SYNTHESIS AND CHARACTERIZATION OF SOME TRANSITION METAL COMPLEXES FOR HOMOCOUPLING OF GRIGNARD REAGENTS

Thesis

Submitted in partial fulfilment of the requirements for the degree of
DOCTOR OF PHILOSOPHY

by

APARNA P.I.

DEPARTMENT OF CHEMISTRY
NATIONAL INSTITUTE OF TECHNOLOGY KARNATAKA,
SURATHKAL, MANGALORE - 575025
March, 2014

DECLARATION

I hereby *declare* that the Research Thesis entitled “SYNTHESIS AND CHARACTERIZATION OF SOME TRANSITION METAL COMPLEXES FOR HOMOCOUPLING OF GRIGNARD REAGENTS” which is being submitted to the National Institute of Technology Karnataka, Surathkal in partial fulfilment of the requirements for the award of the Degree of Doctor of Philosophy in Chemistry is a *bonafide report of the research work carried out by me*. The material contained in this Research Thesis has not been submitted to any University or Institution for the award of any degree.

Aparna P.I.
Reg. No: 090703CY09F01
Department of Chemistry

Place: NITK-Surathkal
Date:

CERTIFICATE

This is to *certify* that the Research Thesis entitled “SYNTHESIS AND CHARACTERIZATION OF SOME TRANSITION METAL COMPLEXES FOR HOMOCOUPLING OF GRIGNARD REAGENTS” submitted by Mrs. Aparna P.I. (Register Number: 090703CY09F01) as the record of the research work carried out by her, is *accepted as the Research Thesis submission* in partial fulfilment of the requirements for the award of degree of Doctor of Philosophy.

Research Guide

Chairman - DRPC

DEDICATION

I am dedicating my thesis to my loving parents, P. Parameshwari and P. Ishwara Bhat who are my soul, strength and life. Without whom I could not have made it here. Their endless love, support and confidence kept me working when I wanted to give up.

This thesis is dedicated to the memory of my Late grandmother, Rathnamma, who raised me and taught me to speak. Her love, care, strength, thirst for education and faith in me till the last moment of her life gave me a new appreciation for the meaning and importance of 'education.' I am dedicating my thesis to my grandparents Late Panjigadde Ramakrishna Bhat-Late Shankari amma, Late Panjaje Shankara Bhat-Late Savithri amma and I am dedicating this thesis to my dearest uncle Late P.S. Vijayashankar. Their memories continue to regulate my life.

I am dedicating the thesis to my beloved in-laws, Shashiprabha and Mahalingeshwara Bhat whose understanding, love, care and faith throughout my research life made it possible today.

This thesis would be incomplete without a mention of the support given to me by my cherished husband, Dr. Harisha Kinilakodi, to whom this thesis is dedicated. He was my own "soul out of my soul," who kept my spirits up when the muses failed me. Without his unconditional support when this thesis seemed interminable, I doubt it would ever have been completed.

I am dedicating my work to my beloved brother Shrikrishna P.I., who is my strength, best friend, mentor, guide and cheerleader. I dedicate thesis to my sisters Usha and Dr. Chethana, brother-in-laws Shivashankara Bhat and Dr. Ramachandra Bhat for their support, encouragement and care. I dedicate this thesis to my cousin brother Tushar, for being with me throughout my work with love and support. I am dedicating my work to my brothers Anish and Ashok who encouraged me throughout my work. I am dedicating my work to my nephew Shwetha, Swathi and Anirudh who brought smile and joy in my life.

I am dedicating my thesis to all my well wishers, especially, S. Venkatramana Bhat, Shankari amma, Parameshwara Bhat K.R., Sharada K., Govinda Bhat, Veena Govinda Bhat, Kaushal, all Panjaje-P.S brothers, Pattaje Lakshmi amma, Kinilakodi Gopalakrishna Bhat, Panjigudde Saraswathi, Jayashree Tondamoole, Gokul Shet, Bhaskara Upadhyaya, Muruva Subramanya Bhat, Late H. Shankara Bhat for constant support and encouragement. My special dedication to V. Raveeshanna for his endless love and care.

I am dedicating my thesis to my research guide, Dr. B. Ramachandra Bhat for opening my eyes, without whom my dream could not have come true today.

I am dedicating this thesis to my Acharya Dr. B. Shridhara Bhat and Savithri Shridhara Bhat for their countless love and care, who inspired my life in all the ways.

I am dedicating this thesis to Padaru Narayana Bhat and P.N. Ambika amma who blessed me with a scholarship and motivated me to persue higher education.

I am dedicating my thesis to Jalli Ishwara Bhat who lightened my life when I was in dark.

I am dedicating my thesis to all my teachers, especially to Yamuna teacher, Vadva Venkatramana Bhat, Late Rajashekhar Rao, Dr. Arun Prakash, Dr. A.P. Radhakrishna and Chandrashekhar Kalchar, who made me what I am today.

I am dedicating this thesis to all my good friends who helped me in good and bad. Especially to Sathish Naik, Rayan, Rajesh, Rammi, Mahesha Poojary, Sandya Rani, Rakesh Kumar Kammaje, Adarsh Hegde, Sarita Alva, Prasad Ananthady, Chaithra, Srijana and Supriya who have been waiting to see their 'appu' as 'Dr. Aparna'.

Finally, at the most, I am dedicating my thesis to the 'Shree Peeta' and the Almighty 'Goddess Devi' for always being with me in all the ways.

ACKNOWLEDGEMENTS

It gives me immense pleasure to express my heartfelt gratitude to my mentor, philosopher and research guide Prof. B. Ramachandra Bhat, Head of the Department, for his insightful guidance, continued inspiration and extreme patience over the years, which made this study possible. I am very much grateful for his unwavering support, invaluable suggestions, generous advice, constructive criticism, balanced approach towards success and failure throughout the study. It was refreshing to work for and with a professional of such a high caliber. It was great experience to learn many aspects from him both as a teacher and a human being.

I would also like to thank my RPAC committee members: Prof. Mahesha A., Department of Applied Mechanics and Prof. D. Krishna Bhat, Department of Chemistry, for spending their valuable time and energy in evaluating my progress and providing thoughtful suggestions.

A special gratitude to Prof. A. Chitharanjan Hegde for motivating me to take-up the research. I have learnt many things from him as a great human being. I sincerely acknowledge Prof. A. Nithyananda Shetty, Prof. A. Vasudeva Adhikari, Prof. D. Krishna Bhat, Dr. Arun M. Isloor, Dr. D. Uday Kumar and Dr. Darshak R. Trivedi for their continuous encouragement and co-operation.

I am grateful to National Institute of Technology Karnataka, Surathkal for providing me research fellowship which made this work possible. I thank Indian Institute of Science, Bangalore for NMR analysis. I would like to thank Head of Department of Chemical Engineering, NITK Surathkal for providing TG and UV analysis throughout my research work. A special thanks to my good friend Miss. Reshma Kayarmar, who helped me in carrying out mass analysis of all my samples.

I would like to mention a word of gratitude to my friend Mrs. Sandya Rani for her help throughout my research work. Whenever I was low, needed a help she was there. I also thank Dr. Ravi K, Dr. Vishnumoorthy, Dr.

Shridhar Malladi, Dr. Murali, Dr. Santhosh, Dr. Sunitha, Dr. Arthi, Vishwanath, Dr. Sujaya, Trithila and Kalaivani for helping me in various stages with fruitful discussions.

Special thanks to Shwetha Panjigadde (IISc) and my best friend Adarsh Hegde (IISc) for helping me in providing the literature whenever I needed throughout my work and for their valuable assistance.

I am very thankful to my fellow researchers for helping me in various stages of this research work. A special thanks to Dr. Ramasubramanian, Dr. Dileep, Dr. Rudresh, Dr. Sampath Kumar, Dr. Ravindra, Mr. Aravinda, Miss. Pooja, Mr. Raghavendra Prasad, Mrs. Lolakshi and Miss. Ansari Rasheeda Maqbool for their good support and cooperation.

I am grateful to the non-teaching staff, Mr. Ashok, Mrs. Kasthuri, Mr. Prashanth, Mr. Pradeep, Mr. Harish, Mrs. Shilpa Kunder, Mrs. Sharmila, Mrs. Deepa and Mrs. Usha who were prompt enough to lend me a helping hand at times of need.

The time spent at NITK was dominated by happy moments. Thanks to all the scholar friends for making my research days at NITK a fun-filled and memorable one. I whole heartedly thank each one of them and wish them success in their research work and all future endeavors.

My intellectual debt is to Mahesha Poojary, Selvam, Raghavendra, Vinay, Suhasini, Lekha, Ranjana, Chinmayi, Swathi and Veena for all the support, cooperation and life experience. They made my stay in NITK more memorable and meaningful.

My special feeling of gratitude to all my teachers-since my childhood till today, because of whom what I am today. I indebt to Dr. B. Shridhara Bhat, Vadva Venkatramana Bhat, Late H.V. Rajashekhar Rao, Prof. M.S. Bhat, Chandrashekhara Kalchar, Dr. Arun Prakash, Adarsha Chokkady, Yamuna teacher for all the inspiration, guidance, care and support given to me throughout my work. I owe my deepest gratitude to Smt. Savithri Shridhara Bhat, Dr. Poornima Ramachandra and Smt. Sunanda Chittaranjan Hegde for their moral support, love and care.

I would like to show my greatest appreciation to my childhood friends, *Sathish Naik, Rayon Antony D'souza, Rajesh Nayak, Rammi for being with me in all the way. I owe a very important debt to my good friends Rakesh Kumar Kammaje, Sarita Alva, Prasad Ananthady, Chaithra, Srijana, Supriya for all the love and support given to me.*

I would like to acknowledge my family members for their unconditional support, understanding, confidence, care and love, especially, my parents, P. Parameshwari-P. Ishwara Bhat; in-laws, Shashiprabha-K. Mahalingeshwara Bhat; brother Shrikrishna P.I; Sisters, Usha, Chethana; brother-in-law, Shivashankara Bhat, Ramachandra Bhat; nephew, Shwetha, Swathi, Anirudh; Cousin brother, Tushar; brothers, Anish, Ashok; well wishers; S. Venkatramana Bhat, K.R. Parameshwara Bhat, Shankari amma, Sharada, Bhaskara Upadhyaya, Dr. Ravishankar K, Smt. Vidya Ravishankar and Ravish V. Nothing can be achieved without the blessings of elders. I like to thank each and every member of my family whose good wishes worked like a guiding lamp on the road leading to my goal. Most importantly, I wish to thank my husband Dr. Harisha Kinilakodi for his cooperation, care and love.

I remain thankful to all those who helped me directly/indirectly for the completion of this research work. Finally, I salute and thank the Almighty Goddess Devi and 'Shri Peeta' for always being with me giving me the strength, patience, knowledge and resources leading to the success of this research work.

Thank you.
Aparna P.I.

ABSTRACT

The biaryl motif plays a significant role in the multidisciplinary fields ranging from natural product synthesis to supramolecular chemistry. Transition metal catalyzed homocoupling reaction is one of the powerful tools for the synthesis of symmetrical biaryls. Though, modern methods of oxidative homocoupling reactions have successively focused on the development of high-yielding reactions, establishing a more efficient catalytic routes where the same outcome is accomplished, but reactions with - reduced waste, in fewer steps, under mild reaction conditions and minimum catalyst loading - is still a challenge.

In this thesis, we have discussed about the development of a catalytic methodology for the homocoupling of Grignard reagents to synthesis symmetrical biaryls in a single step. The ruthenium, palladium, cobalt, nickel and copper complexes were synthesized using dmit (2-thioxo-1,3-dithiole-4,5 dithiolate), ON and ONO Schiff bases and triphenylphosphine ligands. The synthesized complexes catalyzed the reaction effectively at room temperature. In the present study, Grignard reagents were synthesized *in situ* which avoids all the synthetic difficulties regarding isolation of Grignard reagents. The reaction system utilized atmospheric oxygen as a green oxidant, making the system environmentally friendly. The reaction is compatible with diverse functionalities. This study also focuses on the large impact of electronic properties of ancillary and reactive ligands on the yield and scope of homocoupling reaction. The operational simplicity, minimum byproduct, low catalyst loading, usage of green oxidant, mild reaction conditions, tolerant for diverse functionalities, higher yield and chemoselectivity makes the present catalytic system synthetically attractive for the large scale synthesis of symmetrical biaryls.

Key words: biaryl, homocoupling reaction, transition metal complex, Schiff base, Grignard reagent, atmospheric oxygen, green oxidant

CONTENTS

DECLARATION

CERTIFICATE

DEDICATION

ACKNOWLEDGEMENTS

ABSTRACT

CHAPTER 1

INTRODUCTION

CHAPTER 2

SCOPE AND OBJECTIVES

CHAPTER 3

METHODS, SYNTHESIS AND CHARACTERIZATION

CHAPTER 4

CATALYTIC APPLICATION

CHAPTER 5

SUMMARY AND CONCLUSIONS

NOMENCLATURE

DMF	Dimethyl formamide
DMSO	Dimethyl sulfoxide
THF	Tetrahydrofuran
GC	Gas Chromatography
FT-IR	Fourier Transform Infra Red Spectroscopy
UV-vis	Ultraviolet Visible Spectroscopy
LMCT	Ligand to metal charge transitions
ILCT	Intra ligand charge transitions
TGA	Thermogravimetric Analysis
NMR	Nuclear Magnetic Resonance
ESIMS	Electrron Spray Ionization Mass Spectra
dmit	2-thioxo-1,3-dithiole-4,5-dithiolate
NLO	Non Linear Optics

CHAPTER 1

INTRODUCTION

This chapter speaks about the introduction to coordination compounds. The significance of transition metal complexes in catalysis has been briefly addressed. It also introduces the basics of coupling reaction.

1.1 INTRODUCTION TO COORDINATION COMPOUNDS

Coordination chemistry is one of the most active research areas in inorganic chemistry. Alfred Werner's coordination theory in 1893 was the first attempt to explain the bonding in coordination complexes and his pioneering contribution to the study of coordination chemistry fetched him the Nobel Prize in Chemistry in 1913. Research has come long way from the time of Werner in terms of the growth that the coordination chemistry has experienced over the last few decades. With the variety of the coordination compounds being discovered and their stereochemistry being solved, the applications of these compounds have also widened. Coordination chemistry encompasses multidisciplinary fields as bioinorganic chemistry, medicine, catalysis, material science, dyes, toxicology, photonics, microelectronics, optical materials etc. Moreover, there is an ever increasing academic, commercial and biological interest on the metal complexes due to its interesting electrical, optical and magnetic properties.

1.1.1 The metal complexes and ligands

A complex is a species that contains a central metal ion or atom (M), surrounded by ions or molecules called ligands (L).

$$M + L \longrightarrow ML$$

In other words, a complex is a combination of Lewis acid (the central metal atom) with a number of Lewis bases (the ligands), a Lewis acid being an electron pair acceptor and a Lewis base being an electron pair donor. The Lewis bases attached to the metal ion in such compounds are called ligands. These may be simple ions such as Cl^-, small molecules such as H_2O or NH_3, larger molecules such as $H_2NCH_2CH_2NH_2$ or $N(CH_2CH_2NH_2)_3$, or even macromolecules, such as proteins. The atom in the ligand that forms the bond to the central atom is called the donor atom, because it donates the electrons used in bond formation. Ligands bind to the metal center through electron pair donation called as coordination bond. Ligands bind to the metal center through sharing of electrons called as covalent bond.

The majority of ligands are either neutral or anionic. Those which coordinate to a metal ion through a single atom are described as monodentate or unidentate. Examples of such ligands include water, ammonia, chloride etc. Where two donor atoms can be used to bind to a metal ion, as with $H_2NCH_2CH_2NH_2$, the ligand is said to be bidentate and where several donor atoms are present in a single ligand as with $N(CH_2CH_2NH_2)_3$, the ligand is said to be polydentate. When a bi- or polydentate ligand uses two or more donor atoms to bind to a single metal ion, it is said to form a chelate complex (from the Greek for claw) (Shriver and Atkins 2004). Cyclic compounds which contain donor atoms oriented so that they can bind to a metal ion and which are large enough to encircle it are known as macro cyclic proligands. Bicyclic proligands are also known which can completely encapsulate a metal ion. Sometimes ligands can bind to more than one metal ion in a bridging arrangement.

A wide range of ligands appear in coordination complexes. A variety of elements may function as donor atoms towards metal ions, but the most commonly encountered are nitrogen, phosphorus, oxygen, sulfur and the halides. In addition, a large number of metal complexes which contains carbon donor atoms are known as organometallic compounds.

The nature of a bond between metal ion and a donor atom in a coordination compound depends upon various factors like the nature of the metal ion, oxidation state of metal ions, nature of donor atoms, structure of the ligands, steric factors and metal-ligand orbital interaction. Similarly, the coordination number and geometry varies depending on the nature of the metal ion, as well as on the nature of the ligand. With a given number of ligands, each metal complex adopts one of a number of energetically favourable geometries.

Although, coordination compounds are formed by almost all transition metals, lanthanide series metals and some of the non metals like silicon etc., especially transition metals form a large number of complexes with variety of molecules. This is mainly because of their ability to exhibit variable oxidation states, coordination geometry and lower energy vacant *d-orbitals*.

Chemistry of ruthenium with respect to coordination and organometallic behavior has been extensively studied among platinum group metals due to their interesting structure and properties. Ruthenium exhibits a wide range of oxidation states +8 to -2. Most common oxidation states being +3 and +2 for classical type ligands and 7, 5, -1 are the least common. Small π-donor ligands such as O^{2-}, F^- and N^{3-} stabilizes the higher oxidation states and π-acceptor ligands such as PR_3, CO stabilize lower oxidation states. Ligands which are good σ donors but show no substantial π-acceptor or donor properties are usually associated with Ru(II) and Ru(III).

Palladium and its compounds are one of the mostly used catalysts in the C-C coupling reactions especially in Suzuki Miyaura coupling reactions. Many industrial important reactions like Heck reactions, Wacker processes utilizes palladium as main catalyst. Palladium has the ability to absorb hydrogen up to 900 times of its own volume and thus it is used as catalyst for hydrogenation reactions, petroleum cracking and dehydrogenation reactions.

A number of cobalt complexes are used as driers for the conversion of liquids to solids and in inks, paints, varnishes and other surface coatings. The most important among them are cobalt soaps, which are complexes of carboxylate anions such as oleate, stearate, naphthenate, octanoate etc. Cobalt octanoates and naphthenates have been investigated as driers for linseed oil on paper. Cobalt complexes find various applications as additives for polymers. Cobalt complexes were used as efficient catalysts in the variety of catalytic transformations and it emerged as a potential area of research for further development.

The electronic configuration of Ni is [Ar] $3d^8$ $4s^2$. Although 0 or +2 oxidation states are normal for Ni, the +1 and +3 states can exist under certain conditions. Finely divided Ni is used as a catalyst for hydrogenating vegetable oils. A number of nickel complexes of Schiff bases have been shown to possess fungicidal and bacterial activity. Nickel complexes are used in heterogeneous catalysis, electroplating and in making pigments and ceramics. The development of nickel complexes for C–C bond forming reactions is an attractive area of endeavor, in part owing to the utility of its heavy metal congener palladium in coupling catalysis. Significantly, the lower cost and excellent redox properties of nickel make this objective economically as well as synthetically alluring. But, certain disadvantages of Ni and its complexes are associated with toxicity, human carcinogenesis and skin allergies (Sigel et al. 2005).

The applications of copper complexes are extremely varied and of great importance. Copper complexes are widely used as polymer additives, fungicides and crop protectors. They are also used in antifouling paints and as fungicides for textiles. Bis(acetylacetonato)copper(II) has been used as a source of copper in copper-vapour lasers and it has also been investigated as a substitute for silver iodide as an ice-nucleating agent for the initiation of rainfall. Copper phathalocyanine is more effective as smoke retardant for polystyrene than such complexes of other first row transition metals. Bis(acetylacetonato)copper(II) is employed in the protection of fabrics against fungicidal attack. Copper complexes are reported to be more active fungicides than similar iron, cobalt and nickel complexes. The complexes were found to be more effective than the free ligands. Many copper complexes found variety of applications in the area of catalysis ranging from oxidation reactions, hydrogenation reactions, epoxidation reactions, coupling reactions etc. and gives the platform for further development in this field.

The search for appropriate ligands for effectively controlling the stability and reactivity of metal complexes has been an important topic of coordination and organometallic chemistry research. Among the various ligands, sulfur ligands, Schiff base ligands and phosphine ligands are very important and have been studied extensively because of their attractive chemical and physical properties and their wide range of applications in numerous scientific areas.

1.1.2 Metal - sulfur complexes

Metal complexes with sulfur-containing chelating ligands attract strong attention of researchers due to a number of their unique physical and chemical properties. Among such ligands, dithiolate ligands have been studied most extensively. Dithiolene ligands are unsaturated bidentate ligands wherein the two donor atoms are sulphur. Complexes containing dithiolene ligand have been subject of much interest since the mid 1960s when a major research effort, particularly by the groups of Schrauzer, Holm and McCleverty led to the discovery of synthetic routes to ditithiolene complexes of most of the transition metals. Mccleverty introduced the term ‘dithiolene’ to give a general name for the ligand that doesn’t specify a particular oxidation state.

The dithiolene complexes of transition metals are a class of covalent compounds with a number of unusual properties, the most relevant to this report being their very intense electronic transition in the Near-IR region. A second important property of the dithiolene is their ability to exist in several clearly defined oxidation states, mainly due to the delocalized nature of dithiolenes, which are connected through fully reversible redox steps. The third and rather useful characteristic of the dithiolenes is their high thermal and photochemical stability. At present, studies are performed on potential applications of dithiolene complexes, which are related to their magnetic, conducting and non-linear optical properties, superconductivity and liquid crystalline properties. However, the use of sulfur ligands in reactions catalyzed by transition metals is still relatively unexplored compared with other ligands.

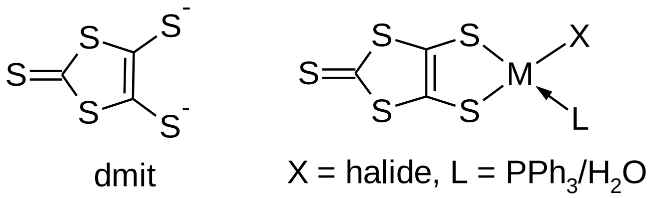

Figure 1.1 General representation of dmit ligand and Dithiolate complex

Specificity of electronic structure of dithiolene metal complexes gives rise to diversity of their practically important properties for materials science and electronics. Among them, dithiolate ligands, especially $C_3S_5^{2-}$, $C_8H_4S_8^{2-}$ and related ligands have been studied extensively (Galloway et al. 1994, Zuo et al. 1996, Deplano et al. 2010, Matsubayashi et al. 2002, Saito et al. 2000). From the viewpoint of potential application as catalysts in organic synthesis, metal complexes containing dmit (dmit=2-thioxo-1,3-dithiole-4,5-dithiolate) or $C_3S_5^{2-}$ ligands (Fig. 1.1) offer a number of important advantages: (1) the metal oxidation state is determined by ligands X and it can change in a predictable mode (e.g., as a result of reductive elimination and oxidative addition, which constitute the basis of coupling reaction); (2) weaker binding of ligand provides the possibility for reversible dissociation and substrate coordination (Ananikov et al. 2008).

Due to the delocalized nature of dithiolenes, metal dithiolenes often exist in multiple oxidation states. These properties were recognized as indications of a type of bonding different from what was previously known for transition-metal complexes. The reason was found to lie in a high degree of electron delocalization in these systems, which also manifests itself in the intense electronic transitions at unusually low energies, not unlike the absorptions seen in extended organic π-systems. The electron delocalization is not limited to the ligand, but includes the metals to give rise to cyclic delocalization.

Many complexes of sulfur-containing ligands have received considerable attention because of their applications in analytical chemistry, new materials, catalysis and their relevance to bioinorganic systems. They have been found to exhibit good third-order NLO properties (Fan et al. 2010), building blocks for organic, organometallic and coordination-complex, electrical conductors (Piotraschke et al. 1995, Robertson and Cronin 2002 and Kobayashi et al. 2004) and superconductors (Cassoux 1999 and Kato 2004) due to its redox activity, pseudo-aromaticity and propensity for stabilizing unusual coordination geometries. Such research has lead to a large body of recent information on both the individual dithiolene complexes and the functional materials derived from them.

Nickel and copper dithiolate complexes were studied by Alkam et al. (1997) and discussed about the influence of substituent within the ligand on the complexes. Cassoux (1999) was synthesized Ni and Pd dithiolate (dmit) complexes and studied their superconducting properties, electrical behavior, unconventional magnetic properties and nonlinear optical (NLO) behavior. Oxidized species of Ru(II)-dithiolato complexes were studied by Natsuaki et al. (2000). Moutloali et al. (2002) synthesized binuclear nickel complexes containing dithiolato Schiff base ligands and by electrochemical behavior it was proven the possibility of electronic coupling of two nickel centres even though the nickel-sulfur bond was especially a *sigma*-bond.

In the studies of Martins et al. (2002), an ancillary ligand, *cis*-1,2-bis(diphenylphosphine)ethene, dppen, was used as a strong chelating ligand to avoid polymeric, insoluble, material of thiolate complex. Hossain et al. (2003) developed Ru-dithiolate complexes and their studies showed that binding of the ligands to the metal site are accomplished either by activation of S-H/S-S/P-C and C-H bonds of the ligands or by simple coordination through the donor atoms depending on the ligand geometry as well as the reaction condition. Thermal decomposition studies of Ni and Pd dithiolate complexes were analyzed by Bernado da Cruz et al. (2006).

The combination of dithiolate and phosphorous ligands were used for the complexation with Ru, Rh metals (Adams et al.2007 and Rivas et al. 2009) and their properties were studied for various applications.

Ananikov et al. (2009) calculated the binding energy of Pd-analogs of dithiolate complexes and showed that Sulfur-containing ligands formed weaker complexes with palladium.

Electrochemical studies of Fe-dithiolate compounds carried out by Charreteur et al. (2010) demonstrates that electron-withdrawing groups have a pronounced effect on both the reduction potentials and the electron transfer process.

Many Ni, Co, Cu, Cd complexes containing dithiolate ligands were synthesized and extensively investigated for third order non linear optical properties (Hou et al. 2008, Wang et al. 2008, de Bonneval et al. 2010, Deplano et al. 2010, Deplano et al. 2010, Jin et al. 2012, Starodub et al. 2012). The third order nonlinear optical properties of Ni(III) complexes of dmit ligand was investigated by Wang et al. (2010). Quantum-chemical study of Ni(III), Co(III) and Cu(III) complexes containing benzene-1,2-dithiolate ligands were studied by Soralova et al. (2011).

Hoffmann et al. (2013) developed Cu complex of dmit ligand and discussed the g-factor and hyperfine splitting correlation line for the CuS_4 using extended molecular orbital calculations for crystal field of distorted tetrahedral geometry.

Jankowska et al. (2013) studied the metal organic framework (MOF) of Zn complexes and studies showed that dmit compounds can be entrapped inside metal organic framework materials such as MOF-5 and particularly ZIF-8. The resulted pigments are resistant for washing with water, which is in a contrast to zeolite matrices. Wrixon et al. (2014) were synthesized the dithiolate complexes of Ni, Pd and Pt from oxidative addition of $[(MeO)_2C_6H_2S_2]_2$ to zero-valent Ni, Pd and Pt complexes in the presence of diphenylphosphinoethane (dppe) under microwave conditions.

Though, dithiolene complexes are active catalysts in a considerable number of catalysis reactions (Bayon et al.1999, Pellissier 2007, Rivas et al. 2009) less explored to coupling reactions which makes it a great interest area of study.

1.1.3 Metal-Schiff base complexes

Schiff bases, named after Hugo Schiff (1834-1915) and their transition metal complexes continue to be of interest even after over hundred years of study. Schiff bases are organic compounds containing azomethine group (>C=N) and have the general structure R-N=C-R' where R and R' are aryl, alkyl, cycloalkyl or heterocyclic groups which may be variously substituted. Often they are referred to as anils, imines or azomethines. Schiff bases can be prepared by condensing carbonyl compounds and an aliphatic or aromatic amines accompanied by the elimination of water molecules. The presence of a dehydrating agent normally favours the formation of Schiff bases (Scheme 1).

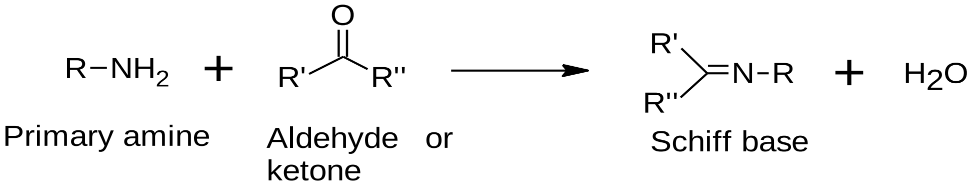

Scheme 1 Synthesis of Schiff base

The bonding ability of the ligands depends on the nature of atoms that act as coordination site, their electro negativity and steric factors. By virtue of the presence of lone pair of electrons on the nitrogen atom, electron donating character of the double bond and low electro negativity of nitrogen, N of the azomethine group

(>C=N) act as good donor site and Schiff base as active ligands. The chelating ability of the Schiff bases combined with the ease of preparation and flexibility in varying the chemical environment about the C=N group makes it an interesting ligand in coordination chemistry.

Transition metal complexes with oxygen and nitrogen donor Schiff bases are of particular interest because of their ability to possess unusual configurations, be structurally liable and their sensitivity to molecular environments (Garcia-Vazquez et al. 1999, Cucciolito et al. 2005, Ghosh et al. 2007). The two donor atoms O and N of the chelated Schiff bases exert two opposite electronic effects: the phenolate oxygen is a hard donor known to stabilize the higher oxidation state of the metal atom where as imine nitrogen is soft donor and accordingly, will stabilize the lower oxidation state of the metal. Thereby, tuning the performance of metals in a large variety of useful catalytic transformations. These ligands can coordinate from a monodentate (Tian et al., 1997) to a nonadentate (Archibald et al., 1994) fashion to a metal ion.

Schiff base complexes are known to offer (i) ease and flexibility of the synthetic procedure; (ii) diverse properties and (iii) use as biological models or biologically active compounds.

The Schiff base complexes are known for their biological properties such as antibacterial agents (Rosu et al. 2011, Shujah et al. 2011, Mandal et al. 2011, Singh and Biyala 2006, Chohan et al. 2006), antifungal agents (Chohan et al. 2010, Shanker et al. 2009, Parekh et al. 2006), anti tumour drugs (Lee et al. 2010, Pradeepta et al. 2013, Adsule et al. 2006, Zhong et al. 2006, Friaza et al. 2006) antimicrobial activities (Raman et al. 2005, Badiger et al. 2012). Further, Schiff base complexes are important due to their oxygen binding ability (Jones et al. 1979), complexing ability for various toxic metals (Sawony and Riederer 1977). Schiff base complexes of zinc found application as electroluminescent materials (Yu et al. 2007). Many Schiff base complexes are attracting material chemistry mainly for nonlinear optical materials (Costes et al. 2005, Trujillo et al. 2010; Anitha et al. 2012; Kumar et al. 2010; Lenoble et al. 1998; Averseng et al. 1999), conducting materials, liquid crystals, metal sensors (Ganjali et al. 2004, Saadeh et al. 2012), polymer films (Vilas-Boas et al.

1997) and so on. Schiff base complexes are emerging as analytical reactants because of their capability to determine several organic and inorganic substances (Cimernman et al. 1997). Many Schiff base complexes found applications in heterogeneous catalysis. Among these polymer supported (Gupta et al. 2009; Gupta and Sutar 2007; Syamal and Singh 1993) and zeolite encapsulated Schiff base complexes are the most widely used heterogeneous catalysts (Jin et al. 2006).

The Schiff bases derived from 4-aminoantipyrine are of interest mainly due to their appreciable biological applications. A broad spectrum of bioactive 4-aminoantipyrine derivatives has been studied for analgesic, antibacterial, anti-inflammatory, antimicrobial activities (Ismail 2000, Raman et al. 2004, Raman et al. 2005, Raman et al. 2008, Omar et al. 2009, Raman et al. 2010, Abdel rehman et al. 2010, Mahalingam et al. 2010, Sharma and Chandra 2011, Rosu et al. 2011, Leelavathy et al. 2013). The NLO properties of such complexes were studied with great interest (Arun et al. 2010). Though, 4-amino antipyrine Schiff base complexes found applications in the various catalytic transformations such as epoxidation reactions (Bernado et al. 1996), oxidation reactions (Biava and Singorella 2010), very less work has been reported for coupling reaction so far.

The products of condensation of aminonaphthalene sulfonic acids, which are polydentate ligands, play a special role among diverse chelating Schiff bases. The complexes of 2-Amino-1-naphthalene Sulfonic acid were extensively used in the manufacture of a large number of azo dyes and pigments (Chao and Yang 1995, Hishara et al. 2007). Napthylamine-derived azo-linked Schiff bases and their Ni(II), Cu(II) and Zn(II) complexes have found application especially in the dye industry (Erdem et al. 2009). Sulfonic salts are soluble in water. Sulfonic acid and its salts present in organic dyes provide useful function of water solubility and or improve the washfastness of dyes due to their capabiltity of binding more tightly to the fabric. They are widely used in the detergent industry (Akerman et al. 2004). Sulfonic acid derivatives were used as spectrofluorimetric reagents for the detection of metals (Al-Kindy et al. 2008, Mansouri et al. 2011, Wu et al. 2013). The sulfonic acid derivatives found as good catalysts in esterification, alkylation and condensation reactions (Hello et al. 2013). Alkylbenzene sulfonic acid is the largest-volume synthetic surfactant because of its relatively low cost, good performance, the fact that it can be dried to a stable powder and the biodegradable environmental friendliness. Sulfonic acid salts and esters are intermediates widely used in organic synthesis and particularly phenolic compounds and cation exchange resins. They are synthetic intermediate for a number of biologically active compounds and pharmaceutical candidates (Wong et al. 1996, Tandon et al. 2009, Iqbal et al. 2013).

The Schiff bases derived from 2-aminophenol have been studied extensively for varieties of applications. Aziz et al. (2012) studied the catalytic activity of metal complexes of Mn, Co, Ni, Cu and Zn derived from N-salicylidene-o-aminophenol for the aerobic oxidation of benzaldehyde to benzoic acid. These ligands and complexes also showed good antibacterial and antifungal activities. Kagkelari et al. (2009) developed electroluminescence devices from the gallium(III) complexes of N-salicylidene-o-aminophenol and its 5-methyl and 5-bromo derivatives. Amino phenol derivatised square planar Ni(II) complexes were well characterized by Bag et al. (2013). Numerous complexes found importance in various biological studies such as antibacterial, antimicrobial, antioxidant and DNA cleavage activities (Mohamed and Abd El-Wahab 2005, Mohamed 2006, Singh et al. 2010, Kavitha et al. 2013, Subbaraj et al. 2014). Many complexes were investigated for NLO properties (Chavan and Bharate 2013). Co, Ni, Cu and Zn complexes of 2-aminophenol and 2,4-dihydroxybenzaldehyde were investigated for non linear optical properties of organic chromophores (Ananthi et al. 2012). Cariati et al. (2004) were studied cyclopalladated chromophores for third order non-linear optical activities. Aminophenol derivatized Schiff base complexes were extensively studied in various catalytic applications such as epoxidation of olefines (Chatterrjee et al. 2000), oxidation reactions (Pasini et al. 2006, Simandi et al. 2003, Chatterjee et al. 2004, Mukherjee et al. 2006, Chittilappilly et al. 2008), Diels–Alder cycloaddition reaction (Kubota et al. 2006), acylation of alcohols (Niasari et al. 2005).

The Schiff base complexes found ample applications in homogeneous catalysis. This is mainly due to their ability of controlling the catalytic activity by changing the donor atoms and the coordination sites. Biittcber et al. (1993) studied the Co(II), Ni(II) and Cu(II) complexes with derivatives of salen and tetrahydrosalen for oxidative dehydrogenation reactions. The influence of ligand modification on complexation with metals were studied. Epoxidation of terminal olefins were investigated by Bernardo et al. (1996) using chiral schiff base complexes of Mn, Ni, Co, Cu with diiminobinaphthyl or diiminocyclohexyl moieties. Clercq and Verpoort (2002) were developed ruthenium schiff base complexes for radical polymerization reactions. Himeda et al. (2003) reported the efficient catalytic activity of [CpRh(bpy)Cl]Cl in the transfer hydrogenation of a wide variety of ketones in aqueous formic acid solution under mild reaction conditions.

Good C-C coupling activity of Palladium(II) complex with bidentate phosphine sulfide ligands was investigated by Aizawa et al. (2007) and was reasoned to the *pi*-accepting ability of the phosphine sulfide S atom which stabilizes the catalytically active Pd(0) species electronically and weak *sigma*-donation of the S atom which did not block the formation and a subsequent reaction of the Pd(II) substrate adduct in the catalytic cycle.

Many V and Co oxidation reactions (Rajagopalan et al.2008, Ando et al. 2007) were studied. Long et al. (2009) studied the Ni and Pd complexes for olefin polymerization and influence of steric effect on coordinated geometry was investigated.

Many Ru-schiff base complexes were studied (Karvembu et al. 2002, Padma et al. 2009, Jayabalakrishnan et al. 2010) for aryl-aryl coupling reaction biological activity studies and could obtain 30-40% yield of biphenyl.

Kumar et al. 2009 studied the Pd(II) with chalcogenated Schiff bases of 2-hydroxybenzophenone complexes for Heck and Suzuki reaction under aerobic condition. Cui et al. 2010 developed amino-salicylaldimine–palladium(II) complexes bearing 5-methyl-3-(R-1-ylmethyl)-salicylaldimine ligands for suzuki and heck reactions under air towards activated aryl bromides. Iron complexes containing Schiff base and PPh_3 was subjected to oxidation of alcohol to aldehide with excellent yield by Sandya and Bhat (2010). Catalytic activities of the Mn(II) complexes with bidentate N,N'-imine-pyridine and N,N'-imine-quinoline-type donor ligands were studied by Sood et al. (2013) for ethene polymerization which indicated single-site polymerization behavior.

Schiff base complexes have been amongst the most widely studied coordination compounds in the past few years, since they are becoming increasingly important as biochemical, analytical and antimicrobial reagents.

1.1.4 Metal-phosphine ligand complexes

Organophosphines or phosphine ligands (PR_3) are among the most common ancillary ligands used in organometallic chemistry with excellent tunable and sigma-donar, pi-accepter abilities, owing to their ability to stabilize low metal oxidation states (Philips et al. 2004). They are probably the most widely used ligands in catalysis field (Garrou 1985, Fogg et al. 1994, Matteoli et al. 1995, Moldes et al. 1998, Li et al. 2002, Horvath et al. 2004, Tsai et al. 2005, Sharma and Samuelson 2006, Jackson et al. 2006, Deb et al. 2011, Tamhiz et al. 2012, Sisodiya et al. 2012, Duanmu et al. 2014). These can influence both steric and electronic properties of the catalytic species. Phosphine ligands have the advantage that they can be tailored to a greater extent by varying the R group inorder to vary electronic and steric properties and to modify the solubility of their metal complexes (Prabhakaran et al., 2011). In homogeneous catalysis, this can be a very useful tool in order to change the activity or selectivity of the catalyst.

Tertiary phosphines stabilize wide variety of metal complexes (Nadri et al. 2009, Aswin et al. 2013). They coordinate to the metals in relatively high to low oxidation states. Conventionally, metal-phosphine bonding has been described as a ligand to metal σ bond plus metal to ligand π back bond using the acceptor character of the empty 3*d* orbitals on the phosphorus atom. Orpen and Connelly (1985) used structural data to confirm the theoretical studies (Xiao et al. 1983) suggesting that the σ^* phosphine orbitals are π-acid in character and act as the π- acceptor for the metal *d* electron back bond. Phosphines have lone pair of electron on central P atom that can be donated to a metal. These ligands are strong σ donor and weak π-acceptor. π-acidity varies depending on the R group. Alkyl phosphines have week π acidity, whereas aryl, dialkylamino and alkoxy groups are successively more effective in promoting π acidity. The electronic flexibility of PR_3 is the reason it forms so many complexes. Traditional phosphine complexes of metals, particularly those of palladium, have played an extremely important role in the development of homogeneous catalysis. They have shown high catalytic activity and selectivity. But most of the phosphine complexes are relatively less air stable.

Garcia-Vazquez et al. (1999) synthesized metallic complexes of bidentate thiolates containing nitrogen and phosphorous donor atom via electrochemical reactions. The study revealed that the polymerization tendency of the dmit ligands can be modulated by introducing bulky group to the coordination geometry. An increase in the volume will reduces the degree of polymerization as a result of steric hindrance.

Recently, extensive research efforts have been invested in the development of catalysts based on the Schiff base and triphenylphosphine transition metal complexes (Leeuwen et al. 2000, Wolf et al. 2006, Huang et al. 2009, Deb et al. 2011, Xu et al. 2012). This would result in complexes with higher air stability along with good catalytic activity. Aizawa et al. (2007) studied C-C couling reaction catalysed by Palladium(II) complex with bidentate phosphine sulfide ligands. The exploration of chemistry of bis(phosphino)amines possessing electron-donating methoxy-substituents on an aryl ring when coordinated to palladium was studied by Biricik et al. (2010) and successfully applied for Heck and Suzuki coupling. Catalytic activity of the complexes were evaluated and compared with the conventional Pd(II) and Pd(0) complexes with phosphines. Hydrosilylation reaction via rhodium complexes employing 2-imidazolium phosphinesas ligands by Li et al. (2010) showed that enhancement in the catalytic activity was due to the presence of phosphine atom.

Palladium-catalyzed cross coupling of aryltrimethylammonium triflates with grignard reagents studies were carried out by Reeves et al. (2010) and showed that variation to a more bulky or more electron-rich phosphine afford lower yields.

Organometallic synthesis represents a notable component of catalysis in industry. The development of industrial processes, carried out by transition metal complexes, includes the choice of the metal centre as well as the synthesis of ligands able to affect positively the course of the reaction. Thus, a continuous interest is addressed toward the synthesis and the characterization of new ligands and complexes for more active, stable and selective catalysts.

1.2 COORDINATION COMPOUNDS AND CATALYSIS

Coordination compounds are important not only because of their interesting chemistry, but because of their numerous applications. These compounds are widely present in the mineral, plant and animal worlds and are known to play many important functions in the area of analytical chemistry, metallurgy, biological systems, industry and medicine. Coordination compounds are the basis for a number of therapeutic drugs, chemical sensors, colouring agents etc. Amongst major application of coordination compounds as catalysts, which serve to alter the rate of many industrially important chemical reactions.

The term catalysis was coined by Berzelius around 1836 (Laidler 1982) after observing changes in substances when they came into contact with small amounts of species called “ferments”. Catalysis is the process by which the rate of a chemical reaction (or biological process) is altered by means of the addition of a species known as a catalyst to the reaction. Catalyst is not consumed by the reaction itself. That is, the catalyst may participate in multiple chemical transformations during the reaction, but at the end of the reaction, the catalyst is regenerated unchanged. Often only a very small amount of catalyst is needed to increase the rate of the reaction. A catalyst works by providing an alternative reaction pathway to the reaction product. The rate of the reaction is increased as this alternative route has lower activation energy than the reaction route not mediated by the catalyst. Lower the activation energy, the faster the rate of the reaction. Nowadays, the definition of catalyst in use is “*A catalyst is a* substance which increases the rate at which a chemical reaction approaches equilibrium without becoming itself permanently involved”. Thus catalyst facilitates the establishment of equillibria and is capable of greatly enhancing product selectivity. Catalyts allow chemical transformations to be performed with increased efficiency, minimal waste and reduced energy consumption.

In organometallic catalysis, activation energy decreases through coordination of substituent to a transition metal center, thus promoting the reaction. Furthermore, a catalyst enhances product selectivity by accelerating just one of the competing reaction sequences when alternative routes exist. Thus, important processes can be carried out under industrially feasible conditions of pressure and temperature simply by using a catalyst.

It is not surprising that the vast majority of products of the chemical industry involve a catalyst at some stage in their manufacture. This applies to bulk chemicals produced on a large scale as the starting materials for innumerable end products, such as alcohols, ketones, carboxylic acids, hydrocarbon such as olefins and dienes that can be polymerized to polyolefins and also increasingly to fine chemicals, i.e., high added-value compounds produced on a smaller scale, as well as pharmaceuticals.

1.2.1 Catalytic cycle and intermediates

Consider a hypothetical metal complex ML_n (M = metal, L = ligand, n= number of ligands) that acts as a catalyst for a given process. Assume catalytic cycle consisting of different catalytic intermediates. The stable metal complex added to the reaction at the beginning, ML_n, is called the precatalyst or the catalyst precursor. One complete catalytic cycle is derived from one molecule of the precatalyst and produces one molecule of the product. Turnover frequency in terms of a catalytic cycle is therefore the number of times the cycle is completed in unit time.

Information about the catalytic cycle and catalytic intermediates is obtained by four methods: kinetic studies, spectroscopic investigations, studies on model compounds and theoretical calculations. Kinetic studies and the macroscopic rate law provide information about the transition state of the rate-determining step. Apart from the rate law, kinetic studies often include effects of isotope substitution and variation of the ligand structure on the rate constants.

Spectroscopic studies may be carried out under the actual catalytic conditions. These are referred to as in situ spectroscopic investigations. Ultraviolet, Infrared and multinuclear NMR spectroscopy have been used to identify homogeneous catalytic intermediates. These spectroscopic methods, if they are to be used for studying reactions under drastic conditions (i.e., high pressure and temperature), require careful choice of construction material and design of the spectroscopic cell. However, if the catalytic conditions are too drastic, it may not be possible to record spectra under such conditions. In such cases, spectroscopic monitoring is done under less severe conditions.

Both kinetic studies and spectroscopic investigations have certain inherent limitations. Kinetic studies are informative about the slowest step and at best can provide only indirect information about the fast steps. Spectroscopic detection of a complex, catalytically active or not, requires a minimum level of concentration. It is possible that the catalytically active intermediates never attain such concentrations and therefore are not observed. Conversely, the species that are seen by spectroscopy may not necessarily be involved in the catalytic cycle.

The third method is based on the study of model compounds. Model compounds are fully characterized metal complexes that are assumed to approximate the actual catalytic intermediates. Studies on the reactions of such compounds can yield valuable information about the real intermediates and the catalytic cycle. With the advent of computational speed and methods, quantum-mechanical and other theoretical calculations are also increasingly used to check whether theoretical predictions match with experimental data.

1.2.2 Types of catalysts

The numerous catalysts known today can be classified according to various criteria: structure, composition, area of application, or state of aggregation (Fig. 1.2). Broadly catalysts can be classified into two groups according to the state of aggregation in which they act. They are heterogeneous catalysts and homogeneous catalysts. There are also intermediate forms such as homogeneous catalysts attached to solids known as immobilized catalysts (Hetrogenized homogenious catalysts) and biocatalysts.

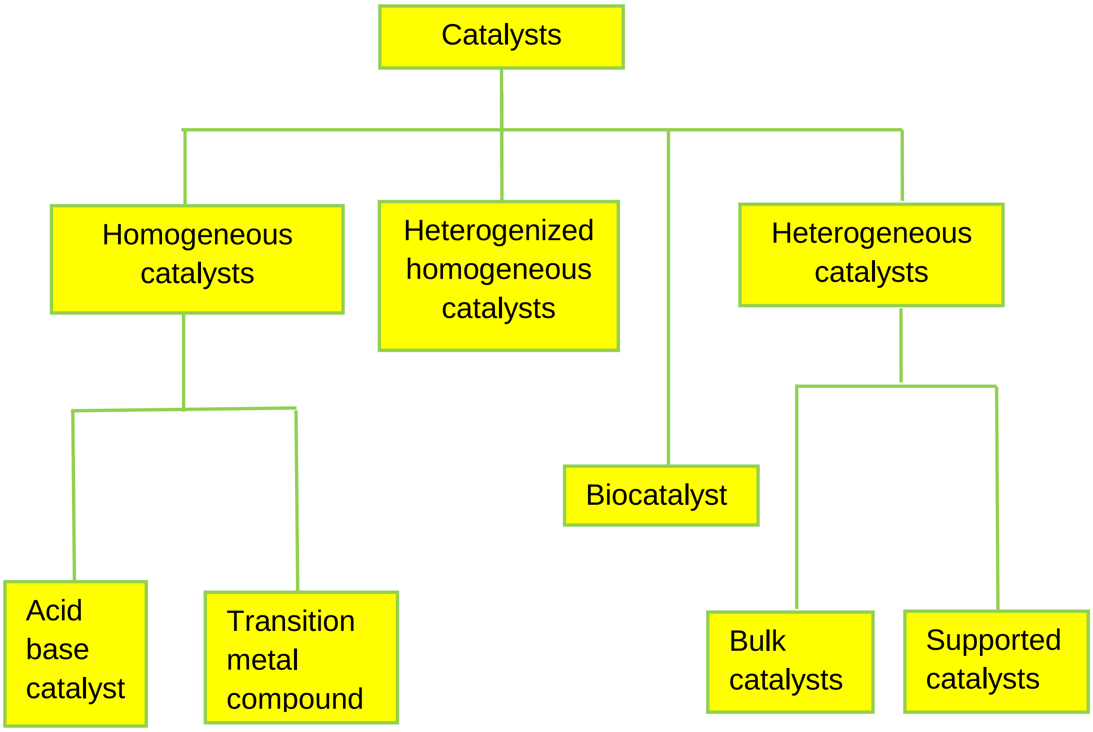

Figure 1.2 Types of catalysts

In homogeneous catalysis, both the catalyst and the reactant are in the same phase. Generally, homogeneous catalytic processes take place in a uniform gas or liquid phase. Homogeneous catalysts are generally well defined chemical compounds or coordination compounds, which, together with the reactants, are molecularly dispersed in the reaction medium. Metal complexes and organometallic compounds are the important homogeneous catalysts. These catalysts are soluble in the reaction medium and are used in the production of high purity, high value chemicals. Usually, homogeneous catalytic reactions are very complex and proceed as a closed cycle of linked chemical reactions which involve different intermediate species. However, they exhibit high efficiency and selectivity and operate at milder conditions of temperature and pressure. Moreover, homogeneous catalysts of definite stoichiometry and structure can be easily made with more reproducibility.

Heterogeneous catalysis take place between several phases. Generally the catalyst is a solid and the reactants are gases or liquids. Heterogeneous catalysis is based on surface phenomena where atoms that are available at the surface of a solid are those which activate substrates. They are mainly used for the production of large scale commodity chemicals and in petrochemical industry. One attractive feature of heterogeneous catalysts is their high stability which makes it suitable for wide range of operating conditions and extra steps are not needed to separate the product from the catalyst.

Both homogeneous and heterogeneous catalysts were extensively used in industry since the beginning of the twentieth century. But, heterogeneous catalysis has grown at a faster rate than homogeneous catalysis in industry. The main technical problem in the use of homogeneous systems is the separation of catalysts from reactants and products, which is practically very easy in the case of heterogeneous catalysts. The deactivation of homogeneous catalysts by the self aggregation of the active sites may also restrict its application in industrial processes, whereas heterogeneous catalysts are relatively more stable. The above mentioned facts may be the reason for the slow growth of homogeneous catalyst systems in industry. However, the ability of homogeneous systems to catalyze a variety of specifically designed chemical transformations promises lot of scope for future developments.

1.2.3 Transition metals/compounds as catalysts

Transition metals and their compounds are often good catalysts. Transition metal catalysts can be homogeneous catalysts or heterogeneous catalysts. Transition metals and transition metal oxides tend to be used as heterogeneous catalysts, their ions and complexes are usually employed as catalysts in homogeneous contexts.

The ability of transition metal ions to change oxidation state makes them suitable as homogenous catalysts. A new activated complex can be formed with the catalyst, because transition metals are able to form stable compounds in more than one oxidation state.

Typical common features of transition metals and their compounds are the presences of *d* electrons/incompletely filled *d*-orbitals. Transition metal atoms have one *s*, three *p* and five *d* orbitals that possess geometrical and energetic features suitable for bonding with the ligands. A compound is said to be coordinatively saturated if the nine potentially bonding orbitals of the metal are completely filled, whose electron count is 18. Such compound would be stable toward nucleophilic attack on the metal because the added electrons will have to occupy orbitals at high energy. Therefore, ligand substitution reactions in such cases proceed by S_N^1 type mechanisms, that is, one ligand dissociates from the complex resulting in a coordinatively unsaturated species, a species having 16 electrons in the valence orbitals of the metal. In other words, when the electron count is less than 18, the metal complex is often classified as coordinatively unsaturated. The coordinatively unsaturated complex would then bind with other potential ligands rather readily. This switching of electron count between 16 and 18 drives the catalytic cycle.

High reactivity may also result from easy displacement of weakly bound ligands by the substrate. Usually coordinatively saturated complexes follow this route and coordinatively unsaturated complexes do follow this type of reactivity also. In other words, the ability to form extra bonds or facile displacement of weakly bound ligands, which in many cases may just be solvent molecules, are both manifestations of coordinative unsaturation. Thus ligand dissociation or some other similar mechanism generates coordinative unsaturation. The substrates are activated by direct interaction with small, highly electropositive metal ions.

Coordinative unsaturation can sometimes be induced by using bulky ligands. A few such ligands can take up most of the space around the metal atom and prevent the presence of a full complement of ligands. So due to steric constraints, an 18-electron count, which only a full complement of ligands can give, is not achieved. As an example, nickel in the zero oxidation state requires the presence of four monodentate phosphorus ligands to give an electron count of 18. However, if these ligands are bulky, then steric repulsion between them causes ligand dissociation and the following equilibrium is established. The species NiL_3 on the right-hand side of the equilibrium has an electron count of 16 and is coordinatively unsaturated.

$$NiL_4 \longrightarrow NiL_3 + L, L=PPh_3$$

Thus, transition metals and their compounds can act as electron banks that lend out electrons at appropriate time and store them for chemical species at other times. This kind of ability is the basis for the catalytic activity of certain transition metal complexes to a great extent. Upon coordination to a metal ion, changes take place in the electronic distribution in a ligand, which result in the modification of the reactivity of the ligand molecule, at times dramatically.

1.3 TRANSITION METAL CATALYZED HOMOGENEOUS REACTIONS

In the last three decades homogeneous catalysis has undergone major growth. Many new processes with transition metal catalysts (Fig. 1.3) have been developed and many new products have become available.

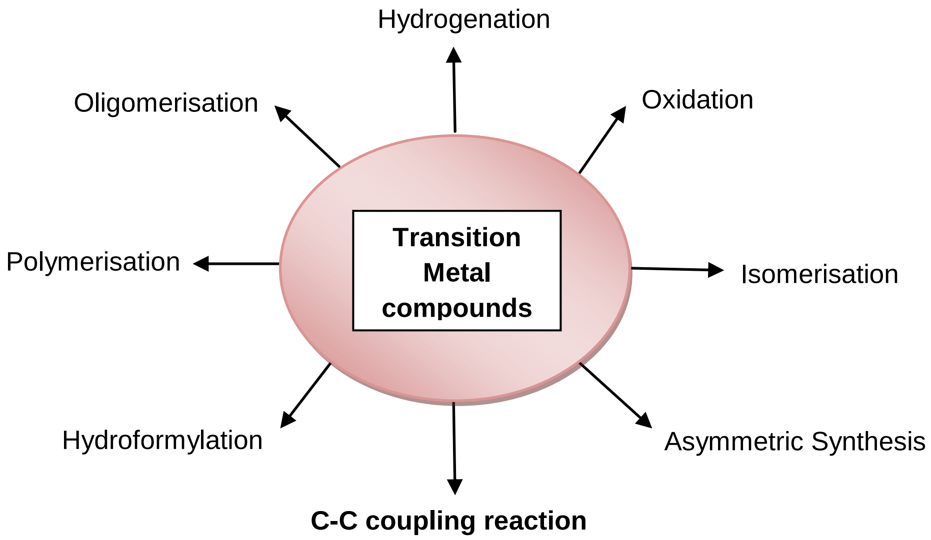

Figure 1.3 Some industrially important metal catalyzed homogeneous reactions

The continuous search for biologically active molecules for the pharmaceutical and agrochemical industries is probably one of the largest areas of research in which synthetic organic chemistry plays a fundamental role. There is a constant need for the development of new methods for selective carbon-carbon and carbon-heteroatom bond formation which are very useful tools for the fine chemical industry. Among various industrially important metal catalyzed homogeneous reactions C-C coupling reactions plays central role.

1.3.1 C-C coupling reactions

A coupling reaction in organic chemistry is a catch-all for a range of reactions in organometallic chemistry where two hydrocarbon fragments are coupled with the aid of a metal catalyst supported by suitable ligands. Broadly speaking, there are two types of coupling reactions, namely, cross coupling and homocoupling. Cross coupling involve reaction between two chemically distinct partners, allowing control over both halves of the resulting molecule. Homocoupling couples a molecule to itself, often in a reductive or oxidative fashion.

1.3.1.1 Cross coupling reactions

Transition metal catalyzed cross-coupling reactions are the milestone in the synthetic organic chemistry. Cross coupling reactions often involve aryl, alkenyl, or alkyl halides or pseudo halides as one reaction partner, with a much greater variety in the other reaction partner.

The Ullmann reaction or Ullmann coupling is a coupling reaction between aryl halides with copper. The traditional version of the Ullmann reaction requires harsh reaction conditions and the reaction has a reputation for erratic yields.

A Kumada coupling or Kumada-Corriu coupling is a cross coupling reaction in organic chemistry between an alkyl or aryl Grignard reagent and an aryl or vinyl halocarbon catalyzed by nickel or palladium.

The Heck reaction is the chemical reaction of an unsaturated halide (or triflate) with an alkene and a base and palladium catalyst to form a substituted alkene. The reaction is performed in the presence of an organopalladium catalyst.

Sonogashira coupling is a coupling reaction of terminal alkynes with aryl or vinyl halides. Typically, two catalysts are needed for this reaction (eg. a zerovalent palladium complex and a halide salt of copper(I)).

The Negishi coupling is a cross coupling reaction in organic chemistry involving an organozinc compound, an organic halide and a nickel or palladium catalyst creating a new carbon-carbon covalent bond.

The Stille coupling reaction is a chemical reaction coupling an organotin compound with sp^2-hybridized organic halide catalyzed by palladium. The reaction is usually performed under inert atmosphere using dehydrated and degassed solvent, as oxygen causes the oxidation of the palladium catalyst and promotes homo-coupling of organic stannyl compounds and these side reactions lead to a decrease in the yield of the desired cross-coupling reaction.

The Suzuki reaction is the organic reaction of an aryl- or vinyl-boronic acid with an aryl- or vinyl-halide catalyzed by a palladium(0) complex. It is widely used to synthesize poly-olefins, styrenes, substituted biphenyls and has been extended to incorporate alkyl bromides.

Hiyama coupling is a palladium or nickel-catalyzed cross coupling reaction of organosilanes with organic halides or triflates. Hiyama coupling reaction is promoted by activation of the organosilane with fluorides.

The Buchwald-Hartwig reaction is a coupling reaction between an aryl halide and an amine in presence of base and a palladium catalyst forming a new carbon-nitrogen bond.

The Fukuyama coupling is a coupling reaction taking place between a thioester and an organozinc halide in the presence of a palladium catalyst. The reaction product is a ketone.

Amongst cross-coupling reactions, the Heck or Stille reaction, the Suzuki-Miyaura reaction is a superior coupling reaction in terms of catalyst used and reaction conditions.

1.3.2 Organometallic reagents in coupling reactions

With the synthesis of diethylzinc in 1849, E. Frankland laid the foundation stone for modern organometallic chemistry. The reactivity of an organometallic species increases with increased ionic character of the carbon-metal bond. The use of highly reactive species, such as organolithium reagents, selectivity is often compromised. Furthermore, reduced tolerance towards functional groups such as esters, cyano groups and ketones are observed. On the other hand, the less reactive organometallic species, such as organo zinc, -tin or -boron compounds, require transition metal catalysts, such as palladium or nickel complexes, to promote the reaction of these nucleophiles, giving access to the broad field of transition metal catalyzed transformations.

Though, Organomagnesium reagents display a less reactive polar carbon-metal bond than in the corresponding lithium compounds. However, these species are more stable and they still have a high reactivity towards many electrophiles combined with a remarkable functional group tolerance at low temperatures. The application of organomagnesium reagents in organic synthesis suffered a long set back due to a lack of mild preparative methods. The use of Rieke magnesium proved not to be general, since most polar functional groups coordinate to the surface of the activated magnesium and thereby inhibit the oxidative addition of the metal into the carbon-halogen bond (Lee 2000). Recently, a more general method has been developed, which makes use of a low temperature iodine-magnesium exchange reaction (Rottlander et al. 1999). In the wake of this new methodology an array of applications of Grignard reagents in palladium and nickel-catalyzed (Miller 1998) cross-coupling reactions has been developed.

1.4 HOMOCOUPLING OF GRIGNARD REAGENTS - TOOL FOR BIARYL SYNTHESIS

A lot of emphasis is on the development of viable synthetic methods for the synthesis of symmetrical biaryl motif, which plays a substantial role in natural product synthesis (Bringmann et al. 2011), pharmaceuticals (Magano and Dunetz 2011), asymmetric catalysis (Chelucci and Thummel 2002, Wurz 2007), synthesis of biomolecules (Evano et al. 2008, Vallee et al. 2010) and materials with specialized optical and electronic properties (Pu 1998). Due to high efficiency and broad application, transition metal catalyzed homo-coupling of Grignard reagents have become one of the most powerful methods for their synthesis (Alberico et al. 2007).

The Grignard reaction, reported in 1900 by Victor Grignard (Nobel Prize, 1912), provides the synthetic chemist with one of the most powerful tools for connecting carbon moieties. The homocoupling of aryl Grignard reagents yields respective biaryls using suitable catalysts in specific reaction conditions. Although more than 100 years have passed since Grignard published the preparation of ethereal solutions of organomagnesium halides, the actual mechanism(s) for the formation of the reagents and their structures are still not completely understood.

A wide range of arylmetal compounds has been successfully utilized to date as the nucleophilic partner in biaryl coupling reactions. Out of aryl-lithium (Najera et al. 2003, Nagaki et al. 2011, Toummini et al. 2013), magnesium (Burns et al. 1987, Guan et al. 2010), boron (Amoroso et al. 2010), silicon, copper (Ginah et al. 1990, Hassan et al. 2002), zinc (Hu et al. 2011), or tin (Li et al. 2005) compounds, aryl-magnesium compounds seem ideal for practical synthesis because they are readily available, cheap and environmentally benign (Hatakeyama et al. 2009).

The selection of the solvent in metal-catalyzed homocoupling reactions of Grignard reagents is decisive since the solvent must dissolve both non-polar and polar organic reactants, inorganic bases and organometallic complexes. Many polar aprotic solvents such as tetrahydrofuran, dimethyl formamide, benzene, toluene, diethyl ether are frequently used for homocoupling reaction. The diethyl ether found the best solvent for the Grignard reagent synthesis as ether molecules coordinate to Grignard reagent and stabilize the intermediate complex (Rogers et al. 1980).

The Grignard reagent is formed by the interaction of an alkyl or aryl halide and metallic magnesium in ether solvents (Rogers et al. 1980). The carbon-metal bond is highly polarized leading to considerable carbanion character. Thus the Grignard reagent has significant nucleophilic character and it is also strongly basic. Its nucleophilic character allows it to react with the electrophilic carbon in a reactive ligand or in other words the substrate thus forming the carbon-carbon new bond. Its basic property means that it will react with acidic compounds, such as carboxylic acids, phenols, thiols and even alcohols and water; therefore, reaction conditions must be free from acids and strictly anhydrous. Grignard reagents will also react with oxygen to form hydroperoxides, thus they are highly unstable when exposed to the atmosphere and are generally not isolated from solution.

The formation of Grignard reagent (Scheme. 1.2) occurs at the surface of the Mg metal (Rogers et al. 1980). The studies by Walborsk (1990) showed that iodine can act as surface activator (Yuan and Fang 2012). While forming the Grignard reagent, the metal is oxidized and oraganohalide is reduced to the halide ion and polarized metal-carbon bond with the magnesium. The overall reaction for the formation of Grignard reagents involves an insertion of magnesium into the carbon-halogen bond via an oxidative addition, thereby changing its oxidation state from Mg(0) to Mg(II). The polar Grignard reagent essentially stops the reaction since it forms an insoluble deposit at the metallic surface in most non-polar organic solvents. Protic solvents can not be used to solubilize the material because Grignard reagent, while being an excellent nucleophile, is highly basic. Ether is used to support the reaction, being a relatively polar but aprotic solvent (Rogers et al. 1980). Magnesium, existing as divalent and electron deficient, forms the Grignard reagent and the ether acts as a Lewis acid, coordinating to the Mg and solubilizing it (Scheme 1.3).

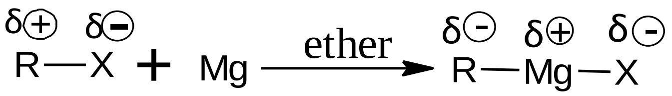

$$\overset{\delta\oplus}{R}-\overset{\delta\ominus}{X} + Mg \xrightarrow{\text{ether}} \overset{\delta\ominus}{R}-\overset{\delta\oplus}{Mg}-\overset{\delta\ominus}{X}$$

Scheme 1.2 Schematic representation of formation of Grignard reagent

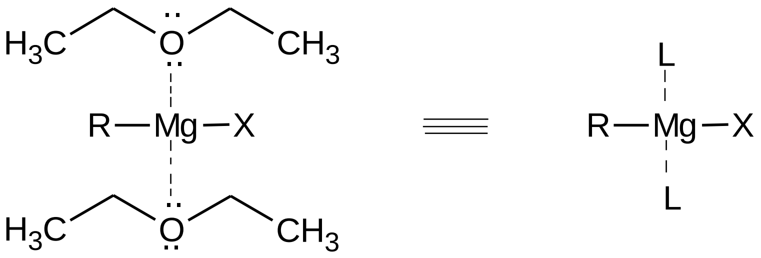

Scheme 1.3 Stabilization of Grignard reagent in diethyl ether

The homocoupling of aryl Grignard reagents yields respective biaryls using suitable catalysts in specific reaction conditions. To date, various simple metal salts have been used as catalysts for the synthesis of biaryls. There are many reports of coupling reactions that use a variety of metal reagents such as $NiCl_2$, $CuCl_2$, $TiCl_4$, $Ce(OTf)_4$, $FeCl_3$, $MnCl_2$ $Pd(OAc)_2$ and Cu(I) triflate in stoichiometric or catalytic amounts in the presence of a reoxidant (Inoue et al. 2000, Cepanec et al. 2007). The demand of a stoichiometric amount of an organic oxidant or an extra ligand limits their use in industrial scale applications.

An ideal oxidant for any large scale oxidation reaction should be easily accessible, cheap and non-toxic. Many coupling reactions utilized 1,2-dihaloalkane (Shekar and Hartwid 2004, Nagano et al. 2005), α-halocarbonyl compounds (Nagano and Hayashi 2005), 1,3-butadiene, 2-halo-2-butene etc. as oxidants/additives. Kiefer et al. (2013) showed that nitrous oxide can be used as oxidant. Some reactions were utilized extra ligands like pyridine in addition to catalyst and oxidants.

In the search for alternative protocols, greener oxidants like molecular oxygen are gaining much interest of current research as air is the most plentiful oxidant source, which is known to be safe and environmentally benign (Guo et al. 2007, Liu and Lei 2008, Shi et al. 2012). Air is obviously attractive as an oxidant, but reactions are often nonselective and no generally applicable methods exist so far, despite very recent and interesting results. Air-assisted addition of Grignard reagents to olefins to yield alcohol was reported by Nobe et al. (2005). Studies showed that, in presence of pure oxygen yield was less due to much accelerated oxygenation. Recently, Cahiez et al. (2007) developed airobic Mn and Fe catalyzed homocoupling of Alkyl and arylGrignard reagent successfully and peroxo-metal active species was proposed in the mechanism.

Moncomble et al. (2009) devoloped homocoupling reaction for symmetrical biaryl synthesis using $CoBr_2$ as catalyst in presence of manganese dust as reducing agent. Allylchloride was used as an additive. Co^{I}-Co^{III} catalytic cycle was proposed. Good yields were achieved.

Zhou and Xue (2009) studied homocoupling of Grignard chlorides using manganese chloride acts as catalyst and 1,2-dichloroethane acts as oxidizing agent. Reaction conditions optimized with various parameters. Studies showed that the electronic property of the substituent on the substrate indeed influences the reaction rate and yield.

The substituent effect on rate of halogen-magnesium exchange reaction was studied by Shi et al. 2012. The results showed that as distance increases between bromine and the substituent under consideration, the effects of substituent decreases.

The studies by Felkin and Swierczewski (1975) showed that Grignard reagent can reduce the Schiff base.

The influence of the electronic and steric effects of substituents attached in the ortho, meta and para positions of substrate was discussed by Percec et al. (1995). A novel palladium-catalyzed homocoupling reaction initiated by transmetallation of palladium enolates was studied by Lei and Zhang (2002).

Shekar and Hartwid 2004 studied the homocoupling of Alkyl, allyl and arylGrignard reagent in the presence of Pt catalyst and 1,2-dichlorometane as oxidant. In their study, distinct electronic effects on reductive eliminations of symmetrical and asymmetrical bis-aryl platinum complexes was discussed.

Hashim et al. (2006) reported Ni(0) mediated Homocoupling reactions to synthesis symmetrical biaryls in presence of Zn as reducing agent. The report showed the importance of iodide ion as bridging ion between Ni and Zn in electron transfer process (Hashim et al. 2005) and stabilizes coordinatively unsaturated Ni(0) species. It showed the necessity of PPh_3 ligand in Ni-mediated homocoupling reactions.

The first example of biaryl cross-coupling utilizing unactivated aryl fluorides under phosphine free palladium conditions is reported by Dankwardt (2005). The studies showed that palladium catalysts are less reactive in the oxidative addition chemistry when compared to their nickel counterparts.

Wu et al. 2013 reported homocoupling of Grignard reagents using Fe(III) complex with NHC bidentate ligand as catalyst. In their study, lower yield of coupling yield was obtained when reaction involved *in situ* generation of Grignard reagents.

The problem encountered with the most reported homocoupling methods is two step synthetic route, where the organometallic compounds are prepared first and then in a separate reaction converted into the biaryl product. The catalytic processes with minimum steps and reduced waste are the most desirable.

A new mentality of the organic chemist is focused on the design of new tendencies and methodologies able to make the already known chemical transformations simpler, faster, cheaper, greener and in general, more efficient processes. In particular, increasing attention has been paid to the ‘green chemistry’ of these processes that reduce or eliminate the use or generation of hazardous substances (Eissen 2002). The idea of atom-economical reactions may be a useful concept in helping to promote thinking in the direction of sustainable chemistry (Mingos 2004).

1.4.1 General catalytic steps involved in homocoupling reaction

i) Oxidative addition

It is the reaction of molecule X-Y with a low valent coordinatively unsaturated metal complex M^nL_m under bond cleavage forming two new bonds. Metal increases its formal oxidation state by two units, namely, M^n is oxidized to M^{n+2} and atoms, groups of atoms or molecules are added to the metal center, thus increases the coordination number of metal center by 2.

ii) Transmetalation

Transmetalation is a type of organometallic reaction that involves the transfer of ligands from one metal to another. It has the general form of $M_1R + M_2R' \rightarrow M_1R' + M_2R$, where R and R' can be, but are not limited to an alkyl, aryl, alkynyl, allyl, halogen or pseudo-halogen group. The reaction is usually an irreversible process due to thermodynamic and kinetic reasons. Thermodynamics will favor the reaction based on the electronegativities of the metals and kinetics will favor the reaction if there are empty orbitals on both metals. There are different types of transmetalation including redox-transmetalation and redox-transmetalation/ligand exchange. During transmetalation the metal-carbon bond is activated, leading to the formation of new metal-carbon bonds.

iii) Reductive elimination

It is a unimolecular decomposition pathway and reversal of oxidative addition- the metal ion is formally reduced with elimination of ligands. It is often the last step in catalytic cycle. Reductive elimination involves loss of two ligands from cis configuration from the metal centre and their combination to form single elimination product. By reductive elimination both the coordination number and formal oxidation state of the metal M^{n+2} reduced by 2 units to generate M^{n}. The M^{n+2} is reduced to Mn and the reaction is named reductive elimination. Without reductive elimination the reaction ends as a stoichiometric one.

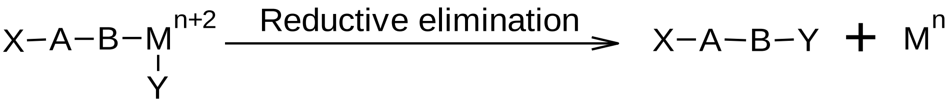

$$X-A-B-\underset{\mid \atop Y}{M}^{n+2} \xrightarrow{\text{Reductive elimination}} X-A-B-Y + M^{n}$$

The potential of transition metal homogeneous catalysis to provide a short, clean and cost-effective process is obvious. At the same time, processes that provide high yield of the desired product are also quite valuable. Therefore, cost-effective processing is becoming increasingly important. The focus of research should lie in realizing shorter synthetic routes. C-C bond formation reactions have an enormous scope for research to develop newer and highly efficient catalysts and cost effective production.

CHAPTER 2

SCOPE AND OBJECTIVES

The chapter presents the outline of the present work highlighting the main objectives.

2.1 SCOPE AND OBJECTIVES

The synthesis of biaryls is of particular interest to industry as shown by their broad application in multidisciplinary fields. The wide scope of applications of such compounds in organic synthesis demands efficient methods for their preparation. Homocoupling of Grignard reagent is one of the synthetic methods for the preparation of symmetrical biaryls.

Metal complexes play a central role in many organic transformations as versatile catalyst. Transition metal complexes with sulfur ligands, particularly dmit (2-thioxo-1,3-dithiole-4,5-dithiolate) or C_3S_5 ligands, are active catalysts in a considerable number of homogeneous reactions due to its electron density delocalization, possibility of reversible and accessible oxidation states. But these ligands are less explored for coupling reactions. Bulky groups such as phosphine ligands or chelating Schiff bases reduces the tendency of dmit ligands towards polymerization. The Schiff bases containing oxygen and nitrogen donor atoms are of great interest due to their ability to tune the electronic properties of metal center to a greater extent and thus help in enhancing the catalytic activity of metal complexes. Triphenylphosphine are important in homogeneous catalysis because of their capability of tuning both steric and electronic properties of metal complexes. Thus they can increase the catalytic activity by bringing the changes in the steps involved in catalytic cycle. It has also been seen in literature that metal complexes with Schiff base ligand blend with triphenylphosphine perform several efficient catalytic processes due to their stability, ease of preparation and structural variability. The combination of dmit, Schiff base and triphenylphosphine ligands are not used as catalysts so far and has drawn attention to do the research for the benefit of biaryl synthesis. Collectively, all these factors inspired us to incorporate dmit, Schiff bases and triphenylphosphine as ligands in the synthesis of transition metal complexes and to investigate their catalytic efficiency in the homocoupling of Grignard reagents under mild conditions. Relatively little work has been done so far on the synthesis of such metal complexes of ruthenium, palladium, cobalt, nickel and copper. The transition metal catalyzed homocoupling of Grignard reagents are the efficient tool for the synthesis of symmetrical biaryls. Arylmagnesium halides are found to be better nucleophilic partner due to its low cost, ready availability and environment benign nature. Solvent plays an important role and aprotic polar solvents found appropriate choice for the homocoupling reaction. Though, a wide range of other metal compounds has been successfully utilized to date as catalysts, the need for stoichiometric amount of organic oxidants, extra ligand or additives often hampers their general application towards industrial scale production of biaryls. These drawbacks spawned the developments of coupling procedures of alternative milder methods with utmost significance relying on the use of natural oxidant 'oxygen' as green oxidant. Though, modern methods of transition metal catalyzed oxidative homocoupling reactions are achieving high yield with good selectivity and diverse functionalities, but the reactions with reduced waste, in fewer steps, under mild reaction conditions with minimum catalyst loading - is still a challenge.

In view of the growing demand for the biaryls synthesis and based on the literature survey, the present research work is intended to synthesize Ru(III), Pd(IV), Co(III)/(II), Ni(III)/(II) and Cu(III)/(II) complexes with dmit, triphenylphosphine and Schiff base ligands. The catalytic efficiency of the synthesized complexes were examined for the homocoupling of aryl Grignard reagents using air as the oxidant at room temperature in a single step.

The objectives of this research work are as follows:

- To synthesize series of metal complexes of ruthenium, palladium, cobalt, nickel and copper containing dmit and triphenylphosphine (PPh_3) as ligands.
- To synthesize a series of Schiff base ligands from the condensation of 4-aminoantipyrine/2-aminonaphthalene-1-sulfonicacid/2-aminophenol/ with salicylaldehyde/substituted salicylaldehydes.

- To synthesize a series of metal complexes of cobalt, nickel and copper containing above synthesized Schiff base and triphenylphosphine/dmit ligands.

- To characterize the synthesized ligands and complexes by analytical, spectral (NMR, Mass, UV-Vis and FT-IR), thermal and magnetic studies.

- To use the synthesized complexes as homogeneous catalyst for the homocoupling of aryl Grignard reagents and to analyze reaction product by gas chromatographic technique.

- To study the effect of solvent, time, catalyst concentration and influence of air on the yield of coupling products.

- To study the effect of variations in the ancillary and reactive ligands on the catalytic activity.

- To investigate the mechanism involved in the coupling reaction by UV-Vis spectral analysis of the reaction mixture and hence to propose the probable mechanism.

CHAPTER 3

METHODS, SYNTHESIS AND CHARACTERIZATION

In this chapter, a brief description of the general reagents employed in this study and purification procedures adopted wherever necessary are described. It addresses the analytical and physical methods used for the characterization of ligands and complexes synthesized. The chapter details the information on the synthesis and characterization of ligands and metal complexes of Ru(III), Pd(IV), Co(II)/Co(III), Ni(II)/Ni(III) and Cu(II)/Cu(III). This chapter also includes the experimental procedures for the catalytic studies performed using the synthesized complexes.

3.1 INTRODUCTION

The dmit-Schiff base-triphenylphosphine-transition metal complexes are expected to be attractive catalysts because of their chemical and thermal stability. Considerable attention has been paid in recent years to the synthesis of these complexes because they are considered to constitute the potential application in homogeneous catalysis.

3.2 EXPERIMENTAL

3.2.1 Materials

All the chemicals used were of analytical grade. Solvents were purified and dried according to standard procedure (Vogel 1989). 4-aminoantipyrene, 2-aminonaphthalene-1-sulfonic acid, o-aminophenol, salicyladehyde, 2,4-dihydroxy-benzaldehyde, 5-nitrosalicyladehyde, 2-hydroxy-1-naphthaldehyde, $M(CH_3COO)_2$ (M = cobalt, nickel and copper), $RuCl_3.3H_2O$, $PdCl_2$, $CoCl_{2.}6H_2O$, $NiCl_{2.}6H_2O$ and $CuCl_{2.}2H_2O$ were purchased from Sigma Aldrich and were used without further purification. The metal precursors, $[MCl_2(PPh_3)_2]$ [M = Ru, Pd, Co, Ni and Cu] were synthesized as per the reported procedure (Stephenson and Wilkinson 1966, Oskooie et al. 2007, Venanzi 1958).

3.2.2 Experimental techniques

A variety of physicochemical methods were used to characterize the structure of Schiff base ligands and their metal complexes. A brief account of the methods employed is given below.

3.2.2.1 C H N S analysis

The C, H, N and S contents of the ligands and their metal complexes were determined by microanalysis using Thermoflash EA1112 series elemental analyzer.

3.2.2.2 Magnetic measurements

The magnetic susceptibilities of the complexes were carried out at room temperature on a Sherwood UK magnetic susceptibility balance using ($HgCo(NCS)_4$) as solid calibrant. The solid sample was tightly packed into a weighed sample tube to a suitable length (l) and the sample weight (m) was noted. This packed sample tube was placed into tube holder of the balance and the reading (R) was taken. The mass susceptibility, χ_g, was calculated using the formula,

$$\chi_g = [\, C_{bal} \times l \times (R - R_0)] \div [10^9 \times m]$$

where: l = the sample length (cm)

m = the sample mass (g)

R = the reading for the tube plus sample

R_0 = the empty tube reading

C_{bal} = the balance calibration constant

The molar susceptibility was calculated as, $\chi_m = \chi_g \times$ molecular formula of the complex. The molar susceptibility was then corrected with diamagnetic contribution. The effective magnetic moment, μ_{eff}, was calculated using the following expression:

$$\mu_{\mathrm{eff}} = 2.83\sqrt{\mathrm{T}} \times \mathrm{X_A}$$

where X_A is the corrected molar susceptibility.

The theoretical magnetic moments were calculated using the formula

$$\mu_{eff} = \sqrt{n(n + 2)}\ \mathrm{BM}$$

where n is the number of unpaired electrons.

3.2.2.3 NMR spectra

^{1}H NMR spectra were recorded in Bruker AMX 400 instrument using TMS as internal standard. The spectra of the ligands were recorded in $CDCl_3$ and that of the complexes were recorded in DMSO. ^{31}P NMR spectra were recorded in Bruker AMX 400 instrument in DMSO with H_3PO_4 as a reference.

3.2.2.4 Infrared Spectra

FT-IR spectra were recorded on a Thermo Nicolet Avatar FT-IR spectrometer as KBr powder in the frequency range 400-4000 cm^{-1}. The importance of FT-IR spectroscopy lies in the fact that characteristic infrared absorption of a group occurs at about the same frequency irrespective of the molecule in which the group is present.

3.2.2.5 Electronic spectra

Electronic spectra of ligands and complexes were measured on Analytikjena S-600 UV–vis spectrophotometer in the 200-800 nm range. Electronic spectral studies were carried out mainly in a structural diagnostic perspective so as to supplement any information obtained from magnetic studies.

3.2.2.6 Thermo gravimetric analysis

TG-DTA-DTG analysis of the complexes were carried out under air and nitrogen at a heating rate of 10 ºC min^{-1} using a Perkin Elmer Pyres Diamond TG/DTA analyzer. Each mass loss consideration from the TG plot can be assigned to the decomposition or volatilization of a particular group.

3.2.2.7 Mass spectra

Electron Spray Mass spectra of the complexes were recorded on a Jeol SX 102/Da-600 spectrometer.

3.2.2.8 Gas chromatography

The coupling product analysis was carried out using GC (Shimadzu 2014, Japan); the instrument has a 5% diphenyl and 95% dimethyl siloxane Restek capillary column (30 m length and 0.25 mm diameter) and a flame ionization detector (FID).

3.3 SYNTHESIS OF LIGANDS

3.3.1 Synthesis of dmit ligand (2-thioxo-1,3-dithiole-4,5-dithiolate)

The dmit ligand was synthesized *in situ* as earlier reported work with some modification (Wang et al. 2008). The dmit ligand was synthesized by the addition of CS_2 (1 mmol) to the sodium methoxide solution (10 ml). [The sodium methoxide solution was obtained by the addition of Na metal (2 mmol) in methanol (10 ml)].

3.3.2 Synthesis of 4-{[(E)-(2,4-dihydroxyphenyl)methylidene]amino}-1,5-dimethyl-2-phenyl-1,2-dihydro-3H-pyrazol-3-one (L_1)

The schiff base $\mathbf{L_1}$ was obtained by the condensation of 4-Aminoantipyrine and 2,4-dihdroxybenzaldehyde (Selvakumar et al. 2007) (Fig. 3.1). Solution of 4-Aminoantipyrine (2.03g, 10 mmol) in ethanol was added drop wise to a solution of 2,4-dihdroxybenzaldehyde (2,4-DHB) (1.38g, 10 mmol) in ethanol. The mixture was stirred at room temperature for 15 minutes and then refluxed for 4 h. The yellow colored solid product was filtered, washed with ethanol and dried in *vacuo*. Yield: 72% M.P: 234^0C

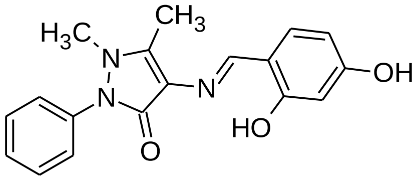

Figure 3.1 Structure of $\mathbf{L_1}$

3.3.3 Synthesis of 4-{[(E)-(2-hydroxyphenyl)methylidene]amino}-1,5-dimethyl-2-phenyl-1,2-dihydro-3H-pyrazol-3-one (L_2)

The Schiff base **L₂** (Fig 3.2) was obtained by the condensation of 4-Aminoantipyrine and salicylaldehyde (Hokelek et al. 2001). Solution of 4-Aminoantipyrine (2.03 g, 10 mmol) in ethanol was added drop wise to a solution of salicylaldehyde (1.22 g, 10 mmol) in ethanol. The mixture was stirred at room temperature for 15 minutes and then refluxed for 2 h. The yellow colored solid product was filtered, washed, recrystallized with ethanol and dried *in vacuo*.

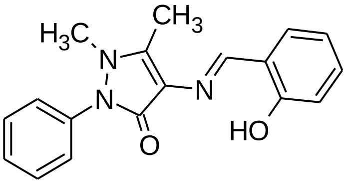

Figure 3.2 Structure of **L₂**

3.3.4 Synthesis of 4-{[(E)-(2-hydroxy-5-nitrophenyl)methylidene]amino}-1,5-dimethyl-2-phenyl-1,2-dihydro-3H-pyrazol-3-one (L₃)

The Schiff base **L₃** (Fig. 3.3) was obtained by the condensation of 4-Aminoantipyrine and 5-nitrosalicylaldehyde (Anupama and Gyana 2013). Solution of 4-Aminoantipyrine (2.03 g, 10 mmol) in ethanol was added drop wise to a solution of 5-nitrosalicylaldehyde (1.67 g, 10 mmol) in ethanol. The mixture was stirred at room temperature for 15 minutes and then refluxed for 2 h. The yellow colored solid product was filtered, washed, recrystallized with ethanol and dried *in vacuo*.

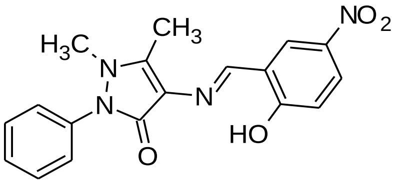

Figure 3.3 Structure of **L₃**

3.3.5 Synthesis of 4-{[(E)-(2-hydroxynaphthalen-1-yl)methylidene]amino}-1,5-dimethyl-2-phenyl-1,2-dihydro-3H-pyrazol-3-one (L₄)

The Schiff base **L₄** (Fig. 3.4) was obtained by the condensation of 4-Aminoantipyrine and 2-hydroxy-1-naphthaldehyde (Issa et al. 2005). Solution of 4-

Aminoantipyrine (2.03 g, 10 mmol) in ethanol was added drop wise to a solution of 2-hydroxy-1-naphthaldehyde (1.72 g, 10 mmol) in ethanol. The mixture was stirred at room temperature for 15 minutes and then refluxed for 2 h. The yellow colored solid product was filtered, washed, recrystallized with ethanol and dried *in vacuo*.

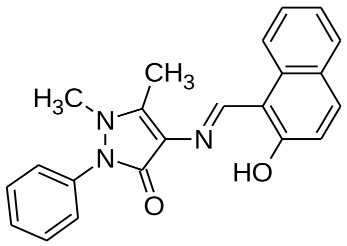

Figure 3.4 Structure of $\mathbf{L_4}$

3.3.6 Synthesis of 2-[N-(substituted 2,4-dihydroxyphenylmethylidene)]aminonapthalene-1-sufonic acid (L_5)

The ligand $\mathbf{L_5}$ (Fig. 3.5) was synthesized by the similar method described in the literature (Skorokhod et al. 2002, Asnani and Sahare 2013). A 1:1 equimolar ethanolic solution of 2-aminonaphthalene-1-sulfonic acid (1 mmol) and 2,4-dihydroxybenzaldehyde (1 mmol) were mixed and heated for 2 h. with constant stirring. The characteristic yellow precipitate obtained was filtered, washed, recrystallized from ethanol and dried *in vacuo.*

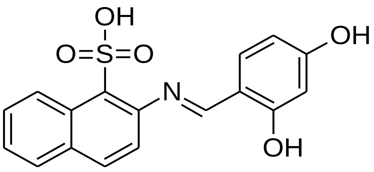

Figure 3.5 Structure of $\mathbf{L_5}$

3.3.7 Synthesis of 4-[(2-hydroxyphenylimino)methyl]benzene-1,3-diol (L_6)

The ligand $\mathbf{L_6}$ (Fig. 3.6) was synthesized according to the reported procedure (Mulazimoglu et al. 2009). The ligand was prepared by drop wise addition of a solution of the 2-aminophenol (0.1582 g, 3 mmol) in 10 mL ethanol to a stirred solution of 2,4-dihydroxybenzaldehyde (0.4144 g, 3 mmol) in 10 mL ethanol. After the addition was completed, the mixture was stirred at room temperature for 3 h. The characteristic orange colored precipitate obtained was filtered, purified by recrystallization from ethanol and dried in *vacuo.* Yield:-70-80%

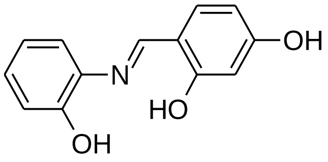

Figure 3.6 Structure of **L$_6$**

3.4 SYNTHESIS OF COMPLEXES

3.4.1 Synthesis of Ru(III), Pd(IV), Co(II), Ni(II) and Cu(III) complexes (C$_1$-C$_5$) containing dithiolato and triphenylphosphine ligands

The complexes **(C$_1$–C$_5$)** were prepared under strictly anhydrous conditions (Scheme 3.1). To a methanol (20 ml) solution containing CS_2 (0.2 ml, 3mmol) and sodium metal (0.144 g, 6 mmol) was added metal precursor $[MCl_2(PPh_3)_2]$ (M = Ru, Pd, Co, Ni and Cu) (1 mmol) with constant stirring. The mixture was refluxed for 5 h. The solid product obtained was filtered, washed with methanol, petroleum ether (60-80 ºC) and dried in *vacuo*. Yield: 60-69%

3.4.2 Synthesis of Co(II), Ni(II) and Cu(II) Complexes (C$_6$-C$_8$) containing O,N,O-Schiff base (L$_1$) and triphenylphosphine ligands

Complexes **(C$_6$-C$_8$)** were prepared under strictly anhydrous conditions (Scheme 3.2). To a methanolic solution of metal precursor $[MCl_2(PPh_3)_2]$ (M = Co, Ni and Cu) (1 mmol), **L$_1$** (1 mmol) in methanol was added drop wise with constant stirring. The mixture was refluxed for 4 h. The product obtained was filtered, washed with methanol, petroleum ether (60-80 ºC) and dried in *vacuo.* Yield: 54 -76%

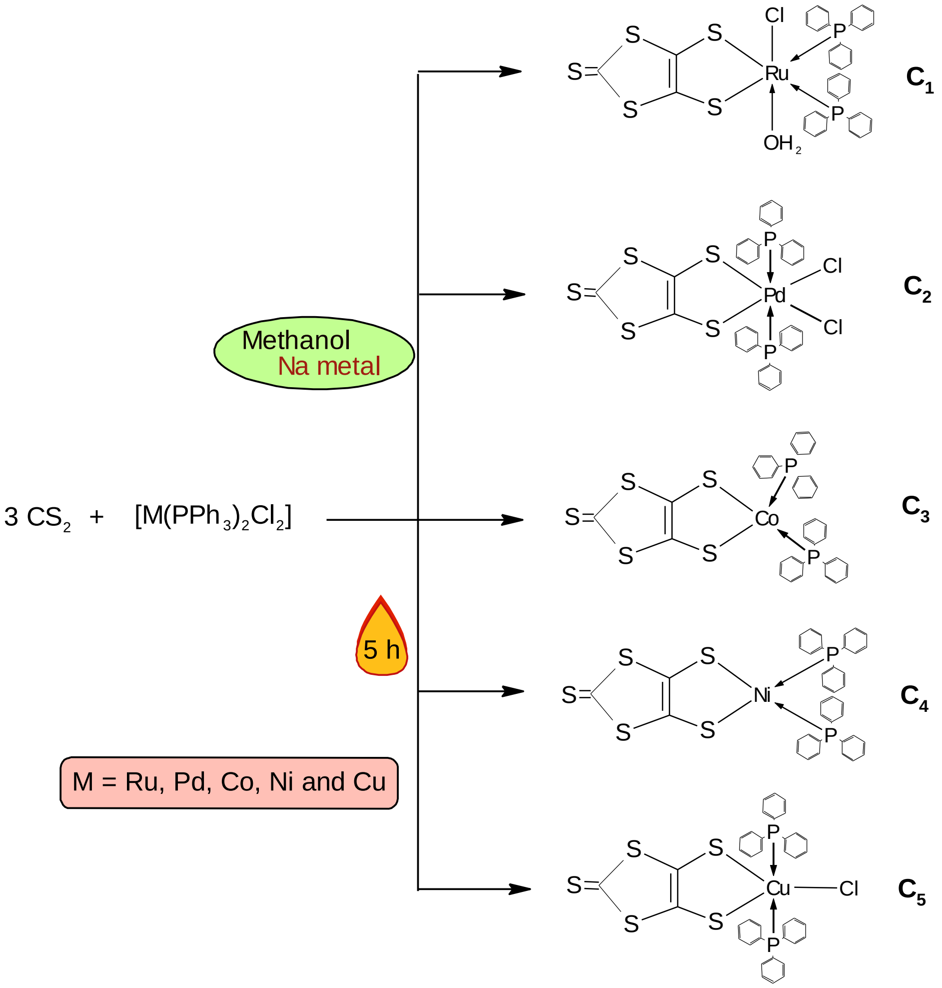

Scheme 3.1 Synthesis of $\mathbf{C_1}$-$\mathbf{C_5}$ complexes

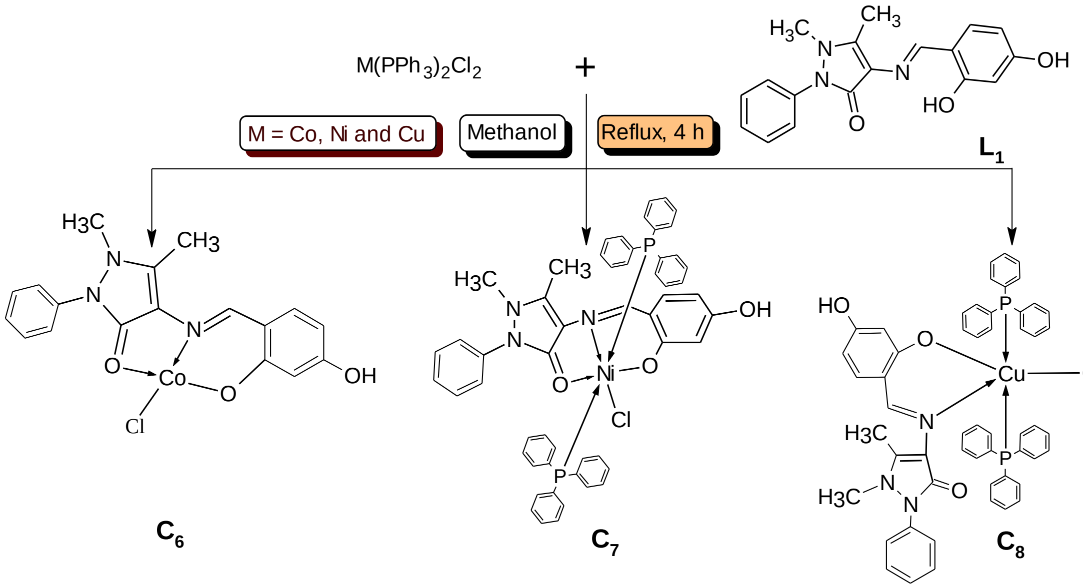

Scheme 3.2 Synthesis of $\mathbf{C_6}$-$\mathbf{C_8}$ complexes

3.4.3 Synthesis of Co(III), Ni(III) and Cu(III) Complexes (C_9-C_{11}) containing O,N,O-Schiff base (L_1) and dmit ligands

Complexes **(C_9-C_{11})** were prepared under strictly anhydrous conditions (Scheme 3.3). To a methanolic (20 ml) solution containing CS_2 (0.2 ml, 3mmol) and sodium metal, was added **L_1** (1 mmol) and metal acetate [$M(CH_3COO)_2$] (M = Co, Ni and Cu) (1 mmol) with constant stirring. The mixture was refluxed for 4 h. The solid product obtained was filtered, washed with methanol, petroleum ether (60-80 ºC) and dried in *vacuo*. Yield: 59-67%

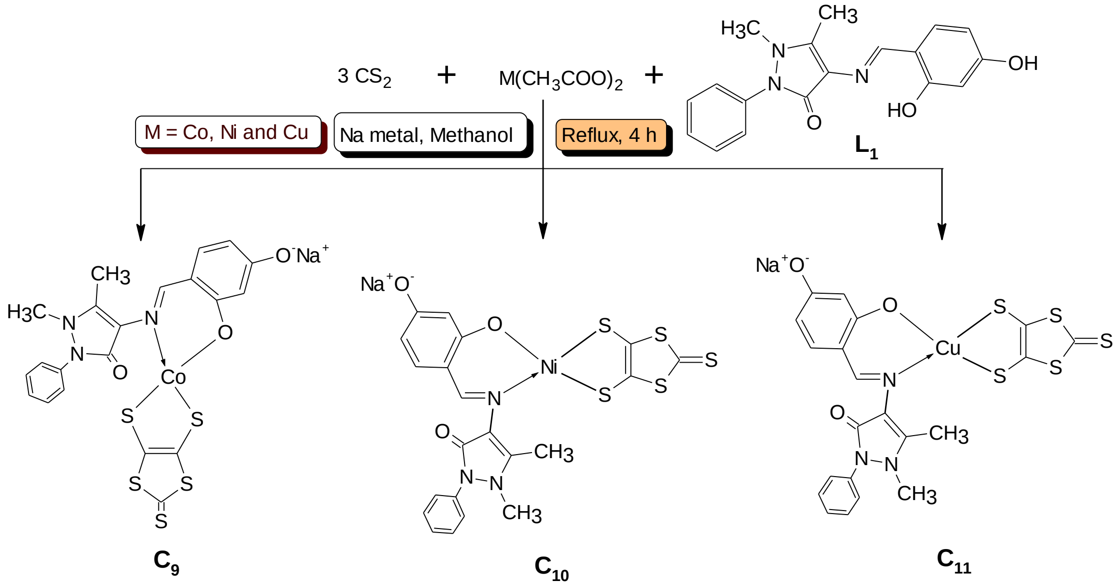

Scheme 3.3 Synthesis of **C_9-C_{11}** complexes

3.4.4 Synthesis of Ni(II) complexes (C_{12}-C_{14}) containing O,N,O-Schiff Base (L_2-L_4) and triphenylphosphine ligands

Complexes **(C_{12}-C_{14})** were prepared under strictly anhydrous conditions (Scheme 3.4). To a sodium methoxide solution of **L** (**L_2-L_4**, 1 mmol), metal precursor [$NiCl_2(PPh_3)_2$] (1 mmol) in methanol was added drop wise with constant stirring. The mixture was refluxed for 4 h. The product obtained was filtered, washed with methanol, petroleum ether (60-80 ºC) and dried in *vacuo*. Yield: 64 -73%.

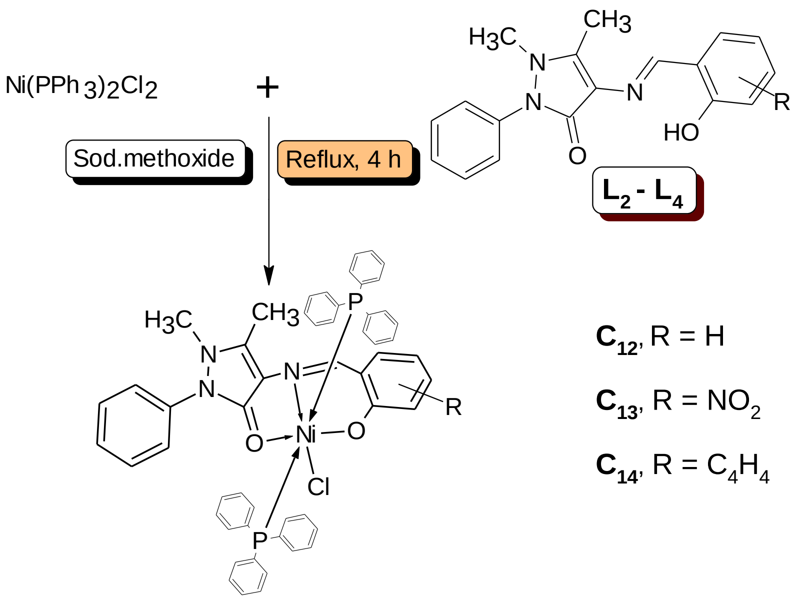

Scheme 3.4 Synthesis of **C$_{12}$-C$_{14}$** complexes

3.4.5 Synthesis of Ni(III) complexes containing O,N,O-Schiff Base (L$_2$-L$_4$) and dmit ligands

Complexes **(C$_{15}$-C$_{17}$)** were prepared under strictly anhydrous conditions (Scheme 3.5). To a methanolic (20 ml) solution containing CS_2 (0.2 ml, 3mmol) and sodium metal, was added **L** (**L$_2$-L$_4$**, 1 mmol) and metal acetate, $Ni(CH_3COO)_2$ (1 mmol) with constant stirring. The mixture was refluxed for 4 h. The solid product obtained was filtered, washed with methanol, petroleum ether (60-80 ºC) and dried in *vacuo*. Yield: 54-68%.

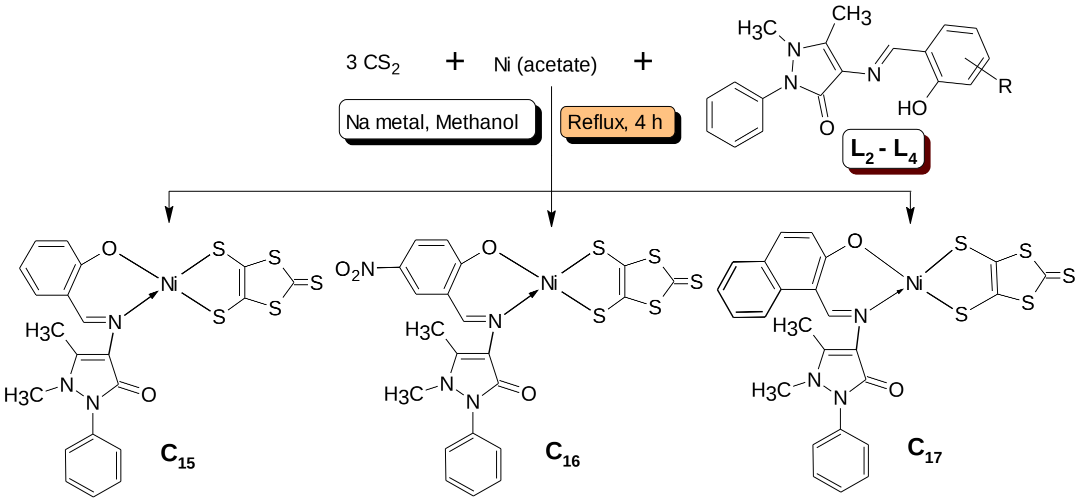

Scheme 3.5 Synthesis of **C$_{15}$-C$_{17}$** complexes

3.4.6 Synthesis of Co(II), Ni(II) and Cu(II) Complexes (C_{18}-C_{20}) containing N,O-Schiff base (L_5) and triphenylphosphine ligands

Complexes **(C_{18}-C_{20})** were prepared under strictly anhydrous conditions (Scheme 3.6). To a sodium ethoxide solution of metal precursor $[MCl_2(PPh_3)_2]$ (M = Co, Ni and Cu) (1 mmol), **L_5** (1 mmol) in ethanol was added drop wise with constant stirring. The mixture was refluxed for 4 h. The product obtained was filtered, washed with ethanol, petroleum ether (60-80 ºC) and dried in *vacuo.* Yield: 54 -76%

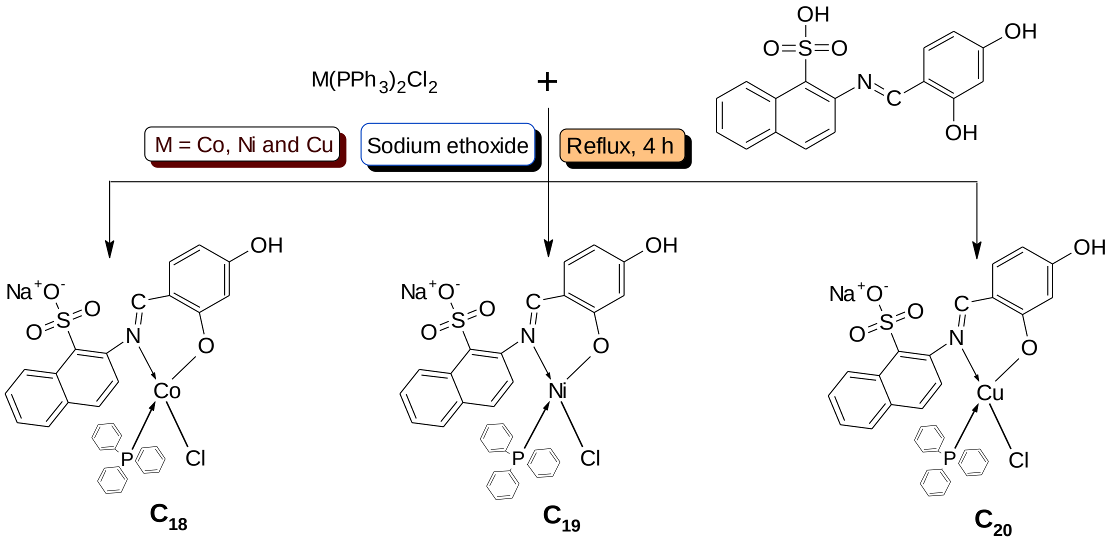

Scheme 3.6 Synthesis of **C_{18}-C_{20}** complexes

3.4.7 Synthesis of Co(II), Ni(II) and Cu(II) Complexes (C_{21}-C_{23}) containing N,O-Schiff base (L_5) and dmit ligands

Complexes **(C_{21}-C_{23})** were prepared under strictly anhydrous conditions (Scheme 3.7). To a methanolic (20 ml) solution containing CS_2 (0.2 ml, 3mmol) and sodium metal, was added **L_5** (1 mmol) and metal acetate $[M(CH_3COO)_2]$ (M = Co, Ni and Cu) (1 mmol) with constant stirring. The mixture was refluxed for 4 h. The solid product obtained was filtered, washed with methanol, petroleum ether (60-80 ºC) and dried in *vacuo*. Yield: 59-67%

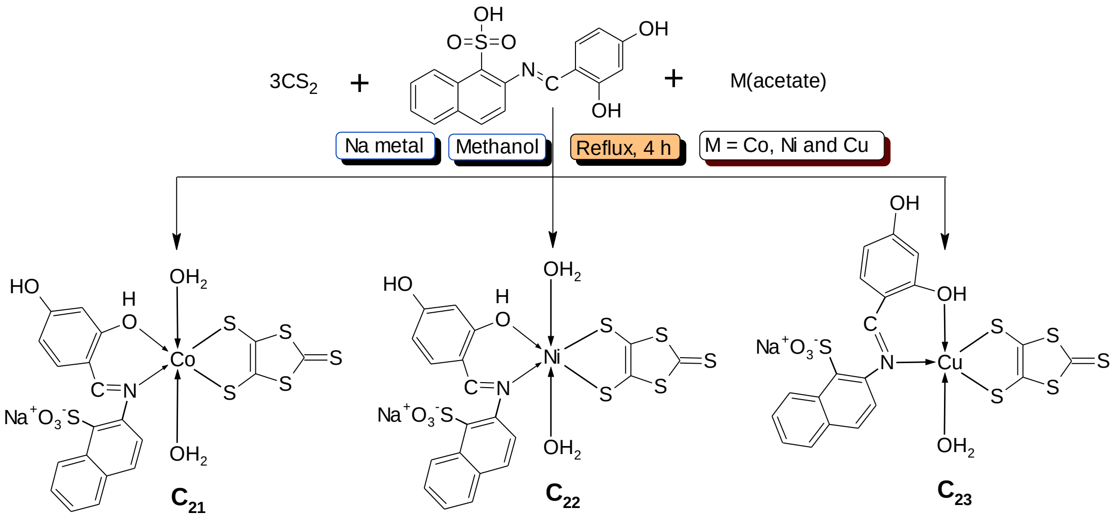

Scheme 3.7 Synthesis of $\mathbf{C_{21}}$-$\mathbf{C_{23}}$ complexes

3.4.8 Synthesis of Co(III), Ni(II) and Cu(III) Complexes ($\mathbf{C_{24}}$-$\mathbf{C_{26}}$) containing O,N,O-Schiff base ($\mathbf{L_6}$) and triphenylphosphine ligands

Complexes ($\mathbf{C_{24}}$-$\mathbf{C_{26}}$) were prepared under strictly anhydrous conditions (Scheme 3.8). To a ethanolic solution of metal precursor $[MCl_2(PPh_3)_2]$ (M = Co, Ni and Cu) (1 mmol), $\mathbf{L_6}$ (1 mmol) in ethanol was added drop wise with constant stirring. The mixture was refluxed for 4 h. The product obtained was filtered, washed with ethanol, petroleum ether (60-80 ºC) and dried in *vacuo.* Yield: 54 -76%

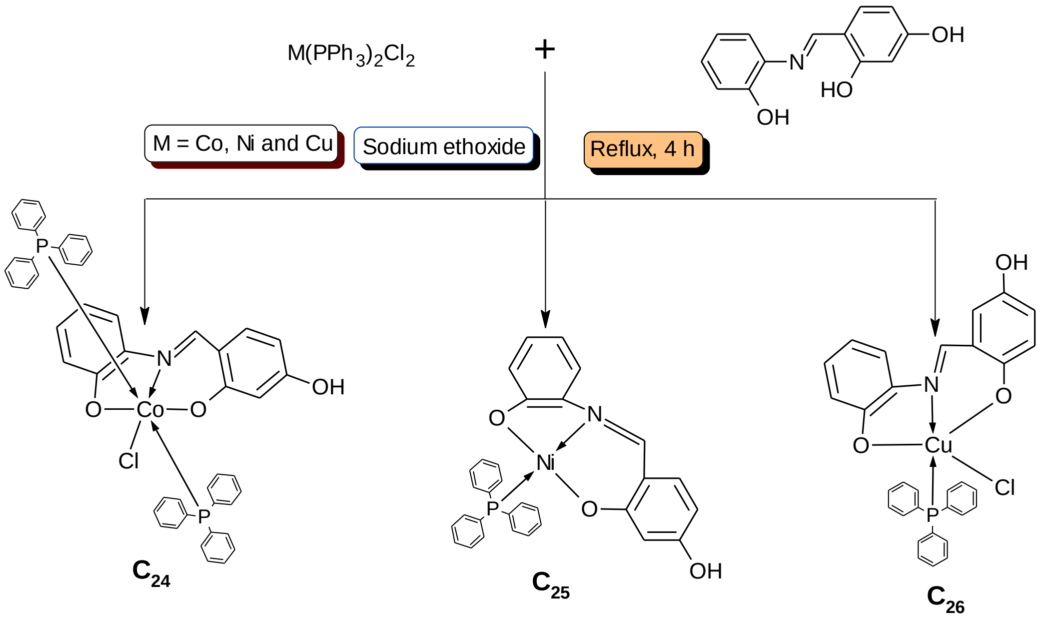

Scheme 3.8 Synthesis of $\mathbf{C_{24}}$-$\mathbf{C_{26}}$ complexes

3.4.9 Synthesis of Co(II), Ni(II) and Cu(II) Complexes (C_{27}-C_{29}) containing O,N,O-Schiff base (L_6) and dmit ligands

Complexes **(C_{27}–C_{29})** were prepared under strictly anhydrous conditions (Scheme 3.9). To a methanolic (20 ml) solution containing CS_2 (0.2 ml, 3mmol) and sodium metal, was added **L_6** (1 mmol) and metal acetate [$M(CH_3COO)_2$] (M = Co, Ni and Cu) (1 mmol) with constant stirring. The mixture was refluxed for 4 h. The solid product obtained was filtered, washed with methanol, petroleum ether (60-80 ºC) and dried in *vacuo*. Yield: 59-67%.

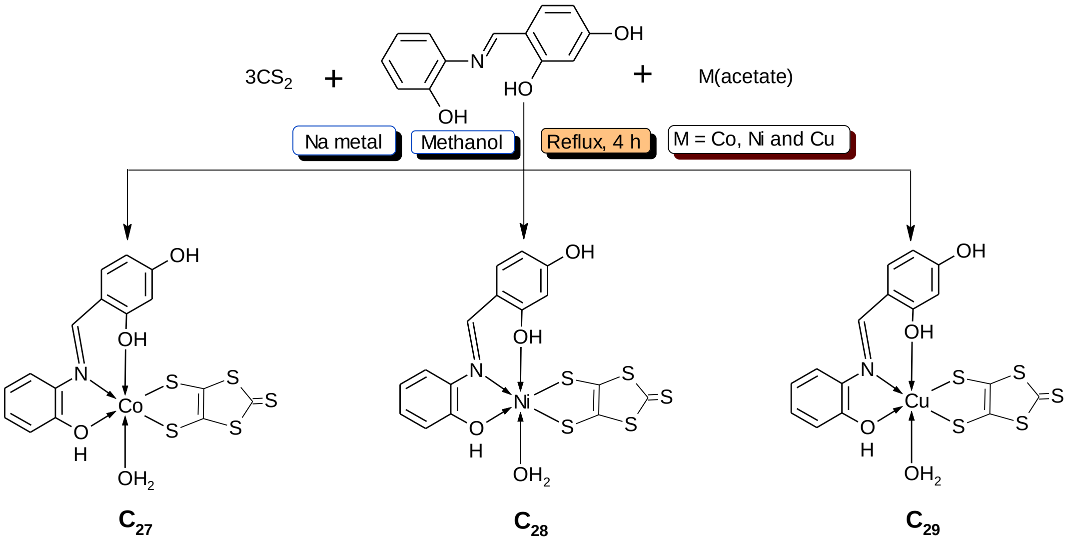

Scheme 3.9 Synthesis of **C_{27}-C_{29}** complexes

3.5 CHARACTERIZATION

3.5.1 Characterization of complexes (C_1-C_5)

Generally, dmit ligands have a tendency to form the metal bridges with geometries of variable nuclearities. This tendency towards polymerization can be reduced by introducing a bulky group into the coordination sphere. In this study, triphenylphosphine (PPh_3) metal precursors [$M(PPh_3)_2Cl_2$] were used instead of simple metal salts or metal acetate. The bulkiness of the PPh_3 lowers the degree of polymerization which is associated with its steric hindrance, justifies its selection.

The reaction of 3:1 equimolar ratios of CS_2 and the metal precursor [$M(PPh_3)_2Cl_2$] (M=Ru, Pd, Co, Ni and Cu) yielded the complexes **C_1-C_5** in moderate to good yield. The dmit ligand was synthesized *in situ*, by the addition of CS_2 in a methanol solution containing sodium metal. To this reaction mixture, metal precursor was added with constant stirring and refluxed for 5 h. The solid product obtained was filtered, washed with methanol and ether and dried in *vacuo*. Synthesized complexes were air stable, soluble in DMSO and DMF.

3.5.1.1 Physical and analytical studies

The physical properties and analytical data of the complexes **C_1-C_5** are given in the Table 3.1. The elemental analyses (C, H, S) data were in good agreement with the proposed empirical formulae of the complexes, respectively.

Table 3.1 The physical properties and analytical data of **C_1-C_5**

Compound (Colour)	Molecular formula	M.P. (°C)	Yield (%)	Elemental analysis data*		
				C	H	S
C_1 (Brown)	$C_{39}H_{32}ClOP_2RuS_5$	235	72	53.43 (53.50)	3.64 (3.68)	18.26 (18.31)
C_2 (Yellowish brown)	$C_{39}H_{30}Cl_2P_2PdS_5$	242	56	52.04 (52.15)	3.33 (3.37)	17.79 (17.85)
C_3 (Dark brown)	$C_{39}H_{30}CoP_2S_5$	345	69	60.05 (60.06)	3.85 (3.88)	20.53 (20.56)
C_4 (Dark brown)	$C_{39}H_{30}NiP_2S_5$	330	74	60.07 (60.08)	3.85 (3.88)	20.53 (20.56)
C_5 (Pale brown)	$C_{39}H_{30}ClCuP_2S_5$	295	61	57.03 (57.13)	3.65 (3.69)	19.50 (19.55)

* Found (Calculated) %

3.5.1.2 Electronic absorption and magnetic susceptibility measurement studies

The electronic absorption spectra of all the complexes **C_1-C_5** (Table 3.2, Fig. 3.7) were recorded in DMSO. Spectra showed three bands in the region 240-680 nm. In the spectra of all the complexes, the bands appearing in the region 275-416 nm are assigned to intra ligand charge transfer transitions (ILCT) (Sureshann and Bhattacharya 1998). In the spectra of **C_1** band at 418 nm can be assigned to ligand to metal charge transfer transition (LMCT) and 560-664 nm are due to the d-d forbidden transitions which are the characteristic of ruthenium(III) octahedral complex (Jayabalakrishnan et al. 2003). It was further confirmed by its magnetic moment of 1.81 BM, which showed **C_1** is one-electron paramagnetic in nature. The complex **C_2** showed LMCT at 436 nm and its diamagnetic behavior confirms the octahedral geometry. The absorption maximum at 480 nm can be assigned to the d-d transition and magnetic moment of 4.07 BM supports the tetrahedral structure for **C_3**. The characteristic absorption peak at 680 nm can be attributed to the square planar geometry of the complex **C_4** which was supported by its diamagnetism i.e $\mu_{eff} = 0$ (Salem et al. 2008). The complex **C_5** showed maximum absorption at 536 nm and can be attributed to trigonal bipyramidal for Cu(III) complex which is diamagnetic in nature (Ondrejovic et al. 2001).

Table 3.2 Electronic absorption spectral and Magnetic Susceptibility measurement results of the complexes **C_1-C_5**

Compound	λ_{max} (nm)	Assignment	μ_{eff} (BM)	Geometry
C_1	275, 358, 367, 389 418 560, 607, 664	ILCT LMCT d-d forbidden transition	1.81	Octahedral
C_2	261, 348, 364, 416 436	ILCT LMCT	diamagnetic	Octahedral
C_3	295, 340, 374, 413 480	ILCT d-d transition	4.07	Tetrahedral
C_4	281, 371, 409 478, 680	ILCT LMCT d-d forbidden transition	diamagnetic	Square planar
C_5	273, 338, 370, 411 440, 477 536	ILCT LMCT d-d transition	diamagnetic	Trigonal bipyramidal
LMCT=Ligand to Metal Charge Transfer transition. ILCT=Intra Ligand Charge Transfer transition.				

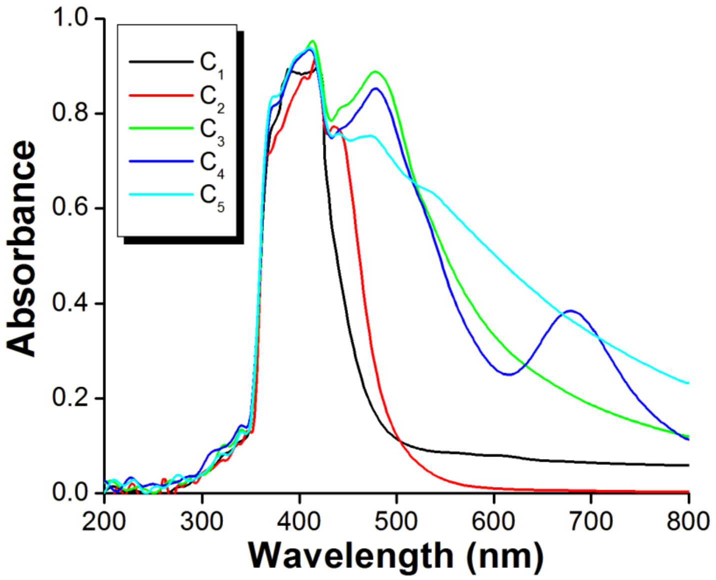

Figure 3.7 Electronic absorption spectra of the complexes **C_1-C_5**

3.5.1.3 FT-IR analysis

Selected FT-IR bands of the complexes are listed in Table 3.3. The FT-IR spectra of all the complexes **C_1-C_5** exhibit strong bands in the region 1429-1432 and 1226-1247 cm^{-1}, which can be assigned to C=C stretching vibration of dmit (Zuo et al. 1996). The bands in the regions 1021-1051 cm^{-1} and 948-996 cm^{-1} can be attributed to C=S and C-S stretching vibrations, respectively. The bands in the region 611-637 cm^{-1} can be credited to SC=CS twisting mode (Wang et al. 2008, Zinenko et al. 2003, Adams et al 2006). In the spectrum of **C_1** the band appeared around 3383 cm^{-1} is due to ν(O-H) vibration of coordinated water molecule. In addition to these modes, coordinated water exhibited $\delta_r(H_2O)$ rocking near 849 cm^{-1} and $\delta_w(H_2O)$ wagging near 533 cm^{-1} (Refat et al. 2013 and Abdel Aziz et al. 2012). The bands due to triphenylphosphine were observed in the expected region (Bhowon et al. 1999). The FT-IR spectra of complexes **C_1** is shown in Fig. 3.8.

Table 3.3 FT-IR spectral data of the complexes **C_1-C_5**

Compound	ν(C=C)	ν(C=S)	ν(C-S)	ν(SC=CS)	ν(O-H)	bands due to PPh_3
C_1	1431, 1226	1053	972	619	3383	1086, 747, 691, 511
C_2	1432	1051	993	622	-	1094, 745.5, 694, 514
C_3	1432,	1025	996	611	-	1099, 747, 689, 507
C_4	1429, 1247	1021	994	631	-	1096, 747, 685, 507
C_5	1431	1041	948	637	-	1092, 741, 692, 504

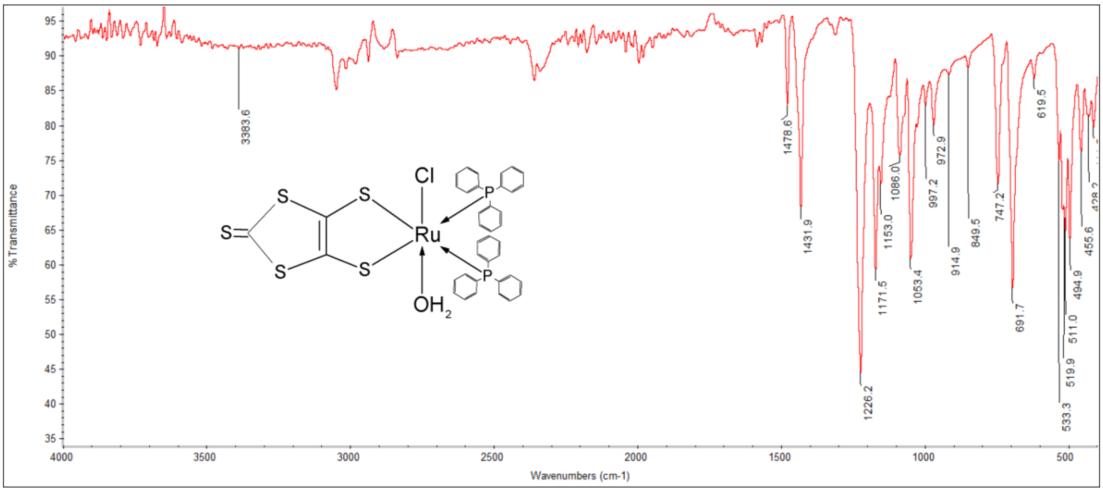

Figure 3.8 FT-IR spectrum of complex **C_1**

3.5.1.4 NMR analysis

The ^1H NMR spectra of the complexes **C_2**, **C_4** and **C_5** showed resonance at 7.08–7.8 ppm as set of multiplets which has been assigned to the aromatic protons that of coordinated triphenylphosphine groups present in the complexes. $^{31}P\{^1H\}$ NMR spectra of the complex **C_4** (Table 3.4) exhibit a sharp singlet in the range 43.33 ppm supporting the presence of the triphenylphosphine groups in *cis*-position. The complexes **C_2** and **C_5** showed at 30.02 and 26.49 ppm corresponding to trans-triphenylphosphine groups. These results indicating that the electrons are transferred from phosphorous to metal atoms to cause the P nucleus to be deshielded downfield and the chemical shifts increased in comparison with free triphenylphosphine (Schoonover et al. 1978). The ^{1}H NMR and ^{31}P{^{1}H} NMR spectra of the complex **C_4** are shown in the Fig. 3.9. and Fig. 3.10, respectively.

Table 3.4 ^{31}P NMR chemical shifts of the complexes

Complex	Chemical shift (ppm)
C_2	30.02
C_4	43.33
C_5	26.49
PPh_3	-5.75

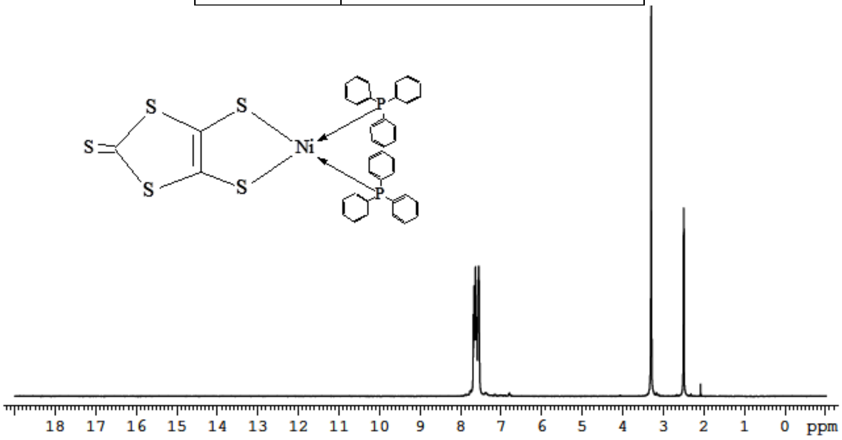

Figure 3.9 ^{1}H-NMR spectrum of complex **C_4**

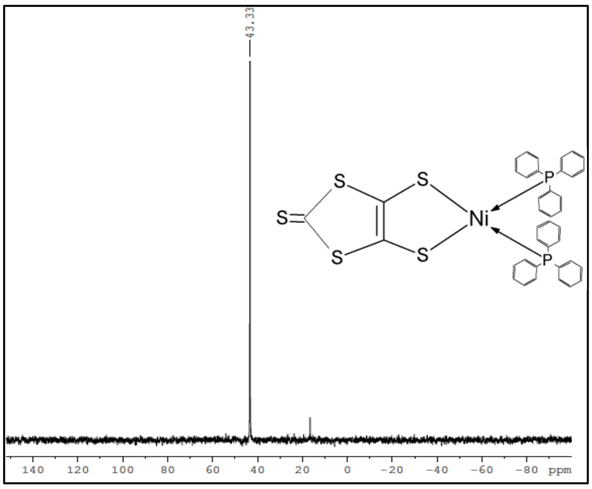

Figure 3.10 The ^{31}P{^{1}H} NMR spectrum of complex **C_4**

3.5.1.5 ESI Mass measurements

In the mass spectra of the complexes, the molecular weight of the complexes correspond to the presence of the dmit, triphenylphosphine ligands and chloride group in the synthesized complexes confirming the assumed structure. The ESI-MS spectra of the complex $\mathbf{C_1}$ is shown in the Fig. 3.11. The expected molecular weight and the observed molecular weight of the complexes are given in the Table 3.5.

Table 3.5 ESIMS data of $\mathbf{C_1}$-$\mathbf{C_5}$

Complex	Expected mass	Observed mass
$\mathbf{C_1}$	875.5	875.9
$\mathbf{C_2}$	898.2	899.3
$\mathbf{C_3}$	779.8	779.2
$\mathbf{C_4}$	779.6	779.0
$\mathbf{C_5}$	819.9	820.5

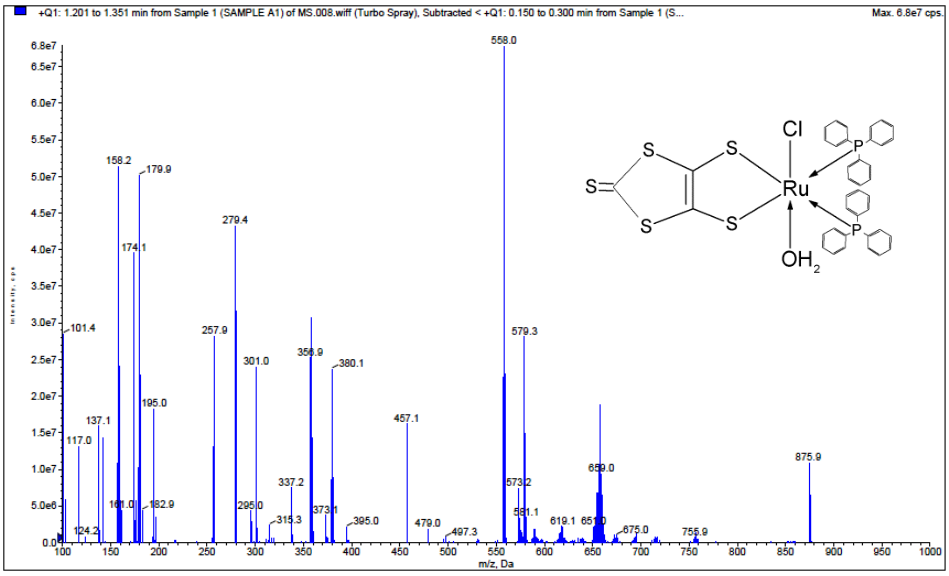

Figure 3.11 ESIMS spectrum of complex $\mathbf{C_1}$

3.5.1.6 Thermal analysis

The thermal analysis results of the complexes are represented in the Table 3.6**.** In all cases, the ligand moiety was removed first leaving the respective metal oxide as the decomposition residue. In the complexes **C_1**, **C_2** and **C_5** chloride moiety was removed first in the temperature range 171-215 °C followed by the PPh_3 and C_3S_5 moiety in the temperature range 215-401 °C. Similarly, in the complexes **C_3** and **C_4** PPh_3 molecule decomposed initially followed by C_3S_5 moiety in the mentioned temperature region. The thermal decomposition behaviors of the complexes reflected the structural information as well. The simultaneous TG-DTG curves of **C_1** is shown in the Fig. 3.12.

Table 3.6 Thermal analyses data for the complexes **C_1-C_5**

Complex	stage	TG temp. range (°C)	Removed group	TG mass loss (%)		Residue	Residue found (calcd.)%
				Found	Calcd.		
C_1	I	170-215	H_20+Cl	6.3	6.1	½(Ru_2O_3)	12.4 (14.2)
	II	215-371	2(PPh_3)+C_3S_5	77.5	82.2		
C_2	I	160-211	2(Cl)	7.9	7.8	PdO_2	17.0 (15.4)
	II	211-401	2(PPh_3)+C_3S_5	80.7	80.2		
C_3	I	198-299	2(PPh_3)	68.5	67.1	CoO	8.3 (9.6)
	II	300-465	C_3S_5	25.3	25.1		
C_4	I	203-319	2(PPh_3)	65.3	67.1	NiO	9.2 (9.5)
	II	380-536	C_3S_5	25.9	25.1		
C_5	I	179-183	Cl	5.0	4.3	½(Cu_2O_3)	11.4 (14.7)
	II	220-284	2(PPh_3)+C_3S_5	88.9	87.8		

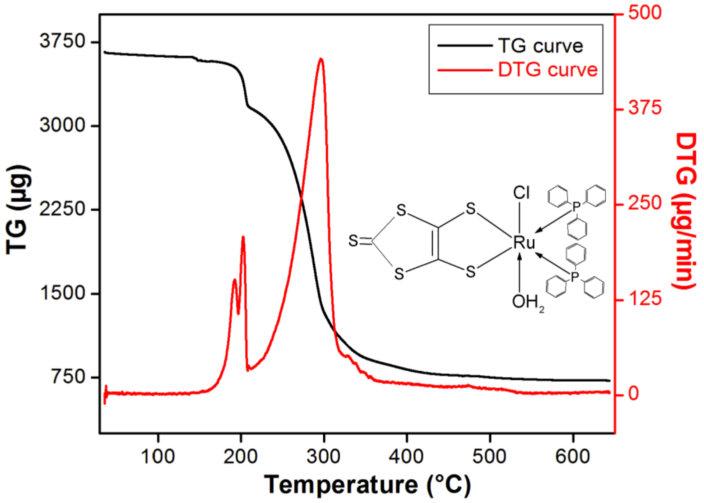

Figure 3.12 TG and DTG curve of complex **C_1**

3.5.2 Characterization of complexes (**C_6-C_{11}**)

Higher the steric requirements of the ligands lower the degree of association. This reduction in the degree of association can also be achieved by simultaneous coordination of the metal to other donor atoms, either by introduction of an additional neutral ligand or by use of chelating ligands containing other donor groups along with the thiolate sulfur atom. Hence, Schiff base containing nitrogen and oxygen as donor atoms has been selected for the complexation along with the dmit ligand. Since, Schiff bases containing -OH group close to azomethine group will act as multidentate versatile ligand and will form complexes of variable oxidation state with great structural stability, we have chosen ONO-tridentate Schiff bases for the complexation. Metal acetates were used as metal precursors for the synthesis of complexes **C_9-C_{11}**. Dithiolate free metal complexes **C_6-C_9** were synthesized from the combination of Schiff base and PPh_3 metal precursors to compare the catalytic activity with above said PPh_3 free metal complexes **C_9-C_{11}**.

All the complexes were colored and found to be air stable in solid state at room temperature and non-hygroscopic in nature. They were found to be soluble in DMSO and DMF.

3.5.2.1 Physical and analytical studies

The Physical properties and analytical data of the complexes **C_6-C_{11}** are given in the Table 3.7. The elemental analyses (C,H,N,S) data were in good agreement with the proposed empirical formulae of the ligand and complexes, respectively.

Table 3.7 The Physical properties and analytical data of **C_6-C_{11}**

Compound (Colour)	Molecular formula	M.P. (°C)	Yield (%)	Elemental analysis data*			
				C	H	N	S
L_1 (Yellow)	$C_{18}H_{17}N_3O_3$	234	72	66.85 (66.86)	5.27 (5.30)	12.98 (13.00)	-

C_6 (Orange)	$C_{18}H_{16}ClCoN_3O_3$	170	54	51.81 (51.88)	3.83 (3.87)	10.07 (10.08)	-
C_7 (Yellowish green)	$C_{54}H_{46}ClN_3NiO_3P_2$	280	65	68.84 (68.92)	4.89 (4.93)	4.42 (4.47)	-
C_8 (Light yellow)	$C_{54}H_{46}ClCuN_3O_3P_2$	240	76	68.43 (68.57)	4.85 (4.90)	4.43 (4.44)	-
C_9 (Green)	$C_{21}H_{15}CoN_3NaO_3S_5$	270	61	41.93 (42.06)	2.49 (2.52)	6.98 (7.01)	26.62 (26.74)
C_{10} (Dark green)	$C_{21}H_{15}N_3NaNiO_3S_5$	320	65	42.00 (42.08)	2.48 (2.52)	6.99 (7.01)	26.73 (26.75)
C_{11} (Dark green)	$C_{21}H_{15}CuN_3NaO_3S_5$	295	63	41.55 (41.74)	2.47 (2.50)	6.92 (6.95)	26.38 (26.53)

* Found (calculated) %

3.5.2.2 Electronic absorption and magnetic susceptibility measurement studies

The electronic absorption spectrum of **L_1** in DMSO (Fig. 3.13) displays four main bands. The bands appearing in the region of 278 nm are assigned to the π-π^* transitions of the aromatic rings. The band at 315–340 nm are due to the n-π^* transition of the C=O and C=N groups. The longer wavelength band at 390 nm can be assigned to intramolecular charge transfer transitions. The charge transfer will originate from 4-aminoantipyrine ring as an origin to the C=N group as a sink (Selvakumar et al. 2007). The electronic absorption spectra of the complexes **C_6-C_{11}** show three bands in the region 272-641 nm. In the spectra of all the complexes, the bands appearing in the region 272-411 nm can be credited to ILCT. In the spectra of **C_6** band at 416 nm corresponds to LMCT and low intense bands observed in the range of 513 nm must be due to d-d transition which confirms the presence of tetrahedral cobalt(II) complex. It is further supported by its magnetic moment of 4.13 BM, which shows **C_6** is three-electron paramagnetic in nature (Abdalrazaq et al. 2010). The complex **C_7** shows LMCT at 411 nm and d-d transition band at 511-658 nm supports its octahedral geometry, which is supported by its magnetic moment of 3.26 (Patel et al. 2007). The **C_8** shows LMCT at 414 nm. The absorption maximum at 545 nm and 641 nm are assigned to the d-d transition and magnetic moment of 1.92 BM corresponds to the trigonal bipyramidal structure of the complex **C_8** (Mishra et al. 2004). The **e**lectronic absorption spectra of the complexes **C_6-C_8** is shown in the Fig. 3.13. The spectra of the complexes **C_9**, **C_{10}** and **C_{11}** show LMCT in the range of 411-446 nm. The **C_{10}** shows the d-d transition at 479 nm. The complex **C_9** is tetrahedral and is supported by its magnetic moment value of 4.14 BM. The complex **C_{10}** and **C_{11}** are square planar in nature which is confirmed by their magnetic moment of 2.6 and diamagnetic behavior, respectively (Cukurovali et al. 2001 and Issa et al. 2005). The **e**lectronic absorption spectra of the complexes **C_9-C_{11}** are shown in the Fig. 3.14. Electronic absorption spectral results and Magnetic Susceptibility measurement data of the complexes **C_6-C_{11}** are summarized in the Table 3.8.

Table 3.8 The electronic absorption spectral results and magnetic susceptibility measurement data of the ligand and complexes **C_6-C_{11}**

Compound	λ_{max} (nm)	Assignment	μ_{eff} (BM)	Geometry
L_1	278 315, 340 390	π - π^*, Ar π - π^* of C=O and C=N CT	-	-
C_6	288, 340, 396 416 513	ILCT LMCT d-d transition	4.13	Tetrahedral
C_7	288, 334 411 511, 563, 658	ILCT LMCT d-d forbidden transition	3.26	Octahedral
C_8	305, 403 414 545, 641	ILCT LMCT d-d transition	1.92	Trigonal bipyramidal
C_9	272, 310, 351,405 415, 446	ILCT LMCT	4.14	Tetrahedral

C_{10}	292, 338, 370 411, 443 479	ILCT LMCT d-d forbidden transition	2.6	Square planar
C_{11}	275, 345, 395 416, 437	ILCT LMCT	-	Square planar
CT= Intramolecular Charge Transfer transitions ILCT=Intra Ligand Charge Transfer transitions. LMCT=Ligand to Metal Charge Transfer transitions.				

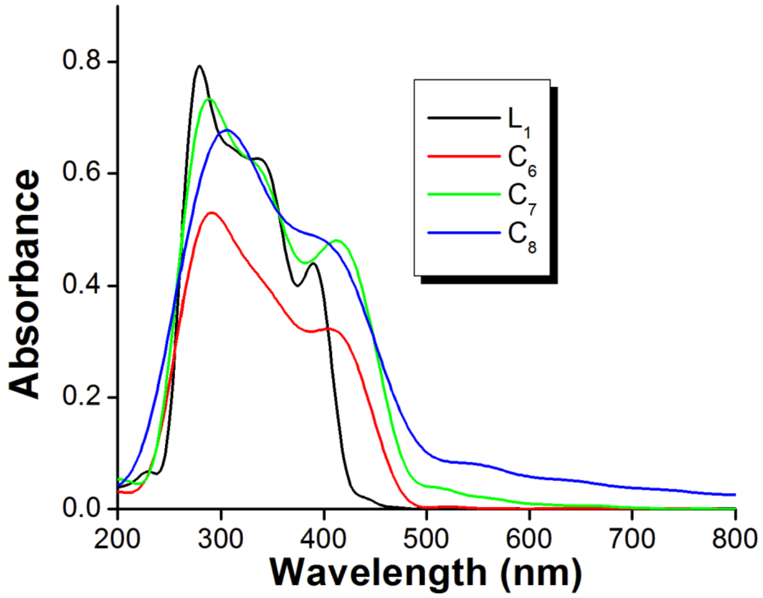

Figure 3.13 The electronic absorption spectra of the ligand **L_1** and complexes **C_6-C_8**

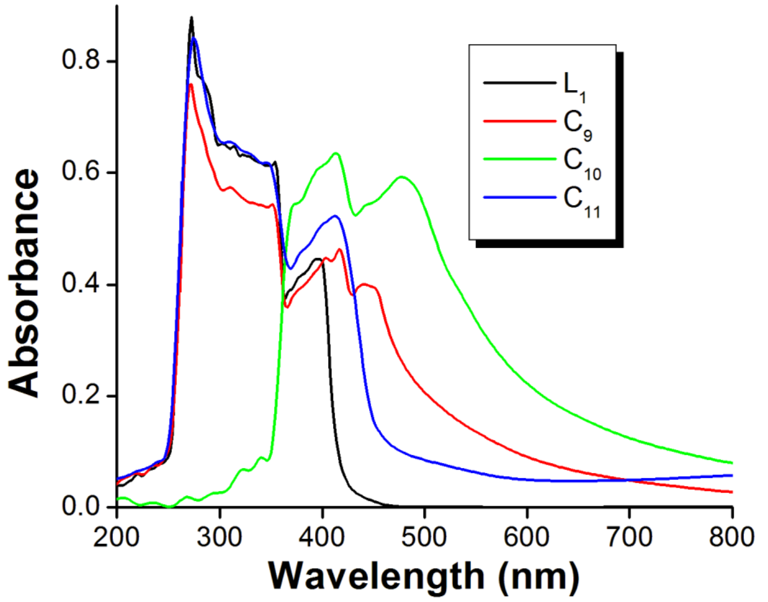

Figure 3.14 The electronic absorption spectra of the ligand **L_1** and complexes **C_9-C_{11}**

3.5.2.3 FT-IR analysis

Selected FT-IR bands of the complexes **C_6-C_{11}** are listed in Table 3.9. The FT-IR spectra of the ligand (Fig. 3.15) exhibit intense bands at 1605 and 1576 cm^{-1} corresponding to antipyrine exocyclic ketone *ν*(C=O) and azomethine *ν*(CH=N), respectively. The band in the region 1314 cm^{-1} is assigned to phenolic ν(C–O). Thus ligand is tridentate in nature with O,N,O coordination sites. Usually, the *ν*(CH=N) band occurs at an around 1600-1590 cm^{-1}, which is shifted here to lower wave number due to the contribution of the CH=N in an intramolecular hydrogen bond (Issa et al. 2005). On complexation, *ν*(CH=N) shifted to lower frequencies i.e. 1568-1525 cm^{-1} which confirms N (azomethine) coordination. In the spectra of the complexes **C_6** and **C_7**, *ν*(C=O) shifted to higher frequencies 1615-1618 cm^{-1} which confirms the involvement of antipyrine exocyclic ketonic oxygen in the complexation. There is no significant *ν*(C=O) shift in the rest of the complexes symbolizing the non-involvement of carbonyl oxygen in the complexation (Selvakumar et al. 2007). In all the complexes, phenolic ν(C–O) is shifted to higher wave number suggesting the coordination of phenolic oxygen to the metal ion (Arunachalam et al. 2009 and Nakamoto 1971). Eventhough **L_1** is tridentate in nature, it behaves as bidentate ligand in the complexes **C_8-C_{11}** by coordinating the phenolic oxygen of phenyl ring and nitrogen of the azomethine group leaving the antipyrine exocyclic ketonic oxygen free (Rosu et al. 2011, Selvakumar et al. 2007). The steric strain imposed by the methyl substitution on the antipyrine moiety restricts the ligand to bidentate coordination (Selvakumar et al. 2007). In **C_6** and **C_7**, **L_1** acts as tridentate ligand. In the complexes **C_6** and **C_7**, the bands due to triphenylphosphine were observed in the expected region (Nguyen et al. 2010). IR spectra of **C_9-C_{11}** exhibit strong bands in the region 1216-1221 cm^{-1}, which is assigned to C=C stretching vibration of dmit (Zuo et al. 1996). The bands in the regions 1022-1028 cm^{-1} and 965-990 cm^{-1} can be attributed to C=S and C-S stretching vibrations respectively (Wang et al. 2008, Zinenko et al. 2003, Adams et al 2006). The bands in the region 609-615 cm^{-1} is assigned to SC=CS twisting mode. Besides, all the complexes show bands corresponding to *ν*(M-N) and *ν*(M-O) in the region 437-451 and 516-525 cm^{-1}, respectively (Nguyen et al. 2010).

The FT-IR spectra of the complexes **L_1, C_7** and **C_{10}** are shown in the Fig. 3.15-Fig. 3.17**.**

Table 3.9 FT-IR spectral data of the ligand **L_1** and complexes **C_6-C_{11}**

Assignment (cm^{-1})	**L_1**	**C_6**	**C_7**	**C_8**	**C_9**	**C_{10}**	**C_{11}**
ν(C=O)	1605	1615	1618	1604	1600	1603	1602
ν(CH=N)	1576	1536	1538	1566	1525	1567	1568
ν(C-O)	1314	1334	1337	1319	1324	1320	1318
ν(C=C)	-	-	-	-	1216	1221	1217
ν(C=S)	-	-	-	-	1022	1022	1028
ν(C-S)	-	-	-	-	990	987	965
ν(SC=CS)	-	-	-	-	612	615	609
bands due to PPh_3	-	-	1071 749 693	1092 742 691	-	-	-

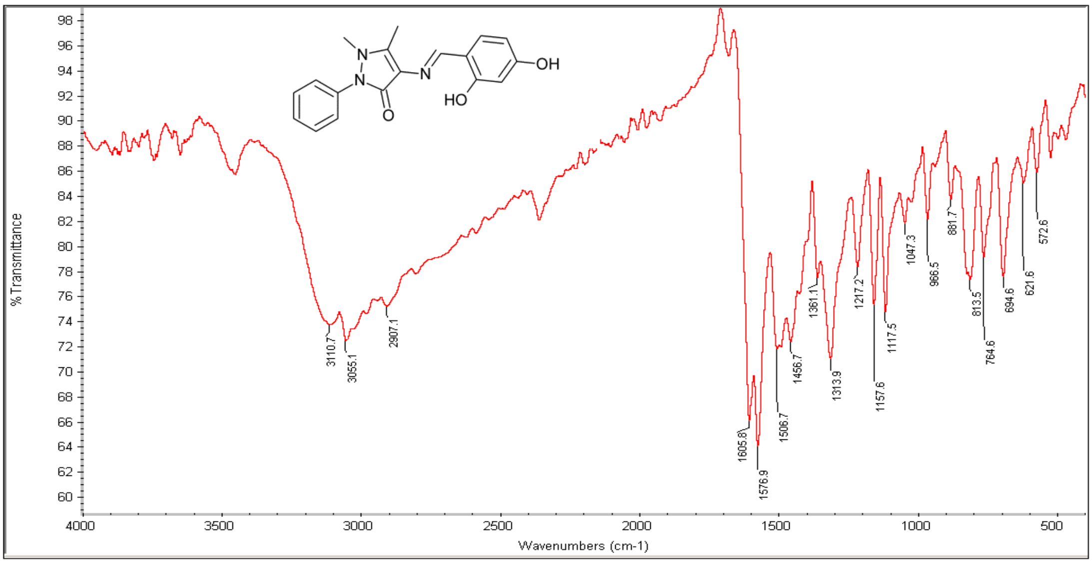

Figure 3.15 FT-IR spectrum of **L_1**

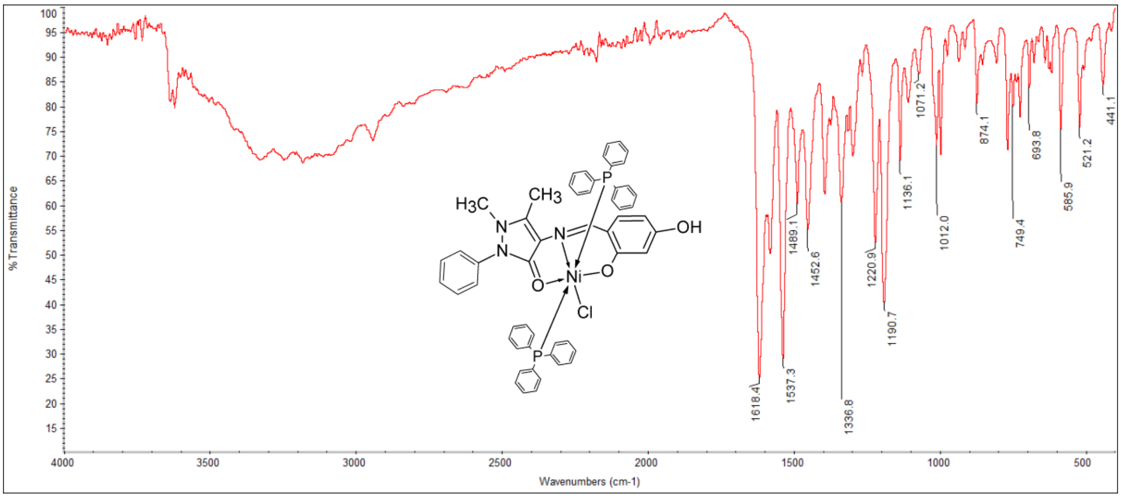

Figure 3.16 FT-IR spectrum of $\mathbf{C_7}$

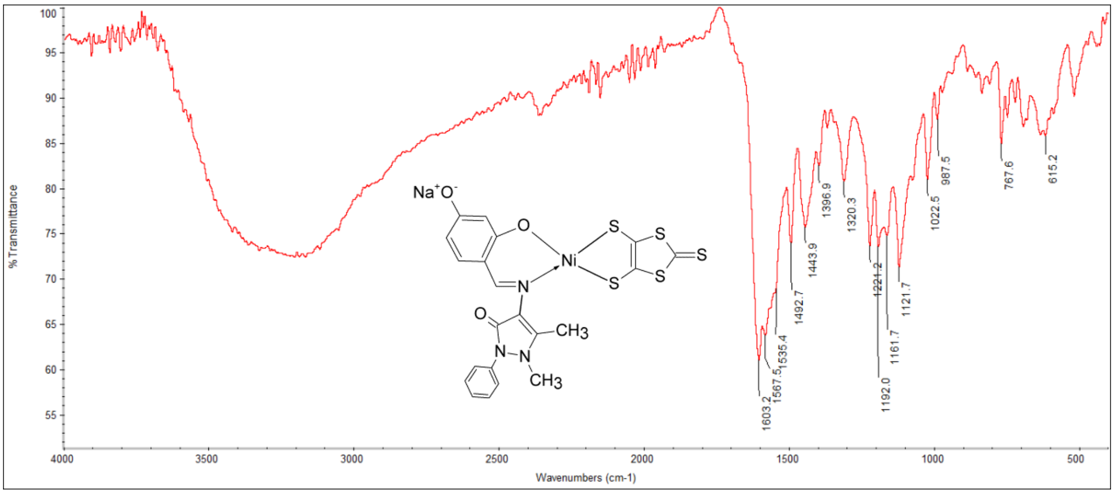

Figure 3.17 FT-IR spectrum of $\mathbf{C_{10}}$

3.5.2.4 NMR analysis

The ^{1}H NMR spectra of the ligand and the complex $\mathbf{C_{11}}$ display two sharp signals (3H) at δ 2.35-2.37 and δ 3.10-3.19 ppm corresponding to the (=C-CH_3) and N-CH_3 groups, respectively. The complex $\mathbf{C_{11}}$ show multiplets at δ 6.2-7.6 ppm due to the aromatic proton signals for the coordinated ligand. A singlet (1H) observed at 9.56 ppm in the spectra of ligand has been assigned to azomethine proton (–CH=N) (Raman et al. 2008). ^{1}H NMR spectra of the complex exhibited almost the same values for azomethine proton as that of the ligand. Although we expected a shift on the position of CH=N signal for the NMR spectra of the complex, a significant shift could not be observed. But the presence of CH=N signal with variation in peak intensity compared to that of the ligand shows that ligand coordinate to the metal ion through azomethine nitrogen (Ilhan et al. 2007). A sharp singlet (1H) appeared for *o*-OH proton of the ligand in the region δ 13.32 ppm is absent in the complex shows that the phenolic oxygen coordinates after deprotonation. The ^{1}H NMR spectra of $\mathbf{L_1}$ and $\mathbf{C_{11}}$ are given in the Fig. 3.18 and Fig. 3.19.

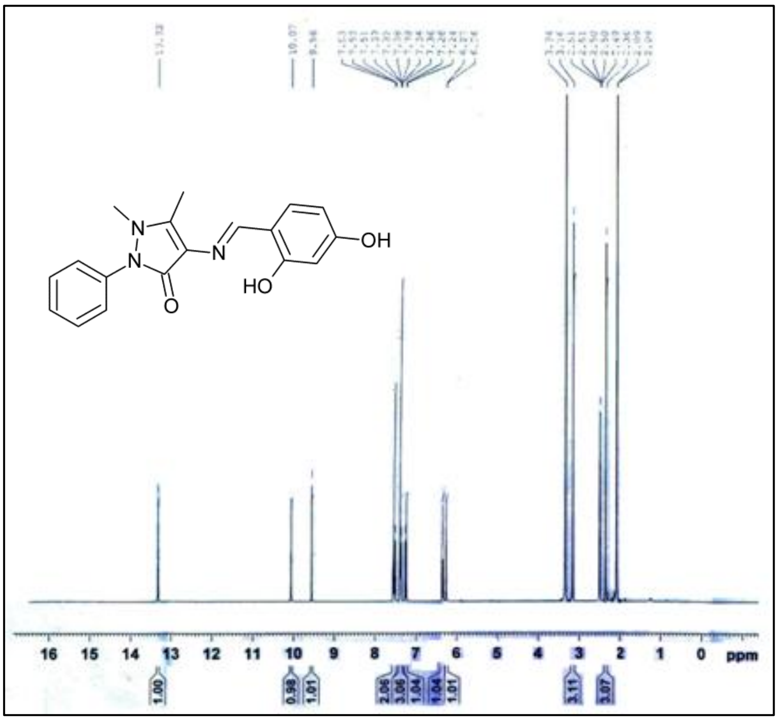

Figure 3.18 ^{1}H NMR spectrum of $\mathbf{L_1}$

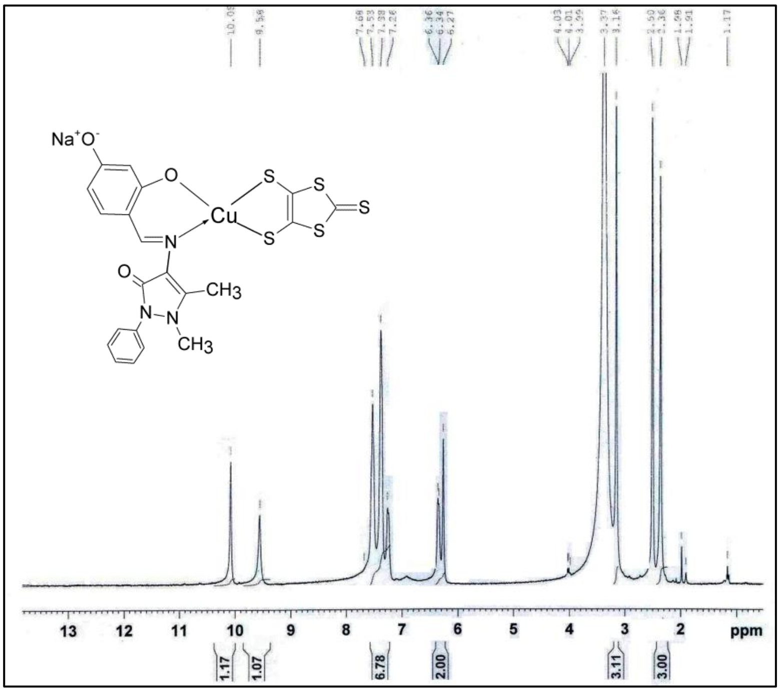

Figure 3.19 ^{1}H NMR spectrum of **C_{11}**

3.5.2.5 ESI Mass measurements

In the mass spectra of the complexes, the molecular weight of the complexes correspond to the presence of the dmit, Schiff base, triphenylphosphine ligands and chloride group in the synthesized complexes confirming the assumed structure. The ESI-MS spectra of the complex **C_{10}** is shown in the Fig. 3.20. Similarly, expected molecular weight and the observed molecular weight of the complexes are given in the Table 3.10.

Table 3.10 ESIMS data of **C_6-C_{11}**

Complex	Expected mass	Observed mass
C_6	416.7	416.9
C_7	941.1	941.4
C_8	945.9	946.9
C_9	599.6	600.9
C_{10}	599.3	600.0
C_{11}	604.2	606.4

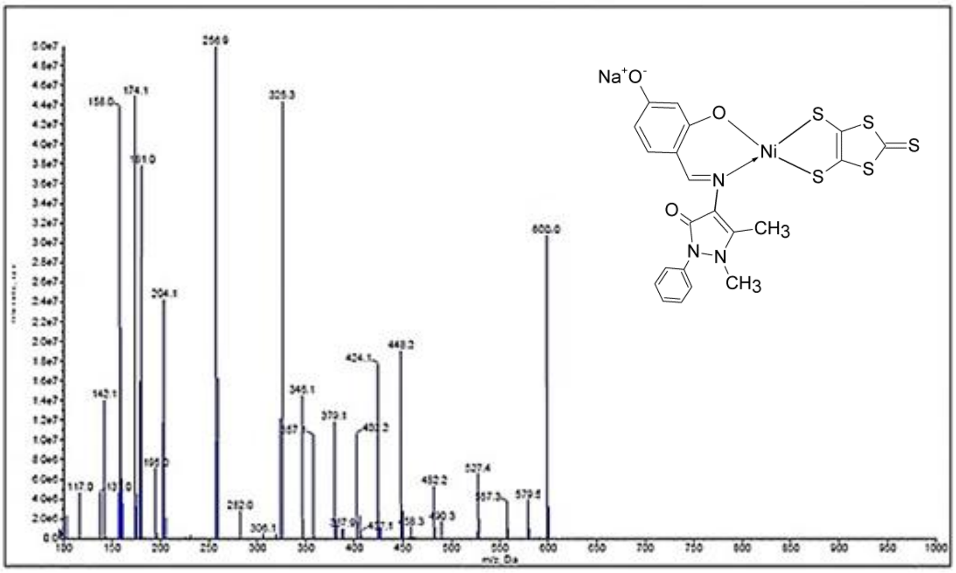

Figure 3.20 ESIMS spectrum of complex $\mathbf{C_{10}}$

3.5.2.6 Thermal analysis

The thermal analyses results of the complexes are represented in the Table 3.11. In all cases the ligand moiety is removed first leaving the respective metal oxide as the decomposition residue. In the complexes $\mathbf{C_6}$-$\mathbf{C_8}$, chloride moiety is removed in the temperature range of 195-352 °C followed by ligand and PPh_3 in the temperature range of 195-658 °C and 450-524 °C, respectively. Similarly in the complexes $\mathbf{C_9}$-$\mathbf{C_{11}}$, C_3S_5 decomposes initially in the temperature range of 182-445 °C followed by ligand moiety in the temperature range of 401-697 °C, respectively. The simultaneous TG-DTG curves of complexes $\mathbf{C_7}$ and $\mathbf{C_{10}}$ are shown in the Fig. 3.21 and Fig. 3.22, respectively.

Table 3.11 Thermal analyses data for the complexes **C_6-C_{11}**

Complex	stage	TG temp. range (°C)	Removed group	TG mass loss (%)		Residue compound	Residue found (calc.) %
				Found	Calc.		
C_6	I	222-322	Cl	08.07	08.52	CoO	16.98
	II	322-658	L	75.75	77.59		(17.98)
C_7	I	310-318	Cl	04.02	03.77	NiO	06.26
	II	335-393	L	33.90	34.36		(07.93)
	III	450-524	2 (PPh_3)	55.66	55.66		
C_8	I	195-296	L	31.86	32.90	CuO	09.80
	II	325-352	Cl	06.45	07.12		(08.09)
	III	353-479	2 (PPh_3)	50.80	53.30		
C_9	I	324-445	C_3S_5	32.32	33.93	1/2(Co_2O_3)	16.90
	II	480-511	L	57.97	55.97		(14.35)
C_{10}	I	324-395	C_3S_5	33.82	33.94	1/2(Ni_2O_3)	11.59
	II	431-462	L	56.50	56.00		(14.32)
C_{11}	I	182-373	C_3S_5	32.4	33.6	1/2(Cu_2O_3)	13.89
	II	401-697	L	53.3	55.4		(13.63)

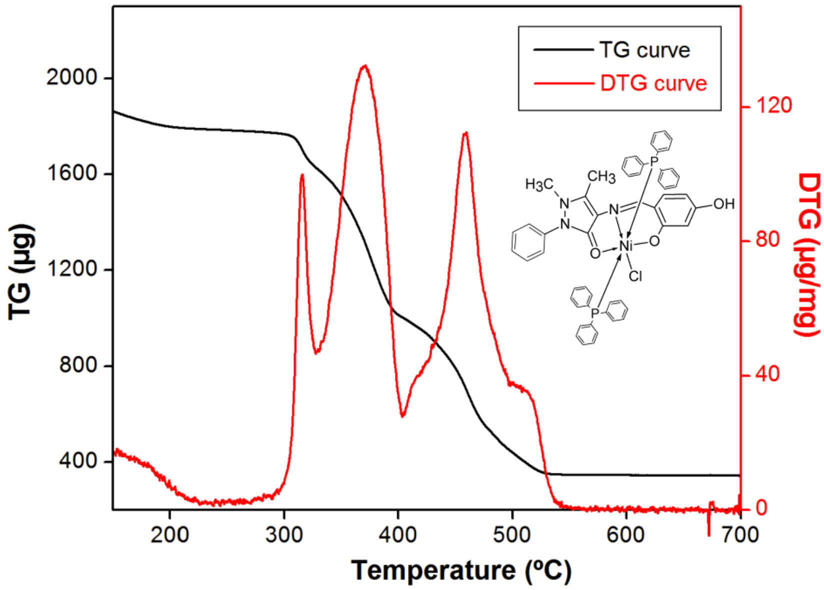

Figure 3.21 TG and DTG curve of complex $\mathbf{C_7}$

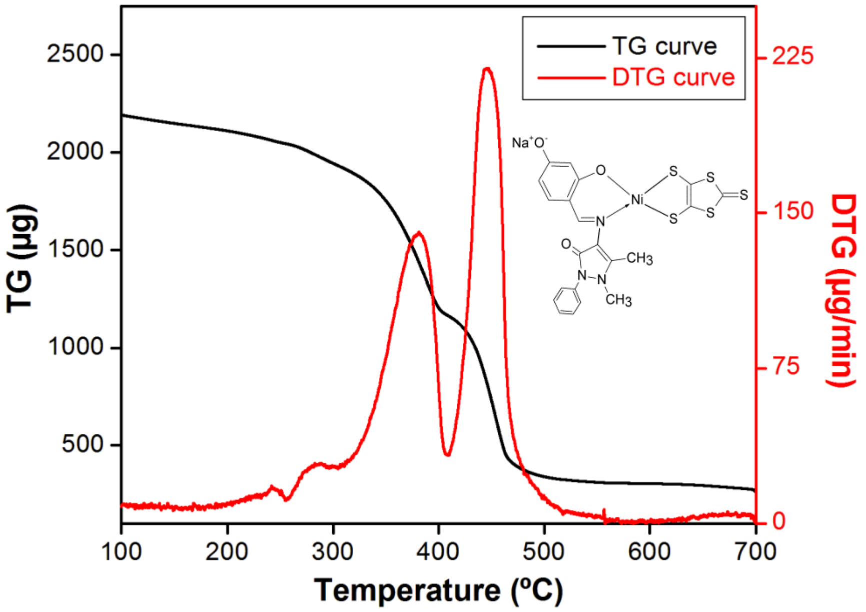

Figure 3.22 TG and DTG curve of complex $\mathbf{C_{10}}$

3.5.3 Characterization of complexes (C_{12}-C_{17})

In particular, the magnitude and character of variation in the reactivity of a coordinated substrate strongly depend on the donor-acceptor properties of ligand. As a rule, ligands possessing moderate overall α-donor/π-acceptor properties insignificantly change their reactivity upon coordination. On the other hand, the reactivity of those ligands which exhibit pronounced donor or acceptor ability should change to a considerably stronger extent upon coordination to a metal center. This has prompted us to explore the catalytic activity of nickel complexes containing Salicylaldehyde derivatised Schiff bases with the substituents of different electronic properties. The steric and electronic effects around the metal core can be fine tuned by incorporating a bulky and/or electron withdrawing or electron donating substituents in the Schiff base moiety. To compare the influence of electronic properties of the ancillary ligand on the catalytic activity, electron donating, electron withdrawing (nitro group) groups were introduced and conjugation was increased by substituting naphthyl ring in the ONO-tridentate ligand frame work.

All the complexes were colored and found to be air stable in solid state at room temperature and non-hygroscopic in nature. They were found to be soluble in DMSO and DMF.

3.5.3.1 Physical and analytical studies

The Physical properties and analytical data of the complexes **C_{12}-C_{17}** are given in the Table 3.12. The elemental analyses (C,H,N,S) data were in good agreement with the proposed empirical formulae of the ligand and complexes, respectively.

Table 3.12 The Physical properties and analytical data of **C_{12}-C_{17}**

Compound (Colour)	Molecular formula	M. P. (°C)	Yield (%)	Elemental analysis data*			
				C	H	N	S
L_2 (Yellow)	$C_{18}H_{17}N_3O_2$	234	72	69.95 (70.34)	5.50 (5.58)	13.60 (13.67)	-
L_3 (Yellow)	$C_{18}H_{16}N_4O_4$	212	68	61.20 (61.36)	4.53 (4.58)	15.86 (15.90)	
L_4 (Yellow)	$C_{22}H_{19}N_3O_2$	170	76	73.55 (73.93)	5.29 (5.36)	11.70 (11.76)	
C_{12} (Green)	$C_{54}H_{46}ClN_3NiO_2P_2$	241	64	70.04 (70.11)	4.97 (5.01)	4.53 (4.54)	-

C_{13} (Light green)	$C_{54}H_{45}ClN_4NiO_4P_2$	320	65	66.77 (66.86)	4.63 (4.68)	5.77 (5.78)	-
C_{14} (Brown)	$C_{58}H_{48}ClN_3NiO_2P_2$	240	73	71.28 (71.44)	4.91 (4.96)	4.30 (4.31)	-
C_{15} (Green)	$C_{21}H_{16}N_3NiO_2S_5$	270	68	44.89 (44.93)	2.85 (2.87)	7.48 (7.49)	28.50 (28.56)
C_{16} (Dark green)	$C_{21}H_{15}N_4NiO_4S_5$	280	54	41.48 (41.59)	2.46 (2.49)	9.21 (9.24)	26.34 (26.44)
C_{17} (Dark green)	$C_{25}H_{18}N_3NiO_2S_5$	295	63	48.98 (49.11)	2.93 (2.97)	6.85 (6.87)	26.12 (26.22)

* Found (calculated) %

3.5.3.2 Electronic absorption and magnetic susceptibility measurement studies

The electronic absorption spectrum of ligands and complexes were taken in DMSO. The spectra of the ligands display four main bands. The bands in the region of 265-280 nm are assigned to the π-π* transitions of the aromatic rings. The band at 309-357 nm involves n-π* transition of the C=O and C=N groups. The longer wavelength band at 390-402 nm can be assigned to an intramolecular charge transfer transition. The charge transfer will originate from 4-aminoantipyrine ring as an origin to the C=N group as a sink (Selvakumar et al. 2007). The electronic absorption spectra of the complexes **C_{12}-C_{17}** showed three bands in the region 283-651 nm. In the spectra of all the complexes, the bands in the region 283-358 nm are assigned to ILCT and the bands in the region 413-416 nm are assigned to LMCT. In the spectra of **C_{12}-C_{14}**, the low intense bands appearing in the range 461-651 nm must be due to d-d transitions corresponding to the presence of high spin octahedral Ni(II) complexes and are further supported by magnetic moment values 3.5, 3.7 and 3.68 BM, respectively (Patel et al. 2007). The characteristic peak at an around 474-502 nm confirms the tetrahedral geometry for the complexes **C_{15}-C_{17}**, which are supported by the magnetic moment of 2.2, 2.4 and 2.6 BM, respectively. Electronic absorption spectral results and Magnetic Susceptibility measurement data of the complexes $\mathbf{C_{12}}$-$\mathbf{C_{17}}$ are summarized in the Table 3.13. The **e**lectronic absorption spectra of the ligands and complexes $\mathbf{C_{12}}$-$\mathbf{C_{17}}$ are shown in the Fig. 3.23 and Fig. 3.24, respectively.

Table 3.13 The electronic absorption spectral results and magnetic susceptibility measurement data of the ligands $\mathbf{L_2}$-$\mathbf{L_4}$ and complexes $\mathbf{C_{12}}$-$\mathbf{C_{17}}$

Compound	λ_{max} (nm)	Assignment	μ_{eff} (BM)	Geometry
$\mathbf{L_2}$	280 315-357 390	π - π*, Ar n - π* of C=O and C=N CT	-	-
$\mathbf{L_3}$	280 309-356 402	π - π*, Ar n - π* of C=O and C=N CT	-	-
$\mathbf{L_4}$	265 320-340 388	π - π*, Ar n - π* of C=O and C=N CT	-	-
$\mathbf{C_{12}}$	285, 330, 351 415 471, 620	ILCT LMCT d-d forbidden transition	3.5	Octahedral
$\mathbf{C_{13}}$	285, 358 416 461, 651	ILCT LMCT d-d forbidden transition	3.7	Octahedral
$\mathbf{C_{14}}$	287, 353 416 477, 591	ILCT LMCT d-d forbidden transition	3.68	Octahedral
$\mathbf{C_{15}}$	288, 350 413 474	ILCT LMCT d-d forbidden transition	2.2	Square planar
$\mathbf{C_{16}}$	283, 348 415 483, 502	ILCT LMCT d-d forbidden transition	2.4	Square planar
$\mathbf{C_{17}}$	286, 347 416 485	ILCT LMCT d-d forbidden transition	2.6	Square planar
CT= Intramolecular Charge Transfer interactions ILCT=Intra Ligand Charge Transfer transition LMCT=Ligand to Metal Charge Transfer transition				

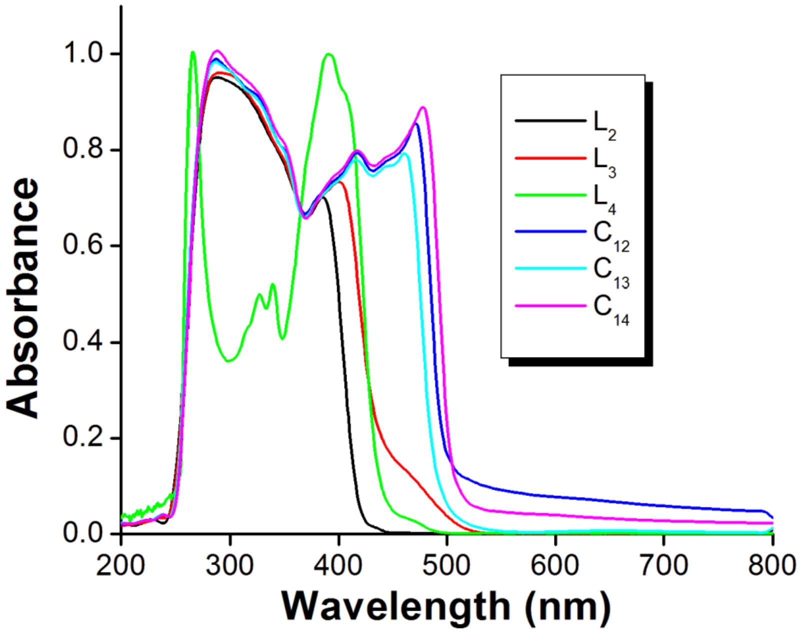

Figure 3.23 The **e**lectronic absorption spectra of the ligands and complexes **C_{12}-C_{14}**

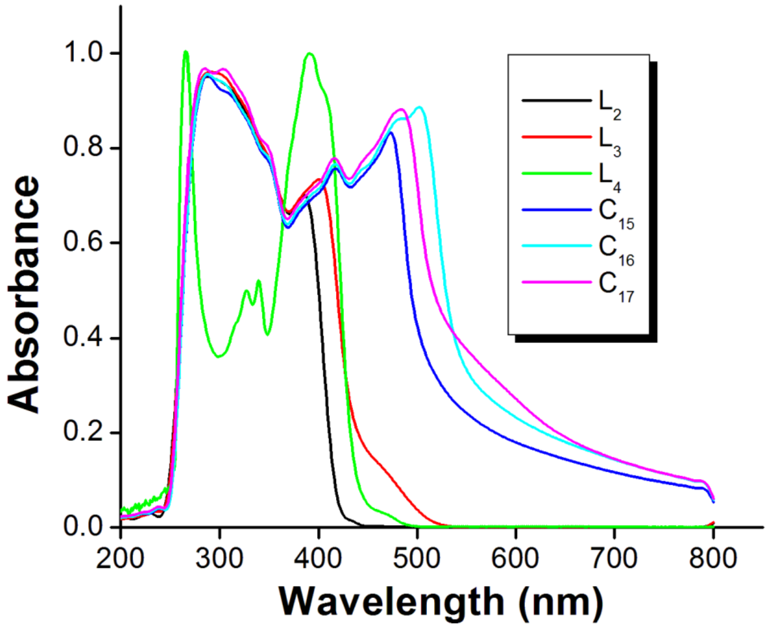

Figure 3.24 The **e**lectronic absorption spectra of the ligands and complexes **C_{15}-C_{17}**

3.5.3.3 FT-IR analysis

Selected FT-IR bands of the ligand and complexes **C_{12}-C_{17}** are listed in Table 3.14. The FT-IR spectra of the ligands exhibit intense bands at 1635-1650 and 1610-1620 cm^{-1} corresponding to antipyrine exocyclic ketone *ν*(C=O) and azomethine *ν*(CH=N), respectively. The band in the region 1285-1310 cm^{-1} is assigned to phenolic ν(C–O). Thus ligand is tridentate in nature with O,N,O coordination sites (Issa et al. 2005). In the spectra of all complexes, *ν*(CH=N) shifted to lower frequencies i.e. 1590-1604 cm^{-1} which confirms N (azomethine) coordination on complexation. In the spectra of complexes **C_{12}-C_{14}**, *ν*(C=O) shifted to lower frequencies, 1612-1621 cm^{-1} confirms the coordination through antipyrine exocyclic ketonic oxygen. There is no significant *ν*(C=O) shift in the rest of the complexes symbolizing the non-involvement of carbonyl oxygen in the coordination to the metal ion (Selvakumar et al. 2007). The ν(C–O) is shifted to higher wave number in all the complexes suggesting the coordination of phenolic oxygen to metal ion (Arunachalam et al. 2009 and Nakamoto 1971). In the complexes **C_{12}-C_{14}**, Schiff base acts as ONO-tridentate ligand and in the complexes **C_{15}-C_{17}** it binds the metal ions in a bidentate fashion through the phenolic oxygen of phenyl ring and nitrogen of the azomethine group leaving the antipyrine exocyclic ketonic oxygen free. The steric strain imposed by the methyl substitution on the antipyrine moiety restricts the ligand towards bidentate coordination from its tridentate nature. Thus, the ligands act as both tridentate and bidentate ligands with ONO and NO coordination sites, respectively. The bands due to triphenylphosphine were observed in the expected region for the complexes **C_{12}-C_{14}**, respectively (Nguyen et al. 2010). IR spectra of **C_{15}-C_{17}** exhibit strong bands in the region 1240-1249 cm^{-1}, which is assigned to C=C stretching vibration of dmit (Zuo et al. 1996). The bands in the regions 1033-1038 cm^{-1} and 993-996 cm^{-1} can be attributed to C=S and C-S stretching vibrations, respectively. The bands in the region 636-640 cm^{-1} is assigned to SC=CS twisting mode (Wang et al. 2008, Zinenko et al. 2003, Adams et al 2006). Besides, all the complexes show bands corresponding to *ν*(M-N) and *ν*(M-O) in the region 437-451 and 516-525 cm^{-1}, respectively (Nguyen et al. 2010). The FT-IR spectra of **L_2** and **C_{12}** are as shown in the Fig. 3.25-Fig. 3.26, respectively.

Table 3.14 FT-IR spectral data of the ligands and complexes **C$_{12}$-C$_{17}$**

Compound	ν(C=O)	ν(CH=N)	ν(C-O)	ν(C=C)	ν(C=S)	ν(C-S)	ν(SC=CS)	ν(PPh$_3$)
L$_2$	1650	1591	1303	-	-	-	-	-
L$_3$	1665	1620	1285	-	-	-	-	-
L$_4$	1635	1618	1310	-	-	-	-	-
C$_{12}$	1612	1580	1315	--	-	-	-	1432, 1089, 745, 688
C$_{13}$	1621	1604	1302	-	-	-	-	1072, 747, 697
C$_{14}$	1612	1590	1321	-	-	-	-	1089, 745, 693
C$_{15}$	1652	1600	1326	1245	1038	993	640	-
C$_{16}$	1664	1600	1300	1240	1033	995	641	-
C$_{17}$	1637	1601	1323	1249	1035	996	636	-

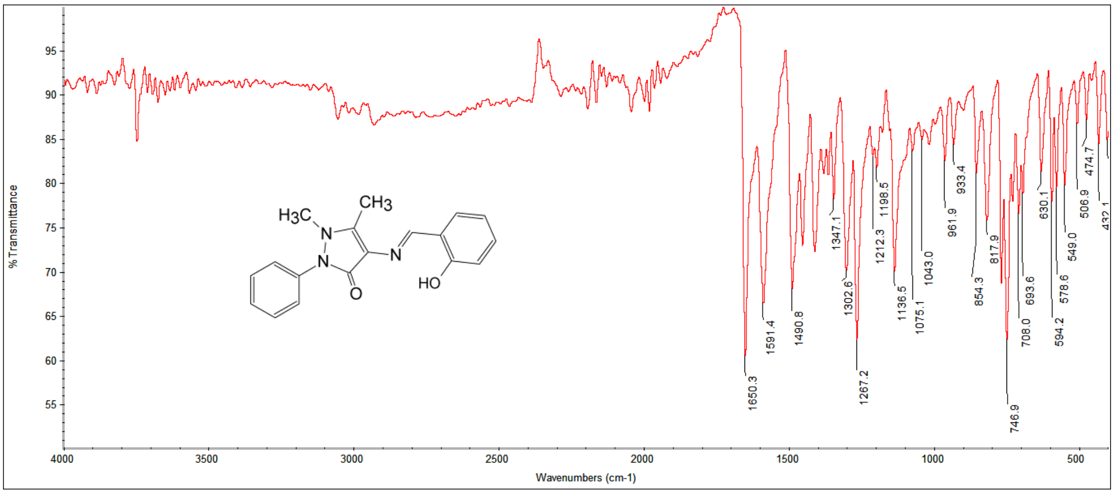

Figure 3.25 FT-IR spectrum of **L$_2$**

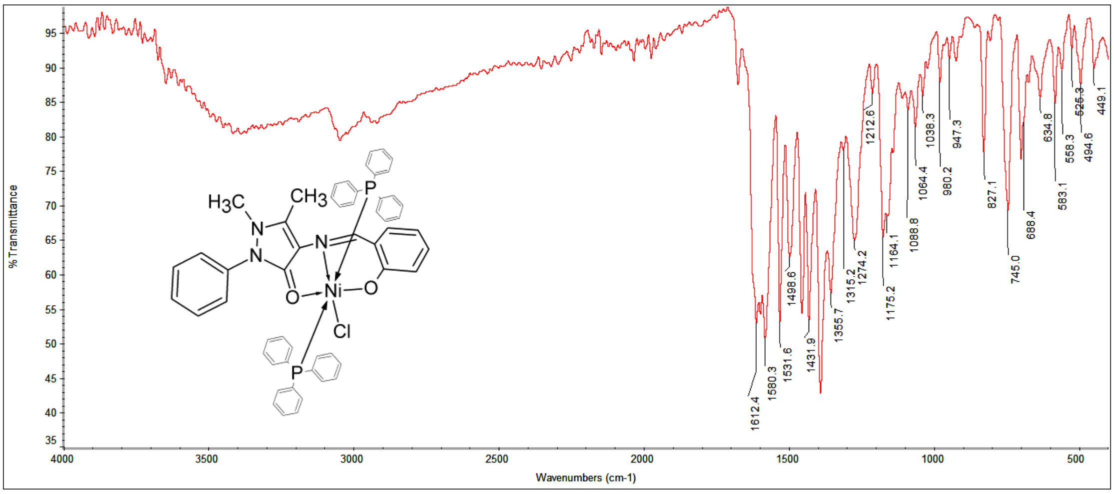

Figure 3.26 FT-IR spectrum of $\mathbf{C_{12}}$

3.5.3.4 ^{1}H NMR analysis

The ^{1}H NMR spectra of the ligands (Fig. 3.27-Fig. 3.28) display two sharp signals (3H) at δ 2.4 and δ 3.10–3.19 ppm corresponding to the (=C-CH_3) and N-CH_3 groups respectively. A singlet (1H) observed at 9.7-10.6 ppm in the spectra of ligands has been assigned to azomethine proton (–CH=N) (Raman et al. 2008). A sharp singlet (1H) appeared for *o*-OH proton of the ligand in the region δ 12-14 ppm.

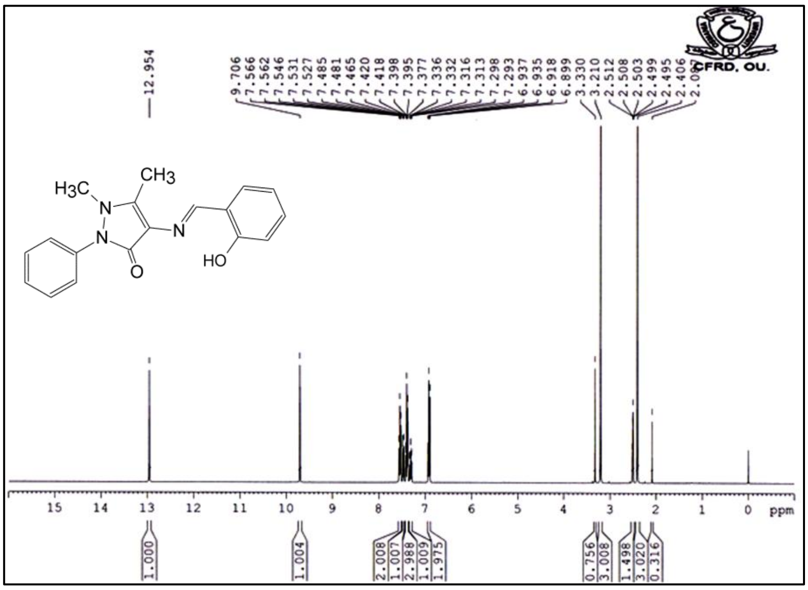

Figure 3.27 ^{1}H NMR spectrum of $\mathbf{L_2}$

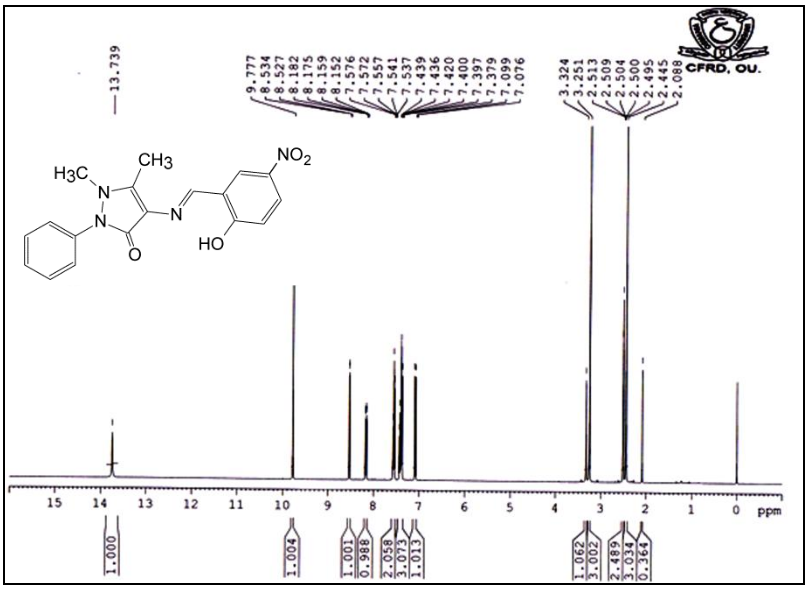

Figure 3.28 ^{1}H NMR spectrum of **L_3**

3.5.3.5 ESI Mass measurements

In the mass spectra of the complexes, the molecular weight of the complexes corresponding to the presence of the dmit, Schiff base, triphenylphosphine ligands and chloride group in the synthesized complexes confirming the assumed structure. The ESI-MS spectra of the complex **C_{12}** is shown in the Fig. 3.29. Similarly, expected molecular weight and the observed molecular weight of the complexes are given in the Table 3.15.

Table 3.15 ESIMS data of **C_{12}-C_{17}**

Complex	Expected mass	Observed mass
C_{12}	925.1	925.1
C_{13}	970.1	970.4
C_{14}	975.1	976.3
C_{15}	561.4	561.3
C_{16}	606.4	607.4
C_{17}	611.4	611.4

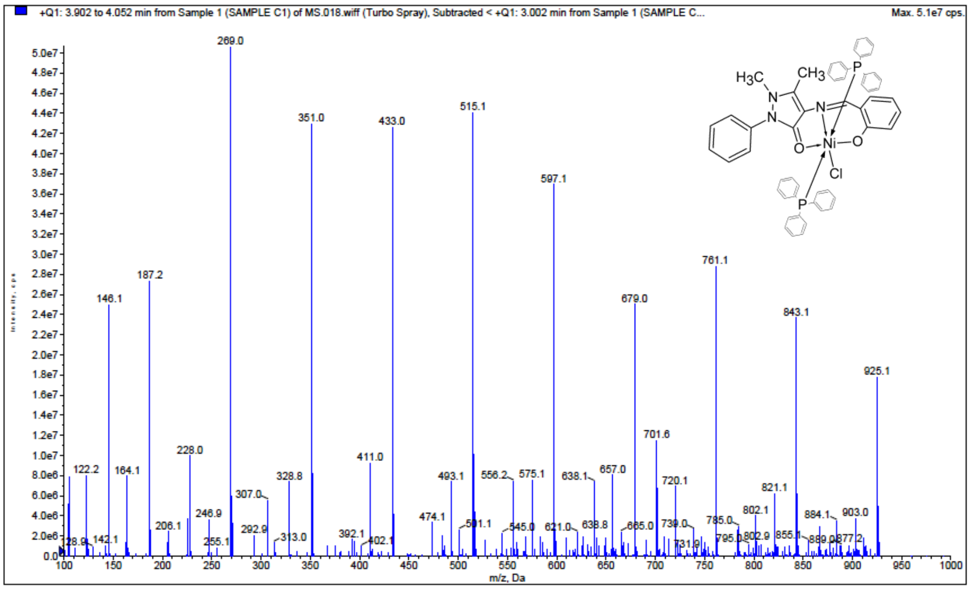

Figure 3.29 ESIMS spectrum of **C_{12}**

3.5.3.6 Thermal analysis

The thermal analyses results of these complexes are represented in the Table 3.16. In all cases the ligand moiety is removed first leaving the respective metal oxide as the decomposition residue. In the complexes **C_{12}-C_{14}**, chloride moiety is removed first in the temperature range of 171-265 °C followed by the ligand and PPh_3 in the temperature range of 218-449 °C and 388-740 °C, respectively. Similarly in the complexes **C_{15}-C_{17}**, C_3S_5 decomposes initially followed by the ligand moiety in the mentioned temperature range (Table 3.16). The thermal decomposition behaviors of these complexes reflects the structural information as well. The thermogram of **C_{12}** and **C_{15}** are as shown in the Fig. 3.30 and Fig. 3.31, respectively.

Table 3.16 Thermal analyses data for the complexes **C_{12}-C_{17}**

Complex	stage	TG temp. range (°C)	Removed group	TG mass loss (%)		Residue compound	Residue found (calc.)%
				Found	Calc.		
C_{12}	I	171-218	Cl	3.09	3.83	NiO	10.83 (8.07)
	II	218-388	L	32.01	33.11		
	III	388-689	2 (PPh_3)	53.06	56.6		
C_{13}	I	225-265	Cl	3.02	3.65	NiO	9.12 (7.69)
	II	265-398	L	34.7	36.2		
	III	398-562	2 (PPh_3)	53.1	53.9		
C_{14}	I	183-226	Cl	3.3	3.64	NiO	6.2 (7.65)
	II	290-449	L	36.8	36.5		
	III	470-740	2 (PPh_3)	55.7	53.7		
C_{15}	I	177-364	C_3S_5	32.8	34.9	1/2(Ni_2O_3)	12.9 (14.7)
	II	394-791	L	55.0	54.5		
C_{16}	I	208-468	C_3S_5	31.5	32.3	1/2(Ni_2O_3)	14.5 (13.6)
	II	468-781	L	54.0	57.9		
C_{17}	I	182-260	C_3S_5	30.9	32.1	1/2(Ni_2O_3)	11.9 (13.5)
	II	260-563	L	57.8	58.2		

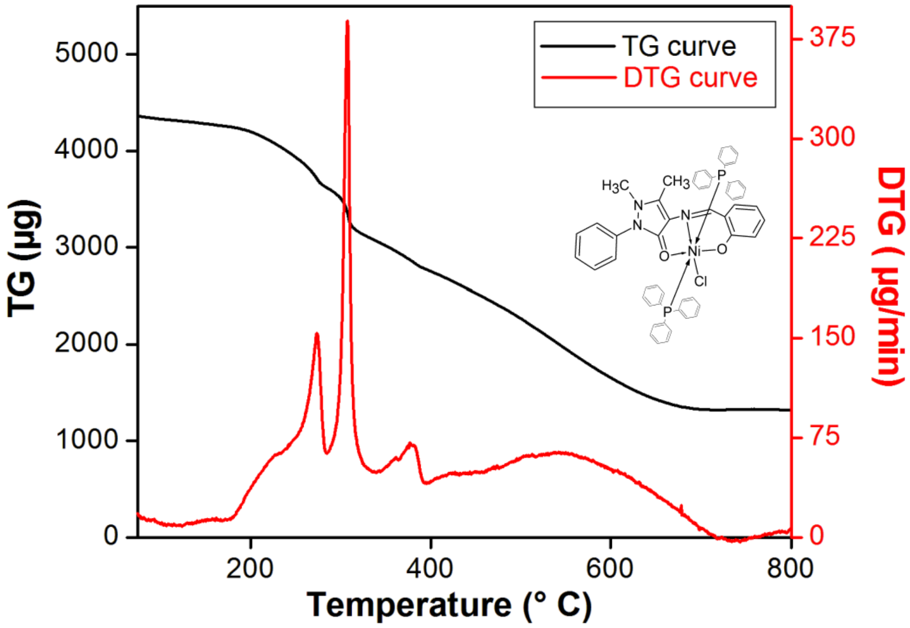

Figure 3.30 TG and DTG curve of complex $\mathbf{C_{12}}$

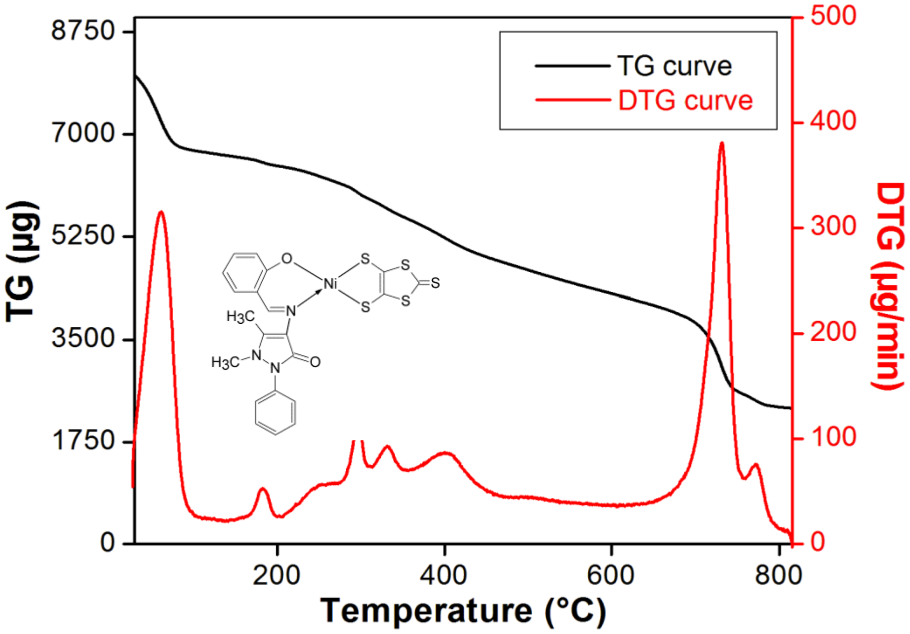

Figure 3.31 TG and DTG curve of complex $\mathbf{C_{15}}$

3.5.4 Characterization of complexes (C_{18}-C_{23})

Electronic effects lie at the heart of all reactivity. In the transition metal chemistry, the electronic properties of both the ligands ancillary to the reaction and ligands participating directly in the reaction affect rates and selectivity. Electronic properties of the ancillary ligands generally control the overall electron density of the transition metal center and can influence the catalytic activity to the considerable extent. The comparison and catalytic activity studies of the complexes due to variation in the ligand environment around metal ion was examined by selecting Salicylaldehyde derivatised ON-bidentate Schiff base for complexation with Co, Ni and Cu metals and their catalytic activity was explored for homocoupling of Grignard reagents.

All the complexes were colored and found to be air stable in solid state at room temperature and non-hygroscopic in nature. They were found to be soluble in DMSO and DMF.

3.5.4.1 Physical and analytical studies

The Physical properties and analytical data of the complexes **C_{18}-C_{23}** are given in the Table 3.17. The elemental analyses (C,H,N,S) data were in good agreement with the proposed empirical formulae of the ligand and complexes, respectively.

Table 3.17 The Physical properties and analytical data of **C_{18}-C_{23}**

Compound (Colour)	Molecular formula	M.P. (°C)	Yield (%)	Elemental analysis data *			
				C	H	N	S
L_5 (Yellow)	$C_{17}H_{12}NO_5S$	234	72	59.47 (59.64)	3.49 (3.53)	4.08 (4.09)	9.33 (9.37)
C_{18} (Brown)	$C_{35}H_{25}ClCoNNaO_5PS$	170	54	58.40 (58.39)	3.47 (3.50)	1.94 (1.95)	4.45 (4.45)
C_{19} (Parrot green)	$C_{35}H_{25}ClNNaNiO_5PS$	320	65	58.39 (58.41)	3.47 (3.50)	1.94 (1.95)	4.44 (4.46)

C_{20} (Brown)	$C_{35}H_{25}ClCuNNaO_5PS$	240	76	57.97 (58.01)	3.45 (3.48)	1.93 (1.93)	4.41 (4.43)
C_{21} (Brown)	$C_{20}H_{15}CoNNaO_7S_6$	270	61	36.56 (36.64)	2.28 (2.31)	2.13 (2.14)	29.25 (29.34)
C_{22} (Brown)	$C_{20}H_{15}NNaNiO_7S_6$	280	67	36.54 (36.65)	2.28 (2.31)	2.13 (2.14)	29.23 (29.35)
C_{23} (Dark green)	$C_{20}H_{13}CuNNaO_6S_6$	295	63	37.37 (37.40)	2.02 (2.04)	2.17 (2.18)	29.84 (29.96)

***** Found (calculated) %

3.5.4.2 Electronic absorption and magnetic susceptibility measurement studies

The electronic absorption spectrum of ligands and complexes were taken in DMSO. The spectra of ligand display three main bands. The bands in the region of 280 nm are assigned to the π - π^* transitions of the aromatic rings. The band at 312–359 nm involves n - π^* transition of the S=O and C=N groups. The electronic absorption spectra of complexes **C_{18}-C_{23}** show three bands in the region 280-697 nm. In the spectra of all the complexes, the bands in the region 280-409 nm assigned to ILCT and the bands in the region 419-422 nm assigned to LMCT. The spectra of the complexes **C_{18}-C_{20}** showed d-d transition in the range 506-697 nm which is the characteristic of tetrahedral geometry and is further confirmed by their magnetic moment values (Patel et al. 2007). The spectra of **C_{21}** showed LMCT in the region 419-456 nm and the spectra of **C_{22}** showed d-d transition in the range 481-515 nm which suggests the octahedral geometry for the complexes and the magnetic moment values for **C_{21}** and **C_{22}** is 4.26 and 3.58 BM, respectively, supports the octahedral geometry. The spectra of **C_{23}** showed d-d transition in the range of 482-562 nm and its magnetic moment value 1.65 BM, confirms trigonal bipyramidal structure. Electronic absorption spectral results (Fig. 3.32 and Fig. 3.33) and Magnetic Susceptibility measurement data of the complexes **C_{18}-C_{23}** are summarized in the Table 3.18.

Table 3.18 The electronic absorption spectral results and magnetic susceptibility measurement data of the complexes $\mathbf{C_{18}}$-$\mathbf{C_{23}}$

Compound	λ_{max} (nm)	Assignment	μ_{eff} (BM)	Geometry
$\mathbf{L_5}$	281 312-359 404	π - π*, Ar π - π* of S=O and C=N CT	-	-
$\mathbf{C_{18}}$	285, 347 414 466, 608, 681	ILCT LMCT d-d transition	4.13	Tetrahedral
$\mathbf{C_{19}}$	306, 348 411 488, 537, 688	ILCT LMCT d-d transition	2.7	Tetrahedral
$\mathbf{C_{20}}$	305 415 499	ILCT LMCT d-d transition	1.99	Tetrahedral
$\mathbf{C_{21}}$	280, 353 413, 456	ILCT LMCT	4.26	Octahedral
$\mathbf{C_{22}}$	286, 357 414, 422 481, 515	ILCT LMCT d-d forbidden transition	3.58	Octahedral
$\mathbf{C_{23}}$	275, 345 414, 420 482, 562	ILCT LMCT d-d transition	1.65	Trigonal bipyramidal
CT= Intramolecular Charge Transfer interactions ILCT=Intra Ligand Charge Transfer transition. LMCT=Ligand to Metal Charge Transfer transition.				

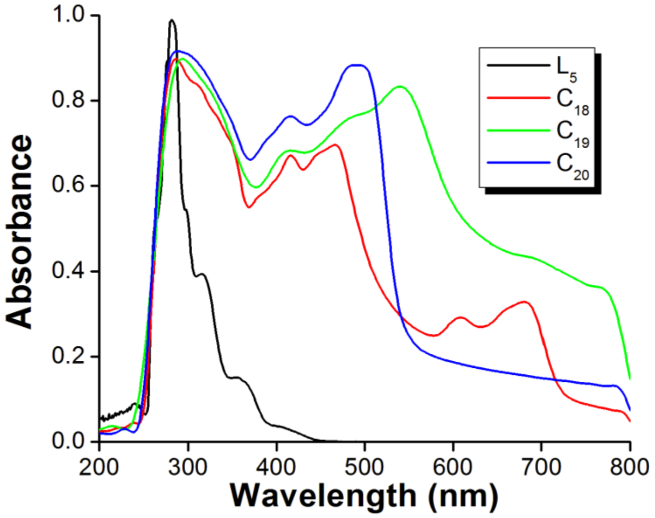

Figure 3.32 The electronic absorption spectra of $\mathbf{L_5}$ and complexes $\mathbf{C_{18}}$-$\mathbf{C_{20}}$

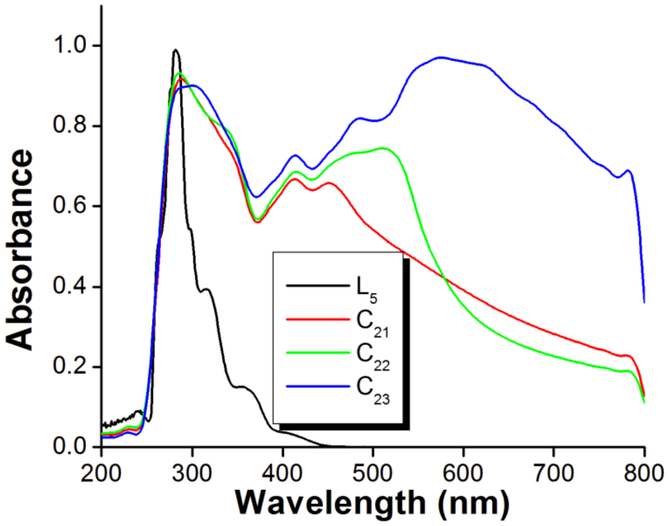

Figure 3.33 The electronic absorption spectra of **L_5** and complexes **C_{21}-C_{23}**

3.5.4.3 FT-IR analysis

Selected FT-IR bands of the ligand and complexes **C_{18}-C_{23}** are listed in Table 3.19. The FT-IR spectra of the ligand (Fig. 3.34) exhibit intense bands at 1617cm^{-1} corresponding to azomethine *ν*(CH=N). The band in the region 1247 cm^{-1} is assigned to phenolic ν(C–O). Thus ligand is bidentate in nature with N,O coordination sites (Issa et al. 2005). In the spectra of the complexes, *ν*(CH=N) shifted to lower frequencies i.e. 1594-1609 cm^{-1} which confirms N (azomethine) coordination on complexation. The ν(C–O) is shifted to lower wave number in all the complexes suggesting the coordination of phenolic oxygen to metal ion (Arunachalam et al. 2009 and Nakamoto 1971). Thus the ligand binds the metal ions in a bidentate fashion through the phenolic oxygen of phenyl ring and nitrogen of the azomethine group. The bands due to triphenylphosphine were observed in the expected region for the complexes **C_{18}-C_{20}** respectively (Nguyen et al. 2010). The FT-IR spectra of complexes **C_{21}-C_{23}** exhibited a broad band around 3381–3299 cm^{-1}, which is assigned to water molecules, ν(OH), associated with the complexes. In addition to these modes, coordinated water exhibited $\delta_r(H_2O)$ rocking near 859-847 cm^{-1} and $\delta_w(H_2O)$ wagging near 550–526 cm^{-1} (Refat et al. 2013 and Abdel Aziz et al. 2012). The FT-IR spectra of complexes exhibit strong bands in the region 1454-1247 cm^{-1}, which is assigned to C=C stretching vibration of dmit. The bands in the regions 1018-1056 cm^{-1} and 931-1002 cm^{-1} can be attributed to C=S and C-S stretching vibrations, respectively. The bands in the region 615-617 cm^{-1} are assigned to SC=CS twisting mode (Zuo et al. 1996). Besides, all the complexes show bands corresponding to *ν*(M-N) and *ν*(M-O) in the region 437-451 and 516-525 cm^{-1} respectively (Nguyen et al. 2010). The FT-IR spectra of $\mathbf{C_{19}}$ and $\mathbf{C_{22}}$ are as shown in Fig. 3.35 and Fig. 3.36, respectively.

Table 3.19 FT-IR spectral data of the ligand and complexes $\mathbf{C_{18}}$-$\mathbf{C_{23}}$

Assignment (cm^{-1})	$\mathbf{L_5}$	$\mathbf{C_{18}}$	$\mathbf{C_{19}}$	$\mathbf{C_{20}}$	$\mathbf{C_{21}}$	$\mathbf{C_{22}}$	$\mathbf{C_{23}}$
ν(OH)	3060	-	-	-	3381	3299	3313
ν(CH=N)	1616	1594	1594	1606	1605	1609	1606
ν(C-O)	1241	1213	1209	1215	1220	1220	1200
ν(C=C)	-	-	-	-	1454, 1247	1427	1428
ν(C=S)	-	-	-	-	1056, 1018	1047	1051
ν(C-S)	-	-	-	-	994	982, 931	954, 1002
ν(SC=CS)	-	-	-	-	617	615	615
$\delta_r(H_2O)$					847	856	859
$\delta_w(H_2O)$					526	541	550
bands due to PPh_3	-	1083 746 682	1085 745 683	1094 742 691	-	-	-

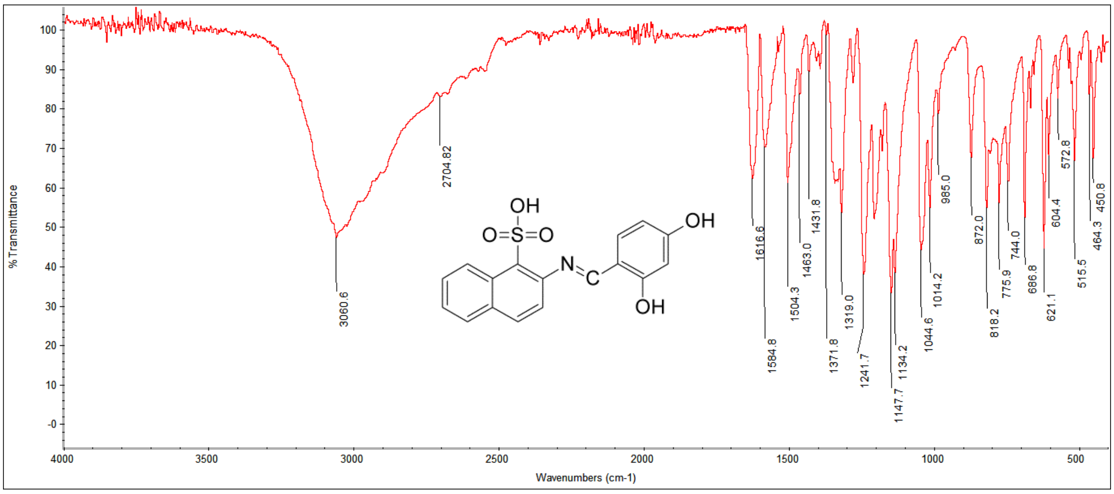

Figure 3.34 FT-IR spectrum of $\mathbf{L_5}$

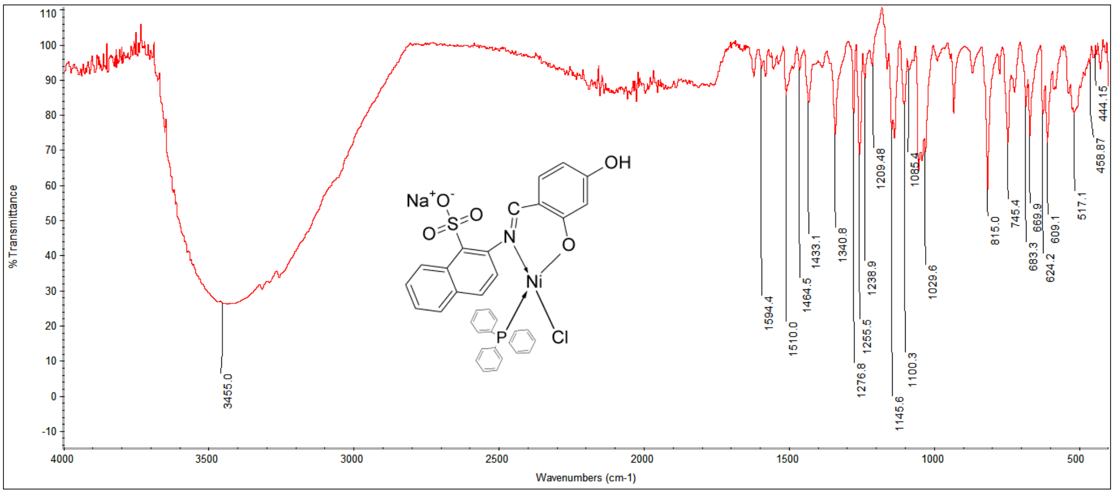

Figure 3.35 FT-IR spectrum of $\mathbf{C_{19}}$

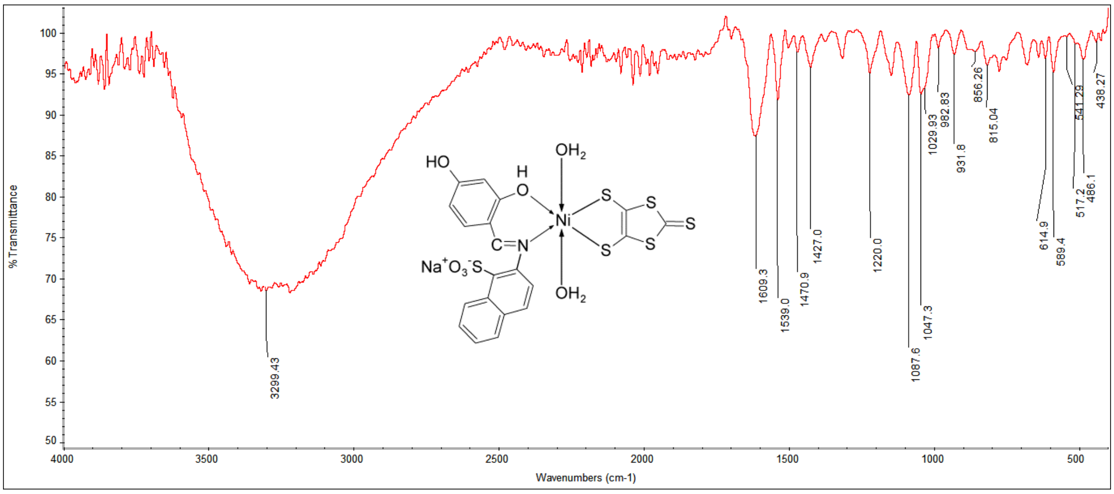

Figure 3.36 FT-IR spectrum of $\mathbf{C_{22}}$

3.5.4.4 NMR analysis

The ^{1}H NMR spectra of the ligand (Fig. 3.37) show multiplets at δ 7.25-8.08 ppm due to the aromatic proton signals. A singlet (1H) observed at 8.18 ppm in the spectra of ligand has been assigned to azomethine proton (–CH=N) (Raman et al. 2008). A sharp singlet (1H) appeared for *o*-OH proton of the ligand in the region δ 15 ppm.

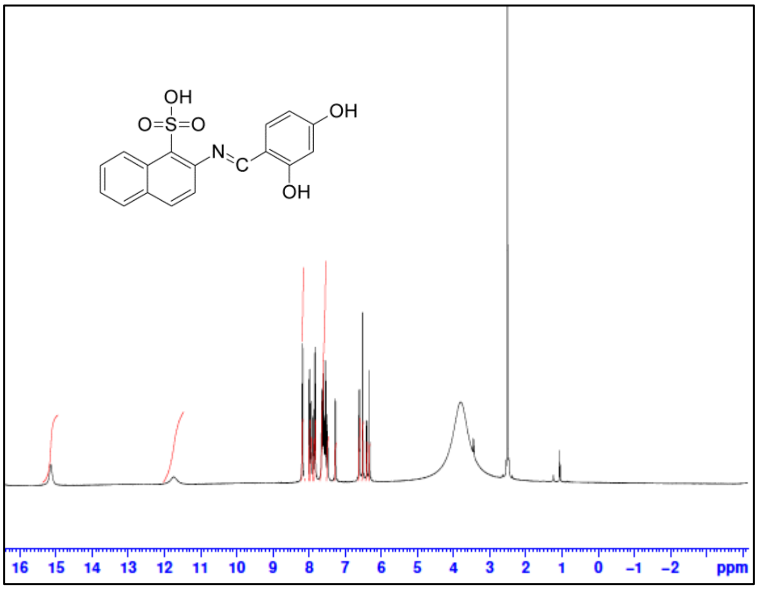

Figure 3.37 ^{1}H NMR spectrum of $\mathbf{L_5}$

3.5.4.5 ESI Mass measurements

In the mass spectra of the complexes, the molecular weight of the complexes correspond to the presence of the dmit, Schiff base, triphenylphosphine ligands and chloride group in the synthesized complexes confirming the assumed structure. The ESI-MS spectra of the complex $\mathbf{C_{22}}$ is shown in the Fig. 3.38. Similarly, expected molecular weight and the observed molecular weight of the complexes are given in the Table 3.20.

Table 3.20 ESIMS data of $\mathbf{C_{18}}$-$\mathbf{C_{23}}$

Complex	Expected mass	Observed mass
$\mathbf{C_{18}}$	719.9	719.1
$\mathbf{C_{19}}$	719.7	719.3
$\mathbf{C_{20}}$	724.6	724.4
$\mathbf{C_{21}}$	655.6	656.3
$\mathbf{C_{22}}$	655.4	656.7
$\mathbf{C_{23}}$	642.2	643.4

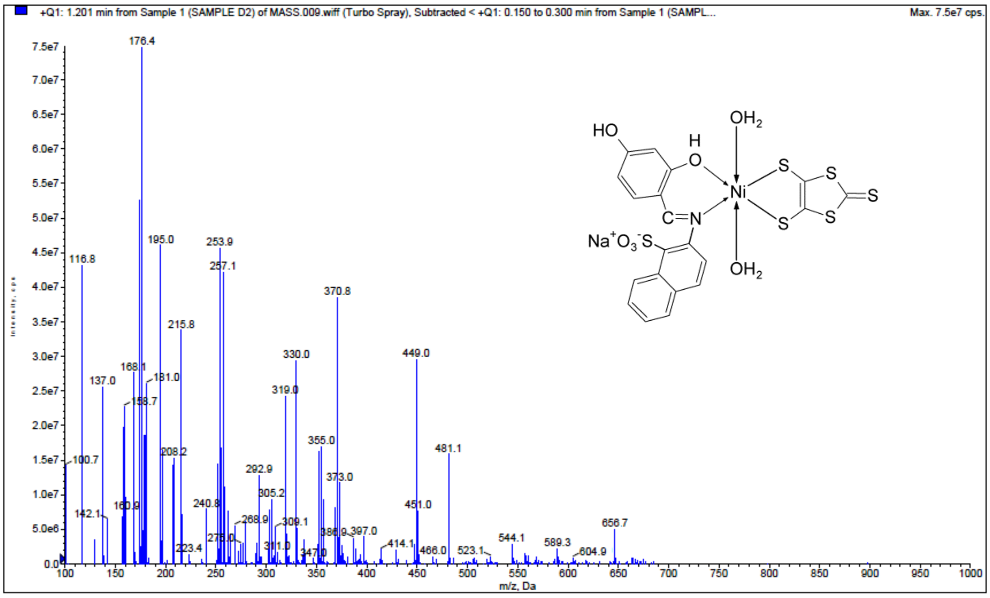

Figure 3.38 ESIMS spectrum of $\mathbf{C_{22}}$

3.5.4.6 Thermal analysis

The thermal analyses results of these complexes are represented in the Table 3.21. In all cases the ligand moiety is removed first leaving the respective metal oxide as the decomposition residue. In the complexes $\mathbf{C_{18}}$-$\mathbf{C_{20}}$, chloride and PPh_3 moiety is removed first in the temperature range 171-404 °C followed by the ligand in the temperature range 373-980 °C. Similarly in the complexes $\mathbf{C_{21}}$-$\mathbf{C_{23}}$, C_3S_5 decomposes initially followed by ligand moiety in the mentioned temperature range. The thermal decomposition behaviors of these complexes reflected the structural information as well. The thermogram of C_{19} and **C_{22}** are shown in Fig. 3.39 and Fig. 3.40, respectively.

Table 3.21 Thermal analyses data for the complexes **C_{18}-C_{23}**

Complex	stage	TG temp. range (°C)	Removed group	TG mass loss (%)		Residue compound	Residue found (calc.)%
				Found	Calc.		
C_{18}	I	166-406	Cl+L	55.4	55.5	CoO	8.1
	II	406-602	PPh_3	36.7	36.6		(10.4)
C_{19}	I	178-544	Cl+L	54.6	55.5	NiO	8.9
	II	373-718	PPh_3	36.8	36.4		(10.3)
C_{20}	I	172-313	Cl+L	54.3	55.1	CuO	9.4
	II	313-733	PPh_3	36.1	36.1		(10.9)
C_{21}	I	150-193	$2(H_2O)$	5.2	5.4	CoO	11.0 (11.3)
	II	193-440	C_3S_5	29.1	29.9		
	III	442-580	L	55.1	55.5		
C_{22}	I II	130-161	$2(H_2O)$	5.4	5.4	$NiO/(Ni_2O_3)$	10.5 (11.3)
		161-533	C_3S_5	29.4	29.8		
		533-785	L	55.2	55.4		
C_{23}	I II	150-189	H_2O	2.6	2.8	$CuO/(Cu_2O_3)$	10.8 (12.3)
		189-556	L	56.5	56.7		
		556-960	C_3S_5	30.1	30.5		

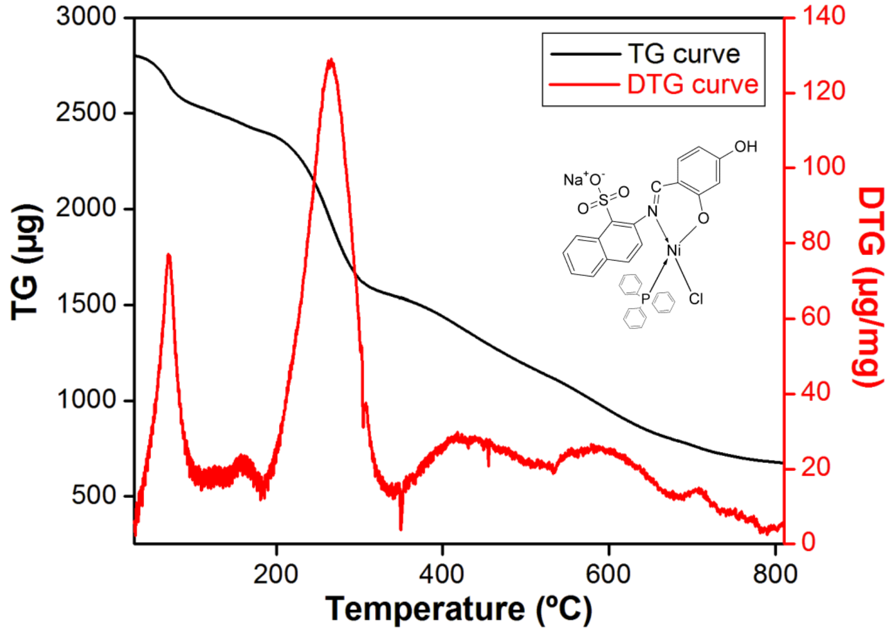

Figure 3.39 TG and DTG curve of complex $\mathbf{C_{19}}$

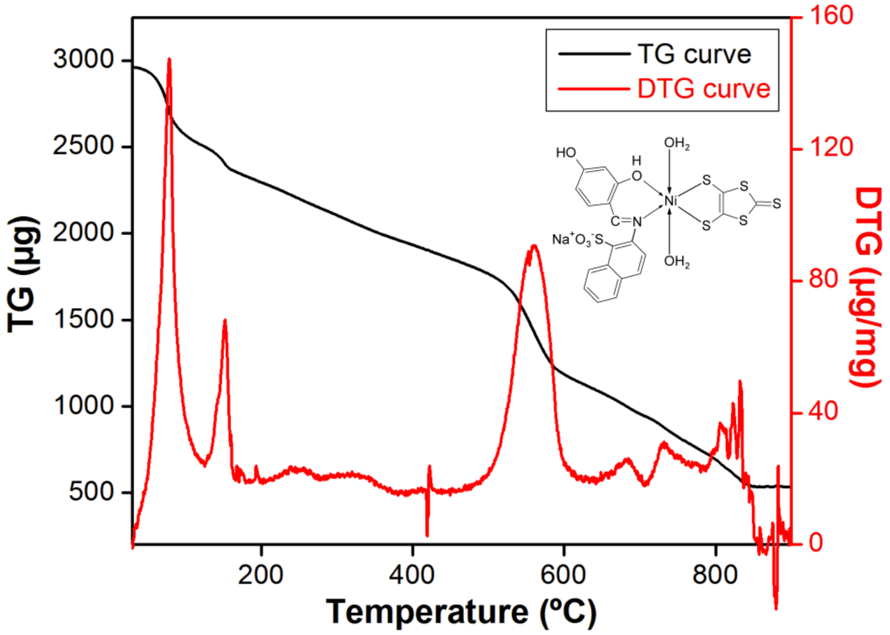

Figure 3.40 TG and DTG curve of complex $\mathbf{C_{22}}$

3.5.5 Characterization of complexes (C_{24}-C_{29})

The presence of lone pair of electrons on the nitrogen atom, electron donating character of the double bond and low electro negativity of nitrogen making N of the azomethine group (>C=N) as a good donor site and Schiff base as active ligands. The electron density around metal atom mainly controls the various steps involved in the catalytic cycle. The presence of phenolic -OH group sufficiently near to the azomethine group of salicylaldimines makes them versatile multidendate ligands complexing with almost all metal ions. Keeping this in mind, we had designed ONO-tridentate Schiff base ligand containing two phenolic -OH groups sufficiently near to azomethine group of salicylaldimines. This gives extra stability to the complexes due to the formation of chelates with five or six membered ring. In addition, the presence of a functional group with replaceable hydrogen atom near to >C=N will be additional factor of stability. This has prompted us to explore the catalytic activity of cobalt, nickel and copper complexes containing ONO-tridentate Schiff base, triphenylphosphine and dmit as ligands.

All the complexes were colored and found to be air stable in solid state at room temperature and non-hygroscopic in nature. They were found to be soluble in DMSO and DMF.

3.5.5.1 Physical and analytical studies

The Physical properties and analytical data of the complexes **C_{24}-C_{29}** are given in the Table 3.22. The elemental analyses (C,H,N,S) data were in good agreement with the proposed empirical formulae of the ligand and complexes, respectively.

Table 3.22 The Physical properties and analytical data of **C_{24}-C_{29}**

Compound (Colour)	Molecular formula	M. P. (°C)	Yield (%)	Elemental analysis data*			
				C	H	N	S
L_6 (Orrange)	$C_{13}H_{11}NO_3$	212	70	67.64 (68.11)	4.77 (4.84)	6.07 (6.11)	-
C_{24} (Dark brown)	$C_{49}H_{39}ClCoNO_3P_2$	280	57	69.39 (69.55)	4.60 (4.65)	1.65 (1.66)	-
C_{25} (Red)	$C_{31}H_{24}NNiO_3P$	320	68	67.98 (67.92)	4.38 (4.41)	2.55 (2.56)	-
C_{26} (Green)	$C_{31}H_{24}ClCuNO_3P$	269	66	63.36 (63.27)	4.08 (4.11)	2.38 (2.38)	-
C_{27} (Brown)	$C_{16}H_{13}CoNO_4S_5$	310	62	38.18 (38.24)	2.58 (2.61)	2.78 (2.79)	31.82 (31.90)
C_{28} (Green)	$C_{16}H_{13}NNiO_4S_5$	> 320	65	38.23 (38.26)	2.58 (2.61)	2.78 (2.79)	31.86 (31.92)
C_{29} (Green)	$C_{16}H_{13}CuNO_4S_5$	> 320	64	37.86 (37.89)	2.56 (2.58)	2.76 (2.76)	31.55 (31.61)

* Found (calculated) %

3.5.5.2 Electronic absorption and magnetic susceptibility measurement studies

The electronic absorption spectrum of **L_6** in DMSO displays three main bands. The bands in the region of 287 nm can be assigned to the π - π* transitions of the aromatic rings. The band at 350-380 nm involves n - π* transition of the C=N groups. The charge transfer will originate from 2-aminophenol ring as an origin to the C=N group as a sink (Selvakumar et al. 2007). In the spectra of all the complexes **C_{24}-C_{29},** the bands in the region 265-398 nm assigned to ILCT and 411-454 nm can be assigned to LMCT. In the spectrum of **C_{24}** band at 618 and 691 nm has been assigned to d-d transition corresponding to cobalt(III) octahedral complex. It is further confirmed by magnetic moment of zero value, shows its diamagnetic nature with d^6 configuration, which can be due to +3 oxidation state of cobalt ion with low spin state

(Abdalrazaq et al. 2010). The complex **C_{25}** shows d-d transition band at 520 nm confirms its square planar geometry, which is supported by its diamagnetic behavior with low spin state of d^8 configuration (Patel et al. 2007). The **C_{26}** shows the absorption maximum at 627 nm which is characteristic of trigonal bipyramidal structure and is confirmed by its diamagnetic behavior and it could be due to d^8 configuration of Cu(III) with low spin state (Mishra et al. 2004). The **e**lectronic absorption spectra of the complexes **C_{27}-C_{29}** shows d-d transition at 630-590 nm which has been assigned to the octahedral geometry of Co(III), Ni(II) and Cu(II) with high spin state. This is supported by their magnetic moment values of 4.93, 2.42 and 1.9 BM, respectively (Cukurovali et al. 2001 and Issa et al. 2005). Electronic absorption spectral results and Magnetic Susceptibility measurement data of the complexes **C_{24}-C_{29}** are summarized in the Table 3.23. The spectra of **C_{24}-C_{26}** and **C_{27}-C_{29}** are given in Fig. 3.41and Fig. 3.42, respectively.

Table 3.23 The electronic absorption spectral results and magnetic susceptibility measurement data of the ligand and complexes **C_{24} - C_{29}**

Compound	λ_{max} (nm)	Assignment	μ_{eff} (BM)	Geometry
L_6	287 350-380 410	π - π*, Ar n - π* of C=N CT	-	-
C_{24}	308 414, 440 618, 691	ILCT LMCT d-d forbidden transition	diamagnetic	Octahedral
C_{25}	286, 383 411, 426 520	ILCT LMCT d-d forbidden transition	diamagnetic	Square planar
C_{26}	285-358 413-454 627	ILCT LMCT d-d transition	diamagnetic	Trigonal bipyramidal
C_{27}	308, 390 475, 620	ILCT d-d forbidden transition	4.93	Octahedral
C_{28}	265, 318, 398 425,448,630	ILCT LMCT d-d forbidden transition	2.42	Octahedral
C_{29}	270-317, 393 429-453, 590	ILCT LMCT d-d forbidden transition	1.9	Octahedral

CT= Intramolecular Charge Transfer interactions
ILCT=Intra Ligand Charge Transfer transition.
LMCT=Ligand to Metal Charge Transfer transition.

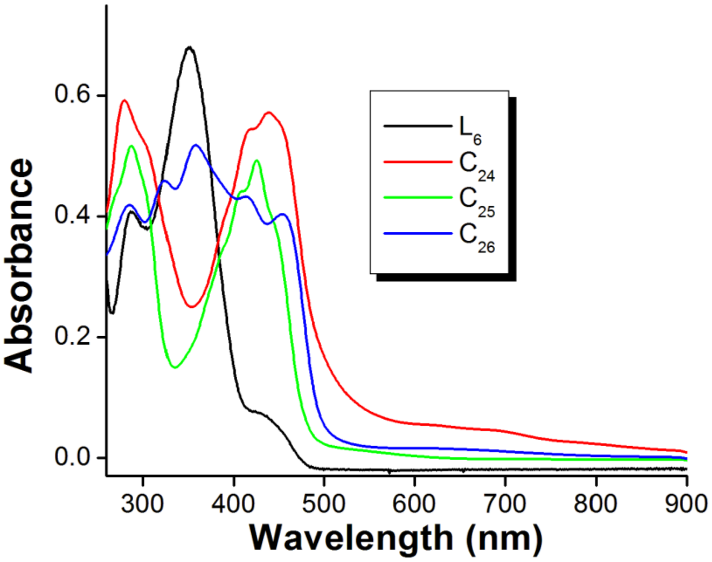

Figure 3.41 The **e**lectronic absorption spectra of the ligands and complexes **C_{24}-C_{26}**

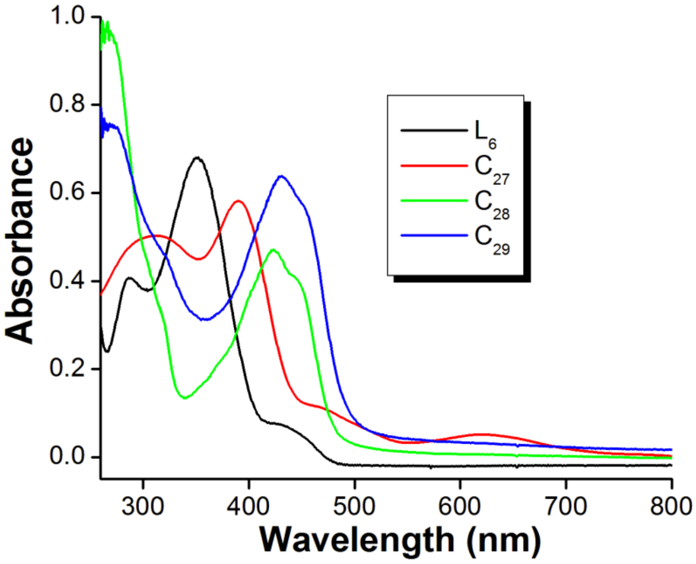

Figure 3.42 The **e**lectronic absorption spectra of the ligands and complexes **C_{27}-C_{29}**

3.5.5.3 FT-IR analysis

Selected FTIR bands of ligand and complexes are listed in Table 3.24. The ligand exhibit broad medium intensity band in the region 2700 cm^{-1} which is assigned to the intermolecular H-bonding vibrations (O-H$^{\cdot\cdot}$N). This situation is common for aromatic azomethine compounds containing o-OH groups (Chukurovali et al. 2001, Tumer et al. 1999). In all the complexes these band disappear completely. The spectrum of the free Schiff base ligand shows the peak of azomethine group -CH=N at 1631 cm^{-1}, which is shifted to lower frequencies in the spectra of all complexes at 1603-1623 cm^{-1}, indicate the involvement of the imine N in the coordination to metal ion. Coordination of the Schiff base to the metal ions through the nitrogen atom is expected to reduce the electron density in the azomethine link and lowers the stretching vibrational motion of ν(C=N). The band in the region 1223 cm^{-1} which is assigned to phenolic ν(C-O) in the free ligand, is shifted to higher wave number in the complexes suggesting the coordination of phenolic oxygen to metal ion. In the complexes **C_{24}-C_{26}**, bands due to triphenylphosphine are also appeared in the expected region. IR spectra of **C_{27}-C_{29}** exhibit strong bands in the region 1421-1438 cm^{-1}, which is assigned to C=C stretching vibration of dmit. The bands in the regions 1018-1056 cm^{-1} and 939-974 cm^{-1} can be attributed to C=S and C-S stretching vibrations respectively (Zuo et al. 1996). The bands in the region 635-640 cm^{-1} is assigned to SC=CS twisting mode. The spectra of complexes **C_{27}-C_{29}** exhibited a broad band around 3382-3233 cm^{-1}, which is assigned to water molecules, ν(OH), associated with the complexes. In addition to these modes, coordinated water exhibited $\delta_r(H_2O)$ rocking near 835-853 cm^{-1} and $\delta_w(H_2O)$ wagging near 535-555 cm^{-1} (Refat et al. 2013 and Abdel Aziz et al. 2012). The weak-to-very weak bands in the two ranges (550-480 cm^{-1}) and (460-430 cm^{-1}), respectively, are assigned to the stretching frequencies of the ν(M-O) and ν(M-N) bands (Refat et al. 2013 and Abdel Aziz et al. 2012), which confirmed the attachment of ligand to the center metal ions through the phenolic oxygen atoms and the azomethine nitrogen. In all the complexes the strong band around 2900-3200 cm^{-1} is due to the presence of ν(O-H) vibration of coordinated Schiff base. (Nguyen et al. 2010). The FT-IR spectra of the ligand **L_6**, complexes **C_{24}** and **C_{28}** are shown in the Fig. 3.43-Fig. 3.45, respectively.

Table 3.24 FT-IR spectral data of the ligand $\mathbf{L_6}$ and complexes $\mathbf{C_{24}}$-$\mathbf{C_{29}}$

Assignment (cm^{-1})	$\mathbf{L_6}$	$\mathbf{C_{24}}$	$\mathbf{C_{25}}$	$\mathbf{C_{26}}$	$\mathbf{C_{27}}$	$\mathbf{C_{28}}$	$\mathbf{C_{29}}$
ν(OH)	3051	3373	3210	3398	3382	3334	3232
ν(CH=N)	1631	1605	1623	1606	1604	1610	1603
ν(C-O)	1223	1241	1242	1237	1243	1261	1268
ν(C=C)	-	-	-	-	1438	1421	1432
ν(C=S)	-	-	-	-	1033	1018	1056
ν(C-S)	-	-	-	-	939	954	974
ν(SC=CS)	-	-	-	-	638	635	640
$\delta_r(H_2O)$	-	-	-	-	853	849	835
$\delta_w(H_2O)$	-	-	-	-	543	553	544
bands due to triphenylphosphine	-	1083 740, 691	1099 743 691	1092 741 690	-	-	-

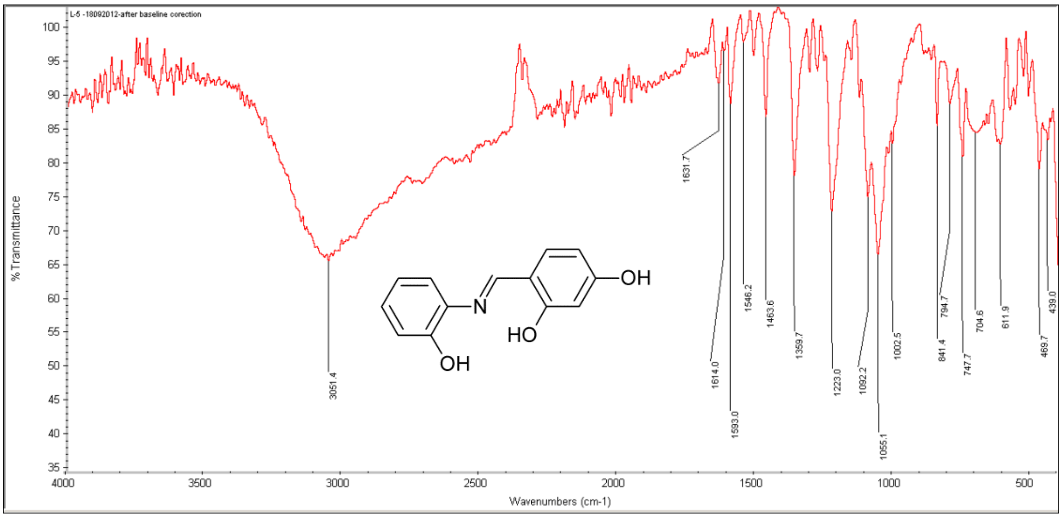

Figure 3.43 FT-IR spectrum of $\mathbf{L_6}$

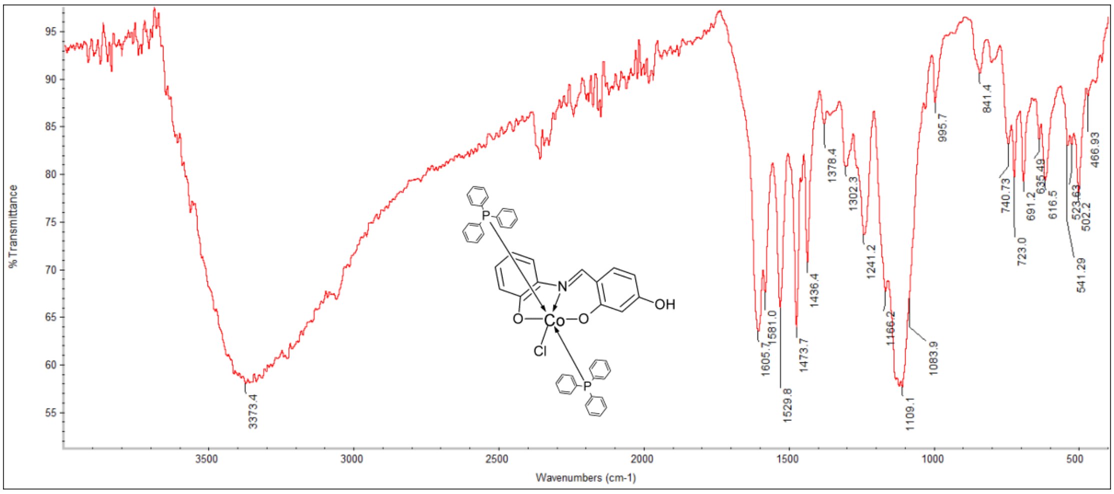

Figure 3.44 FT-IR spectrum of $\mathbf{C_{24}}$

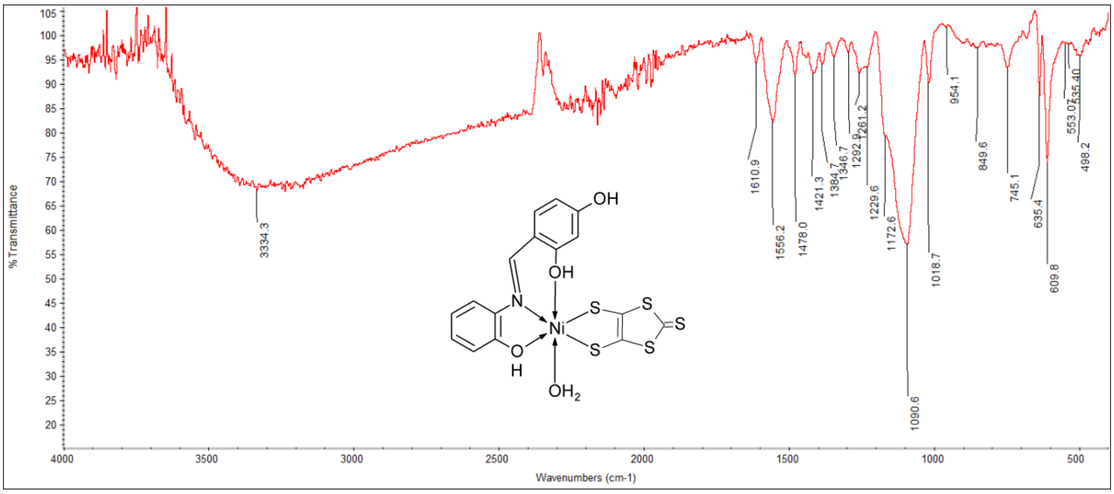

Figure 3.45 FT-IR spectrum of $\mathbf{C_{28}}$

3.5.5.4 NMR analysis

The ^{1}H NMR spectra of the complexes $\mathbf{C_{24}}$-$\mathbf{C_{26}}$ (Table 3.25) show multiplets at δ 6.3-8.9 ppm as set of multiplets which has been assigned to the aromatic protons that of coordinated triphenylphosphine groups present in the complexes and that of the Schiff base ligand. A singlet (1H) observed at 8.9 ppm in the spectra of ligand has been assigned to azomethine proton (–CH=N) (Raman et al. 2008) which shows significant shift in the spectra of all the complexes confirms that ligand coordinate to the metal ion through azomethine nitrogen. A sharp singlet appeared for *o*-OH proton of the ligand in the region δ 13.7 ppm and 9.6 ppm is absent in the complexes shows that the phenolic oxygen coordinates after deprotonation. ^{31}P{^{1}H} NMR spectra of the complexes **C_{24}-C_{26}** (Table 4.41) exhibit a sharp singlet in the range 42.3-43.3 ppm supporting the presence of the triphenylphosphine groups in the complex. The ^1H NMR and ^{31}P NMR spectra of **C_{24}** is shown in the Fig. 3.46 - Fig. 3.47, respectively.

Table 3.25 ^1H NMR and ^{31}P NMR chemical shifts of the complexes

Complex	Chemical shift (ppm)	
	^1H	^{31}P
C_{24}	6.3-8.9	43.3
C_{25}	6.1-8.8	42.3
C_{26}	6.2-8.6	42.8

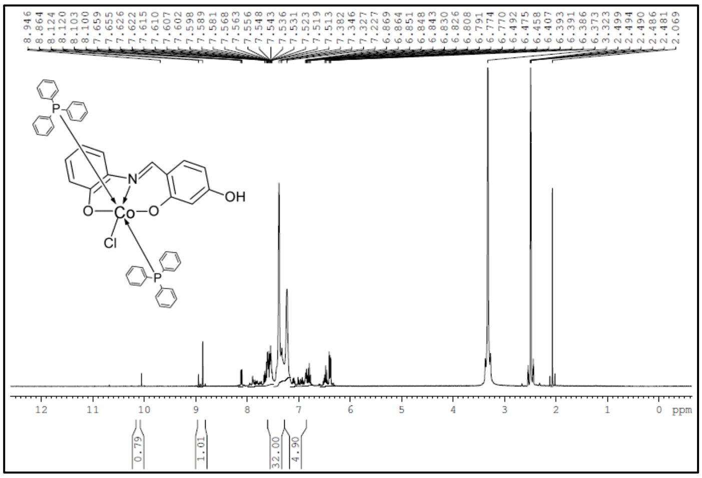

Figure 3.46 ^1H NMR spectrum of **C_{24}**

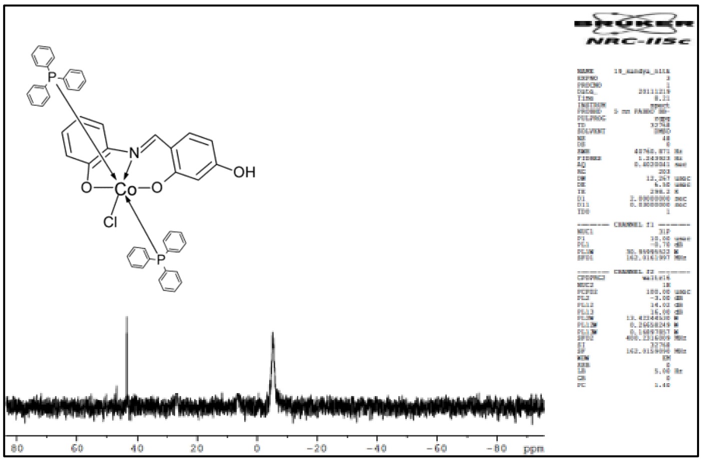

Figure 3.47 ^{31}P NMR spectrum of **C_{24}**

3.5.5.5 ESI Mass measurements

In the mass spectra of the complexes, the molecular weight of the complexes correspond to the presence of the dmit, Schiff base, triphenylphosphine ligands and chloride group in the synthesized complexes confirming the assumed structure. The ESI-MS spectra of the complex **C_{24}** is shown in the Fig. 3.48. Similarly expected molecular weight and the observed molecular weight of the complexes are given in the Table 3.26.

Table 3.26 ESIMS data of **C_{24}-C_{29}**

Complex	Expected mass	Observed mass
C_{24}	846.1	847.3
C_{25}	548.1	547.2
C_{26}	588.4	587.1
C_{27}	502.5	502.8
C_{28}	502.2	502.1
C_{29}	507.1	507.1

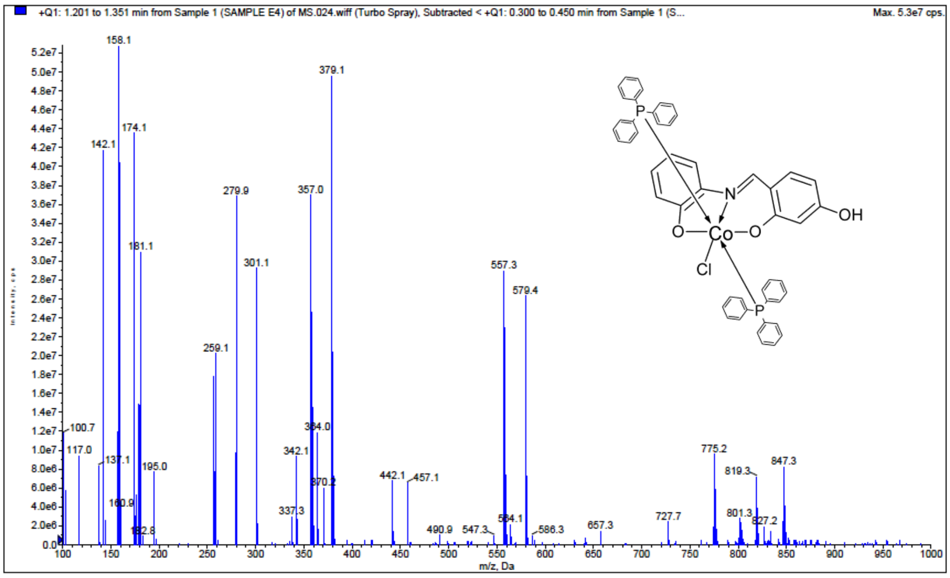

Figure 3.48 ESIMS spectrum of **C_{24}**

3.5.5.6 Thermal analysis

The thermal analyses results of these complexes are represented in the Table 3.27. In all cases the ligand moiety is removed first leaving the respective metal oxide as the decomposition residue. In the complexes **C_{24}-C_{26},** chloride and ligand moiety is removed first in the respective temperature range followed by the PPh_3 moiety. Similarly in the complexes **C_{27}-C_{29},** water molecule and ligand moiety decomposes initially followed by ligand C_3S_5 moiety in the mentioned temperature range. The thermal decomposition behaviors of these complexes reflected the structural information as well. The thermogram of **C_{24}** and **C_{28}** is as shown in the Fig. 3.49 and Fig. 3.50, respectively.

Table 3.27 Thermal analyses data for the complexes **C_{24}-C_{29}**

Complex	stage	TG temp. range (°C)	Removed group	TG mass loss (%)		Residue compound	Residue found (calc.)%
				Found	Calc.		
C_{24}	I II III	197-286 286-500 500-867	Cl L 2(PPh_3)	4.42 26.8 61.4	4.1 25.6 61.8	CoO or 1/2(Co_2O_3)	7.38 (8.8)
C_{25}	I II	197-384 384-660	L (PPh_3)	39.1 47.4	41.5 47.9	NiO	13.5 (13.6)
C_{26}	I II	170-373 571-788	Cl+L (PPh_3)	38.3 45.5	39.7 44.6	CuO or 1/2(Co_2O_3)	16.2 (15.6)
C_{27}	I II	124-321 321-959	(H_2O)+L C_3S_5	49.2 39.0	49.1 38.1	CoO	11.8 (12.8)
C_{28}	I II	148-684 684-910	(H_2O)+L C_3S_5	48.5 39.1	49.2 39.0	NiO	12.4 (11.8)
C_{29}	I II	153-404 404-908	(H_2O)+L C_3S_5	47.5 38.3	48.7 38.7	CuO	14.2 (12.6)

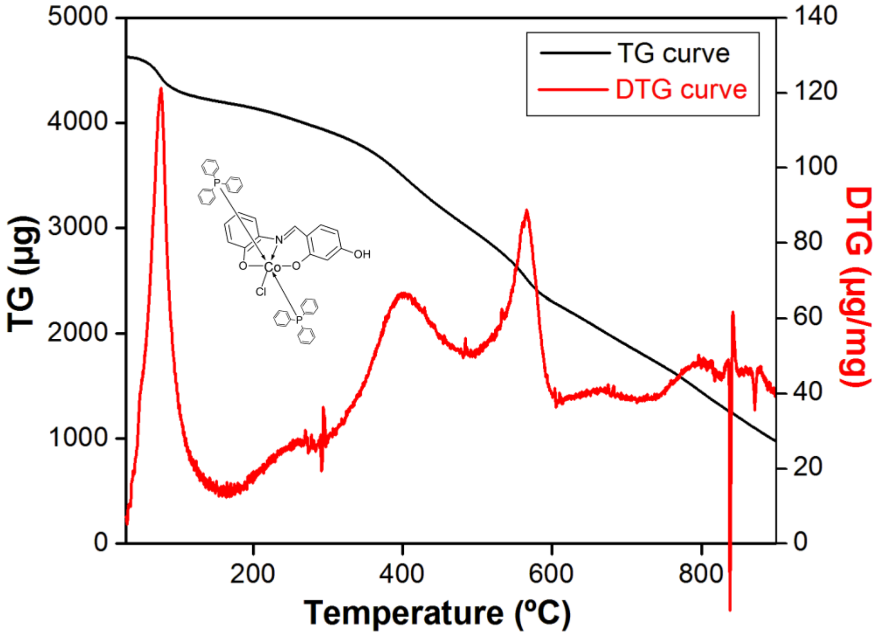

Figure 3.49 TG and DTG curve of complex $\mathbf{C_{24}}$

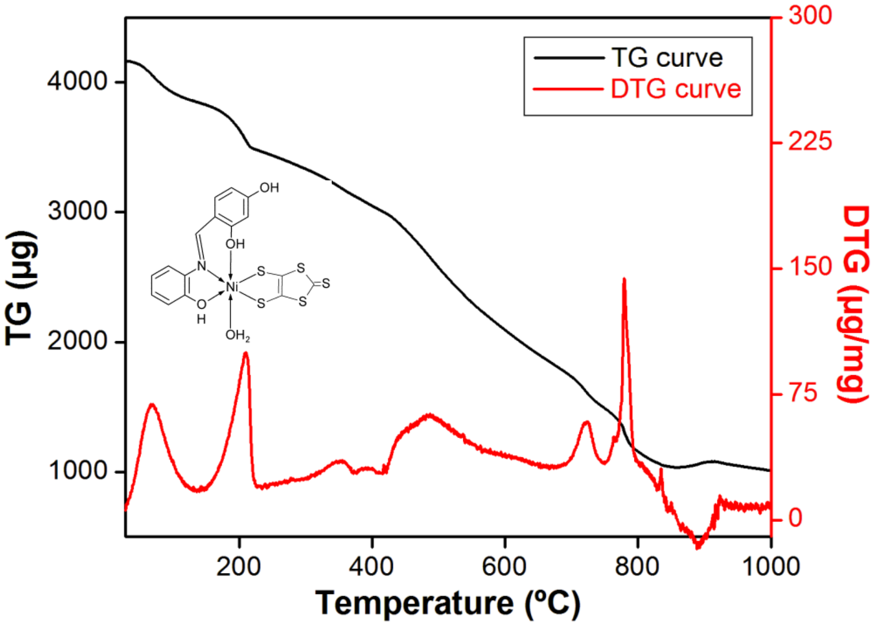

Figure 3.50 TG and DTG curve of complex $\mathbf{C_{28}}$

3.6 GENERAL PROCEDURE FOR HOMOCOUPLING OF ARYL GRIGNARD REAGENTS

3.6.1 Homocoupling of aryl Grignard reagents (1a-1h)

The coupling reaction was carried out according to the reported procedure (Padma et al. 2009) with modification. Magnesium turnings (13 mmol, 0.320 g atom) were placed in a two necked round bottom flask with a calcium chloride guard tube. A crystal of iodine was added. Aryl halide (2 mmol of total 10 mmol) in 5 ml of anhydrous diethyl ether was added with stirring at room temperature. Initially, increase in the temperature of the reaction mixture was observed and the appearance of turbidity after few minutes indicated the initiation of the reaction. The remaining aryl halide (8 mmol) in 5 ml of ether was added drop wise and the reaction mixture was stirred for 40 minutes. To the reaction mixture, chosen catalyst was added. The reaction mixture darkened immediately upon addition of the catalyst. The stirring was continued till required time. Then reaction mixture was cooled and hydrolyzed with a saturated solution of 10% aqueous ammonium chloride. After extraction with ether (3x50 mL), the combined organic layers were dried over anhydrous magnesium sulfate. All volatiles were removed under reduced pressure and the product obtained was compared well with authentic samples using gas Chromatography.

3.6.2 Homocoupling of functionalized aryl Grignard reagents (1i-1j)

Magnesium turnings (13 mmol, 0.320 g atom) were placed in a two necked round bottom flask with a calcium chloride guard tube. A crystal of iodine was added. Aryl halide (2 mmol of total 10 mmol) in 5 ml of anhydrous diethyl ether was added with constant stirring maintaining the reaction mixture at -5 °C to avoid the decomposition of Grignard reagent. Initially, increase in the temperature of the reaction mixture was observed and the appearance of turbidity after few minutes indicated the initiation of the reaction. The remaining aryl halide (8 mmol) in 5 ml of ether was added drop wise and the reaction mixture was stirred for 40 minutes. To the reaction mixture, chosen catalyst was added. The reaction mixture darkened immediately upon addition of the catalyst. The stirring was continued till required time. Then reaction mixture was cooled and hydrolyzed with a saturated solution of 10% aqueous ammonium chloride. After extraction with ether (3x50 mL), the combined organic layers were dried over anhydrous magnesium sulfate. All volatiles were removed under reduced pressure and the product obtained was compared well with authentic samples using gas Chromatography. Schematic representation of homocoupling of Grignard reagents is as shown in Scheme 3.10.

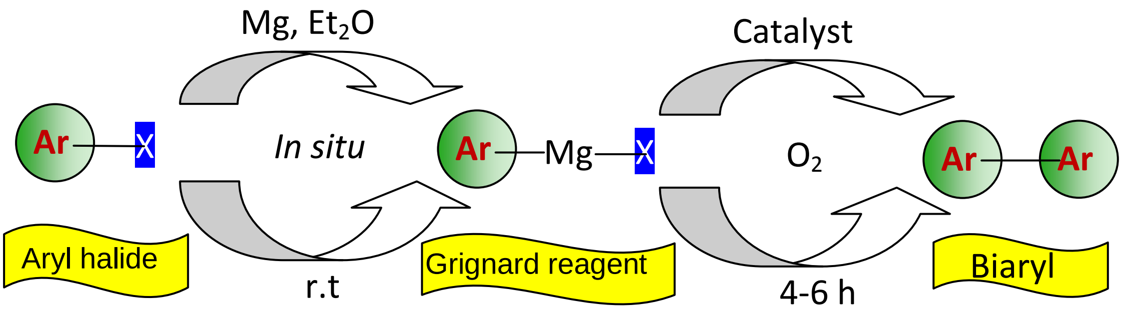

Scheme 3.10 Schematic representation of homocoupling of Grignard reagents to biaryls

3.6.3 Product analysis

The initial column temperature of GC was increased from 60 °C to 150 °C at the rate of 10 °C/min and then to 220 °C at the rate of 40 °C/min. Nitrogen gas was used as the carrier gas. The temperatures of the injection port and FID were kept constant at 150°C and 250°C, respectively, during product analysis. The retention time for different compounds was determined by injecting pure compounds under identical gas chromatography conditions.

CHAPTER 4

CATALYTIC APPLICATION

This chapter focuses on the development of "one-pot" catalytic system for the homocoupling of variety of aryl Grignard reagents using the synthesized complexes. The reaction conditions were optimized to accomplish this transformation. The scope of the method is discussed and in many instances, the factors that govern the efficiency of the process are elaborated. The proposed mechanisms were embedded for the present catalytic system based on the UV-vis studies of the reaction mixtures.

4.1 CATALYTIC ACTIVITY STUDIES OF C_1-C_5

In the present catalytic methodology, Grignard reagents were synthesized *in situ* from metallic magnesium, which is inexpensive, readily available and environmentally friendly. The synthesized Grignard reagents were converted into biaryl compounds with the aid of a metal catalyst in a single step. The handling of commercially available Grignard reagents is very difficult owing to their highly basic and hygroscopic nature, which usually needs special attention during the experiments. As *in situ* preparations avoid the workup procedures for the isolation of Grignard reagents, the present method is very simple and economical. The important surface activation of magnesium turnings was achieved with iodine crystals (Yuan and Fang 2012). The initial addition of aryl halide during the preparation of the Grignard reagent is very important. Various side products were observed when the aryl halides were added quickly, mainly ROH (R is 'aryl'). When bromobenzene was used as the aryl halide, we obtained phenol as the main side product (Kiefer et al. 2013). With controlled addition of the aryl halides, the respective Grignard reagents were yielded. The thus-formed Grignard reagent afforded biaryls in good to high yields when treated with a catalytic amount of **C_1-C_5**. In our study, atmospheric oxygen was employed as the oxidant. No extra ligand, additives, or oxidants were needed and this renders the current reaction environmentally friendly and cost-effective. Notably, the coupling reaction proceeded smoothly even at room temperature and, therefore, the catalytic system is energy-efficient.

The reaction conditions for the coupling of phenylmagnesium bromide (**1e**) were optimized with respect to

- solvent

- time
- catalyst concentration

4.1.1 Solvent effect

Solvents play a crucial role in the coupling reactions. The catalytic activities of the complexes **C_1-C_5** were checked in tetrahydrofuran, diethyl ether and benzene with atmospheric oxygen as the oxidant (Table 4.1). The best conversion was observed in diethyl ether as ether molecules coordinate with Grignard reagent and thus helps in stabilizing the intermediate complex (Rogers et al. 1980, Fox and Whitesell 2009) (entry 2). The least conversion was observed in benzene. Since, non-polar organic solvent forms insoluble deposit at the metallic surface and thus gradually inhibits the formation of polar Grignard reagent. The order of increasing percentage yield in tested solvents follows, benzene < tetrahydrofuran < diethyl ether.

Table 4.1 Optimization of homocoupling of phenylmagnesium bromide (**1e**) in different solvents[a]

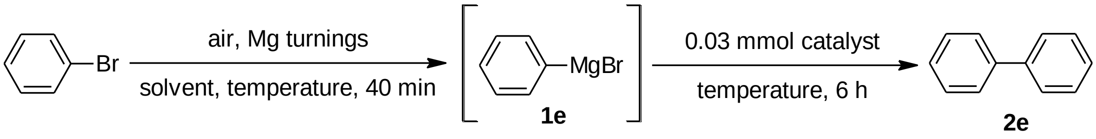

Entry	Solvent	Temperature (°C)	Yield (%)[b]				
			C_1	**C_2**	**C_3**	**C_4**	**C_5**
1	tetrahydrofuran	60	62	28	45	58	16
2	**diethyl ether**	**r.t[c]**	**76**	**42**	**60**	**70**	**31**
3	benzene	40	36	13	21	27	09

[a] Reaction conditions: Mg turnings (0.320 g), bromobenzene (10 mmol), catalyst (0.03 mmol), solvent (10 ml).
[b] GC yield based on the amount of bromobenzene.
[c] r.t = room temperature.

4.1.2 Effect of reaction time

The dependence of product yield on the reaction time was investigated by analyzing the reaction mixture at regular intervals of time. As observed in Fig. 4.1, the yield was increased with reaction time and total reaction time of 6 h at room temperature gave a constant conversion of the highest yield (entry 7). The results are tabulated in the Table 4.2.

Table 4.2 Optimization of homocoupling of phenylmagnesium bromide (**1e**)[a] w.r.to time

Tr. No.	Time (min)	Yield (%)[b]				
		C_1	**C_2**	**C_3**	**C_4**	**C_5**
1	0	0	0	0	0	0
2	60	19.8	9.7	12.8	17.4	3.2
3	120	32.5	11.5	28.3	31.1	8.5
4	180	48.6	16.4	39.4	43.2	16.2
5	240	63.8	27.5	43.7	54.3	19.4
6	300	68.4	38.3	51.3	65.8	23.7
7	**360**	**75.9**	**42.4**	**60.2**	**70.3**	**31.2**
8	420	74.3	42.1	60.1	70.3	31.0
9	480	74.8	41.9	59.8	70.2	31.0
10	540	74.1	42.2	59.7	70.1	30.9
11	600	74.9	42.3	59.7	70.1	30.9

[a] Reaction conditions: Mg turnings (0.320 g), bromobenzene (10 mmol), catalyst (0.03 mmol), Et_2O (10 ml).

[b] GC yield based on the amount of bromobenzene.

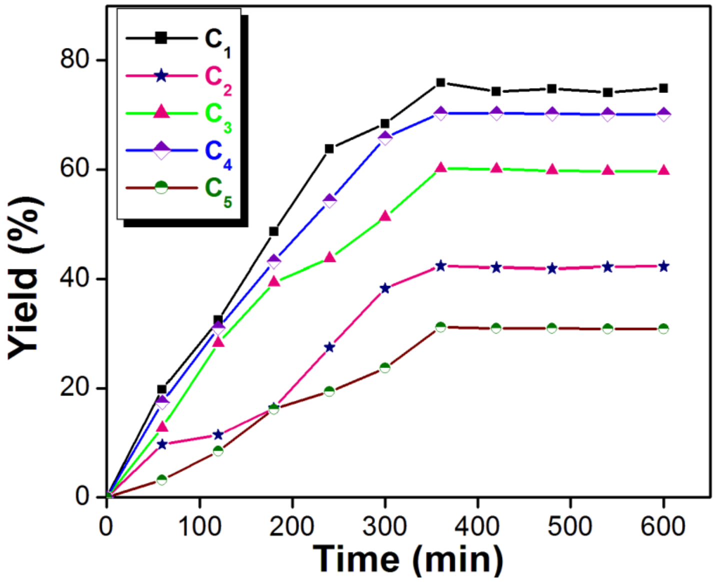

Figure 4.1 Effect of reaction time on the yield of bromobenzene to biphenyl

4.1.3 Effect of catalyst loading and influence of air on the reaction

To study the effect of catalyst concentration on the coupling yield, substrate to catalyst ratio was varied from total catalyst amount 0.01 mmol to 0.05 mmol (Table 4.3). Herewith we describe the effect of **C_1** concentration on the coupling of **1e** in detail. From the catalytic activity studies it was observed that, increase in catalyst loading increases the coupling yield and after reaching the optimum concentration further increase of catalyst amount did not affect the yield of coupling product significantly and remained almost constant. The use of 0.03 mmol of **C_1** afforded the highest yield of 76 % (entry 6). Interestingly, negligible amount of product was observed in the absence of **C_1** featuring the catalytic role of the complex as the efficient catalyst (entry 1). Notably, the present coupling can be readily scaled up to the reaction of 50.0 mmol of the aryl halide using 0.15 mmol of the catalyst, which afford 74 % of biaryl with a negligible amount of side products. This further supports the efficiency of the synthesized complex as competent catalyst for the homocoupling reaction (entry 10). The yields were not very sensitive to the catalyst loading at higher concentration. This could be reasoned to the fact that, the reactions conducted at high catalyst loading might experience rate-limiting mass-transfer of oxygen gas into solution (Steinhoff et al. 2006). Indeed, the solubility of oxygen in most of the solvents is poor and its rate of dissolution is very low. Hence, at high catalyst loading the fixation of oxygen might be taking place. The mass-transfer effects are especially significant for aerobic reactions because of the susceptibility of the reduced catalyst to decompose into inactive metal. Thus, slow transfer of oxygen gas into solution not only affects the reaction rate but also contributes to catalyst decomposition. Catalyst decomposition might be associated with catalyst aggregation. If the catalyst decomposes during the course of the reaction, the concentration of active metal catalyst will decrease and the rate will decrease proportionately. It should be noted that, mass-transfer limitation effects include the invariance of the rate on catalyst above a threshold concentration (Steinhoff et al. 2006).

The present reaction system was highly influenced by air. The reaction affords a good coupling yield in the presence of atmospheric oxygen. We have investigated the feasibility of the coupling reaction under an inert (argon) atmosphere using 0.03 mmol of catalyst (entry 9, Table 4.9). But, insignificant amount of product was detected. This can be attributed to the lack of formation of peroxo-ruthenium(III) active species. This serendipitous discovery suggested the necessity of atmospheric oxygen and its role as oxidant in present reaction system. Similar trend was observed for rest of the complexes.

Table 4.3 Effect of catalyst concentration and influence of air on the yield of coupling product[a]

Entry	Amount of complex **C$_1$** (mmol)	Yield(%)[b]
1	**No catalyst**	**01.1**
2	0.01	19.7
3	0.015	32.3
4	0.02	47.3
5	0.025	61.2
6	**0.03**	**75.9**
7	0.04	75.6
8	0.05	74.9
9[c]	**0.03**	**04.2**
10[d]	**0.15**	**74.0**

[a] Reactions were carried out with 10 mmol of bromobenzene in presence of atmospheric molecular oxygen.
[b] GC yield based on the amount of bromobenzene.
[c] Inert atmosphere (argon).
[d] With 50.0 mmol of bromobenzene in the presence of 0.15 mmol catalyst for 10 h.

4.1.4 Scope of the reaction

This promising results encouraged to extend the scope of the reaction to various aryl Grignard reagents (Table 4.4). Thus, simple and functionalized biaryl compounds were synthesized in good yields (entries 1–10). Introduction of methyl group at the *ortho*-position of the aryl Grignard reagent **1b** resulted in lesser yield of the product (entry 2). 4-Methoxy- and 2- methoxyphenylmagnesium bromide can be efficiently converted into the corresponding biaryls **2c** and **2d**, respectively, under similar conditions (entries 3 and 4). It was noteworthy that the present reaction system was tolerant of aryl chloride functionality (entry 6). Also it allowed the coupling of heteroaryl Grignard reagent **1g** successfully (entry 7). Although sterically demanding substrate **1h** required higher reaction temperature and longer reaction time, it gave the corresponding biaryl **2h** in moderate yield (entry 8). The reaction was chemoselective; thus, nitrile, or nitro groups were tolerated (entries 9 and 10).

Enhanced yields of coupling products were obtained with the Grignard reagents containing electron donating groups (**1a, 1b, 1c** and **1d**) compared to the yields of those with electron withdrawing groups (**1f**, **1i** and **1j**). This can be attributed to two factors: the yield of Grignard reagent and the reductive elimination step. The yield of Grignard reagent increases with the aryl halide attached to an electron donating group compared to that with the aryl halide attached to an electron withdrawing group. A higher yield of Grignard reagent results in a higher yield of coupling product (Seyferth 2009). Another factor can be attributed to the faster reductive elimination from the complex with the aryl halide attached to an electron donating group than from the complex with the aryl halide attached to an electron withdrawing group. The electron withdrawing group on the aryl halide increases the strength of the M-C bond and makes it more ionic; the increase in ionic character increases the thermodynamic bond strength (Hartwig 2007). Thus, aryl halides with electronic properties that increase the strength of the M-C bond tend to decrease the thermodynamic driving force for the reductive elimination. In all these experiments, formations of cross-coupling products were very less.

Table 4.4 Homocoupling of Grignard reagents with atmospheric oxygen as an oxidant[a]

Entry	RMgBr	Product	Yield (%)[b]				
			C_1	**C_2**	**C_3**	**C_4**	**C_5**
1	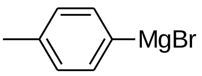 **1a**	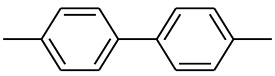 **2a**	**83**	49	66	79	38
2	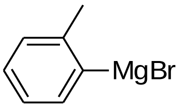 **1b**	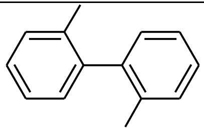 **2b**	**74**	42	56	67	24
3	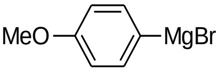 **1c**	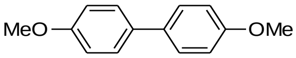 **2c**	**89**	53	72	83	41
4	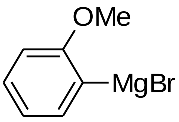 **1d**	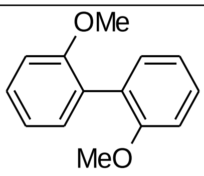 **2d**	**72**	37	57	65	27
5	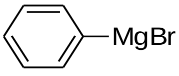 **1e**	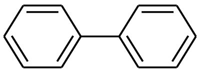 **2e**	**76**	42	60	70	31
6	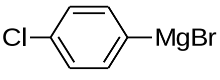 **1f**	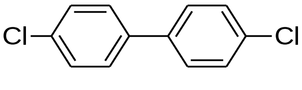 **2f**	**71**	36	55	63	26
7	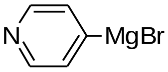 **1g**	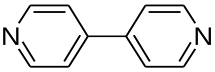 **2g**	**70**	34	50	62	23

8[c]	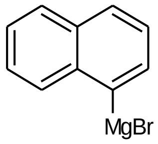 **1h**	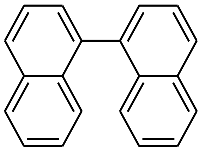 **2h**	**65**	30	46	60	17
9[d]	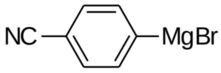 **1i**	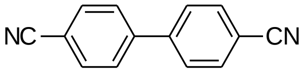 **2i**	**62**	26	44	57	13
10[d]	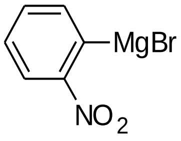 **1j**	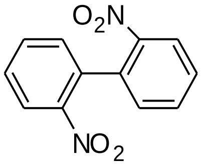 **2j**	**64**	29	42	60	15

[a] Reaction conditions: Mg turnings (0.320 g), aryl halide (10 mmol), catalyst (0.03mmol), Et_2O (10 ml).
[b] GC yield based on the amount of aryl halide.
[c] In THF, 60 °C, 10 h.
[d] reactions at -5 °C to room temp.

4.1.5. Proposed mechanism

The proposed mechanism is depicted in Fig. 4.2 for the **C_1** catalyzed reaction. A low valent ruthenium species is generated by the Grignard reagent, which is a strong reducing agent (Ramnial et al. 2007) and is involved in the catalytic cycle (Xu et al. 2006). The oxidative addition of atmospheric oxygen to the low valent ruthenium complex (a) forms a peroxo-ruthenium(IV) intermediate (b), which is the key step of this catalytic cycle (Hossain et al. 2003, Ourari et al. 2011). It then reacts with two equivalents of RMgX to give the biarylruthenium(IV) intermediate (c) and XMgOOMgX (Cahiez et al. 2007). Thus, the formed biarylruthenium(IV) intermediate (c) undergoes a rapid reductive elimination, which eventually yields the homocoupling product Ar-Ar and ruthenium(II). It can be reasonably supposed that the formation of the unstable ruthenium(IV) species (c) is required to achieve a very quick reductive elimination to give (d) and that the best way to favor the reductive elimination is to increase the oxidation state of the metal.

The formation of the peroxo-ruthenium(IV) intermediate was confirmed by the UV-vis spectral analysis (Fig. 4.2). The absorption peak of the catalytic reaction mixture that appears at 398 nm can be attributed to the peroxo-ruthenium(IV) intermediate (Joseph et al. 2002) and its absence from the reaction carried out under inert conditions further confirms the necessity of atmospheric oxygen for the present catalytic system. Various iron (Cho et al. 2011), cobalt (Cho et al. 2010), nickel (Cho et al. 2009, Zapata-Rivera et al. 2012), copper (Zapata-Rivera et al. 2011) and palladium (Adamo et al. 2006, Popp et al. 2009)-catalyzed reactions are well established with such peroxo complexes as the catalytic intermediate.

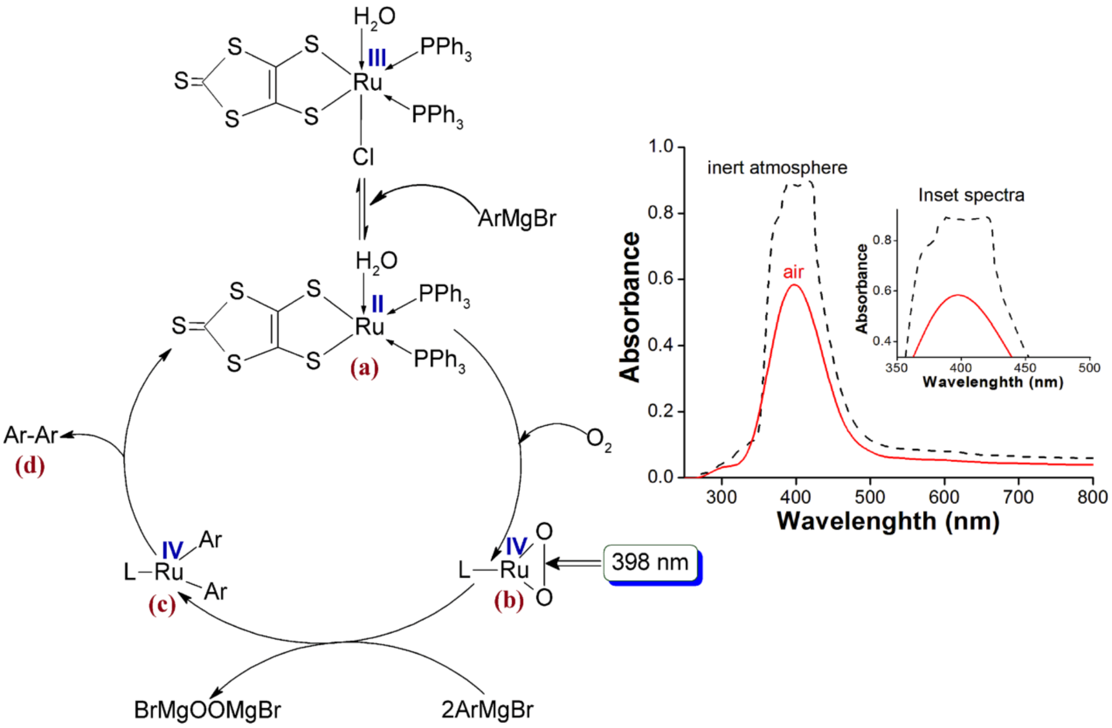

Figure 4.2 Proposed mechanism for the homocoupling of Grignard reagent using the complex $\mathbf{C_1}$

Based on the above studies, the general mechanism for homocoupling of the Grignard reagent using the metal complexes $\mathbf{C_2}$-$\mathbf{C_5}$ can be proposed as given in the Fig. 4.3 and Fig. 4.4, respectively.

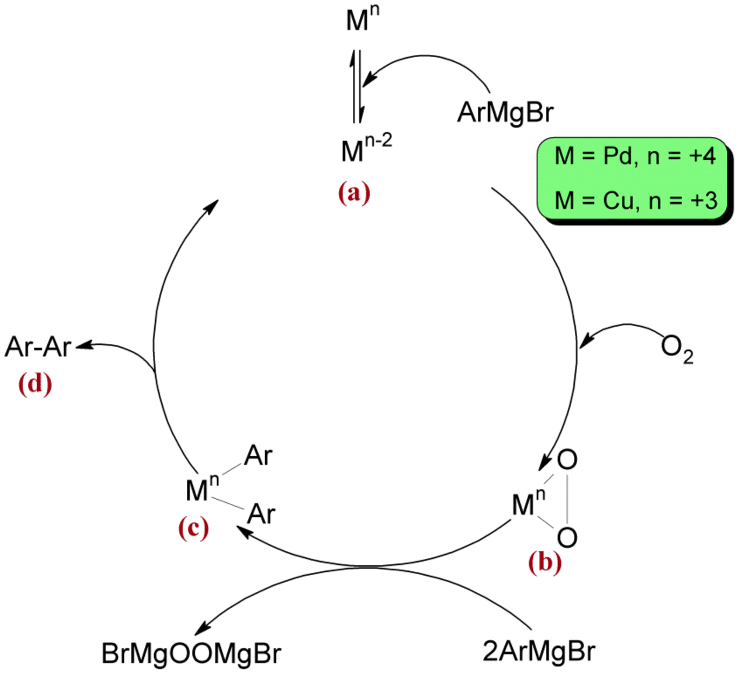

Figure 4.3 Proposed mechanism for the homocoupling reaction using the complexes **C_2** and **C_5**

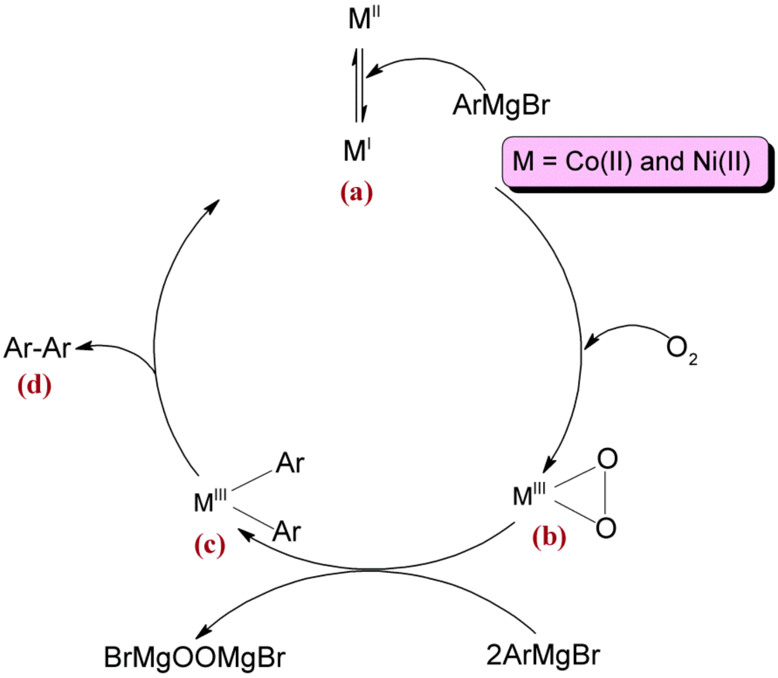

Figure 4.4 Proposed mechanism for the homocoupling reaction using the complexes **C_3** and **C_4**

From the catalytic activity studies it was observed that the complex **C_1** showed the highest catalytic activity compared to the rest of the complexes which can be attributed to its variable oxidation states and faster reductive elimination to yield the coupling product in good yield. This can be due to the fact that reductive elimination to form C-C bond occurs faster from the three- and five-coordinate intermediate complexes than from four- or six- coordinate complexes (Hartwig 2007). Hence lesser yield was observed from **C_2** which was assumed to exhibit four-coordinate intermediate complex by the dissociation of two ligands and thus typically undergo slower reductive elimination. The complex **C_4** gave coupling product in good yield than **C_3** which can be due to its electron rich three-coordinate intermediate complex that facilitates faster oxidative addition reaction, in turn results in the higher yield of the coupling product. The complex **C_5** showed the least catalytic activity. This may be due to the difficulty in the two-electron oxidation of Cu(I) in association with the greater stability due to its completely filled *d-orbitals*.

4.2 CATALYTIC ACTIVITY STUDIES OF C_6-C_{11}

The reaction conditions for the coupling of phenylmagnesium bromide (**1e**) were optimized with respect to

- solvent
- time
- catalyst concentration

4.2.1 Solvent effect

The catalytic activities of the complexes **C_6-C_{11}** were checked in tetrahydrofuran, diethyl ether and benzene using atmospheric oxygen as the oxidant (Table 4.5). The best conversion was observed in diethyl ether as ether molecules actually coordinate with and thus helps in stabilizing the Grignard reagent (entry 2). The least conversion was observed in benzene, since the formation of polar Grignard reagent stops in most non-polar organic solvents as it forms an insoluble deposit at the metallic surface. The order of increasing percentage yield in tested solvents follows, benzene < tetrahydrofuran < diethyl ether.

Table 4.5 Optimization of homocoupling of phenylmagnesium bromide (**1e**)[a] in different solvents

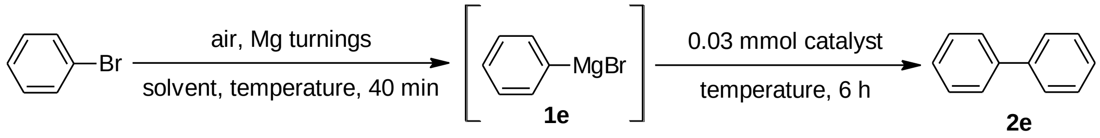

Entry	Solvent	Temperature (°C)	Yield (%)[b]					
			C_6	**C_7**	**C_8**	**C_9**	**C_{10}**	**C_{11}**
1	tetrahydrofuran	60	39	42	14	27	45	11
2	**diethyl ether**	**r.t[c]**	**68**	**83**	**39**	**62**	**89**	**33**
3	benzene	40	22	29	5	19	33	6

[a] Reaction conditions: Mg turnings (0.320 g), bromobenzene (10 mmol), catalyst (0.03 mmol), solvent (10 ml).
[b] GC yield based on the amount of bromobenzene.
[c] r.t = Room temperature.

4.2.2 Effect of reaction time

The dependence of product yield on the reaction time for the coupling of **1e** was studied by analyzing the reaction mixture at regular intervals of time under similar reaction conditions. The yield increased with reaction time (Fig. 4.5). The complexes **C_6**, **C_8**, **C_9** and **C_{11}** required 6 h to achieve maximum yield. The total reaction time of 5.5 h at room temperature gave a constant conversion of the highest yield for **C_7**. Among all the complexes **C_6-C_{11}**, the complex **C_{10}** yielded the maximum in minimum time of 5 h. The results are tabulated in the Table 4.6.

Table 4.6 Optimization of homocoupling of phenylmagnesium bromide (**1e**)[a] w.r.to time

Tr. No.	Time (min)	Yield (%)[b]					
		C_6	**C_7**	**C_8**	**C_9**	**C_{10}**	**C_{11}**
1	0	0.0	0.0	0.0	0.0	0.0	0.0
2	60	18.3	27.3	4.3	16.2	33.6	3.2
3	120	27.4	43.2	12.8	21.5	49.7	10.4

4	180	38.7	51.6	18.7	32.7	62.4	16.6
5	240	47.6	62.2	23.5	39.2	73.5	22.3
6	**300**	51.2	71.1	29.4	46.3	**89.2**	26.9
7	**330**	59.3	**82.7**	32.2	53.3	88.9	31.2
8	**360**	**68.4**	82.6	**39.3**	**62.2**	89.1	**33.3**
9	420	68.2	82.4	38.8	62.1	88.4	33.2
10	480	68.3	81.9	39.1	62.2	89.0	33.3
11	540	68.4	82.3	38.9	62.0	88.9	33.2
12	600	67.9	82.2	39.0	61.9	89.1	33.0

[a] Reaction conditions: Mg turnings (0.320 g), bromobenzene (10 mmol), catalyst (0.03 mmol), Et_2O (10 ml).

[b] GC yield based on the amount of bromobenzene.

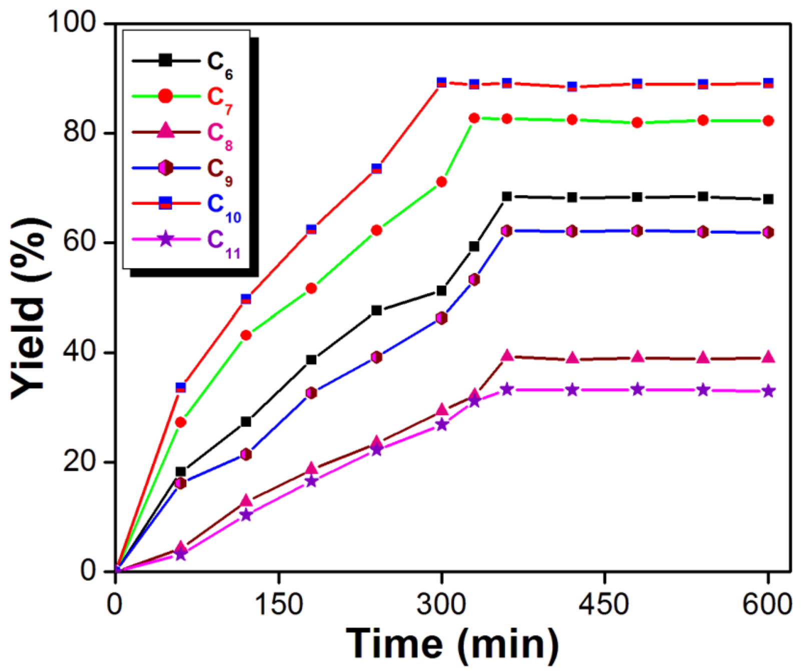

Figure 4.5 Effect of reaction time on the yield of bromobenzene to biphenyl

4.2.3 Effect of catalyst loading and influence of air on the reaction

To study the effect of catalyst concentration on the reaction, substrate to catalyst ratio was varied from total catalyst amount 0.01 mmol to 0.05 mmol (Table 4.7). Herewith we describe the effect of the concentration of the complex **C_{10}** on the coupling of **1e** in detail. The yield increased with increase in catalyst loading after reaching optimum concentration further increase of catalyst amount did not affect the yield of coupling product significantly and remained almost constant. At higher catalyst loading the yields were not very sensitive. The reason is the same as discussed in *section 4.1.3*. The highest value of 89 % yield was obtained with 0.025 mmol of catalyst loading (entry 5). The efficiency of the complex **C_{10}** should be underlined since, in the absence of nickel(III) complex, only traces of coupling product was observed featuring the catalytic role of the complex for the present system (entry 1). Notably, the present coupling can be readily scaled up to the reaction of 50.0 mmol of the aryl halide using 0.125 mmol of the catalyst, which afford 83 % of biaryl with a negligible amount of side products. This further supports the efficiency of the synthesized complex as competent catalyst for the homocoupling reaction (entry 10). The feasibility of the coupling reaction was investigated under an inert atmosphere (argon). Surprisingly, a lower yield was obtained which may be due to the lack of formation of peroxo-nickel(III) active species (entry 9). This emphasizes the role of atmospheric oxygen as an effective oxidant in the present study. Similar trend was observed for rest of the complexes and they achieved maximum yield with the amount of 0.03 mmol.

Table 4.7 Effect of the concentration of **C_{10}** on the yield of coupling product[a]

Entry	Amount of complex (**C_{10}**) (mmol)	Yield(%)[b]
1	**No catalyst**	**01.1**
2	0.01	31.4
3	0.015	42.5
4	0.02	67.3

5	**0.025**	**89.2**
6	0.03	88.9
7	0.04	88.8
8	0.05	88.7
9[c]	**0.025**	**07.2**
10[d]	**0.125**	**83.0**

[a] Reactions were carried out with 10 mmol of bromobenzene in presence of atmospheric molecular oxygen.
[b] GC yield based on the amount of bromobenzene.
[c] Inert atmosphere (argon).
[d] With 50.0 mmol of bromobenzene in the presence of 0.125 mmol catalyst for 10 h.

4.2.4 Scope of the reaction

This promising result encouraged us to extend the scope of the reaction to various aryl Grignard reagents (Table 4.8). Thus, simple and functionalized biaryl compounds were synthesized in good yields (entries 1-10). Introduction of methyl group at the *ortho*-position of the aryl Grignard reagent **1b** resulted in somewhat lower yield of the homocoupling product (entry 2). 4-Methoxy- and 2-methoxyphenylmagnesium bromide can be efficiently converted into the corresponding biaryls **2c** and **2d**, respectively, under similar conditions (entries 3 and 4). It is noteworthy that the present reaction system is tolerant of aryl chloride functionality (entry 6). Also it allows the coupling of heteroaryl Grignard reagent **1g** successfully (entry 7). Although sterically demanding substrate **1h** required higher reaction temperature and longer reaction time, it gave the corresponding biaryl **2h** in moderate to good yield (entry 8). The reaction is chemoselective; thus, nitrile, or nitro groups are tolerated (entries 9 and 10). It was observed that electron donating group on Grignard reagent (**1a, 1b, 1c** and **1d)** enhances the yield of coupling product compared to that of electron withdrawing group (**1f**, **1i** and **1j**). The reason can be explained same as discussed in the *section 4.1.4*. In all these experiments, formations of cross-coupling products were very less.

Table 4.8 Homocoupling of Grignard reagents with atmospheric oxygen as an oxidant using **C_6-C_{11}** complexes[a]

Entry	RMgBr	Product	Yield (%)[b]					
			C_6	**C_7**	**C_8**	**C_9**	**C_{10}**	**C_{11}**
1	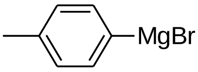 **1a**	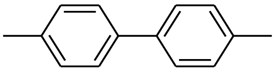 **2a**	74	**86**	43	68	**94**	39
2	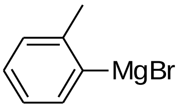 **1b**	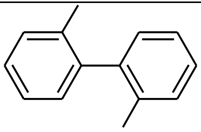 **2b**	61	**75**	34	59	**82**	27
3	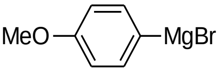 **1c**	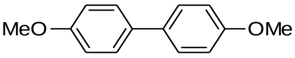 **2c**	78	**92**	50	73	**97**	46
4	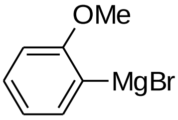 **1d**	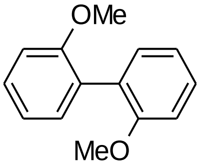 **2d**	63	**79**	37	59	**86**	30
5	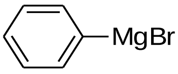 **1e**	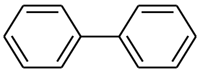 **2e**	68	**83**	39	62	**89**	33
6	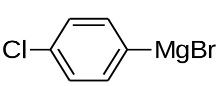 **1f**	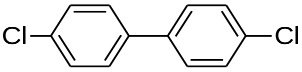 **2f**	64	**76**	35	56	**83**	29
7	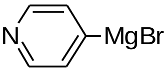 **1g**	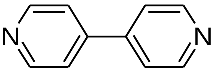 **2g**	59	**73**	33	52	**78**	25
8[c]	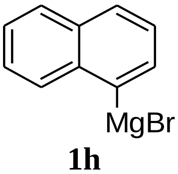 **1h**	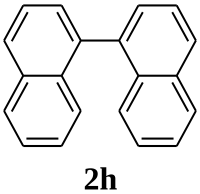 **2h**	53	**68**	28	51	**75**	20

9[d]	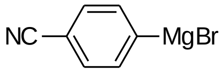 **1i**	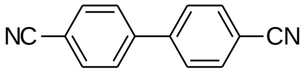 **2i**	45	**61**	24	46	**69**	15
10[d]	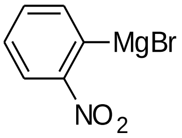 **1j**	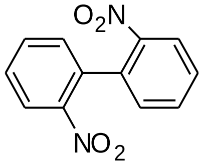 **2j**	49	**65**	26	49	**71**	17

[a] Reaction conditions: Mg turnings (0.320 g), aryl halide (10 mmol), catalyst (0.03mmol), Et_2O (10 ml).
[b] GC yield based on the amount of aryl halide.
[c] In THF, 60 °C, 10 h.
[d] reactions at -5 °C to room temp.

4.2.5 Proposed mechanism

The proposed mechanism is depicted in Fig. 4.6 for $\mathbf{C_7}$ catalyzed reaction. A low valent nickel species is generated by the Grignard reagent, which is a strong reducing agent (Ramnial et al. 2007) and is involved in the catalytic cycle. The oxidative addition of molecular oxygen to a low valent nickel complex **(a)** forms peroxo-nickel(III) intermediate **(b)** which is the key step of this catalytic cycle (Cho et al. 2009). It then reacts with two equivalents of RMgX to give biarylnickel(III) intermediate **(c)** and XMgOOMgX (Tsou and Kochi 1979, Cahiez et al. 2007). Thus formed biarylnickel(III) intermediate **(c)** undergoes rapid reductive elimination which eventually yields homocoupling product Ar-Ar and Ni(I) is regenerated. It is very reasonable to think that the formation of the unstable nickel(III) species (**c**) is required to achieve a very quick reductive elimination that gives (**d**) as the best way to favor the reductive elimination is to increase the oxidation state of the metal.

The formation of peroxo-nickel(III) intermediate was confirmed by the UV-vis spectral analysis (Fig. 4.6). The absorption peak of the catalytic reaction mixture that appeared at 419.2 nm can be attributed to peroxo-nickel(III) intermediate (Cho et al. 2009) and its absence in the reaction mixture carried out under inert condition further confirms the necessity of molecular oxygen for the present catalytic system.

Various iron (Cho et al. 2011), cobalt (Cho et al. 2010), nickel (Cho et al. 2009, Zapata-Rivera et al. 2012), copper (Zapata-Rivera et al. 2011) and palladium (Adamo et al. 2006, Popp et al. 2009)-catalyzed reactions are well established with such peroxo complexes as the catalytic intermediate.

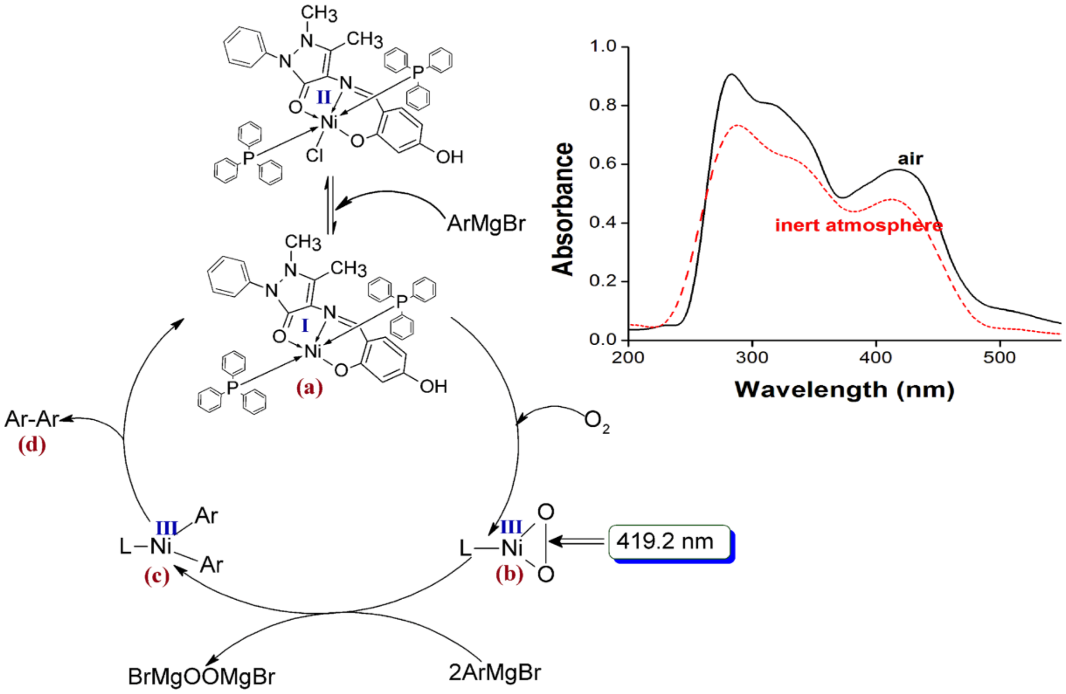

Figure 4.6 Proposed mechanism for the homocoupling of Grignard reagent using the complex **C_7**

Based on the above studies, the general mechanism for homocoupling of the Grignard reagent using the metal complexes **C_6**, **C_8** and **C_9–C_{11}** can be proposed as given in the Fig. 4.7 and Fig. 4.8, respectively.

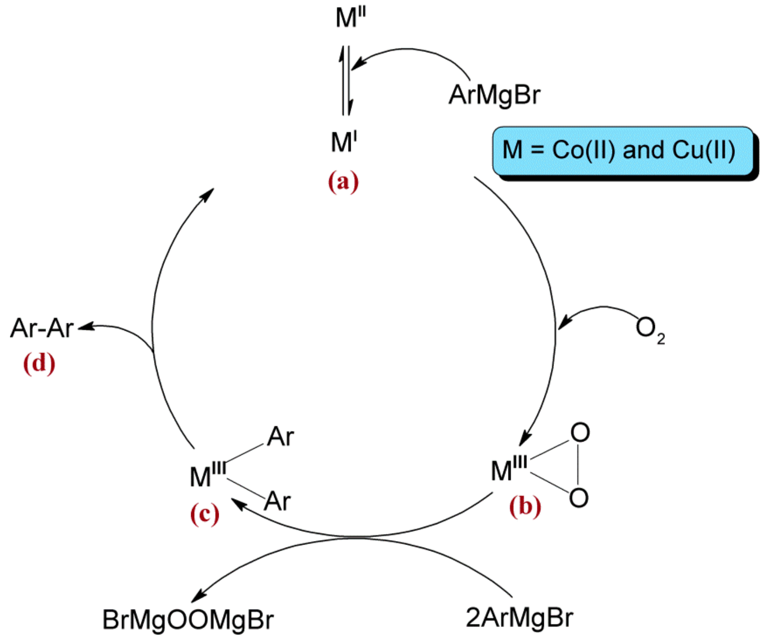

Figure 4.7 Proposed mechanism for the homocoupling reaction using the complexes **C_6** and **C_8**

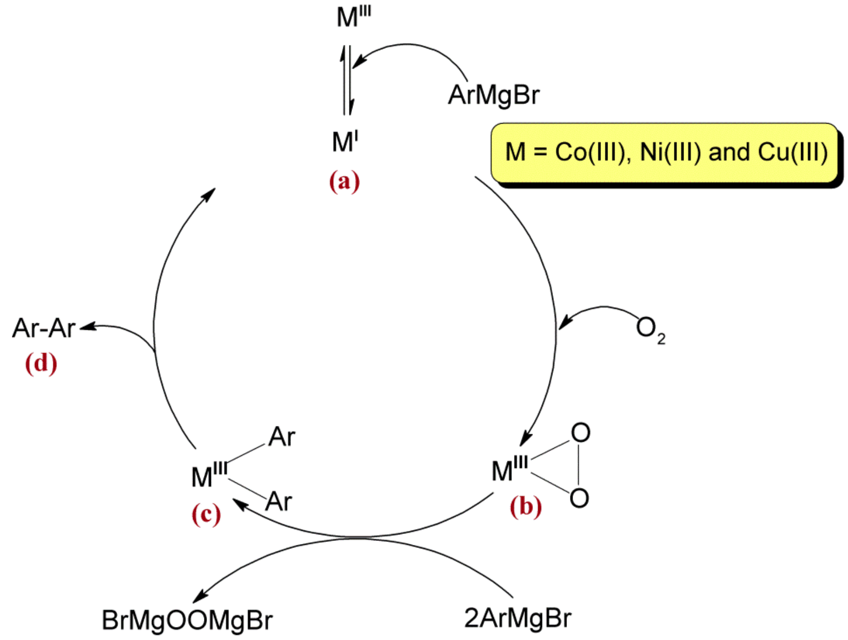

Figure 4.8 Proposed mechanism for the homocoupling reaction using the complexes **C_9-C_{11}**

From the catalytic activity studies, it was observed that, among the complexes containing Schiff base and PPh_3 ligands, complex **C_7** showed the highest catalytic activity which can be attributed to the faster reductive elimination to afford biaryls in good yield. The presence of triphenylphosphine groups which is more hindered ancillary ligand made the reductive elimination faster in the complex **C_7** than the complex **C_6** which is free from the triphenylphosphine ligand. This effect presumably arises from a relief in steric congestion upon generation of the free organic product and resulting metal center with a reduced coordination number (Hartwig 2007). The lesser catalytic activity of the complex **C_8** can be attributed to the difficulty in the two-electron oxidation of Cu(I) in association with the greater stability due to its completely filled *d-orbitals*. The triphenylphosphine free metal complexes blend with both Schiff base and dithiolate ligands also showed very good catalytic activity. Among them, **C_{10}** exhibits the highest catalytic efficiency. This can be attributed to its tendency to undergo faster oxidative addition (Anderson et al. 1997) than **C_9** which are under the same ligand environment and oxidation state. This is due to the electron rich nickel center. Hence lesser yield of biaryl was obtained from the catalytic activity of the complex **C_9** than that of **C_{10}**. The least catalytic activity of **C_{11}** can be attributed to the difficulty in the two-electron oxidation of Cu(I) in association with the greater stability due to its completely filled *d-orbitals*. Among the cobalt complexes, **C_6** showed higher coupling yield. This may be due to the higher stability of the complex **C_9** in association with the chelating dithiolate ligand which made it less reactive. Among nickel complexes, **C_{10}** showed the maximum activity. Comparatively lesser catalytic activity of **C_7** can be attributed to its steric hindered triphenylphosphine ligand which slowers the association of incoming substrate to the metal center. Among copper complexes, **C_8** gave better yield than **C_{11}**. This can be reasoned to the faster reductive elimination in the complex **C_8** than that compared to the complex **C_{11}**. It can be attributed to its steric hindered triphenylphosphine ligand which undergoes faster reductive elimination than triphenylphosphine free **C_{11}**.

4.3 CATALYTIC ACTIVITY STUDIES OF C_{12}-C_{17}

The reaction conditions for the coupling of phenylmagnesium bromide (**1e**) were optimized with respect to

- solvent
- time
- catalyst concentration

4.3.1 Solvent effect

The catalytic activities of the complexes **C_{12}-C_{17}** were checked in tetrahydrofuran, diethyl ether and benzene with atmospheric oxygen as the oxidant (Table 4.9). The best conversion was observed in diethyl ether as ether molecules actually coordinate with and thus helps in stabilizing the Grignard reagent (entry 2). The least conversion was observed in benzene, since the formation of polar Grignard reagent stops in most non-polar organic solvents as it forms an insoluble deposit at the metallic surface. The order of increasing percentage yield in tested solvents follows, benzene < tetrahydrofuran < diethyl ether.

Table 4.9 Optimization of homocoupling of phenylmagnesium bromide (**1e**) in different solvents[a]

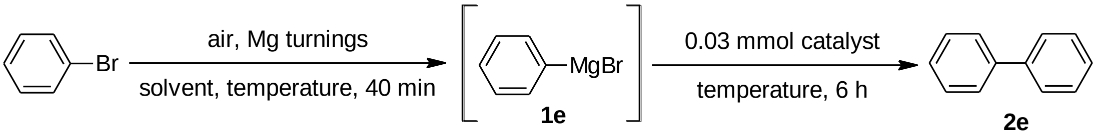

Entry	Solvent	Temp.(°C)	Yield (%)[b]					
			C_{12}	**C_{13}**	**C_{14}**	**C_{15}**	**C_{16}**	**C_{17}**
1	tetrahydrofuran	60	28	17	33	32	22	39
2	**diethyl ether**	**r.t[c]**	**68**	**61**	**73**	**74**	**67**	**80**
3	benzene	40	16	9	20	18	13	26

[a] Reaction conditions: Mg turnings (0.320 g), bromobenzene (10 mmol), catalyst (0.03 mmol), solvent (10 ml).

[b] GC yield based on the amount of bromobenzene.

[c] r.t = Room temperature.

4.3.2 Effect of reaction time

The dependence of product yield on the reaction time for the coupling of **1e** was studied by analyzing the reaction mixture at regular intervals of time under identical reaction conditions. The yield increased with reaction time (Fig.4.9). The complexes (**C_{12}-C_{16}**) achieved maximum yield in 6 h. The complex **C_{17}** yielded the maximum in minimum time of 5.5 h. The results are tabulated in the Table 4.10.

Table 4.10 Optimization of homocoupling of phenylmagnesium bromide (**1e**) w.r.to time[a]

Tr. No.	Time (min)	Yield (%)[b]					
		C_{12}	**C_{13}**	**C_{14}**	**C_{15}**	**C_{16}**	**C_{17}**
1	0	0.0	0.0	0.0	0.0	0.0	0.0
2	60	18.3	16.2	23.5	20.2	17.3	29.2
3	120	27.4	21.5	32.6	29.4	24.7	37.3
4	180	38.7	32.7	40.4	42.6	37.4	43.2
5	240	47.6	39.2	49.6	51.3	43.5	57.6
6	300	51.2	46.3	58.2	54.5	47.4	69.2
7	**330**	55.3	53.3	63.3	62.7	58.5	**80.2**
8	**360**	**68.2**	**61.4**	**73.0**	**74.0**	**67.2**	79.9
9	420	68.1	61.2	72.8	74	66.9	79.8
10	480	67.8	60.9	72.7	73.9	66.3	79.2
11	540	67.9	61.3	73	73.6	65.9	79.5
12	600	68.0	61.1	72.9	73.8	66.2	79.9

[a] Reaction conditions: Mg turnings (0.320 g), bromobenzene (10 mmol), catalyst (0.03 mmol), Et_2O (10 ml).
[b] GC yield based on the amount of bromobenzene.

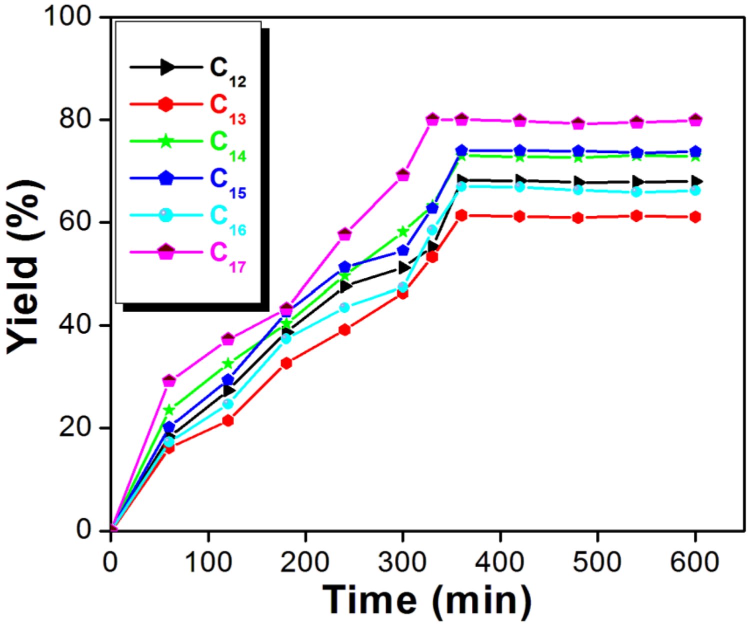

Figure 4.9 Effect of reaction time on the yield of bromobenzene to biphenyl

4.3.3 Effect of catalyst loading and influence of air on the reaction

To study the effect of catalyst concentration on the reaction, substrate to catalyst ratio was varied from total catalyst amount 0.01 mmol to 0.05 mmol (Table 4.11). Herewith we describe the effect of the concentration of the complex **C_{17}** on the coupling of **1e** in detail. The yield increased with increase in catalyst loading and reaches to the highest value of 80 % with 0.03 mmol of catalyst loading (entry 5). The yields were not very sensitive to the catalyst loading at higher concentration and can be explained same as discussed in the *section 4.1.3*. The efficiency of the complex **C_{17}** should be underlined since, in the absence of nickel(III) complex, only traces of coupling product was observed (entry 1). The present coupling can be readily scaled up to the reaction of 50.0 mmol of the aryl halide using 0.15 mmol of the catalyst and gave 78 % of biaryl with negligible amount of byproducts (entry 10). This further supports the efficiency of the synthesized complex as competent catalyst for the homocoupling reaction.

We have investigated the feasibility of the coupling reaction under an inert (argon) atmosphere using 0.03 mmol of catalyst (entry 9, Table 4.9). But, insignificant amount of product was detected. This can be attributed to the lack of formation of peroxo-nickel(III) active species. This signifies the role of atmospheric oxygen as the oxidant and its necessity in present reaction system. Similar trend was observed for rest of the complexes.

Table 4.11 Effect of the concentration of $\mathbf{C_{17}}$ on the yield of coupling product[a]

Entry	Amount of complex ($\mathbf{C_{17}}$) (mmol)	Yield(%)[b]
1	No catalyst	01.1
2	0.01	28.4
3	0.015	39.5
4	0.02	64.3
5	0.025	72.5
6	**0.03**	**80.2**
7	0.04	79.5
8	0.05	78.3
9[c]	**0.03**	**05.2**
10[d]	**0.15**	**78.0**

[a]Reactions were carried out with 10 mmol of bromobenzene in presence of atmospheric molecular oxygen.

[b] GC yield based on the amount of bromobenzene.

[c] Inert atmosphere (argon).

[d] With 50.0 mmol of bromobenzene in the presence of 0.15 mmol catalyst for 10 h.

4.3.4 Scope of the reaction

This promising result encouraged us to extend the scope of the reaction to various aryl Grignard reagents (Table 4.12). Thus, simple and functionalized biaryl compounds were synthesized in good yields (entries 1–10). Introduction of methyl group at the *ortho*-position of the aryl Grignard reagent **1b** resulted in somewhat lower yield of the homocoupling product (entry 2). 4-Methoxy- and 2-methoxyphenylmagnesium bromide can be efficiently converted into the corresponding biaryls **2c** and **2d**, respectively, under similar conditions (entries 3 and 4). It is noteworthy that the present reaction system is tolerant of aryl chloride functionality (entry 6). Also it allows the coupling of heteroaryl Grignard reagent **1g** successfully (entry 7). Although sterically demanding substrate **1h** required higher reaction temperature and longer reaction time, it gave the corresponding biaryl **2h** in moderate to good yield (entry 8). The reaction is chemoselective; thus, nitrile, or nitro groups are tolerated (entries 9 and 10). It was observed that electron donating group (**1a, 1b, 1c** and **1d**) on Grignard reagent enhances the yield of coupling product compared to that of electron withdrawing group (**1f**, **1i** and **1j**). The reason is the same as explained in the *section 4.1.4.*

Table 4.12 Homocoupling of Grignard reagents with atmospheric oxygen as an oxidant using **C_{12}-C_{17}** complexes[a]

Entry	RMgBr	Product	Yield (%)[b]					
			C_{12}	**C_{13}**	**C_{14}**	**C_{15}**	**C_{16}**	**C_{17}**
1	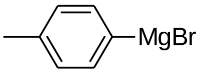 **1a**	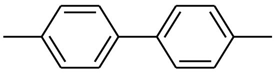 **2a**	73	65	78	79	75	**89**
2	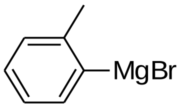 **1b**	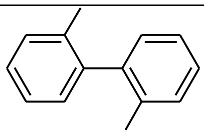 **2b**	61	53	66	67	63	**77**
3	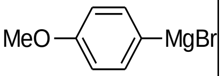 **1c**	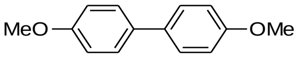 **2c**	77	69	82	83	79	**93**
4	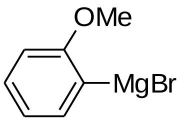 **1d**	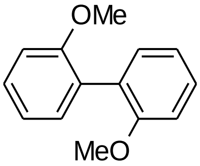 **2d**	64	58	70	71	65	**79**
5	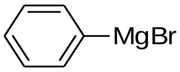 **1e**	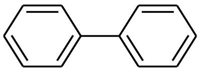 **2e**	68	61	73	74	67	**80**
6	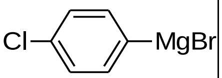 **1f**	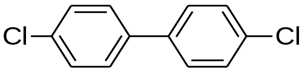 **2f**	63	57	68	69	63	**74**

7	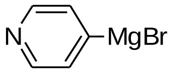 **1g**	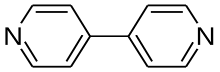 **2g**	58	53	64	67	59	**69**
8[c]	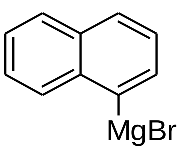 **1h**	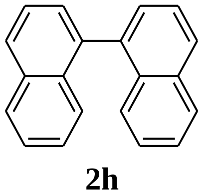 **2h**	54	51	60	64	56	**66**
9[d]	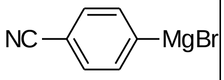 **1i**	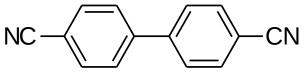 **2i**	49	43	56	58	51	**61**
10[d]	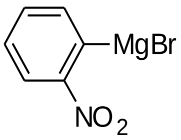 **1j**	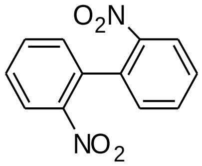 **2j**	53	47	59	60	52	**63**

[a] Reaction conditions: Mg turnings (0.320 g), aryl halide (10 mmol), catalyst (0.03mmol), Et_2O (10 ml).

[b] GC yield based on the amount of aryl halide.

[c] In THF, 60 °C, 10 h.

[d] reactions at -5 °C to room temp.

4.3.5 Proposed mechanism

The proposed mechanism is depicted in Fig. 4.35 for **C_{12}** catalyzed reaction. A low valent nickel species is generated by the Grignard reagent, which is a strong reducing agent (Ramnial et al. 2007) and is involved in the catalytic cycle. The oxidative addition of molecular oxygen to a low valent nickel complex **(a)** forms peroxo-nickel(III) intermediate **(b)** which is the key step of this catalytic cycle (Cho et al. 2009). It then reacts with two equivalents of RMgX to give biarylnickel(III) intermediate **(c)** and XMgOOMgX (Tsou and Kochi 1979, Cahiez et al. 2007). Thus formed biarylnickel(III) intermediate **(c)** undergoes rapid reductive elimination which eventually yields homocoupling product Ar-Ar and Ni(I) is regenerated. It is very reasonable to think that the formation of the unstable nickel(III) species (**c**) is required to achieve a very quick reductive elimination that gives (**d**) as the best way to favor the reductive elimination is to increase the oxidation state of the metal.

The formation of peroxo-nickel(III) intermediate was confirmed by the UV-vis spectral analysis. The absorption peak of the catalytic reaction mixture that appeared at 421.1 nm can be attributed to peroxo-nickel(III) intermediate (Cho et al. 2009) and its absence in the reaction mixture carried out under inert condition further confirms the necessity of molecular oxygen for the present catalytic system. Various iron (Cho et al. 2011), cobalt (Cho et al. 2010), nickel (Cho et al. 2009, Zapata-Rivera et al. 2012), copper (Zapata-Rivera et al. 2011) and palladium (Adamo et al. 2006, Popp et al. 2009)-catalyzed reactions are well established with such peroxo complexes as the catalytic intermediate.

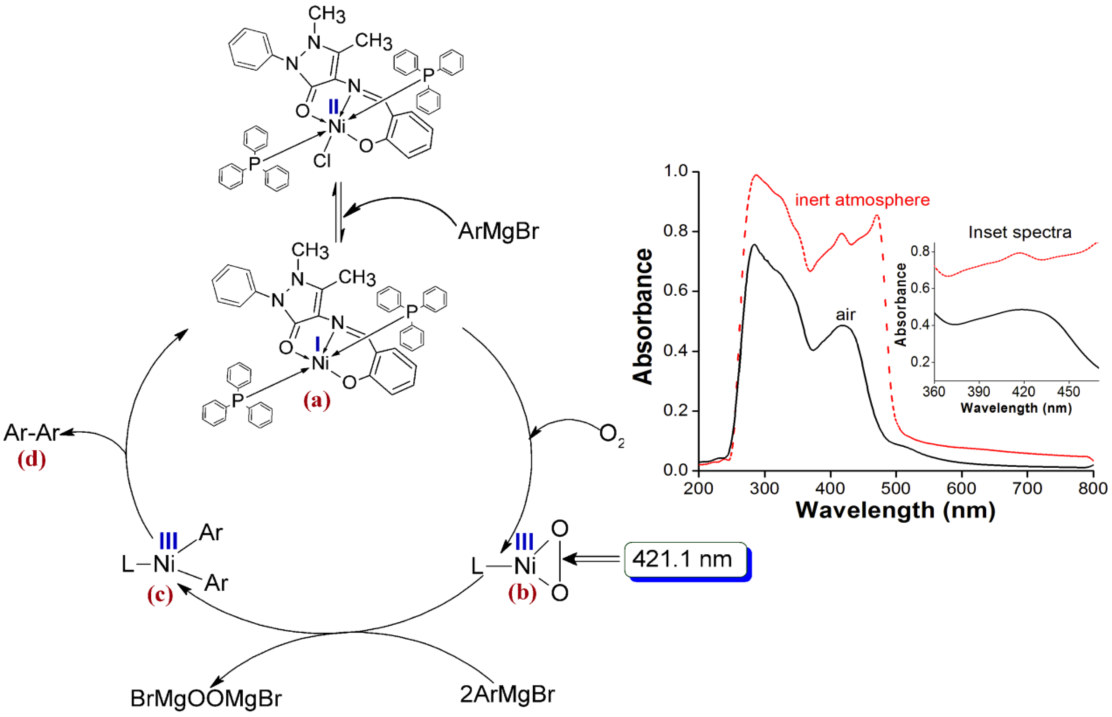

Figure 4.10 Proposed mechanism for the homocoupling of Grignard reagent using the complex **C_{12}**

Based on the above studies, the general mechanism for homocoupling of the Grignard reagent using the metal complexes **C_{13}-C_{14}** and **C_{15}-C_{17}** can be proposed as given in Fig. 4.11 and Fig. 4.12, respectively.

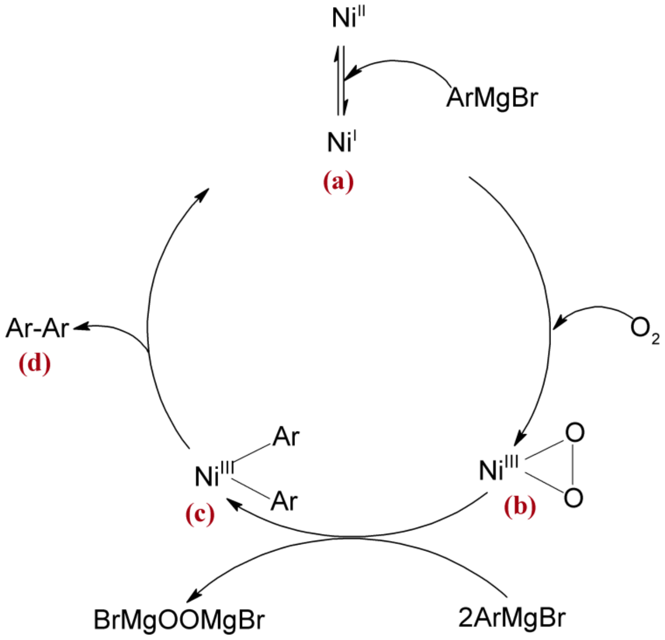

Figure 4.11 Proposed mechanism for the homocoupling of Grignard reagent using the complexes $\mathbf{C_{13}}$ and $\mathbf{C_{14}}$

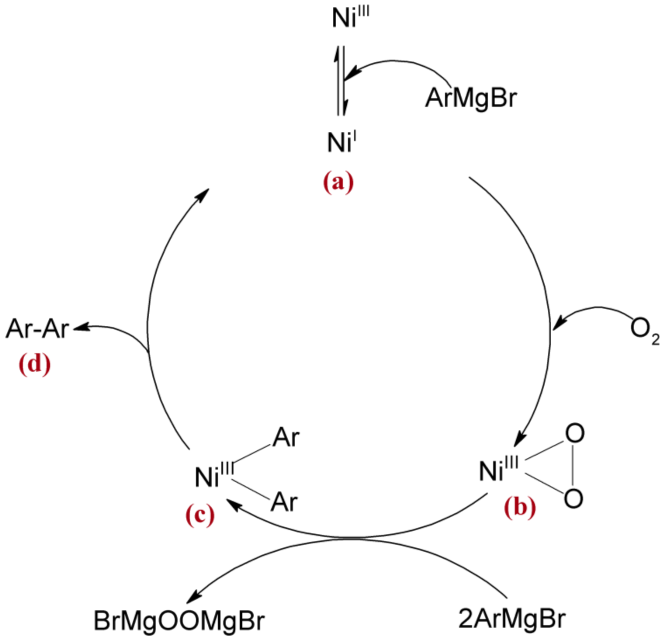

Figure 4.12 Proposed mechanism for the homocoupling of Grignard reagent using the complexes $\mathbf{C_{15}}$-$\mathbf{C_{17}}$

The catalytic activities exhibited a strong dependence on the ancillary ligands utilized for the catalyst. In present study, difference in catalytic activities is mainly due to the variation in the substituents of Schiff base ligands (ancillary ligands). The ligands may affect all three steps involved in the catalytic cycle, but the catalysts which accelerate the rate-determining step will be desirable. The highest catalytic activity was observed for **C_{14}** among **C_{12}-C_{14}** and **C_{17}** among **C_{15}-C_{17}** catalyzed reactions, respectively. This could be credited to the tendency for oxidative addition reaction. Oxidative addition usually occurs faster from more electron-rich metal centers than from more electron-poor metal centers possessing similar steric properties. This effect can be rationalized using thermodynamic arguments. If the reaction is considered an overall oxidative process at the metal, then the reaction will be more favored thermodynamically when the metal center of the reactant is more electron-rich. In the complexes **C_{14}** and **C_{17}**, delocalization of π-electrons in naphthyl ring makes the nickel center electron rich, making the metal more nucleophilic and thus facilitating the oxidative addition step in a faster rate. The least catalytic activity of complexes **C_{13}** among **C_{12}-C_{14}** and **C_{16}** among **C_{15}-C_{17}** can be credited to its electron withdrawing ancillary ligand which decreases the electron density around metal centre which makes the metal less nucleophilic and thus tend to undergo oxidative addition more slowly. The complexes (**C_{15}-C_{17}**) containing dmit and Schiff base ligands showed better catalytic activity than the complexes (**C_{12}-C_{14}**) with triphenylphosphine and Schiff base ligand which can be attributed to its steric hindered triphenylphosphine ligand which slower the association of incoming substrate to the metal center.

4.4 CATALYTIC ACTIVITY STUDIES OF C_{18}-C_{23}

The reaction conditions for the coupling of phenylmagnesium bromide (**1e**) were optimized with respect to

- solvent
- time
- catalyst concentration

4.4.1 Solvent effect

The activities of the complexes **C_{18}-C_{23}** were checked in different solvents, tetrahydrofuran, diethyl ether, benzene, etc., with molecular oxygen as oxidant (Table 4.13). The best conversion was observed in diethyl ether as ether molecules actually coordinate with and thus helps in stabilizing the Grignard reagent (entry 2). The least conversion was observed in benzene, since the formation of polar Grignard reagent stops in most non-polar organic solvents as it forms an insoluble deposit at the metallic surface. The order of increasing percentage yield in tested solvents follows, benzene < tetrahydrofuran < diethyl ether.

Table 4.13 Optimization of homocoupling of phenylmagnesium bromide (**1e**)[a] in different solvents

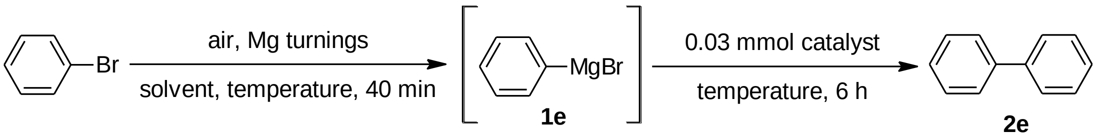

Entry	Solvent	Temp. (°C)	Yield (%)[b]					
			C_{18}	**C_{19}**	**C_{20}**	**C_{21}**	**C_{22}**	**C_{23}**
1	tetrahydrofuran	60	34	43	22	25	38	17
2	**diethyl ether**	**r.t[c]**	**64**	**81**	**51**	**57**	**75**	**45**
3	benzene	40	21	33	14	18	26	9

[a] Reaction conditions: Mg turnings (0.320 g), bromobenzene (10 mmol), catalyst (0.03 mmol), solvent (10 ml).
[b] GC yield based on the amount of bromobenzene.
[c] r.t = Room temperature.

4.4.2 Effect of reaction time

The dependence of product yield on reaction time for the coupling of **1e** was studied by analyzing the reaction mixture at regular intervals of time under similar reaction conditions. The yield increased with reaction time (Fig. 4.13). The complexes required 6 h to achieve the maximum yield. Among all the complexes **C_{18}–C_{23}**, the complex **C_{22}** yielded the maximum. The results are tabulated in the Table 4.14**.**

Table 4.14 Optimization of homocoupling of phenylmagnesium bromide (**1e**) w.r.to time [a]

Tr. No.	Time (min)	Yield (%) [b]					
		C_{18}	**C_{19}**	**C_{20}**	**C_{21}**	**C_{22}**	**C_{23}**
1	0	0.0	0.0	0.0	0.0	0.0	0.0
2	60	14.1	19.4	7.2	11.1	23.0	3.2
3	120	19.3	23.2	12.8	14.3	38.2	10.4
4	180	28.6	31.6	18.7	24.2	43.5	16.6
5	240	33.8	45.2	27.5	31.5	51.2	22.3
6	300	45.4	56.1	31.4	44.2	58.5	26.9
7	330	55.3	60.7	42.2	50.3	66.2	31.2
8	**360**	**63.8**	**81.2**	**51.1**	**57.3**	**74.8**	**44.9**
9	420	63.6	81.0	51.0	57.2	74.4	44.7
10	480	63.5	80.9	50.9	57.2	74.0	44.7
11	540	63.4	80.9	50.8	57.1	73.9	44.6
12	600	63.2	80.7	50.8	57.0	73.1	44.5

[a] Reaction conditions: Mg turnings (0.320 g), bromobenzene (10 mmol), catalyst (0.03 mmol), Et_2O (10 ml).
[b] GC yield based on the amount of bromobenzene.

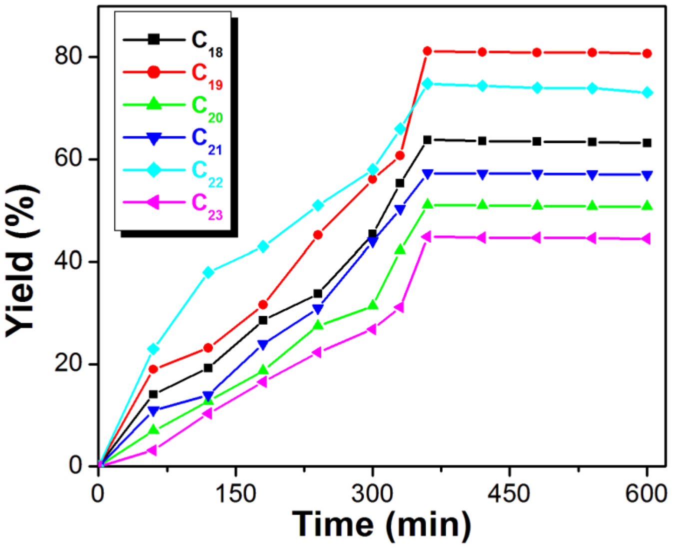

Figure 4.13 Effect of reaction time on the yield of bromobenzene to biphenyl

4.4.3 Effect of catalyst loading and influence of air on the reaction

To study the effect of catalyst concentration on the reaction, substrate to catalyst ratio was varied from total catalyst amount 0.01 mmol to 0.05 mmol (Table 4.15). Herewith we describe the effect of the concentration of the complex $\mathbf{C_{22}}$ on the coupling of **1e** in detail. The yield increased with increase in catalyst loading and reaches to the highest value of 75% with 0.03 mmol of catalyst (entry 6). At higher catalyst loading the yields were not very sensitive. The reason is the same as discussed in *section 4.1.3*. The efficiency of the complex $\mathbf{C_{22}}$ should be underlined since, in the absence of nickel(III) complex, only traces of coupling product was observed featuring the catalytic role of the complex for the present system (entry 1). Notably, the present coupling can be readily scaled up to the reaction of 50.0 mmol of the aryl halide using 0.15 mmol of the catalyst, which afford 70 % of biaryl with a negligible amount of side products. This further supports the efficiency of the synthesized complex as competent catalyst for the homocoupling reaction (entry 10).

The feasibility of the coupling reaction was investigated under an inert atmosphere (argon). A lower yield was obtained can be attributed to the lack of formation of peroxo-nickel(III) active species (entry 9). This emphasizes the role of atmospheric oxygen as an effective oxidant in the present study. Similar trend was observed for rest of the complexes and they achieved maximum yield with the amount of 0.03 mmol.

Table 4.15 Effect of the concentration of $\mathbf{C_{22}}$ on the yield of coupling product[a]

Entry	Amount of complex ($\mathbf{C_{22}}$) (mmol)	Yield(%)[b]
1	**No catalyst**	**01.1**
2	0.01	29.4
3	0.015	40.5
4	0.02	54.3
5	0.025	63.2
6	**0.03**	**74.9**
7	0.04	72.8

8	0.05	72.7
9[c]	**0.03**	**05.2**
10[d]	**0.15**	**70.0**

[a] Reactions were carried out with 10 mmol of bromobenzene in presence of atmospheric molecular oxygen.
[b] GC yield based on the amount of bromobenzene.
[c] Inert atmosphere (argon).
[d] With 50.0 mmol of bromobenzene in the presence of 0.15 mmol catalyst for 10 h.

4.4.4 Scope of the reaction

This promising result encouraged us to extend the scope of the reaction to various aryl Grignard reagents (Table 4.16). Thus, simple and functionalized biaryl compounds were synthesized in good yields (entries 1–10). Introduction of methyl group at the ortho-position of the aryl Grignard reagent **1b** resulted in somewhat lower yield of the homocoupling product (entry 2). 4-Methoxy- and 2-methoxyphenylmagnesium bromide can be efficiently converted into the corresponding biaryls **2c** and **2d**, respectively, under similar conditions (entries 3 and 4). It is noteworthy that the present reaction system is tolerant of aryl chloride functionality (entry 6). Also it allows the coupling of heteroaryl Grignard reagent **1g** successfully (entry 7). Although sterically demanding substrate **1h** required higher reaction temperature and longer reaction time, it gave the corresponding biaryl **2h** in moderate to good yield (entry 8). The reaction is chemoselective; thus, nitrile, or nitro groups are tolerated (entries 9 and 10). It was observed that electron donating group on Grignard reagent (**1a**, **1b**, **1c** and **1d**) enhances the yield of coupling product compared to that of electron withdrawing group (**1f**, **1i** and **1j**). The reason can be explained as discussed in the *section 4.1.4*. In all these experiments, formations of cross-coupling products were very less.

Table 4.16 Homocoupling of Grignard reagents with atmospheric oxygen as an oxidant using $\mathbf{C_{18}}$-$\mathbf{C_{23}}$ complexes [a]

Entry	RMgBr	Product	Yield (%)[b]					
			$\mathbf{C_{18}}$	$\mathbf{C_{19}}$	$\mathbf{C_{20}}$	$\mathbf{C_{21}}$	$\mathbf{C_{22}}$	$\mathbf{C_{23}}$
1	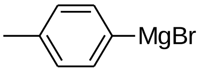 **1a**	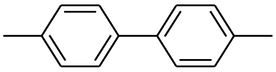 **2a**	70	**84**	55	63	**81**	51
2	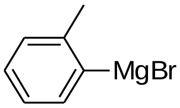 **1b**	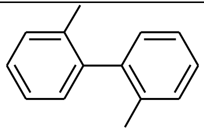 **2b**	60	**73**	47	54	**71**	43
3	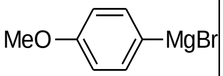 **1c**	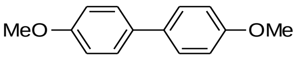 **2c**	75	**90**	60	70	**87**	55
4	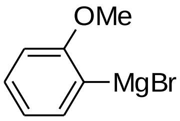 **1d**	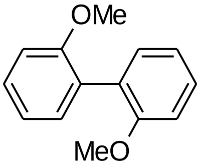 **2d**	62	**75**	49	55	**70**	44
5	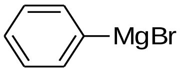 **1e**	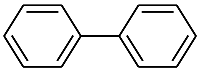 **2e**	64	**81**	51	57	**75**	45
6	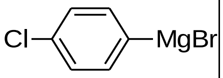 **1f**	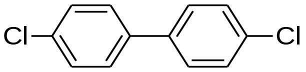 **2f**	59	**73**	45	53	**69**	42
7	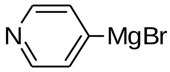 **1g**	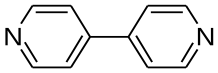 **2g**	54	**70**	42	48	**65**	38

8^c	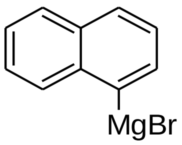 **1h**	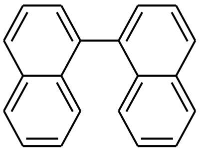 **2h**	52	**66**	37	44	**64**	30
9^d	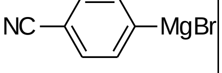 **1i**	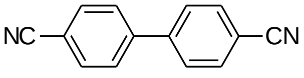 **2i**	48	**60**	33	40	**59**	24
10^d	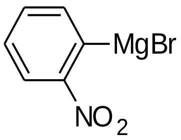 **1j**	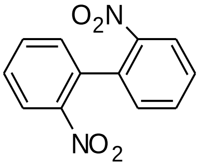 **2j**	50	**63**	35	43	**62**	27

[a] Reaction conditions: Mg turnings (0.320 g), aryl halide (10 mmol), catalyst (0.03mmol), Et_2O (10 ml).
[b] GC yield based on the amount of aryl halide.
[c] In THF, 60 °C, 10 h.
[d] reactions at -5 °C to room temp.

4.4.5 Proposed mechanism

A proposed mechanism is depicted in Fig. 4.14 for **C_{19}** catalyzed reaction. . A low valent nickel species is generated by the Grignard reagent, which is a strong reducing agent (Ramnial et al. 2007) and is involved in the catalytic cycle. The oxidative addition of molecular oxygen to a low valent nickel complex **(a)** forms peroxo-nickel(III) intermediate **(b)** which is the key step of this catalytic cycle (Cho et al. 2009). It then reacts with two equivalents of RMgX to give biarylnickel(III) intermediate **(c)** and XMgOOMgX (Tsou and Kochi 1979, Cahiez et al. 2007). Thus formed biarylnickel(III) intermediate **(c)** undergoes rapid reductive elimination which eventually yields homocoupling product Ar-Ar and Ni(I) is regenerated. It is very reasonable to think that the formation of the unstable nickel(III) species (**c**) is required to achieve a very quick reductive elimination that gives (**d**) as the best way to favor the reductive elimination is to increase the oxidation state of the metal.

The formation of peroxo-nickel(III) intermediate was confirmed by the UV-vis spectral analysis. The absorption peak of the catalytic reaction mixture that appeared at 419 nm can be attributed to peroxo-nickel(III) intermediate (Cho et al.

2009) and its absence in the reaction mixture carried out under inert condition further confirms the necessity of molecular oxygen for the present catalytic system. Various iron (Cho et al. 2011), cobalt (Cho et al. 2010), nickel (Cho et al. 2009, Zapata-Rivera et al. 2012), copper (Zapata-Rivera et al. 2011) and palladium (Adamo et al. 2006, Popp et al. 2009)-catalyzed reactions are well established with such peroxo complexes as the catalytic intermediate.

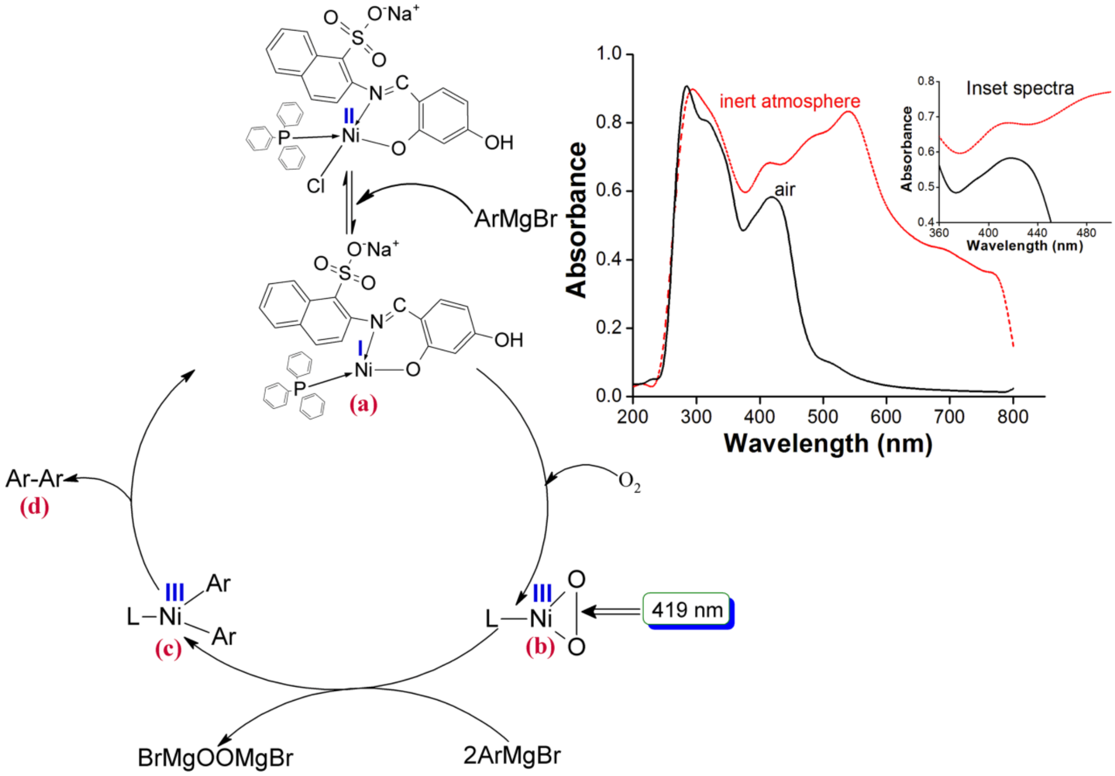

Figure 4.14 Proposed mechanism for the homocoupling of Grignard reagent using the complex **C_{19}**

The general mechanism for homocoupling of the Grignard reagent using the metal complexes **C_{18}** and **C_{20}-C_{23}** can be proposed as given in the Fig. 4.15.

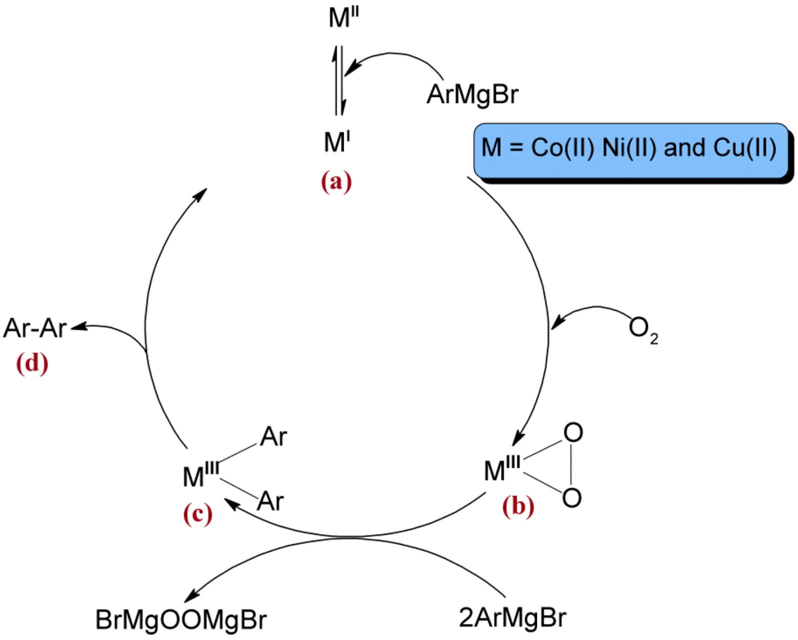

Figure 4.15 Proposed mechanism for the homocoupling reaction using the complexes $\mathbf{C_{18}}$ and $\mathbf{C_{20}}$-$\mathbf{C_{23}}$

From the catalytic activity studies it was observed that, among the complexes ($\mathbf{C_{18}}$-$\mathbf{C_{20}}$) containing Schiff base and PPh_3 ligands, complex $\mathbf{C_{19}}$ showed the highest catalytic activity which can be attributed to the faster oxidative addition reaction to afford biaryls in good yield. This must be due to its electron rich metal center compared to that of $\mathbf{C_{18}}$. The lesser catalytic activity of complex $\mathbf{C_{20}}$ can be attributed to the difficulty in the two-electron oxidation of Cu(I) in association with the greater stability due to its completely filled *d-orbitals*. The triphenylphosphine free metal complexes ($\mathbf{C_{21}}$-$\mathbf{C_{23}}$) blend with both Schiff base and dithiolate ligands also showed very good catalytic activity. Among them, $\mathbf{C_{22}}$ showed the highest catalytic efficiency which can be attributed to its tendency to undergo oxidative addition faster than from the cobalt complex under the same ligand environment and oxidation state due to the electron rich metal center. The catalytic activity of $\mathbf{C_{23}}$ yielded the least amount of catalytic product which can be once again attributed to the difficulty in the two-electron oxidation of Cu(I) in association with the greater stability due to its completely filled *d-orbitals*. Among two sets of complexes ($\mathbf{C_{18}}$-$\mathbf{C_{20}}$) and ($\mathbf{C_{21}}$-$\mathbf{C_{23}}$), complexes containing bidentate Schiff base and triphenylphosphine ligands showed better catalytic activity than that containing dmit and Schiff base complexes. This may be due to the higher stability of the complexes (**C_{21}-C_{23}**) in association with the chelating dithiolate ligand which made it less reactive. Also, it was observed that the bidentate N,O-Schiff base complexes afford lesser yield compared to that of tridentate O,N,O-Schiff base complexes. This can be attributed to their electron poor metal center which slows down the oxidative addition reaction in catalytic cycle.

4.5 CATALYTIC ACTIVITY STUDIES OF C_{24}-C_{29}

The reaction conditions for the coupling of phenylmagnesium bromide (**1e**) were optimized with respect to

- solvent
- time
- catalyst concentration

4.5.1 Solvent effect

The catalytic activities of the complexes **C_{24}-C_{29}** were checked in tetrahydrofuran, diethyl ether and benzene using atmospheric oxygen as oxidant (Table 4.17). The best conversion was observed in diethyl ether as ether molecules actually coordinate with and thus helps in stabilizing the Grignard reagent (entry 2). The least conversion was observed in benzene, since the formation of polar Grignard reagent stops in most non-polar organic solvents as it forms an insoluble deposit at the metallic surface. The order of increasing percentage yield in tested solvents follows, benzene < tetrahydrofuran < diethyl ether.

Table 4.17 Optimization of homocoupling of phenylmagnesium bromide (**1e**) in different solvents [a]

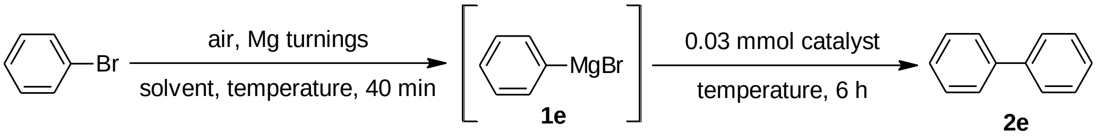

Entry	Solvent	Temp. (°C)	Yield (%)[b]					
			C_{24}	**C_{25}**	**C_{26}**	**C_{27}**	**C_{28}**	**C_{29}**
1	tetrahydrofuran	60	36	57	29	39	49	19
2	**diethyl ether**	**r.t[c]**	**73**	**93**	**71**	**79**	**90**	**43**
3	benzene	40	24	39	17	27	34	10

[a] Reaction conditions: Mg turnings (0.320 g), bromobenzene (10 mmol), catalyst (0.03 mmol), solvent (10 ml).

[b] GC yield based on the amount of bromobenzene.

[c] r.t = Room temperature.

4.5.2 Effect of reaction time

The dependence of product yield on reaction time for the coupling of **1e** was studied by analyzing the reaction mixture at regular intervals of time under similar reaction conditions. The yield increased with reaction time (Fig. 4.16). The complexes **C_{24}**, **C_{26}**, **C_{27}** and **C_{29}** required 5.30 h to achieve maximum yield. The total reaction time of 5.0 h at room temperature gave a constant conversion of the highest yield for **C_{28}**. Among all the complexes **C_{25}-C_{29}**, the complex **C_{25}** yielded the maximum in minimum time of 4.30 h. The results are tabulated in the Table 4.18.

Table 4.18 Optimization of homocoupling of phenylmagnesium bromide (**1e**)[a] w.r.to time

Tr. No.	Time (min)	Yield (%)[b]					
		C_{24}	**C_{25}**	**C_{26}**	**C_{27}**	**C_{28}**	**C_{29}**
1	0	0.0	0.0	0.0	0.0	0.0	0.0
2	60	22.5	44.1	8.5	25.3	36.5	4.5
3	120	36.2	59.9	16.7	31.2	52.6	11.9
4	180	47.5	71.4	22.3	40.2	65.3	18.7
5	240	55.9	82.5	29.7	49.7	75.9	24.3
6	**270**	60.6	**93.2**	41.8	54.6	82.7	28.5
7	**300**	66.8	93.2	58.3	63.8	**89.9**	31.8
8	**330**	**73.3**	93.1	**71.1**	**78.9**	89.7	**42.9**

9	360	73.2	93.0	71.0	78.7	89.7	42.8
10	420	73.1	93.0	70.9	78.7	89.6	42.7
11	480	73.1	92.9	70.7	78.6	89.6	42.7

[a] Reaction conditions: Mg turnings (0.320 g), bromobenzene (10 mmol), catalyst (0.03 mmol), Et_2O (10 ml).
[b] GC yield based on the amount of bromobenzene.

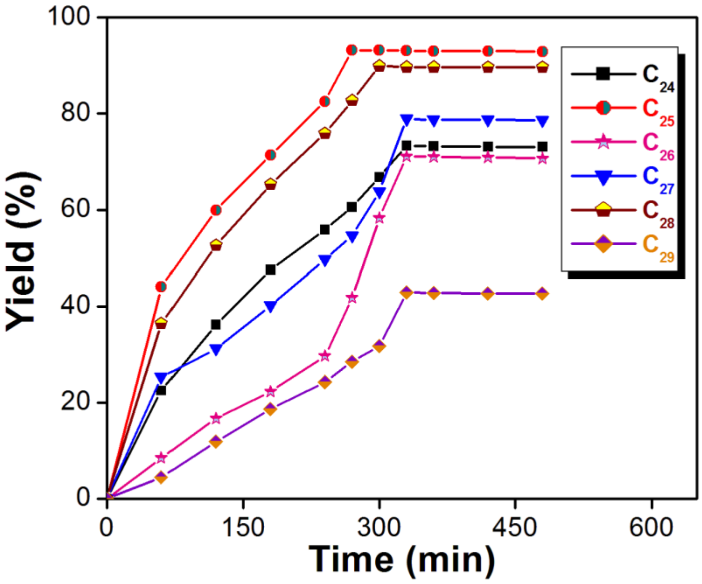

Figure 4.16 Effect of reaction time on the yield of bromobenzene to biphenyl

4.5.3 Effect of catalyst loading and influence of air on the reaction

To study the effect of catalyst concentration on the reaction, substrate to catalyst ratio was varied from total catalyst amount 0.01 mmol to 0.05 mmol (Table 4.19). Herewith we describe the effect of the concentration of the complex $\mathbf{C_{25}}$ on the coupling of **1e** in detail. The yield increased with increase in catalyst loading after reaching optimum concentration further increase of catalyst amount did not affect the yield of coupling product significantly and remained almost constant. At higher catalyst loading the yields were not very sensitive. The reason is the same as discussed in *section 4.1.3*. The highest value of 93% yield was obtained with 0.025 mmol of catalyst loading (entry 5). The efficiency of the complex $\mathbf{C_{25}}$ should be underlined since, in the absence of nickel(III) complex, only traces of coupling product was observed featuring the catalytic role of the complex for the present system (entry 1). Notably, the present coupling can be readily scaled up to the reaction of 50.0 mmol of the aryl halide using 0.125 mmol of the catalyst, which afford 88 % of biaryl with a negligible amount of side products. This further supports the efficiency of the synthesized complex as competent catalyst for the homocoupling reaction (entry 10).

The feasibility of the coupling reaction was investigated under an inert atmosphere (argon). Surprisingly, a lower yield was obtained which may be due to the lack of formation of peroxo-nickel(III) active species (entry 9). This emphasizes the role of atmospheric oxygen as an effective oxidant in the present study. Similar trend was observed for rest of the complexes and they achieved maximum yield with the amount of 0.03 mmol.

Table 4.19 Effect of the concentration of $\mathbf{C_{25}}$ on the yield of coupling product[a]

Entry	Amount of complex ($\mathbf{C_{25}}$) (mmol)	Yield(%)[b]
1	**No catalyst**	**01.1**
2	0.01	42.9
3	0.015	61.5
4	0.02	80.5
5	**0.025**	**93.2**
6	0.03	92.9
7	0.04	91.8
8	0.05	90.6
9[c]	**0.025**	**07.2**
10[d]	**0.125**	**88.5**

[a] Reactions were carried out with 10 mmol of bromobenzene in presence of atmospheric molecular oxygen.
[b] GC yield based on the amount of bromobenzene.
[c] Inert atmosphere (argon).
[d] With 50.0 mmol of bromobenzene in the presence of 0.125 mmol catalyst for 10 h.

4.5.4 Scope of the reaction

This promising result encouraged us to extend the scope of the reaction to various aryl Grignard reagents (Table 4.20). Thus, simple and functionalized biaryl compounds were synthesized in good yields (entries 1–10). Introduction of methyl group at the ortho-position of the aryl Grignard reagent **1b** resulted in somewhat lower yield of the homocoupling product (entry 2). 4-Methoxy- and 2-methoxyphenylmagnesium bromide can be efficiently converted into the corresponding biaryls **2c** and **2d**, respectively, under similar conditions (entries 3 and 4). It is noteworthy that the present reaction system is tolerant of aryl chloride functionality (entry 6). Also it allows the coupling of heteroaryl Grignard reagent **1g** successfully (entry 7). Although sterically demanding substrate **1h** required higher reaction temperature and longer reaction time, it gave the corresponding biaryl **2h** in moderate to good yield (entry 8). The reaction is chemoselective; thus, nitrile, or nitro groups are tolerated (entries 9 and 10). It was observed that electron donating group on Grignard reagent (**1a, 1b, 1c** and **1d)** enhances the yield of coupling product compared to that of electron withdrawing group (**1f**, **1i** and **1j**). The reason can be explained as discussed in the *section 4.1.4*. In all these experiments, formations of cross-coupling products were very less.

Table 4.20 Homocoupling of Grignard reagents with atmospheric oxygen as an oxidant using complexes $\mathbf{C_{24}}$-$\mathbf{C_{29}}^{a}$

Entry	RMgBr	Product	Yield (%)^{b}					
			$\mathbf{C_{24}}$	$\mathbf{C_{25}}$	$\mathbf{C_{26}}$	$\mathbf{C_{27}}$	$\mathbf{C_{28}}$	$\mathbf{C_{29}}$
1	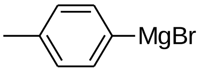 **1a**	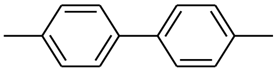 **2a**	77	**96**	74	81	**95**	47
2	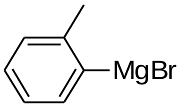 **1b**	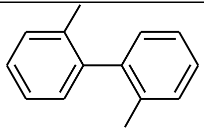 **2b**	64	**85**	58	71	**83**	37
3	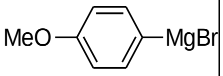 **1c**	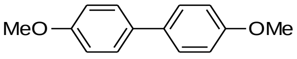 **2c**	80	**98**	77	85	**97**	52
4	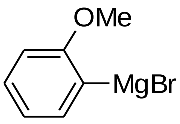 **1d**	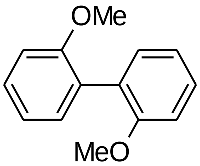 **2d**	67	**89**	64	74	**87**	40

5	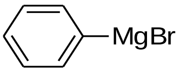 **1e**	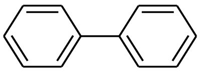 **2e**	73	**93**	71	79	**90**	43
6	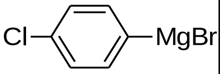 **1f**	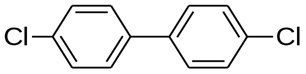 **2f**	68	**87**	59	73	**84**	36
7	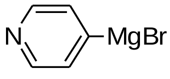 **1g**	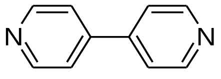 **2g**	63	**83**	51	65	**80**	29
8[c]	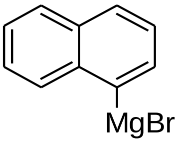 **1h**	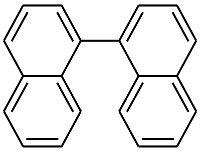 **2h**	56	**78**	46	59	**76**	25
9[d]	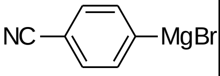 **1i**	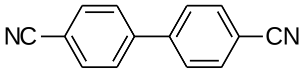 **2i**	50	**72**	37	51	**70**	17
10[d]	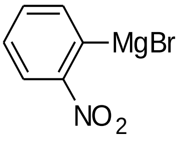 **1j**	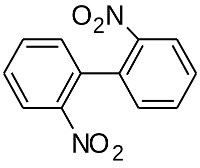 **2j**	53	**74**	41	57	**72**	22

[a] Reaction conditions: Mg turnings (0.320 g), aryl halide (10 mmol), catalyst (0.03mmol), Et_2O (10 ml).

[b] GC yield based on the amount of aryl halide.

[c] In THF, 60 °C, 10 h.

[d] reactions at -5 °C to room temp.

4.5.5 Proposed mechanism

The proposed mechanism is depicted in Fig. 4.17 for $\mathbf{C_{25}}$ catalyzed reaction. A low valent nickel species is generated by the Grignard reagent, which is a strong reducing agent (Ramnial et al. 2007) and is involved in the catalytic cycle. The oxidative addition of molecular oxygen to a low valent nickel complex **(a)** forms peroxo-nickel(III) intermediate **(b)** which is the key step of this catalytic cycle (Cho et al. 2009). It then reacts with two equivalents of RMgX to give biarylnickel(III) intermediate **(c)** and XMgOOMgX (Tsou and Kochi 1979, Cahiez et al. 2007). Thus formed biarylnickel(III) intermediate **(c)** undergoes rapid reductive elimination which eventually yields homocoupling product Ar-Ar and Ni(I) is regenerated. It is very reasonable to think that the formation of the unstable nickel(III) species (**c**) is required to achieve a very quick reductive elimination that gives (**d**) as the best way to favor the reductive elimination is to increase the oxidation state of the metal.

The formation of peroxo-nickel(III) intermediate was confirmed by the UV-vis spectral analysis. The absorption peak of the catalytic reaction mixture that appeared at 420.5 nm can be attributed to peroxo-nickel(III) intermediate (Cho et al. 2009) and its absence in the reaction mixture carried out under inert condition further confirms the necessity of molecular oxygen for the present catalytic system. Various iron (Cho et al. 2011), cobalt (Cho et al. 2010), nickel (Cho et al. 2009, Zapata-Rivera et al. 2012), copper (Zapata-Rivera et al. 2011) and palladium (Adamo et al. 2006, Popp et al. 2009)-catalyzed reactions are well established with such peroxo complexes as the catalytic intermediate.

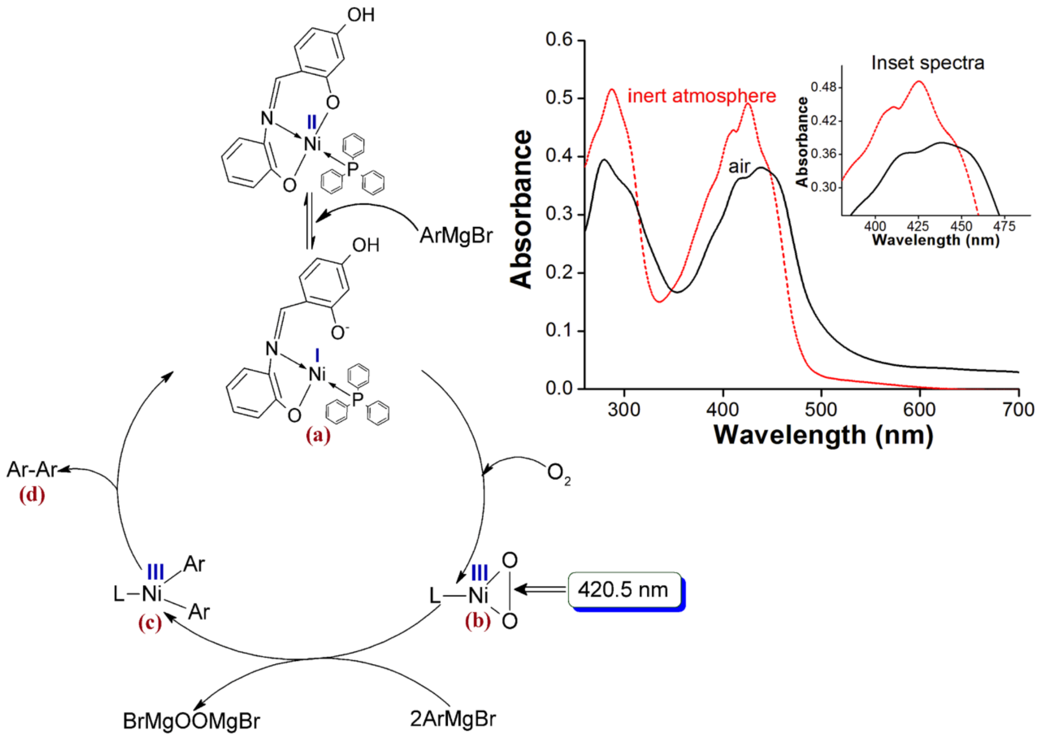

Figure 4.17 Proposed mechanism for the homocoupling of Grignard reagent using the complex **C_{25}**

Based on the above studies, the general mechanism for homocoupling of the Grignard reagent using the metal complexes **C_{24}** and **C_{26}-C_{28}** can be proposed as given in the Fig. 4.18 and Fig. 4.19, respectively.

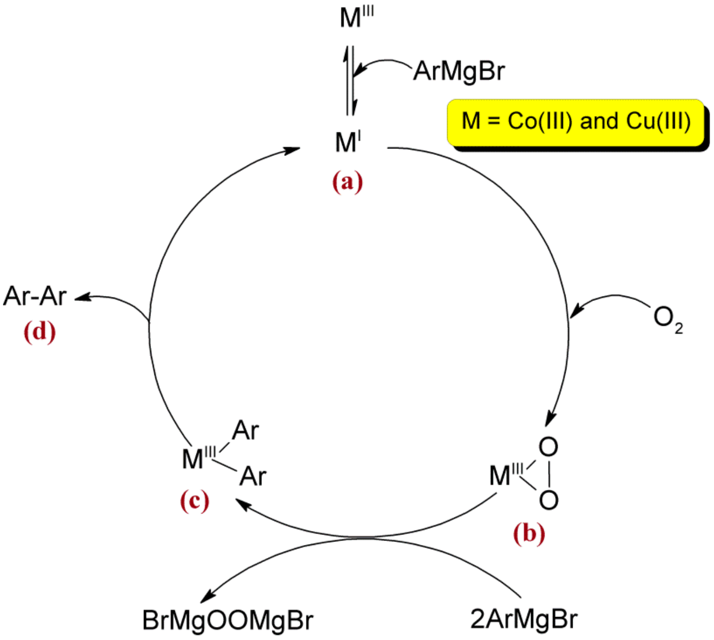

Figure 4.18 Proposed mechanism for the homocoupling of Grignard reagent using the complex **C_{24}** and **C_{26}**

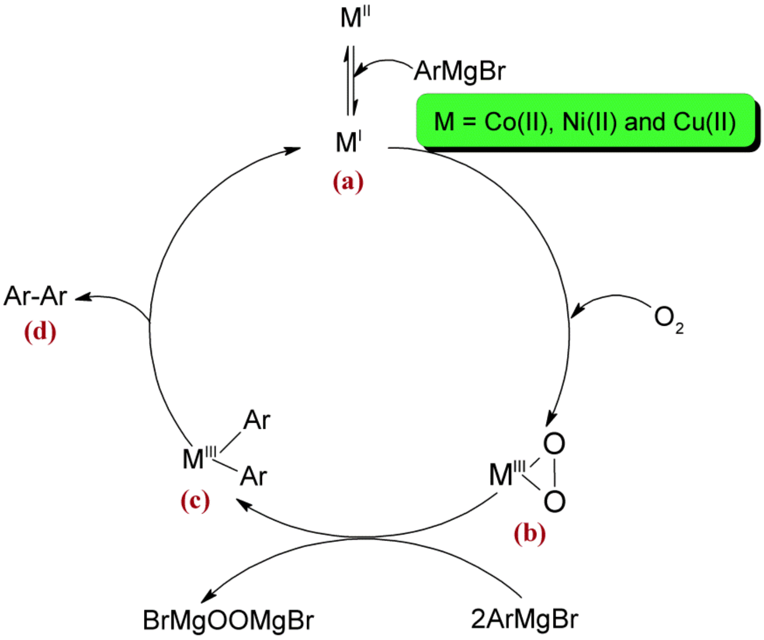

Figure 4.19 Proposed mechanism for the homocoupling of Grignard reagent using the complexes **C_{27}-C_{29}**

From the catalytic activity studies it was observed that, among the complexes containing Schiff base and PPh_3 ligands, complex **C_{25}** showed the highest catalytic activity which can be attributed to the faster oxidative addition step to afford biaryls in good yield. The electron rich metal centre in the complex **C_{25}** allows oxidative addition in a faster rate than the complex **C_{24}** which is surrounded by hindered triphenylphosphine and Schiff base ligand in octahedral fashion which hinders the association of incoming substrate and thus afford lesser yield. The lesser catalytic activity of complex **C_{26}** can be attributed to the difficulty in the two-electron oxidation of Cu(I) in association with the greater stability due to its completely filled *d-orbitals*. The triphenylphosphine free metal complexes blend with both Schiff base and dithiolate ligands also showed very good catalytic activity. Among them, **C_{28}** showed the highest catalytic efficiency which can be attributed to its tendency to undergo oxidative addition faster than from the cobalt complex under the same ligand environment and oxidation state due to the electron rich metal center. This may be the reason for the lesser yield of biaryl from the catalytic activity of the complex **C_{27}** compared to that of **C_{28}**. The catalytic activity of **C_{29}** yielded the least amount of catalytic product which can be once again attributed to the difficulty in the two-electron oxidation of Cu(I) in association with the greater stability due to its completely filled *d-orbitals*. Among cobalt complexes, **C_{27}** showed higher catalytic activity. The presence of bulky triphenylphosphine groups in the complex **C_{24}** may hinder the association of the incoming substrate to the metal center making the oxidative addition reaction slower and eventually affords a lower yield. Among nickel complexes, **C_{25}** showed better activity. Comparatively lesser catalytic activity of **C_{28}** can be attributed to the higher stability of the complex in association with the chelating dithiolate ligand which made it less reactive. Among copper complexes, **C_{26}** gave appreciable yield than from **C_{29}**. The complex **C_{29}** is more stable than **C_{26}** due to the presence of chelating dmit ligand which gives extra stability to the complex and make it less reactive.

4.6 COMPARISON STUDY

4.6.1 Simple metal precursors

For a comparison study, the catalytic activity studies were assessed using metal acetates, metal chlorides and triphenylphosphine metal precursors as catalysts for the homocoupling of Grignard reagents under identical reaction conditions. The reactions were carried out without the addition of either dmit or Schiff base ligands **L_1-L_6.** A reduced yield of coupling product was observed and the results showed that the better yields could be achieved by increasing the amount of catalyst loading. This ensures the effectiveness of synthesized complexes as potential catalysts for the present catalytic system, which gave high yield of biaryls with a minimum amount. The results due to the catalytic activities of metal acetates, metal chlorides and triphenylphosphine metal precursors are tabulated in the Table 4.21-Table 4.23, respectively.

4.6.2 Commercial phenylmagnesium bromide

To establish the significance of present coupling system, the reaction was carried out using commercial phenylmagnesium bromide as the starting material under standard condition (Table 4.24). To our surprise, the yield was lower. This can be interpreted as the difficulty in handling the commercial phenylmagnesium bromide, which is highly basic and hygroscopic in nature (Chen et al. 2009). Most of the reported Grignard reagent based catalytic systems (Zhou and Xue 2009, Cahiez et al. 2007) require a sophisticated set-up to handle the reagents in an inert gas environment in contrast to the present work.

Table 4.21 Homocoupling of phenylmagnesium bromide using metal acetates under atmospheric oxygen[a]

Entry	catalyst (mol %)	time (h)	yield (%)[b]
1	$Co(OAc)_2$ (0.04)	6	7
	$Ni(OAc)_2$ (0.04)	6	10
	$Cu(OAc)_2$ (0.04)	6	2
2	$Co(OAc)_2$ (0.06)	6	9
	$Ni(OAc)_2$ (0.06)	6	17
	$Cu(OAc)_2$ (0.06)	6	3
3	$Co(OAc)_2$ (0.08)	6	13
	$Ni(OAc)_2$ (0.08)	6	22
	$Cu(OAc)_2$ (0.08)	6	5
4	$Co(OAc)_2$ (0.1)	6	16
	$Ni(OAc)_2$ (0.1)	6	26
	$Cu(OAc)_2$ (0.1)	6	7
5	$Co(OAc)_2$ (0.13)	6	18
	$Ni(OAc)_2$ (0.13)	6	29
	$Cu(OAc)_2$ (0.13)	6	9
6	$Co(OAc)_2$ (0.17)	6	23
	$Ni(OAc)_2$ (0.17)	6	32
	$Cu(OAc)_2$ (0.17)	6	13
7	$Co(OAc)_2$ (0.21)	6	29
	$Ni(OAc)_2$ (0.21)	6	37
	$Cu(OAc)_2$ (0.21)	6	17

[a] Standard reaction conditions: Reactions were carried out with 10 mmol of bromobenzene in presence of atmospheric molecular oxygen at room temperature.

[b] GC yield.

Table 4.22 Homocoupling of phenylmagnesium bromide using metal chlorides under atmospheric oxygen[a]

Entry	catalyst (mol %)	time (h)	yield (%)[b]
1	$RuCl_3$ (0.04)	6	12
	$PdCl_2$ (0.04)	6	5
	$CoCl_2$ (0.04)	6	6
	$NiCl_2$ (0.04)	6	8
	$CuCl_2$ (0.04)	6	3
2	$RuCl_3$ (0.06)	6	15
	$PdCl_2$ (0.06)	6	7
	$CoCl_2$ (0.06)	6	9
	$NiCl_2$ (0.06)	6	11
	$CuCl_2$ (0.06)	6	5
3	$RuCl_3$ (0.08)	6	21
	$PdCl_2$ (0.08)	6	11
	$CoCl_2$ (0.08)	6	14
	$NiCl_2$ (0.08)	6	17
	$CuCl_2$ (0.08)	6	8
4	$RuCl_3$ (0.1)	6	25
	$PdCl_2$ (0.1)	6	15
	$CoCl_2$ (0.1)	6	18
	$NiCl_2$ (0.1)	6	21
	$CuCl_2$ (0.1)	6	11
5	$RuCl_3$ (0.13)	6	26
	$PdCl_2$ (0.13)	6	21
	$CoCl_2$ (0.13)	6	23
	$NiCl_2$ (0.13)	6	26
	$CuCl_2$ (0.13)	6	15

6	$RuCl_3$ (0.17)	6	32
	$PdCl_2$ (0.17)	6	24
	$CoCl_2$ (0.17)	6	25
	$NiCl_2$ (0.17)	6	30
	$CuCl_2$ (0.17)	6	19
7	$RuCl_3$ (0.21)	6	40
	$PdCl_2$ (0.21)	6	28
	$CoCl_2$ (0.21)	6	32
	$NiCl_2$ (0.21)	6	37
	$CuCl_2$ (0.21)	6	21

[a] Standard reaction conditions: Reactions were carried out with 10 mmol of bromobenzene in presence of atmospheric molecular oxygen at room temperature.

[b] GC yield.

Table 4.23 Homocoupling of phenylmagnesium bromide using triphenylphosphine metal precursors under atmospheric oxygen[a]

Entry	catalyst (mol %)	time (h)	yield (%)[b]
1	$[Ru(PPh_3)_3Cl_3]$ (0.04)	6	15
	$[Pd(PPh_3)_2Cl_2]$ (0.04)	6	7
	$[Co(PPh_3)_2Cl_2]$ (0.04)	6	9
	$[Ni(PPh_3)_2Cl_2]$ (0.04)	6	11
	$[Cu(PPh_3)_2Cl_2]$ (0.04)	6	5
2	$[Ru(PPh_3)_3Cl_3]$ (0.06)	6	19
	$[Pd(PPh_3)_2Cl_2]$ (0.06)	6	10
	$[Co(PPh_3)_2Cl_2]$ (0.06)	6	12
	$[Ni(PPh_3)_2Cl_2]$ (0.06)	6	15
	$[Cu(PPh_3)_2Cl_2]$ (0.06)	6	8
3	$[Ru(PPh_3)_3Cl_3]$ (0.08)	6	21
	$[Pd(PPh_3)_2Cl_2]$ (0.08)	6	12
	$[Co(PPh_3)_2Cl_2]$ (0.08)	6	14
	$[Ni(PPh_3)_2Cl_2]$ (0.08)	6	17
	$[Cu(PPh_3)_2Cl_2]$ (0.08)	6	10
4	$[Ru(PPh_3)_3Cl_3]$ (0.1)	6	24
	$[Pd(PPh_3)_2Cl_2]$ (0.1)	6	15
	$[Co(PPh_3)_2Cl_2]$ (0.1)	6	16
	$[Ni(PPh_3)_2Cl_2]$ (0.1)	6	19
	$[Cu(PPh_3)_2Cl_2]$ (0.1)	6	13
5	$[Ru(PPh_3)_3Cl_3]$ (0.13)	6	24
	$[Pd(PPh_3)_2Cl_2]$ (0.13)	6	15
	$[Co(PPh_3)_2Cl_2]$ (0.13)	6	18
	$[Ni(PPh_3)_2Cl_2]$ (0.13)	6	21
	$[Cu(PPh_3)_2Cl_2]$ (0.13)	6	14

6	$[Ru(PPh_3)_3Cl_3]$ (0.17)	6	31
	$[Pd(PPh_3)_2Cl_2]$ (0.17)	6	21
	$[Co(PPh_3)_2Cl_2]$ (0.17)	6	24
	$[Ni(PPh_3)_2Cl_2]$ (0.17)	6	26
	$[Cu(PPh_3)_2Cl_2]$ (0.17)	6	15
7	$[Ru(PPh_3)_3Cl_3]$ (0.21)	6	38
	$[Pd(PPh_3)_2Cl_2]$ (0.21)	6	29
	$[Co(PPh_3)_2Cl_2]$ (0.21)	6	33
	$[Ni(PPh_3)_2Cl_2]$ (0.21)	6	35
	$[Cu(PPh_3)_2Cl_2]$ (0.21)	6	19

[a] Standard reaction conditions: Reactions were carried out with 10 mmol of bromobenzene in presence of atmospheric molecular oxygen at room temperature.

[b] GC yield.

Table 4.24 Homocoupling of commercial phenylmagnesium bromide under atmospheric oxygen[a]

Entry	catalyst	mol(%)	time (h)	yield (%)[b]
1	C_1	0.13	6	32
2	C_2	0.13	6	17
3	C_3	0.13	6	27
4	C_4	0.13	6	30
5	C_5	0.13	6	10
6	C_6	0.13	6	29
7	C_7	0.13	6	37
8	C_8	0.13	6	16
9	C_9	0.13	6	25
10	C_{10}	0.13	6	39
11	C_{11}	0.13	6	13
12	C_{12}	0.13	6	30
13	C_{13}	0.13	6	27
14	C_{14}	0.13	6	32
15	C_{15}	0.13	6	33
16	C_{16}	0.13	6	29
17	C_{17}	0.13	6	35
17	C_{18}	0.13	6	28
19	C_{19}	0.13	6	31
20	C_{20}	0.13	6	14
21	C_{21}	0.13	6	26
22	C_{22}	0.13	6	33
23	C_{23}	0.13	6	12
24	C_{24}	0.13	6	29
25	C_{25}	0.13	6	43
26	C_{26}	0.13	6	27

27	C_{27}	0.13	6	32
28	C_{28}	0.13	6	41
29	C_{29}	0.13	6	19

[a] Standard reaction conditions: Reactions were carried out with 10 mmol of commercial phenylmagnesium bromide in the presence of atmospheric oxygen.

[b] GC yield.

4.7 SIGNIFICANCE OF THE PRESENT WORK

- A single step synthesis of symmetrical biaryls from the homocoupling of *in situ* synthesized aryl Grignard reagents has been developed. As *in situ* preparations avoid the workup procedures for the isolation of Grignard reagents, the present method is simple and economical. Most of the reported procedures constitute two step synthetic route, where the organometallic compounds are prepared first and then in a separate reaction converted into the biaryl product (Cahiez et al. 2007, Liu and Lei 2008).

- The reactions were successfully carried out at room temperature using atmospheric oxygen as the oxidant which is safe and environmentally friendly.

- Recently, Chen et al. (2009) developed cobalt catalyzed homocoupling reactions in a single step without proposing a mechanism. From the mechanistic studies of the present coupling system, peroxo-metal(III) active species was proposed and is supported by UV-vis spectral analysis.

- Indeed, most of the reported homocoupling systems demand 2–10 mol% of catalyst (Tao et al. 2006, Xu et al. 2006, Yuan et al. 2008, Chen et al. 2009, Wu et al. 2013), which is quite high in comparison with our reaction system, which utilizes a minimum of 0.1 mol % of catalyst.

CHAPTER 5

SUMMARY AND CONCLUSIONS

5.1 SUMMARY

The metal complexes of ruthenium, palladium, cobalt, nickel and copper with dmit, triphenylphosphine and Schiff base ligands were synthesized. The synthesized ligands and complexes were characterized by analytical, spectral (NMR, ESI Mass, UV-vis and FT-IR), thermal and magnetic studies. These complexes were applied as catalyst for the homocoupling of Grignard reagents for the synthesis of symmetrical biaryls. The Grignard reagents were synthesized *in situ*. The reaction was carried out in a room temperature using environmentally friendly atmospheric oxygen as the oxidant, without using any external organic oxidants. The catalytic activities were optimized with respect to solvent, time and catalyst concentration by taking bromobenzene as the model substrate for all the series of complexes. The influence of air in the present catalytic system was investigated. The quantitative analysis of the reaction products were carried out using gas chromatographic technique. The effect of substrate on the coupling reaction was examined by taking various aryl halides in all the studied catalytic systems. The effect of variation in the ligand frame work on the catalytic activity was also analyzed. The mechanistic studies of the present homocoupling reaction system was carried out by examining the UV-vis spectra of the reaction mixture in all the catalytic systems. Based on these studies, the probable mechanism for the homocoupling of Grignard reagents was proposed.

5.2 CONCLUSIONS

Based on the results of the present investigation, the following important conclusions were drawn:

- The present catalytic system involves *in situ* synthesis of aryl Grignard reagents at room temp using atmospheric oxygen as oxidant affords symmetrical biaryls in a single step. This makes the system simple, green and economical.

- From the mechanistic studies, peroxo-metal(IV) (metal=Ru and Pd) and peroxo-metal(III) (metal=Ni, Co and Cu) were proposed as active species for the present catalytic system.

- The reaction system is tolerant to chloro, nitro, cyano and hetero aryl functionalities and afford good-to-high yields of symmetrical biaryls with a minimum amount of catalyst loading.

- The catalytic activity studies revealed that an electron donating group on the Grignard reagent enhances the yield of the coupling product compared to that of an electron withdrawing group. Also, electron donating group on the ligand frame work enhanced the catalytic activity while electron withdrawing substituents decreased the catalytic activity of the complexes.

- It was observed that complexes containing dmit and Schiff base ligands show better catalytic activity than the complexes containing dmit and triphenylphosphine ligands.

- Among the complexes studied, the highest catalytic activity was observed for the nickel complex C_{25}, containing triphenylphosphine and ONO-tridentate ligand. The copper complex C_5 with dmit and triphenylphosphine ligands showed the least conversion.

- This simple, cost-effective and environmentally friendly catalytic route constitutes an interesting contribution in the large scale synthesis of the symmetrical biaryls.

5.3 SCOPE FOR FUTURE WORK

The following extensions are recommended to the work presented in this thesis:

- The above study can be extended to other structurally related ligands to understand the effect of structure on catalytic activity.

- Study of complexing behavior and catalytic activity of complexes of other metals of the same group to study the variation of size of metal on the catalytic activity.
- The above complexes can be utilized to explore its catalytic activity for cross coupling reactions.
- The above complexes can be utilized to explore its catalytic activity in other reactions.

REFERENCES

Abdalrazaq, E.A., Al-Ramadane, O.M. and Al-Numa, K.S. (2010). "Synthesis and Characterization of Dinuclear Metal Complexes Stabilized by Tetradentate Schiff Base Ligands." *Am. J. Appl. Sci.*, 7(5), 628-633.

Abdel-Rahman, A.A.-H., Ahmed, A.H.A. and Ramiz, M.M.M. (2010). "Synthesis and anti-hbv activity of 4-aminoanti-pyrine derivatives." *Chem. Heterocycl. Comp*., 46(1), 72-78.

Adamo, C., Amatore, C., Ciofini, I., Jutand, A. and Lakmini, H. (2006). "Mechanism of the Palladium-Catalyzed Homocoupling of Arylboronic Acids: Key Involvement of a Palladium Peroxo Complex." *J. Am. Chem. Soc.*, 128, 6829-6836.

Adams, H., Gardner, H.C., McRoy, R.A., Morris, M.J., Motley, J.C. and Torker, S. (2006). "Heterometallic dithiolene complexes formed by stepwise displacement of cyclopentadienyl ligands from nickelocene with $CpMo(S_2C_2Ph_2)_2$." *Inorg. Chem.*, 45, 10967-10975.

Adams, H., Morris, M.J., Riddiough, A.E., Yellowlees, L.J. and Lever, A.B.P. (2007). "Phosphine-substituted dithiolene complexes as ligands: Communication between ruthenium(II) centers through a dimolybdenum bis(dithiolene) core." *Inorg. Chem.*, 46(23), 9790-9807.

Adsule, S., Barve, V., Chen, D., Ahmed, F., Dou, Q.P., Padhye, S. and Sarkar, F.H. (2006). "Novel Schiff base copper complexes of quinoline-2-carboxaldehyde as proteasome inhibitors in human prostate cancer cells." *J. Med. Chem*., 49, 7242-7246.

Aizawa, S., Kondo, M., Miyatake, R. and Tamai, M. (2007). "Application of palladium(II) complex with bidentate phosphine sulfide ligands to palladium-catalyzed C–C coupling reaction." *Inorg. Chim. Acta.*, 360, 2809-2813.

Akerman, D., Phillips, D.A.S. and Taylor, J.A. (2004). "Interaction of oxidative bleach containing detergents with dyes. Part 2: preparation and resistance of hydrazo dyes, derived from aryl diazonium salts and 1-hydroxynaphthalene-4-sulphonic acid, to oxidation by hydrogen peroxide and meta-chloroperbenzoic acid." *Dyes. Pigments,* 62, 249–257.

Alberico, D., Scott, M.E. and Lautens, M. (2007). “Aryl-Aryl bond formation by transition-metal-catalyzed direct arylation.” *Chem. Rev.*, 107, 174-238.

Alkam, H.H., Hatzidimitriou, A., Hadjikostas, C.C. and Tsiamis, C. (1997). “Influence of substituents within bidentate nitrogenous bases on the spectra of mixed-ligand (1,1-dithiolato)copper(II) and nickel(II) chelates.” *Inorg. Chim. Acta.*, 256, 41-50.

Al-Kindy, S.M.Z., Al-Bulushi, S.T. and Suliman, F.E.O. (2008). “Spectrofluorimetric determination of zinc using 8-hydroxy-7-(4-sulfo-1-naphthylazo)-5-quinoline sulfonic acid.” *Spectrochim. Acta. A*, 71, 676–681.

Amorosoa, F., Colussia, S., Zottoa, A.D., Llorcab, J. and Trovarelli, A. (2010). “An efficient and reusable catalyst based on Pd/CeO_2 for the room temperature aerobic Suzuki–Miyaura reaction in water/ethanol.” *J. Mol. Catal. A: Chem.*, 315, 197-204.

Ananikova, V.P., Piroyana, A.O., Gaiduka, K.A., Beletskayab, I.P., Khrustalevc, V.N. and Antipinc, M.Y. (2009). “Sulfur-containing alkenes-A new class of chelating ligands: Synthesis, coordination to palladium and structure of the resulting complexes.” *Russ. J. Org. Chem.*, 45, 1743-1754.

Ananthi, N., Balakrishnan, U., Velmathi1, S., Manjunath, K.B. and Umesh, G. (2012). "Synthesis, Characterization and Third Order Non Linear Optical Properties of Metallo Organic Chromophores." *Opt. Photonics J.*, 2, 40-45.

Anderson, J.C., Namli, H. and Roberts, C.A. (1997). "Investigations into Ambient Temperature Biaryl Coupling Reactions." *Tetrahedron*, 53(44), 15123-15134.

Ando, R., Ono, H., Yagyu, T. and Maeda, M. (2004). “Spectroscopic characterization of mononuclear, binuclear and insoluble polynuclear oxovanadium(IV)–Schiff base complexes and their oxidation catalysis.” *Inorg. Chim. Acta.*, 357, 817-823.

Anitha, C., Sheela, C.D., Tharmaraj, P. and Raja, S.J. (2012). “Synthesis and characterization of VO(II), Co(II), Ni(II), Cu(II) and Zn(II) complexes of chromone based azo-linked Schiff base ligand.” *Spectrochim. Acta. A*, 98, 35-42.

Anupama, B. and Kumari, G.C. (2013). “Cobalt (II) complexes of ONO donor Schiff bases and N, N donor ligands: Synthesis, characterization, antimicrobial and DNA binding study.” *Int. J. Res. Chem. Environ.*, 3(2), 172-180.

Arun, V., Mathewb, S., Robinson, P.P., Jose, M., Nampoori, V.P.N. and Yusuff, K.K.M. (2010). “The tautomerism, solvatochromism and non-linear optical properties of fluorescent 3-hydroxyquinoxaline-2-carboxalidine-4-aminoantipyrine.” *Dyes. Pigments*, 87, 149-157.

Arunachalam, S., Priya, N.P., Jayabalakrishnan, C. and Chinnusamy, V. (2009). “Synthesis, spectral characterization, catalytic and antibacterial studies of new Ru(III) Schiff base complexes containing chloride/bromide and triphenylphosphine/arsine as co-ligands.” *Spectrochim. Acta. A.*, 74, 591–596.

Asnani, A.J. and Sahare, S. (2013). "Synthesis and pharmacological studies of some novel benzoquinoline derivatives." *Asian. J. Pharm. Clin. Res.* 6, 303-308.

Aswin, K., Mansoor, S.S., Logaiya, K. and Sudhan., S.P.N. (2013). “Triphenylphosphine: An efficient catalyst for the synthesis of 4,6-diphenyl-3,4-dihydropyrimidine-2(1H)-thione under thermal conditions.” *Journal of King Saud University – Science*, http://dx.doi.org/10.1016/j.jksus.2013.05.004.

Averseng, F., Lacroix, P.G., Malfant, I., Lenoble, G., Cassoux, P., Nakatani, K., Fanton, I.M., Delaire, J.A. and Aukauloo, A. (1999). “Synthesis, Crystal Structure and Second-Order Nonlinear Optical Properties of a New Bis(salicylaldiminato)nickel(II) Metal Complex.” *Chem. Mater.*, 11(4), 995-1002.

Aziz, A.A.A., Salem, A.N.M., Sayed, M.A. and Aboaly, M.M. (2012). “Synthesis, structural characterization, thermal studies, catalytic efficiency and antimicrobial activity of some M(II) complexes with ONO tridentate Schiff base N-salicylidene-o-aminophenol (saphH_2).” *J. Mol. Struct.*, 1010, 130-138.

Badiger, D.S., Hunoor, R.S., Patil, B.R., Vadavi, R.S., Mangannavar, C.V., Muchchandi, I.S., Patil, Y.P., Nethaji, M. and Gudasi K.B. (2012). “Synthesis, spectroscopic properties and biological evaluation of transition metal complexes of salicylhydrazone of anthranilhydrazide: X-ray crystal structure of copper complex.” *Inorg. Chim. Acta.*, 384, 197-203.

Bag, S., Bhaumik, P.K., Jana, S., Das, M., Bhowmik, P. and Chattopadhyay, S. (2013). "Syntheses and characterizations of square planar nickel(II) complexes with pendant ligands: Examples of bi-dentate bonding modes of potentially tri- and tetra-dentate Schiff bases." *Polyhedron*, 65, 229–237.

Bayo´n, J.C., Claver, C. and Masdeu-Bulto, A.M. (1999). “Homogeneous catalysis with transition metal complexes containing sulfur ligands.” *Coord. Chem. Rev.*, 193–195, 73-145.

Bernardo da Cruz, A.G., Wardell, J.L. and Rocco, A.M. (2006). “The decomposition kinetics of $[Et_4N]_2[M(dmit)_2]$ (M= Ni, Pd) in a nitrogen atmosphere using thermogravimetry.” *Thermochim. Acta*, 443, 217-224.

Bernardo, K., Leppard, S., Robert, A., Commenges, G., Dahan, F. and Meunier, M. (1996). “Synthesis and characterization of new chiral schiff base complexes with diiminobinaphthyl or diiminocyclohexyl moieties as potential enantioselective epoxidation catalysts.” *Inorg. Chem.*, 35, 387-396.

Bhowon, M.G., Wah, H.K. and Narain, R. (1999). “Schiff base complexes of ruthenium(II) and their use as catalytic oxidants.” *Polyhedron*, 18, 341-345.

Biava, H. and Signorella, S. (2010). “Peroxidase activity of dimanganese(III) complexes with the $[Mn_2(\mu\text{-OAc})(\mu\text{-OR})_2]^{3+}$ core.” *Polyhedron*, 29, 1001-1006.

Biittcber, A., Elias, H., Jiiger, E-G., Langfelderova, H., Mazur, M., Miiller, L., Paulus, H., Pelikan, P., Rudolpb, M. and Vakol, M. (1993). “Comparative study on the coordination chemistry of Cobalt(II), Nickel(II) and Copper(II) with derivatives of salen and tetrahydrosalen: Metal-catalyzed oxidative dehydrogenation of the C-N bond in coordinated tetrahydrosalen.” *Inorg. Chem*, 32, 4131-4138.

Biricik, N., Kayan, C., Gümgüma, B., Fei, Z., Scopelliti, R., Dyson, P.J., Gürbüz, N. and Özdemir, I. (2010). “Synthesis and characterization of ether-derivatized aminophosphines and their application in C–C coupling reactions.” *Inorg. Chim. Acta*, 363, 1039-1047.

Bringmann, G., Gulder, T., Gulder, T.M.A. and Breuning, M. (2011) “Atroposelective total synthesis of axially chiral biaryl natural products.” *Chem. Rev.*, 111, 563-639.

Burns, T.P. and Rieke, R.D. (1987). “Highly reactive magnesium and its application to organic syntheses.” *J. Org. Chem.*, 52, 3674-3680.

Cahiez, G., Moyeux, A., Buendia, J. and Duplais, C. (2007). “Manganese- or Iron-Catalyzed Homocoupling of Grignard Reagents Using Atmospheric Oxygen as an Oxidant.” *J. Am. Chem. Soc.*, 129, 13788-13789.

Cariati, F., Caruso, U., Centore, R., De Maria, A., Fusco, M., Panunzi, B., Roviello, A. and Tuzi, A. (2004). “New NLO active cyclopalladated chromophores in main-chain polymers.” *Inorg. Chim. Acta,* 357, 548-556.

Cassoux, P. (1999) “Molecular (super) conductors derived from bis-dithiolate metal complexes.” *Coord. Chem. Rev.*, 185–186, 213-232.

Cepanec, I., Litvic´, M., Udikovic´, J., Pogorelic´, I. and Lovric, M. (2007). “Copper(I)-catalysed homo-coupling of aryldiazonium salts: Synthesis of symmetrical biaryls.” *Tetrahedron*, 63, 5614-5621.

Chao, Y.C. and Yang, S.S. (1995). “Disazo direct dyes derived from 4,4'-diamino derivatives of benzanilide, diphenylamine-2-sulfonic acid and stilbene-2,2'-disulfonic acid.” *Dyes. Pigments*, 29(2), 131-138.

Charreteur, K., Kdider, M., Capon, J-F., Gloaguen, F., Petillon, F.Y., Schollhammer, P. and Talarmin, J. (2010). “Effect of Electron-Withdrawing Dithiolate Bridge on the Electron-Transfer Steps in Diiron Molecules Related to [2Fe]H Subsite of the [FeFe]-Hydrogenases.” *Inorg. Chem.*, 49, 2496–2501.

Chatterjee, D., Mitra, A. and Shepherd, R.E. (2004). “Oxo-transfer catalysis from *t*-BuOOH with C–H bond insertion using tridentate Schiff-base-chelate complexes of ruthenium(III).” *Inorg. Chim. Acta,* 357, 980-990.

Chatterjee, D., Mukherjee, S. and Mitra, A. (2000). “Epoxidation of olefins with sodium hypochloride catalysed by new Nickel(II) –Schiff base complexes.” *J. Mol. Catal. A:Chem.*, 154, 5-8.

Chavan, S.S. and Bharate, B.G. (2013). “Heterobimetallic M(II)/Ru(II) (M = Ni, Zn) complexes containing coordination and organometallic sites: Synthesis, characterization, luminescence and NLO properties.” *Inorg. Chim. Acta,* 394, 598-604.

Chelucci, G. and Thummel, R.P. (2002). “Chiral 2,2′-bipyridines, 1,10-phenanthrolines and 2,2′:6′,2″-terpyridines: Syntheses and applications in asymmetric homogeneous catalysis.” *Chem. Rev.*, 102, 3129-3170.

Chittilappilly, P.S., Sridevi, N. and Yusuff, K.K.M. (2008). “Ruthenium complexes of Schiff base ligands as efficient catalysts for catechol–hydrogen peroxide reaction.” *J. Mol. Catal. A:Chem.*, 286, 92-97.

Cho, J., Jeon, S., Wilson, S.A., Liu, L.V., Kang, E.A., Braymer, J.J., Lim, M.L., Hedman, B., Hodgson, K.O., Valentine, J.S., Solomon, E.I. and Nam, W. (2011). "Structure and reactivity of amononuclear non-haem iron(III)–peroxo complex." *Nature,* 478, 502-505.

Cho, J., Sarangi, R., Annaraj, J., Kim, S.Y., Kubo, M., Ogura, T., Solomon, E.I. and Nam, W. (2009). “Geometric and electronic structure and reactivity of a mononuclear ‘side-on’ nickel(III)–peroxo complex.” *Nat. Chem.*, 1, 568-572.

Cho, J., Sarangi, R., Kang, H.Y., Lee, J.Y., Kubo, M., Ogura, T., Solomon, E.I. and Nam, W. (2010). “Synthesis, structural and spectroscopic characterization and reactivities of mononuclear Cobalt(III)-Peroxo complexes.” *J. Am. Chem. Soc.*, 132, 16977-16986.

Chohan, Z.H., Arif, M., Shafiq, Z., Yaqub, M. and Supuran, C.T. (2006). “In vitro antibacterial, antifungal and cytotoxicactivity of some isonicotinoylhydrazide Schiff bases and their cobalt(II), copper(II), nickel(II) and zinc(II) complexes.” *J. Enz. Inhib. Med. Chem.*, 21, 95-103.

Chohan, Z.H., Sumrra, S.H., Youssoufi, M.H. and Hadda, T.B. (2010). “Metal based biologically active compounds: Design, synthesis and antibacterial/antifungal/cytotoxic properties of triazole-derived Schiff bases and their oxovanadium(IV) complexes.” *Eur. J. Med. Chem.*, 45(7), 2739-2747.

Cimerman, Z., Galic, N. and Bosner, B. (1997). “The Schiff bases of salicylaldehyde and aminopyridines as highly sensitive analytical reagents.” *Anal. Chim. Acta,* 343(1–2), 145-153.

Clercq, B.D. and Verpoort, F. (2002). “A new class of ruthenium complexes containing Schiff base ligands as promising catalysts for atom transfer radical polymerization and ring opening metathesispolymerization.” *J. Mol. Catal. A: Chem.*, 180(1–2), 67-76.

Cordelle, C., Agustin, D., Daran, J-C. and Poli, R. (2010). “Oxo-bridged bis oxo-vanadium(V) complexes with tridentate Schiff base ligands $(VOL)_2O$ (L = SAE, SAMP, SAP): Synthesis, structure and epoxidation catalysis under solvent-free conditions.” *Inorg. Chim. Acta.*, 364, 144-149.

Costes, J.P., Lame`re, J.F., Lepetit, C., Lacroix, P.G., Dahan, F. and Nakatani, K. (2005). “Synthesis, crystal structures and nonlinear optical (NLO) properties of new Schiff-base Nickel(II) complexes. Toward a new type of molecular switch?” *Inorg. Chem.*, 44, 1973-1982.

Cucciolito, M.E., Litto, R.D., Roviello, G. and Ruffo, F. (2005). “O,N,O′ -tridentate ligands derived from carbohydrates in the V(IV)-promoted asymmetric oxidation of thioanisole.” *J. Mol. Catal. A: Chem.*, 236, 176-181.

Cui, J., Zhang, M. and Zhang, Y. (2010). “Amino-salicylaldimine–palladium(II) complexes: New and efficient catalysts for Suzuki and Heck reactions.” *Inorg. Chem. Commun.*, 13, 81-85.

Cukurovali, A., Yilmaz, I. and Ozmen, H. (2001). "Antimicrobial activity studies of the metal complexes derived from substituted cyclobutane sunstituted thiazole Schiff base ligands." *Transit. Met. Chem.* 26, 619-624.

Dankwardt, J.W. (2005). “Transition metal catalyzed cross-coupling of aryl Grignard reagents with aryl fluorides via Pd- or Ni-activation of the C–F bond: an efficient synthesis of unsymmetrical biaryls – application of microwave technology in ligand and catalyst screening.” *J. Organomet. Chem.*, 690, 932–938.

Dayan, O., Özdemir, N., Serbetci, Z., Dinçer, M., Çetinkaya, B. and Büyükgüngör, O. (2012). “Synthesis and catalytic activity of ruthenium(II) complexes containing pyridine-based tridentate triamines (′NNN′) and pyridine carboxylate ligands ($\overset{\frown}{\mathrm{NO}}$).” *Inorg. Chim. Acta.*, 392, 246-253.

de Bonneval, B.G., Kathleen, I., Ching, M.C., Alaryc, F., Bui, T.T. and Valade, L. (2010). “Neutral d8 metal bis-dithiolene complexes: Synthesis, electronic properties and applications.” *Coord. Chem. Rev.*, 254, 1457–1467.

Deb, B., Sarmah, P.P., Saikia, K., Fuller, A.L., Randall, R.A.M., Slawin, A.M.Z., Woollins, J.D. and Dutta, D.K.. (2011). “Rhodium(I) carbonyl complexes of tetradentate chalcogen functionalized phosphines, [P′(X)(CH2CH2P(X)Ph2)3] {X = O, S, Se}: Synthesis, reactivity and catalytic carbonylation reaction.” *J. Organomet. Chem.*, 696(20), 3279-3283.

Denmark, S.E. and Regens, C.S. (2008). “Palladium-Catalyzed Cross-Coupling Reactions of Organosilanols and Their Salts: Practical Alternatives to Boron- and Tin-Based Methods.” *Acc. Chem. Res.*, 41, 1486–1499.

Deplano, P., Pilia, L., Espa, D., Mercuri, M.L. and Serpe, A. (2010). “Square-planar d8 metal mixed-ligand dithiolene complexes as second order nonlinear optical chromophores: Structure/property relationship.” *Coord. Chem. Rev.*, 254, 1434-1447.

Duanmu, C., Wu, L., Gua, J., Xu, X., Feng, L. and Gu, X. (2014). “Magnetic nanoparticle supported triphenylphosphine ligand for the Rh-catalyzed hydroformylation reaction.” *Catal. Commun.*, 48, 45–49.

Erdem, E., Sari, E.Y., Kilincarslan, R. and Kabay, N. (2009). "Synthesis and characterization of azo-linked Schiff bases and their nickel(II), copper(II) and zinc(II) complexes." *Transit. Met. Chem.* (2009) 34, 167–174.

Evano, G., Blanchard, N. and Toumi, M. (2008). “Copper-mediated coupling reactions and their applications in natural products and designed biomolecules synthesis.” *Chem. Rev.*, 108, 3054-3131.

Fan, H., Wang, X., Ren, Q., Li, T., Zhao, X., Sun, J., Zhang, G., Xu, D., Sun, Z. and Yu, G. (2010). “Third-order nonlinear optical properties in $[(C_4H_9)_4N]_2[Cu(C_3S_5)_2]$-doped PMMA thin film using Z-scan technique in picosecond pulse.” *Appl. Phys. A*, 99, 279-284.

Fan, H., Wang, X., Ren, Q., Zhao, X., Zhang, G., Chen, J., Xu, D., Yu, G. and Sun, Z. (2010). “Investigation of the non linear absorption and optical limiting properties of two $[Q]_2[Cu(C_3S_5)_2]$ compounds.” *Opt. Laser Technol.*, 42, 732-736.

Felkin, H. and Swierczewski, G. (1975). “Activation of grignard reagents by transition metal compounds.” *Tetrahedron*, 31, 2735-2748**.**

Fogg, D.E., James, B.R. and Kilner, M. (1994). “A comparison of catalytic activity for imine hydrogenation using Ru ditertiary phosphine complexes, including chiral systems.” *Inorg. Chim. Acta*, 222(1–2), 85-90.

Fox, M.A. and Whitesell, J.K. (2004). "Organic Chemistry." Jones &Bartlett, US, 3rd edn, pp. 615–618.

Friaza, G., Botello, A.F., Perez, J.M., Prieto, M.J. and Moreno, V. (2006). “Synthesis and characterization of palladium(II) and platinum(II) complexes with Schiff base derivatives of 2-pyridincarboxylaldehyde. Study of their interaction with DNA.” *J. Inorg. Biochem.*, 100, 1368-1377.

Galloway, C.P., Doxsee, D.D., Fenske, D., Rauchfuss, T.B., Wilson, S.R. and Yang, X. (1994). “Binary carbon sulfides based on the α-C_3S_5 subunit and related C-S-0, C-S-Cl and C-S-N compounds.” *Inorg. Chem.*, 33, 4537-4544.

Ganjali, M.R., Pourjavid, M.R., Rezapour, M., Poursaberi, T., Daftari, A. and Niasari, M. S. (2004). “Ruthenium(III) Schiff's Base Complex as Novel Chloride Selective Membrane Sensor.” *Electroanalysis*, 16(11), 922-927.

Garcia-Vazquez, J.A., Romero, J. and Sousa, A. (1999). "Electrochemical synthesis of metallic complexes of bidentate thiolates containing nitrogen as an additional donor atom." *Coord. Chem. Rev.*,193-195, 691-745.

Garrou, P.E. (1985). “Transition-metal-mediated phosphorus-carbon bond cleavage and its relevance to homogeneous catalyst deactivation.” *Chem. Rev.*, 85(3), 171-185.

Ghosh, T., Mondal, B., Ghosh, T., Sutradhar, M., Mukherjee, G. and Drew, M.G.B. (2007). “Synthesis, structure, solution chemistry and the electronic effect of para substituents on the vanadium center in a family of mixed-ligand [$V^VO(ONO)(ON)$] complexes.” *Inorg. Chim. Acta.*, 360, 1753-1761.

Ginah, F.O., Donovan, Jr. T.A., Suchan, S.D., Pfennig, D.R. and Ebert, G,W. (1990). “Homocoupling of alkyl halides and cyclization of α,ω-dihaloalkanes via activated copper." *J. Org. Chem.*, 55, 584-589.

Guan, B-T., Lu, X-Y., Zheng, Y., Yu, D-G., Wu, T., Li, K-L., Li, B-J. and Shi, Z-J. (2010). “Biaryl construction through kumada coupling with diaryl sulfates as one-by-one electrophiles under mild conditions.” *Org. Lett.*, 12(2), 396-399.

Guo, Q-X., Wu, Z-J., Luo, Z-B., Liu, Q-Z., Ye, J-L., Luo, S-W., Cun, L-F. and Gong L-Z. (2007). “Highly Enantioselective Oxidative Couplings of 2-Naphthols Catalyzed by Chiral Bimetallic Oxovanadium Complexes with Either Oxygen or Air as Oxidant.” *J. Am. Chem. Soc.*, 129(45), 13927-13938.

Gupta, K.C. and Sutar, A.K. (2007). “Polymer anchored Schiff base complexes of transition metal ions and their catalytic activities in oxidation of phenol.” *J. Mol. Catal. A: Chem.*, 272(1–2), 64-74.

Gupta, K.C. and Sutar, A.K. (2008). “Catalytic activities of Schiff base transition metal complexes.” *Coord. Chem. Rev.*, 252, 1420–1450.

Gupta, K.C., Sutar, A.K. and Lin, C.-C. (2009). “Polymer-supported Schiff base complexes in oxidation reactions.” *Coord. Chem. Rev.*, 253(13–14), 1926-1946.

Hartwig, J.F. (2007). "Electronic Effects on Reductive Elimination To Form Carbon-Carbon and Carbon-Heteroatom Bonds from Palladium(II) Complexes." *Inorg. Chem.*, 46, 1936-1947.

Hashim, J., Glasnov, T.N., Kremsner, J.M. and Kappe, C.O. (2006). "Symmetrical bisquinolones via metal-catalyzed cross-coupling and homocoupling reactions." *J. Org. Chem.*, 71, 1707-1710.

Hassan, J., Se´vignon, M., Gozzi, C., Schulz, E. and Lemaire, M. (2002). "Aryl-Aryl bond formation one century after the discovery of the ullmann reaction." *Chem. Rev.*, 102, 1359-1469.

Hatakeyama, T., Hashimoto, S., Ishizuka, K. and Nakamura, M. (2009). "Highly Selective Biaryl Cross-Coupling Reactions between Aryl Halides and Aryl Grignard Reagents: A New Catalyst Combination of N-Heterocyclic Carbenes and Iron, Cobalt and Nickel Fluorides." *J. Am. Chem. Soc.*, 131, 11949–11963.

Hello, K.M., Adamb, F. and Ali, T.H. (2014). "A solid sulfonic acid catalyst for the solvent free alkylation of phenol." *J. Taiwan. Inst. Chem. Eng.*, 45(1), 134-142.

Hihara, T., Okada, Y. and Morita, Z. (2007). "An analysis of the photo-reactivity of monoazo reactive dyes derived from H-acid and related naphthalene sulfonic acids using the PM5 method." *Dyes. Pigments*, 75, 585-605.

Himeda, Y., Komatsuzaki, N.O., Sugihara, H., Arakawa, H. and Kasuga, K. (2003). "Transfer hydrogenation of a variety of ketones catalyzed by rhodium complexes in aqueous solution and their application to asymmetric reduction using chiral Schiff baseligands." *J. Mol. Catal. A: Chem.*, 195(1–2), 95-100.

Hoffmann, S.K., Goslar, J., Lijewski, S. and Zalewska, A. (2013). "EPR and ESE of CuS_4 complex in $Cu(dmit)_2$: g-Factor and hyperfine splitting correlation in tetrahedral Cu–sulfur complexes." *J. Magn. Reson.*, 236, 7-14.

Hokelek, T., Isiklan, M. and Kilic, Z. (2001). "4-{[(1E)-(2-Hydroxyphenyl)methylidene]amino}-1,5-dimethyl-2-phenyl-2,3-dihydro-1H-pyrazol-3-one." *Acta. Cryst.*, C57, 117-119.

Horváth, H., Laurenczy, G. and Kathó, Á. (2004). "Water-soluble (η6-arene)ruthenium(II)-phosphine complexes and their catalytic activityin the hydrogenation of bicarbonate in aqueous solution." *J. Organomet. Chem.*, 689(6), 1036-1045.

Hossain, G.M.G., Hyder, M.I., Kabir, S.E., Abdul Malik, K.M., Miah, M.A. and Siddiquee, T.A. (2003). "Binuclear ruthenium complexes containing bridging dithiolate and dppm ligands: X-ray structures of [$Ru_2(CO)_4$(m-$SCH_2CH_2CH_2S$)(mdppm)] and [$Ru_2(CO)_4${(m-$SC_6H_3(CH_3)S$}(m-dppm)]." *Polyhedron*, 22, 633-640.

Hou, X-F., Zhang, P-C., Liu, S., Wang, H., Lin, Y-J. and Jin, G-X. (2008). "Synthesis and structures of binuclear half-sandwich cobalt (III) ortho-carboranedithiolato complexes with silyl-bridged bis(cyclopentadienyl) ligands." *J. Organomet. Chem.*, 693, 1462–1468.

Hu, Y-L., Li, F., Gu, G-L. and Lu, M. (2011). "Facile and efficient reductive homocoupling of benzyl and aryl halides catalyzed by ionic liquid [C_{12}mim][$CuCl_2$] in the presence of metallic zinc and copper." *Catal. Lett.*, 141, 467-473.

Huang, P-C. and Hong, F-E. (2009). "Amination and Suzuki coupling reactions catalyzed by palladium complexes coordinated by cobalt-containing monodentate phosphine ligands with bis-trifluoromethyl substituents on bridged arylethynyl: Observation of some unusual metal-containing compounds." *J. Organomet. Chem.*, 694, 113–121.

Ilhan, S., Temel, H., Yilmaz, I. and Sekerci, M. (2007). "Synthesis, structural characterization and electrochemical studies of new macrocyclic Schiff base containing pyridine head and its metal complexes." *J. Organomet. Chem.*, 692, 3855–3865.

Inoue, A., Kitagawa, K., Shinokubo, H. and Oshima, K. (2000). “Simple and efficient ticl$_4$-mediated synthesis of biaryls via arylmagnesium compounds.” *Tetrahedron*, 56, 9601-9605.

Iqbal, J., Saeed, A., Raza, R., Matin, A., Hameed, A., Furtmann, N., Lecka, J., Sévigny, J. and Bajorath, J. (2013). “Identification of sulfonic acids as efficient ecto-5′-nucleotidase inhibitors.” *Eur. J. Med. Chem.*, 70, 685-691.

Ismail, K.Z. (2000). “Synthesis, spectroscopic, magnetic and biological activity studies of copper(II) complexes of an antipyrine Schiff base.” *Transit. Metal. Chem.*, 25, 522-528.

Issa, R.M., Khedr, A.M. and Rizk, H.F. (2005). “UV–vis, IR and 1H NMR spectroscopic studies of some Schiff bases derivatives of 4-aminoantipyrine.” *Spectrochim. Acta A.*, 62, 621-629.

Jackson, S.M., Hughes, C.E., Monfette, S. and Rosenberg, L. (2006). “Structural criteria for the activity of rhodium(I) phosphine complexes in the catalyticdehydrocoupling of di-*n*-hexylsilane.” *Inorg. Chim. Acta*, 359(9), 2966-2972.

Jankowska, A., Florczak, P. and Kowalak, S. (2013). “The MOF matrices for pigments with encapsulated dmit.” *Micropor. Mesopor. Mat.*, 171, 78-81.

Jayabalakrishnan, C., Karvembu, R. and Natarajan, K. (2003). “Ruthenium(III) Schiff Base Complexes: Catalytic Activity in Aryl-Aryl Coupling Reaction and Antimicrobial Activity.” Synthesis and Reactivity in Inorganic and Metal-Organic Chemistry, 33(9), 1535–1553.

Jayabalakrishnan, C., Karvembu, R. and Natarajan, K. (2010). “Ruthenium (III) Schiff Base Complexes: Catalytic Activity in Aryl-Aryl Coupling Reaction and Antimicrobial Activity.” *Synth. React. Inorg. Met.-Org. Chem.*, 9, 1535-1553.

Jin, C., Fan, W., Jia, Y., Fan, B., Ma, J. and Li, R. (2006). “Encapsulation of transition metal tetrahydro-Schiff base complexes in zeolite Y and their catalytic properties for the oxidation of cycloalkanes.” *J. Mol. Catal. A: Chem.*, 249(1–2), 23-30.

Jin, L.T., Wanga, X.Q., Ren, Q., Cai, N.N., Chen, J.W., Li, T.B., Liu, X.T., Wanga, L.N., Zhang, G.H., Zhu, L.Y. and Xua, D. (2012). “Preparation, characterization and third order nonlinear optical properties of the bis(tetrabutylammonium)-[Cd(dmit)$_2$] (dmit=2-thioxo-1,3-dithiol-4,5-dithiolate) for all-optical switching applications at blue–green light band.” *J. Cryst. Growth*, 356, 10-16.

Jones, R.D., Summerville, D.A. and Basalo, F. (1979). “Synthetic oxygen carriers related to biological systems.” *Chem. Rev.*, 79, 139-179.

Joseph, T., Sawant, D.P., Gopinath, C.S. and Halligudi, S.B. (2002). “Zeolite encapsulated ruthenium and cobalt schiff base complexes catalyzed allylic oxidation of α-pinene.” *J. Mol. Catal. A: Chem.*, 184, 289-299.

Kagkelari, A., Papaefstathiou, G.S., Raptopoulou, C.P. and Zafiropoulos, T.F. (2009). "Synthesis and structure of N-salicylidene-o-aminophenolato gallium(III) complexes." *Polyhedron*, 28, 3279-3283.

Karvembu, R., Jayabalakrishnan, C., Dharmaraj, N., Renukadevi, S.V. and Natarajan, K. (2002). “Binuclear ruthenium(III) complexes: synthesis, characterisation, catalytic activity in aryl–aryl couplings and biological activity.” *Transit. Met. Chem.*, 27, 631–638.

Kato, R. (2004). “Conducting metal dithiolene complexes: structural and electronic properties.” *Chem. Rev.*, 104, 5319-5346.

Kavitha, P., Saritha, M. and Reddy, K.L. (2013). “Synthesis, structural characterization, fluorescence, antimicrobial, antioxidant and DNA cleavage studies of Cu(II) complexes of formyl chromone Schiff bases.” *Spectrochim. Acta A*, 102, 159-168.

Kiefer, G., Jeanbourquin, L. and Severin, K. (2013). "Oxidative coupling reactions of Grignard reagents with nitrous oxide." *Angew. Chem.* 125, 6422 –6425.

Kim G-J. and Shin, J-H. (1999). " Application of new unsymmetrical chiral Mn(III), Co(II,III) and Ti(IV) salen complexes in enantioselective catalytic reactions." *Catal. Lett.*, 63, 83–90.

Kobayashi, A., Fujiwara, E. and Kobayashi, H. (2004). “Single-component molecular metals with extended-TTF dithiolate ligands.” *Chem. Rev.*, 104, 5243-5264.

Kubota, K., Hamblett, C.L., Wang, X. and Leighton, J.L. (2006). “Strained silacycle-catalyzed asymmetric Diels–Alder cycloadditions: the first highly enantioselective silicon Lewis acid catalyst.” *Tetrahedron*, 62, 11397-11401.

Kumar, A., Agarwal, M., Singh, A.K. and Butcher, R.J. (2009). “Palladium(II), platinum(II), ruthenium(II) and mercury(II) complexes of potentially tridentate Schiff base ligands of (E, N, O) type (E = S, Se, Te): Synthesis, crystal structures and applications in Heck and Suzuki coupling reactions.” *Inorg. Chim. Acta.*, 362, 3208–3218.

Kumar, H.C.S., Bhat, B.R., Rudresha, B.J., Ravindra, R. and Philip, R. (2010). “Synthesis, characterization of *N,N′*-bis(2-hydroxynaphthalidene)phenylene-1,2-diamine with M(II)(M = Ni, Zn and Fe) Schiff-base complexes and their non-linear optical studies by z-scan technique.” *Chem. Phys. Lett.*, 494(1–3), 95-99.

Lee, S-Y., Hille, A., Frias, C., Kater, B., Bonitzki, B., Wolfl, S., Scheffler, H., Prokop, A. and Gust, R. (2010). “[Ni^{II}(3-OMe-salophene)]: A Potent Agent with Antitumor Activity.” *J. Med. Chem.*, 53, 6064-6070.

Leelavathy, C. and Antony, S.A. (2013). “Synthesis, spectral characterization and biological activity of metal(II) complexes with 4-aminoantipyrine derivatives.” *Spectrochim. Acta Part A*, 113, 346-355.

Leeuwen, P.W.N.M.V., Kamer, P.C.J., Reek, J.N.H. and Dierkes, P. (2000). “Ligand bite angle effects in metal-catalyzed C-C bond formation.” *Chem. Rev.*, 100, 2741-2769.

Lei, A. and Zhang, X. (2002). “A novel palladium-catalyzed homocoupling reaction initiated by transmetallation of palladium enolates.” *Tetrahedron Lett.,* 43, 2525–2528.

Lenoble, G., Lacroix, P.G., Daran, J.C., Bella, S.D. and Nakatani, K. (1998). “Syntheses, Crystal Structures and NLO Properties of New Chiral Inorganic Chromophores for Second-Harmonic Generation.” *Inorg. Chem.,* 37(9), 2158-2165.

Li, J., Peng, J., Bai, Y., Zhang, G., Lai, G. and Li, X. (2010). “Phosphines with 2-imidazolium ligands enhance the catalytic activity and selectivity of rhodium complexes for hydrosilylation reactions.” *J. Organomet. Chem.,* 695(3), 431-436.

Li, J-H., Liang, Y., Wang, D-P., Liu, W-J., Xie, Y-X. and Yin, D-L. (2005). “Efficient stille cross-coupling reaction catalyzed by the $Pd(OAc)_2$/Dabco catalytic system.” *J. Org. Chem.*, 70, 2832-2834.

Li, R.-X., Li, X.-J., Wong, N.-B., Tin, K.-C., Zhou, Z.-Y. and Mak, T.C.W. (2002). “Syntheses and characterizations of iridium complexes containing bidentatephosphine ligands and their catalytic hydrogenation reactions to α,β-unsaturated aldehydes.” *J. Mol. Catal. A: Chem.,* 178(1–2), 181-190.

Liu, W. and Lei, A. (2008). “Efficient Fe-catalyzed homo-coupling of aryl Grignard reagents using O_2 as the oxidant.” *Tetrahedron Lett.*, 49, 610–613.

Long, J-M., Gao, H-Y., Liu, F-S., Song, K-M., Hu, H., Zhang, L., Zhu. F-M. and Wua, Q. (2009). “Nickel and palladium complexes bearing ortho-phenoxy modified anilido-imine ligands: Drastic steric effect on coordinated geometry and catalytic property toward olefin polymerization.” *Inorg. Chim. Acta.*, 362, 3035–3042.

Magano, J. and Dunetz, J.R. (2011). “Large-scale applications of transition metal-catalyzed couplings for the synthesis of pharmaceuticals.” *Chem. Rev.*, 111, 2177-2250.

Mahalingam, V., Chitrapriya, N., Fronczek, F.R. and Natarajan, K. (2010). “New Ru(II)–DMSO complexes of ON/SN chelates: Synthesis, behavior of Schiff bases towards hydrolytic cleavage of C@N bond, electrochemistry and biological activities.” *Polyhedron,* 29, 3363-3371.

Mandal, S., Karmakar, T.K., Ghosh, A.M., Fleck, M. and Bandyopadhyay, D. (2011). “Synthesis, crystal structure and antibacterial activity of a group of mononuclear manganese(II) Schiff base complexes.” *Polyhedron,* 30, 790-795.

Mansouri, A.I., Mirzaei, M., Afzali, D. and Ganjavie, F. (2011). “Catalytic spectrophotometric determination of Mo(VI) in water samples using 4-amino-3-hydroxy-naphthalene sulfonic acid.” *Arab. J. Chem.,* doi:10.1016/j.arabjc.2011.12.009.

Martins, M.A.C., Silva, R.M. and Huffman, J.C. (2002). “Syntheses and characterization of nickel thiolate complexes: X-ray structure of [Ni(SCH$_2$CH$_2$S)(PPh$_2$CH=CHPPh$_2$)].” *Polyhedron,* 21, 421–424.

Matsubayashi, G., Nakano, M. and Tamura, H. (2002). “Structures and properties of assembled oxidized metal complexes with $C_8H_4S_8$ and related sulfur-rich dithiolate ligands.” *Coord. Chem. Rev.*, 226, 143-151.

Matteoli, U., Menchi, G., Bianchi, M., Piacenti, F., Ianelli, S. and Nardelli, M. (1995). “Structure and catalytic activity of phosphine-substituted ruthenium carbonyl carboxylates.” *J. Organomet. Chem.*, 498(2), 177-186.

Mishra, L., Bindu, K. and Bhattacharya, S. (2004). “Spectroscopic studies, structure simulation and phenol binding property of dimetallocyclophanes derived from tetradentate Schiff bases.” *Inorg. Chem. Commun.*, 7, 777-780.

Mohamed, G.G. and Abd El-Wahab, Z.H. (2005). “Mixed ligand complexes of bis(phenylimine) Schiff base ligands incorporating pyridinium moiety Synthesis, characterization and antibacterial activity.” *Spectrochim. Acta Part A*, 61, 1059-1068.

Mohameda, G.G. (2006). “Synthesis, characterization and biological activity of bis(phenylimine) Schiff base ligands and their metal complexes.” *Spectrochim. Acta Part A*, 64, 188-195.

Moldes, I., Encarnación, E., Ros, J., Alvarez-Larena, Á. and Piniella, J.F. (1998). “Ruthenium(II) complexes containing both arene and functionalized phosphines. Synthesis and catalytic activity for the hydrogenation of styrene and phenylacetylene.” *J. Organomet. Chem.*, 566(1–2), 165-174.

Moncomble, A., Floch, P.L. and Gosmini, C. (2009). “Cobalt-catalyzed formation of symmetrical biaryls and its mechanism.” *Chem. Eur. J.*, 15, 4770-4774.

Monfared, H.H., Bikas, R. and Mayer, P. (2010). “Homogeneous green catalysts for olefin oxidation by mono oxovanadium(V) complexes of hydrazone Schiff base ligands.” *Inorg. Chim. Acta.*, 363, 2574-2583.

Moutloali, R.M., Nevondo, F.A., Darkwa, J., Iwuoha, E.I. and Henderson, W. (2002). “Bimetallic nickel complexes with bridging dithiolato Schiff base ligands: synthesis, mass spectral characterisation and electrochemistry.” *J. Organomet. Chem.*, 656, 262-269.

Mukherjee, S., Samanta, S., Roy, B.C. and Bhaumik, A. (2006). Efficient allylic oxidation of cyclohexene catalyzed by immobilized Schiff base complex using peroxides as oxidants.” *Appl. Catal. A-Gen.*, 301, 79-88.

Mulazimoglu, A.D., Mulazimoglu, I.E. and Mercimek B. (2009). "Synthesis, characterizations and investigation of electrochemical behaviours of 4-[(2-hydroxyphenylimino)methyl]benzene-1,3-diol." *E-j. Chem.*, 6(4), 965-974.

Nadri, S., Joshaghani, M. and Rafiee, E. (2009). “Selective arylation of 1,1-disubstituted olefins using a biphenyl-based phosphine in Heck coupling reactions.” *Tetrahedron Lett.*, 50, 5470–5473.

Nagaki, A., Uesugi, Y., Tomida, Y. and Yoshida, J-I. (2011). “Homocoupling of aryl halides in flow: Space integration of lithiation and $FeCl_3$ promoted homocoupling.” *Beilstein. J. Org. Chem.*, 7, 1064-1069.

Nagano, T. and Hayashi, T. (2005). “Iron-catalyzed oxidative homo-coupling of aryl grignard reagents.” *Org. Lett.*, 7(3), 491-493.

Najera, C., Sansano, J.M. and Yus, M. (2003). "Recent synthetic uses of functionalised aromatic and heteroaromatic organolithium reagents prepared by non-deprotonating methods." *Tetrahedron*, 59, 9255–9303.

Nakamoto, K. (1971). "Infrared and Raman Spectra of Inorganic and Coordination Compounds." Wiley–Inter Science, New York.

Natsuaki, K., Nakano, M., Matsubayashi, G. and Arakawa, R. (2000). "Preparation and spectroscopic properties of bis(2,2%-bipyridine)-ruthenium(II) complexes and related complexes with sulfur-rich dithiolato ligands and electrical conductivities of their oxidized species." *Inorg. Chim. Acta*, 299, 112–117.

Nguyen, H.H., Hoang, N. and Abram, U. (2010). "Synthesis and structures of two ruthenium dibenzoylmethane triphenylphosphine mixed ligand complexes." *Transit. Met. Chem.*, 35, 89-93.

Niasari, M.S., Hydarzadeh, S., Amiri, A. and Salavati, S. (2005). "Manganese(III) bis(2-hydroxyanil) acetylacetonato complex as effective catalyst for acylation of alcohols, amines and phenols with acetic anhydride." *J. Mol. Catal. A:Chem.*, 231, 191-195.

Nobe, Y., Arayama, K. and Urabe, H. (2005). "Air-Assisted Addition of Grignard Reagents to Olefins. A Simple Protocol for a Three-Component Coupling Process Yielding Alcohols." *J. Am. Chem. Soc.*, 127, 18006-18007.

Omar, M.M., Mohamed, G.G. and Ibrahim, A.A. (2009). "Spectroscopic characterization of metal complexes of novel Schiff base. Synthesis, thermal and biological activity studies." *Spectrochim. Acta. A*, 73, 358-369.

Ondrejovic, G., Kotocova, A. and Valigura, D. (2002). "Spectrochemical And Electrochemical Properties Of Distorted Pentacoordinate $[Cu(Chel)_2X]Y$ Complexes." *Chem. Pap.*, 56(3), 168-173.

Oskooie, H.A., Heravi, M.M. and Behbahani, F.K. (2007) “A Facile, Mild And Efficient One-Pot Synthesis of 2-Substituted Indole Derivatives Catalyzed By Pd(PPh3)2Cl2.” *Molecules*, 12, 1438-1446.

Ourari, A., Khelafi, M., Aggoun, D., Bouet, G. and Khan, M.A. (2011). “Synthesis, Characterization and Electrochemical Study of Tetradentate Ruthenium-Schiff Base Complexes: Dioxygen Activation with a Cytochrome P450Model Using 1- or 2 Methylimidazole as Axial Bases.” *Adv. Phys. Chem.*, 1-11.

Padma, P.N., Arunachalam, S., Manimaran, A., Muthupriya, D. and Jayabalakrishnan, C. (2009). “Mononuclear Ru(III) Schiff base complexes: Synthesis, spectral, redox, catalytic and biological activity studies*.” Spectrochim. Acta. A,* 72, 670–676.

Parekh, H.M., Panchal, P.K. and Patel, M.N. (2006) “In vitro fungitoxic activity of some Schiff bases and their oxovanadium(IV) complexes” *Taxicol. Environ. Chem*., 88, 579-586.

Pasa, S., Ocak, Y.S., Temel, H. and Kilicoglu, T. (2013). “Synthesis, characterization and catalytic behavior in the Suzuki reaction of Schiff baseand its complexes and the optical properties of nickel complex used in the fabrication of a photodiode.” *Inorg. Chim. Acta*, 405(24), 493-504.

Pasini, A., Bernini, E., Scaglia, M. and Santis, G.D. (1996). “Studies on the oxidation of Cu^{II} complexes of quadridentate schiff bases derived from salicylaldehyde or *ortho*-aminophenol.” *Polyhedron,* 15 (24), 4461-4467.

Patel, R.N., Singh, N. and Gundla, V.L.N. (2007). “Synthesis, Characterization and Superoxide Dismutase Activity of Some Octahedral Nickel(II) Complexes.” *Polyhedron*, 26, 757-762.

Pellissier, H. (2007). “Chiral sulfur-containing ligands for asymmetric catalysis.” *Tetrahedron*, 63, 1297–1330.

Percec, V., Bae, J-Y. Zhao, M. and Hill, D.H. (1995). “Aryl mesylates in metal-catalyzed homocoupling and from phenols via nickel-catalyzed homocoupling of their mesylates cross-coupling reactions. 1. Functional symmetrical biaryls." *J. Org. Chem.*, 60, 176-185.

Piotraschke, J., Pullen, A.E., Abboud, K.A. and Reynolds, J.R. (1995). "The extensively conjugated bimetallic (μ-Tetrathiooxalato) copper(II) complex $(Bu_4N_2)_2[(C_3S_5)CuC_2S_4Cu(C_3S_5)]$ for electrically conducting charge transfer complexes." *Inorg. Chem.*, 34(16), 4011–4012.

Popp, B.V. and Stahl, S.S. (2009). "Mechanism of $Pd(OAc)_2$/Pyridine catalyst reoxidation by O_2: Influence of labile monodentate ligands and identification of a biomimetic mechanism for O_2 activation." *Chem. Eur. J.*, 15, 2915-2922.

Pradeepa, S.M., Naik, H.S.B., Kumar, B.V., Priyadarsini, K.I., Barik, A. and Naik, T.R.R. (2013). "Cobalt(II), Nickel(II) and Copper(II) complexes of a tetradentate Schiff base as photosensitizers: Quantum yield of O2 generation and its promising role in anti-tumor activity." *Spectrochim. Acta A.*, 101, 132-139.

Pu, L. (1998). "1,1′-Binaphthyl dimers, oligomers and polymers: Molecular recognition, asymmetric catalysis and new materials." *Chem. Rev.*, 98, 2405-2494.

Rajagopalan, B., Hu, C., Busch, D.H. and Subramaniam, B. (2008). "The Catalytic Efficacy of Co(salen)(AL) in O_2 Oxidation Reactions in CO_2-Expanded Solvent Media: Axial Ligand Dependence and Substrate Selectivity." *Catal. Lett.*, 123, 46–50.

Raman, N., Jeyamurugan, R., Subbulakshmi, M., Boominathan, R. and Yuvarajan, C.R. (2010). "Synthesis, DNA binding and antimicrobial studies of novel metal complexes containing a pyrazolone derivative Schiff base." *Chem. Pap.*, 64(3), 318-328.

Raman, N., Kulandaisamy, A., Thangaraja, C., Manisankar, P., Viswanathan, S. and Vedhi, C. (2004). "Synthesis, structural characterisation and electrochemical and antibacterial studies of Schiff base copper complexes." *Transit. Metal Chem.*, 29, 129-135.

Raman, N., Raja, J.D. and Sakthivel, A. (2008). “Design, synthesis, spectroscopic characterization, biological screening and DNA nuclease activity of transition metal complexes derived from a tridentate schiff base.” *Russ. J. Coord. Chem.,* 34(6), 400-406.

Raman, N., Thangaraja, C. and Johnsonraja, S. (2005). “Synthesis, spectral characterization, redox and antimicrobial activity of Schiff base transition metal(II) complexes derived from 4-aminoantipyrine and 3-salicylideneacetylacetone.” *Cent. Eur. J. Chem*., 3(3), 537-555.

Ramnial, T., Taylor, S.A., Clyburneab, J.A.C. and Walsby, C.J. (2007). “Grignard reagents in ionic solvents: Electron transfer reactions and evidence for facile Br–Mg exchange.” Chem. Commun., 2066-2068.

Reeves, J.T., Fandrick, D.R., Tan, Z., Song, J.J., Lee, H., Yee, N.K. and Senanayake, C.H. (2010). “Room temperature palladium-catalyzed cross coupling of aryltrimethylammonium triflates with aryl grignard reagents.” *Org. Lett.,* 12(19), 4388-4391.

Refat, M.S., El-Sayed, M.Y. and Adam, A.M.A. (2013). "Cu(II), Co(II) and Ni(II) complexes of new Schiff base ligand: Synthesis, thermal and spectroscopic characterizations." *J. Mol. Struct.*, 1038, 62–72.

Rivas, A.B., Pérez-Torrentea, J.J., Pardeyb, A.J., Masdeu-Bultóc, A.V., Diéguezc, M. and Oroa, L.A. (2009). “Hydroformylation of oct-1-ene catalyzed by dinuclear gem-dithiolato-bridged rhodium(I) complexes and phosphorus donor ligands.” *J. Mol. Catal. A: Chem.,* 300, 121-131.

Robertson, N. and Cronin, L. (2002). “Metal bis-1,2-dithiolene complexes in conducting or magnetic crystalline assemblies.” *Coord. Chem. Rev.,* 227, 93-127.

Rogers, H.R., Hill, C.L., Fujiwara, Y., Rogers, R.J., Mitchell, H.L. and Whitesides, G.M. (1980). “Mechanism of Formation of Grignard Reagents. Kinetics of Reaction of Alkyl Halides in Diethyl Ether with Magnesium.” *J. Am. Chem. Soc.*, 102(1), 217-226.

Rosu, T., Pahontu, E., Maxim, C., Georgescu, R., Stanica, N. and Gulea, A. (2011). "Some new Cu(II) complexes containing an ON donor Schiff base: Synthesis, characterization and antibacterial activity." *Polyhedron*, 30, 154-162.

Saadeh, S.M., Shawish, H.M.A., Dalloul, H.M., EL-Halabi, N.M. and Kh.Daher, B. (2012) "Lead(II) complexes with some SNO and ONO tridentate Schiff base ligands and their evaluation as lead(II) sensors." *Mat. Sci. and Eng.: C*, 32(3), 619-624.

Saito, K., Nakano, M., Tamura, H and Matsubayashi, G. (2002). "Preparation and properties of cyclopentadienyl- and pentamethylcyclopentadienyl-titanium(IV) complexes with the $C_8H_4S_8$ ligand, electrical conductivities of their oxidized species and x-ray crystal structure of $Ti(C_5Me_5)_2(C_8H_4S_8)$." *Inorg. Chem.*, 39, 4815-4820.

Salem, N.M.H., El-Sayed, L. and Iskander, M.F. (2008). "Metal complexe derived from hydrazoneoxime ligands: IV. Molecular and supramolecular structures of some nickel(II) complexes derived from diacetylmonoxime S-benzyldithiocarbazonate." *Polyhedron*, 27, 3215–3226.

Sandya, R. and Bhat, B.R. (2010). "Effective oxidation of alcohols by Iron(III) Schiff base Triphenylphosphine complexes." *Tetrahedron Lett.*, 51, 6403-6405.

Sawony, W. and Riederer. (1977). "Addition compounds with polymeric chromium(II)-Schiff base complexes." *Angew. Chem. Int. Ed. Engl.*, 16, 859-860.

Schoonover, M.W., Kubiak, C.P. and Eisenberg, R. (1978). "Crystal and molecular structure of allylnitrosylbis(triphenylphosphine)ruthenium, Ru(NO)(.eta.3-C3H5)(P(C6H5)3)2." *Inorg. Chem.*, 17, 3050–3055.

Selvakumar, P.M., Suresh, E. and Subramanian, P.S. (2007). "Synthesis, spectral characterization and structural investigation on some 4-aminoantipyrine containing Schiff base Cu(II) complexes and their molecular association." *Polyhedron*, 26, 749–756.

Seyferth, D. (2009). "The Grignard Reagents." *Organometallics*, 28, 1598–1605.

Shahnaz, N., Banik, B. and Das, P. (2013). "A highly efficient Schiff-base derived palladium catalyst for the Suzuki–Miyaura reactions of aryl chlorides." *Tetrahedron Lett.,* 54(22), 2886-2889.

Shanker, K., Rohini, R., Ravinder, V., Reddy, P.M. and Ho, Y.-P. (2009). "Ru(II) complexes of N4 and N2O2 macrocyclic Schiff base ligands: Their antibacterial and antifungal studies." *Spectrochim. Acta. A.,* 73(1), 205-211.

Sharma, A.K. and Chandrab, S. (2011). "Spectroscopic and mycological studies of Co(II), Ni(II) and Cu(II) complexes with 4-aminoantipyrine derivative." *Spectrochim. Acta. A,* 81, 424-430.

Sharma, R.K. and Samuelson, A.G. (2006). "On the key role of water in the allylic activation catalysed by Pd (II) bisphosphinite complexes." *J. Chem. Sci.*, 118(6), 569–573.

Shekhar, S. and Hartwig, J.F. (2004). "Distinct Electronic Effects on Reductive Eliminations of Symmetrical and Unsymmetrical Bis-Aryl Platinum Complexes." *J. Am. Chem. Soc.*, 126, 13016-13027.

Shi, L., Chu, Y., Knochel, P. and Mayr, H. (2012). "Leaving group dependence of the rates of halogen-magnesium exchange reactions." *Org. Lett.*, 14(10), 2602-2605.

Shi, Z., Zhang, C., Tanga, C. and Jiao, N. (2012). "Recent advances in transition-metal catalyzed reactions using molecular oxygen as the oxidant." *Chem. Soc. Rev.*, 41, 3381-3430.

Shujah, S., Rehman, Z., Muhammad, N., Ali, S., Khalid, N. and Tahir, M.N. (2011). "New dimeric and supramolecular organotin(IV) complexes with a tridentate schiff base as potential biocidal agents." *J. Organomet. Chem.*, 696(15-16), 2772-2781.

Simándi, L.I., Simándi, T.M., May, Z. and Besenyei, G. (2003). "Catalytic activation of dioxygen by oximatocobalt(II) and oximatoiron(II) complexes for catecholase-mimetic oxidations of o-substituted phenols." *Coordin. Chem. Rev.*, 245, 85-93.

Singh, B.K., Prakasha, A., Rajour, H.K., Bhojak, N. and Adhikari, D. (2010). “Spectroscopic characterization and biological activity of Zn(II), Cd(II), Sn(II) and Pb(II) complexes with Schiff base derived from pyrrole-2-carboxaldehyde and 2-amino phenol.” *Spectrochim. Acta. A*, 76, 376–383.

Singh, R.V. and Biyala. M.K (2006). “Structuralstudies withn antimicrobial and antifertility activity of a monofunctional bidentate ligand with its boron (III), Palladium(II) and platinum(II) complexes.” *Phosphorus, Sulfur Silicon Relat. Elem*., 181, 1477-1491.

Sisodiya, S., Lazar, A., Shylesh, S., Wang, L., Thiel, W.R. and Singh, A.P. (2012). “Covalently anchored ruthenium–phosphine complex on mesoporous organosilica: Catalytic applications in hydrogenation reactions.” *Catal. Commun.*, 25, 22-27.

Skorokhod, L.S., Seifullina, I.I. and Dzhambek, S.A. (2002). "Nickel(II) and cobalt(II) complexes with products of condensation of 1-aminonaphthalene, 2-aminonaphthalenesulfonic-5 acid and aromatic carbinols." *Russ. J. Coord. Chem*., 28, 684-688.

Sood, A. Räisänen, M.T., Aitola, E., Sibaouih, A., Colacio, E., Ahlgren, M., Nieger, M., Repo, T. and Leskelä, M. (2013). “Synthesis and crystal structure determination of Mn(II) Schiff base complexes and their performance in ethene polymerization.” *Polyhedron*, 56, 221-229.

Šoralová, S., Breza, M. and Gróf, M. (2011). “Quantum-chemical study of transition metal complexes with benzene-1,2-dithiolate.” *Polyhedron*, 30, 307–314.

Starodub, V.A., Vitushkina, S.V., Kamenskyi, D., Anders, A.G., Cheranovskii, V.O., Schmidt, H., Steinborn, D., Potocnak, I., Kajˇnakova´, M., Radva´kova´, A. and Feher, A. (2012). “Peculiarities of crystal structures and magnetic properties of Cu(II) and Ni(II) mixed-ligand complexes on the1,3-dithiole-2-thione-4,5-dithiolatebasis.” *J. Phys. Chem. Solids*, 73, 350-356.

Steinhoff, B.A. and Stahl, S.S. (2006). “Mechanism of Pd(OAc)$_2$/DMSO-catalyzed aerobic alcohol oxidation: Mass-transfer-limitation effects and catalyst decomposition pathways.” *J. Am. Chem. Soc.*, 128, 4348-4355.

Stephenson, T.A. and Wilkinson, G. (1966). “New complexes of ruthenium (II) and (III) with triphenylphosphine, triphenylarsine, trichlorostannate, pyridine and other ligands.” *J. Inorg. Nucl. Chem.*, 28, 945-956.

Subbaraj, P., Ramub, A., Raman, N. and Dharmaraja, J. (2014). “Novel mixed ligand complexes of bioactive Schiff base (E)-4-(phenyl (phenylimino) methyl) benzene-1,3-diol and 2-aminophenol/2-aminobenzoic acid: Synthesis, spectral characterization, antimicrobial and nuclease studies.” *Spectrochim. Acta. A*, 117, 65–71.

Sureshan, C.A. and Bhattacharya, P.K (1998). “Study of olefin epoxidation using binuclear Mn (II) complexes as catalyst in presence and absence of UV light.” *J. Mol. Catal. A: Chem.*, 136, 285-287.

Syamal, A. and Singh, M.M. (1993). “Syntheses and characterization of new cobalt(II) complexes of polystyrene-supported resin containing the Schiff bases derived from 3-formylsalicylic acid and 2-aminophenol, 2-aminobenzyl alcohol or 2-hydroxybenzylamine.” *React. Polym.*, 21(1–2), 45-52.

Tamizh, M.M., Cooper, B.F.T., Macdonald, C.L.B. and Karvembu, R. (2013). “Palladium(II) complexes with salicylideneimine based tridentate ligand and triphenylphosphine: Synthesis, structure and catalytic activity in Suzuki–Miyaura cross coupling reactions.” *Inorg. Chim. Acta*, 394, 391-400.

Tandon, V.K., Maurya, H.K., Mishra, N.N. and Shukla, P.K. (2009). “Design, synthesis and biological evaluation of novel nitrogen and sulfur containing hetero-1,4-naphthoquinones as potent antifungal and antibacterial agents.” *Eur. J. Med. Chem.*, 44, 3130–3137.

Tao, X-C., Zhou, W., Zhang, Y-P., Dai, C-Y., Shen, D. and Huang, M. (2006). “Homocoupling of aryl bromides catalyzed by nickel chloride in pyridine.” *Chin. J. Chem.*, 24(7), 939-942.

Toummini, D., Ouazzani, F. and Taillefer, M. (2013). “Iron-Catalyzed Homocoupling of Aryl Halides and Derivatives in the Presence of Alkyllithiums.” *Org. Lett.*, 15(18), 4690-4693.

Trujillo, A., Fuentealba, M., Carrillo, D., Manzur, C., Ledoux-Rak, I., Hamon, J-R. and Saillard, J-Y. (2010). “Synthesis, Spectral, Structural, Second-Order Nonlinear Optical Properties and Theoretical Studies On New Organometallic Donor-Acceptor Substituted Nickel(II) and Copper(II) Unsymmetrical Schiff-Base Complexes.” *Inorg. Chem.*, 49, 2750–2764.

Tsou, T.T. and Kochi, J.K. (1979). “Mechanism of Biaryl Synthesis with Nickel Complexes.” *J. Am. Chem. Soc.*, 101(25), 7547-7560.

Tumer, M., Koksal, H., Sener, M.K. and Serin, S. (1999). "Antimicrobial activity studies of the binuclear metal complexesderived from tridentate Schiff base ligands." *Transit. Met. Chem.* 24, 414-420.

Vallee, F., Mousseau, J.J. and Charette, A.B. (2010). “Iron-Catalyzed Direct Arylation through an Aryl Radical Transfer Pathway.” *J. Am. Chem. Soc.*, 132, 1514–1516.

Venanzi, L.M. (1958). "Tetrahedral nickel (II) complexes and the factors determining their formtion. Part I. Bistriphenylphosphine nickel(II) compounds." *J. Chem. Soc.*, 719-724.

Vilas-Boas, M., Freire, C., de Castro, B., Christensen, P.A. and Hillman, A.R. (1997). “New insights into the structure and properties of electroactive polymer films derived from [Ni(salen)].” *Inorg. Chem.*, 36, 4919-4929.

Vogel, A.I. (1989). "Textbook of practical organic chemistry." Fifth ed., Longman, London.

Volpe, M., Hartnett, H., Leeland, J.W., Wills, K., Ogunshun, M., Duncombe, B.J., Wilson, C., Blake, A.J., McMaster, J. and Love, J.B. (2009). “Binuclear Cobalt complexes of Schiff-base calixpyrroles and their roles in the catalytic reduction of dioxygen." *Inorg. Chem.*, 48, 5195-5207.

Walborsky, H.M. (1990). "Mechanism of grignard reagent formation. The surface nature of the reaction." *Acc. Chem. Res.*, 23, 286-293.

Wang, X.Q., Ren, Q., Fan, H.L., Chen, J.W., Sun, Z.H., Li, T.B., Liu, X.T., Zhang, G.H., Xua, D. and Liu, W.L. (2010). "Preparation, crystal structure, spectrographic characterization, thermal and third order non linear optical properties of benzyltriethylamine bis(2-thioxo-1,3-dithiole-4,5-dithiolato)nickel(III)." *J. Cryst. Growth*, 312, 2206–2214.

Wang, X.Q., Ren, Q., Zhang, F.J., Guo, W.F., Sun, X.B., Sun, J, Yang, H.L., Zhang, G.H., Hou, X.Q. and Xua, D. (2008). "Preparation, characterization, thermal and third-order nonlinear optical properties of bis(tetraethylammonium)bis(2-thioxo-1,3-dithiole-4,5-dithiolato)cuprate(II)." *Mater. Res. Bull.*, 43, 2342–2353.

Wolf, J., Labande, A., Daran, J.-C. and Poli. R. (2006). "Nickel(II) complexes with bifunctional phosphine–imidazolium ligands and theircatalytic activity in the Kumada–Corriu coupling reaction." *J. Organomet. Chem.*, 691(3), 433-443.

Wong, M.F., Huang, P.P., Brinkworth, R.I., Yashiro, M., Mohanl, P., Fairlie, D.P., Baba, M. and Vermal, S. (1996). "Non-peptide inhibitors of HIV-1 protease. Synthesis and structural evaluation of symmetric and non-symmetric naphthalenesulfonic acid analogues." *Eur. J. Med. Chem.*, 31, 249-255.

Wrixon, J.D., Hayward, J.J., Raza, O. and Rawson, J.M. (2014). "Oxidative addition chemistry of tetrathiocines: synthesis, structures and properties of group 10 dithiolate complexes." *Dalton. Trans.*, 43, 2134-2139.

Wu, F-Y., Zhang, H., Xiao, M. and Han, B-X. (2013). "A dual colorimetric and fluorescent sensor for lead ion based on naphthalene hydrazone derivative." *Spectrochim. Acta. A*, 109, 221–225.

Wu, J., Dai, W., Farnaby, J.H., Hazari, N., Roy, J.J.L., Mereacre, V., Murugesu, M., Powellc, A.K. and Takasea, M.K. (2013). “Synthesis and catalytic activity of iron complexes with bidentate NHC ligands.” *Dalton. Trans.,* 42, 7404-7413.

Wurz, R.P. (2007). “Chiral dialkylaminopyridine catalysts in asymmetric synthesis.” *Chem. Rev.,* 107, 5570-5595.

Xu, C., Hao, X.-Q., Li, Z., Dong, X.-M., Duan, L.-M., Wang, Z.-Q., Ji, B.-M. and Song, M.-P. (2012). “Synthesis, structural characterization and catalytic activity of two *N*-heterocyclic carbene–phosphine palladium(II) complexes.” *Inorg. Chem. Commun.,* 17, 34-37.

Yadav, J.S., Gayathri, K.U., Ather, H., Rehman, H. and Prasad, A.R. (2007). “Utility of semicarbazones as ligands in newly made palladium complex for facile Suzuki homocoupling reaction of alkyl and aryl boronic acids.” *J. Mol. Catal. A: Chem.,* 271, 25–27.

Yu, T., Su, W., Li, W., Hong, Z., Hua, R. and Li, B. (2007). “A schiff base zinc complex and its electroluminescent properties.” *Thin solid Films,* 515(7-8), 4080-4084.

Yuan, C. and Fang, Q. (2012). “A new procedure for the synthesis of p-conjugated polymers via ligand-free iron(III)-catalyzed oxidative homocoupling reaction of grignard reagents.” *RSC Adv.,* 2, 8055-8060.

Zapata-Rivera, J., Caballol, R. and Calzado, C.J. (2011). “Comparing the peroxo/superoxo nature of the interaction between molecular O_2 and b-diketiminato-copper and nickel complexes.” *Phys. Chem. Chem. Phys.,* 13, 20241–20247.

Zapata-Rivera, J., Caballol, R. and Calzado, C.J. (2012). “The role of macrocyclic ligands in the peroxo/superoxo nature of Ni–O2 biomimetic complexes.” *J. Comput. Chem.,* 33, 1407–1415.

Zhong, X., Yi, J., Sun, J., Wei, H.L., Lio, W.S. and Yu, K.B. (2006). "Synthesis and crystal structure of some transition metal complexes with a novel bis-Schiff base ligand and their antitumour activities." *Eur. J. Med. Chem.*, 41, 1090-1092.

Zhou, Z. and Xue, W. (2009). "Manganese-catalyzed oxidative homo-coupling of aryl Grignard chlorides." *J. Organomet. Chem.*, 694, 599-603.

Zinenko, T.N., Starodub, V.A. and Kazachkov, A.R. (2003). "Metal Isotrithionedithiolates as Synthetic Metals." *Russ. J. Coord. Chem.*, 29, 400-407.

Zuo, J-L., Yao, T-M., You, X-Z., Fun, H-K. and Kandasamy, S. (1996). "Syntheses, properties and crystal structures of a series of mixtures of dmit and dmise metal complexes (dmit = 1,3-dithiole-2-thione-4,5-dithiolate, dmise = 1,3-dithiole-2-selone-4,5-dithiolate). Single-crystal ESR study of $[Bu_4N]_2[Cu/Ni(C_3S_{4.4}Se_{0.6})_2]$." *Polyhedron*, 15(20), 3547-3557.

RESEARCH PUBLICATIONS

RESEARCH PUBLICATIONS

(A) Research Papers in International Journals

1. **P.I. Aparna** and Badekai Ramachandra Bhat (2012). “Homocoupling of aryl Grignard reagents to form biaryls using ruthenium(III) complex, [RuCl(C_3S_5)(H_2O)(PPh_3)$_2$].” *J. Mol. Catal. A: Chem.*, 358, 73–78.
2. **Aparna P.I. Bhat**, Fawad Inam and Badekai Ramachandra Bhat (2013). “One-Step Synthesis of Biaryls under Mild Conditions” *Eur. J. Org. Chem.*, 2013, 7139–7144.
3. **Aparna P.I. Bhat**, Fawad Inam and Badekai Ramachandra Bhat. (2013). “Nickel catalyzed one pot synthesis of biaryls under air at room temperature.” *RSC Adv.*, 3, 22191–22198.
4. **Aparna P.I Bhat** and Badekai Ramachandra Bhat. (2014). “Single Step Oxidative Homocoupling of Aryl Grignard Reagents via Co(II), Ni(II) and Cu(II) Complexes under air.” *Appl. Organomet. Chem.*, 28(6), 383-388.
5. **Aparna P.I Bhat** and Badekai Ramachandra Bhat. "Ni(III) catalyzed homocoupling of Grignard reagents for single step synthesis of biaryls: A comparison study of electronic effect of the ancillary and reactive ligands." (Communicated).
6. **Aparna P.I Bhat** and Badekai Ramachandra Bhat. "Octahedral Ni(II)-Schiff base-triphenylphosphine complexes as effective catalysts for homocoupling of Grignard reagents using atmospheric oxygen as oxidant." (Communicated).
7. **Aparna P.I Bhat** and Badekai Ramachandra Bhat. "Cobalt, nickel and copper complexes for direct synthesis of biaryls under air." (Under preparation).
8. **Aparna P.I Bhat** and Badekai Ramachandra Bhat. "Catalytic activity of Cu(III) complexes for one step synthesis of symmetrical biaryls." (Under preparation).

9. **Aparna P.I Bhat** and Badekai Ramachandra Bhat. "Synthesis, characterization and catalytic activity of Co(II) complexes containing dmit-Schiff base-triphenylphosphine ligands for oxidative C-C coupling reaction." (Under preparation).

10. **Aparna P.I Bhat** and Badekai Ramachandra Bhat. "Catalytic activity of Ni(II) complexes containing dmit-Schiff base-triphenylphosphine ligands for direct biaryl construction: A comparison study." (Under preparation).

11. **Aparna P.I Bhat** and Badekai Ramachandra Bhat. "A room temperature direct synthesis of biaryls using Co(III) complexes under air." (Under preparation).

12. **Aparna P.I Bhat** and Badekai Ramachandra Bhat. "Ni(II) catalyzed homocoupling of aryl Grignard reagents using atmospheric oxygen as oxidant: A practical approach." (Under preparation).

(B) Research Papers Presented in National/International Conferences

1. **Aparna P.I**, B. Ramachandra Bhat and S. Vijayanarayana (2010). "Catalytic Activities of Ruthenium(III) Complex Containing C_3S_5 and PPh_3 Ligands." *20th National Symposium on Catalysis for Energy Conversion and Conservation of Environment (NSC-2010)*, 19-22, December, NCCR, Indian Institute of Technology Madras, Chennai, India.

2. **Aparna P.I** and B. Ramachandra Bhat (2011). "Synthesis Characterization and Catalytic application of Ni(II) complex." *National Symposium on Chemistry and Humanity (NSCH-2011)*, 11-12, July, Manipal Institute of Technology, Manipal, India.

3. **Aparna P.I** and B. Ramachandra Bhat (2011). "Green Synthesis of biaryls using Ni(III) complex." *International Conference on Synthetic & Structural Chemistry (ICSSC-2011)*, 8-10, December, Mangalore University, Mangalore, India.

4. **Aparna P.I** and B. Ramachandra Bhat (2011). "One-Step synthesis of biaryls using Co(III) complex." *Indian Council of Chemists conference*, 28-30, December, Osmania University, Hyderabad, India.

5. **Aparna P.I** and B. Ramachandra Bhat (2013). "Efficient Ni(II)-complex catalyzed homo coupling of aryl Grignard reagents in greener reactions." *International Conference on Recent Advances in Material Science and Technology-2013 (ICRAMST-13)*, 17-18, January, National Institute of Technology Karnataka, Surathkal, Mangalore, India.

CURRICULAM VITAE

APARNA P.I.

Temporary Address:

Department of Chemistry

National Institute of Technology Karnataka,

Surathkal, Post Srinivasanagar,

Mangalore - 575025, India.

E-mail: appu.gokula@gmail.com

Phone: +91-9483876575 (M)

EDUCATION

Ph.D. in Chemistry

Area:	Organometallic complex synthesis, Catalysis
Title:	Synthesis and characterization of some transition metal complexes for homocoupling of Grignard reagents
Institute:	Catalysis and Materials Laboratory, National Institute of Technology Karnataka, Surathkal, Mangalore, India.
Advisor:	Dr. B. Ramachandra Bhat
Year:	Thesis submitted (March 2014)

M.Sc. in Chemistry

Project:	Composition modulated multilayered Zn-Fe alloy coatings – synthesis and their characterization
Institute:	Electrochemistry Research Laboratory, National Institute of Technology Karnataka, Surathkal, Mangalore, India.
Advisor:	Dr. A. Chitharanjan Hegde
Year:	2009

RESEARCH PUBLICATIONS

1. **P.I. Aparna** and Badekai Ramachandra Bhat (2012). “Homocoupling of aryl Grignard reagents to form biaryls using ruthenium(III) complex, [RuCl(C_3S_5)(H_2O)(PPh_3)$_2$].” *J. Mol. Catal. A: Chem.*, 358, 73–78.
2. **Aparna P.I. Bhat**, Fawad Inam and Badekai Ramachandra Bhat (2013). “One-Step Synthesis of Biaryls under Mild Conditions” *Eur. J. Org. Chem.*, 2013, 7139–7144.
3. **Aparna P.I. Bhat**, Fawad Inam and Badekai Ramachandra Bhat. (2013). “Nickel catalyzed one pot synthesis of biaryls under air at room temperature.” *RSC Adv.*, 3, 22191–22198.
4. **Aparna P.I Bhat** and Badekai Ramachandra Bhat. (2014). “Single Step Oxidative Homocoupling of Aryl Grignard Reagents via Co(II), Ni(II) and Cu(II) Complexes under air.” *Appl. Organomet. Chem.*, (accepted).

RESEARCH EXPERIENCE

- Synthesis of various Organometallic/transition metal complexes.
- Purification of synthesized compounds.
- The use of metal complexes as homogeneous catalyst for the homocoupling reactions.
- As a senior research fellow, guided one graduate student in the area of catalysis, during the research programme.

TECHNICAL EXPERIENCE

- Having profound instrument operating knowledge of FT-IR, UV-Visible, TGA, Sherwood Magnetic Susceptibility balance and Fluorescence spectrophotometer.
- Skilful in handling Gas Chromatography (Schimadzu GC 2014).
- Having good skill of elucidating he structure of compounds from UV, FT-IR, NMR, Mass and Elemental analysis data.

- Familiar with instruments such as NMR, SEM, TEM, EDAX, Powder XRD and Single crystal XRD.

REFERENCES

1. **Prof. B. Ramachandra Bhat**

   Department of Chemistry,

   National Institute of Technology Karnataka,

   Surathkal-575 025

   Mangalore, India

   Email: chandpoorna@yahoo.com

   Contact No: +91-944953759.

2. **Prof. A. Chitharanjan Hegde**

   Department of Chemistry,

   National Institute of Technology Karnataka,

   Surathkal-575 025

   Mangalore, India

   Email: hegdeac@rediffmail.com

   Contact No: +91-9980360242.